Application of pharmacometric methods to understand warfarin dose response

Qing Xi Ooi

A thesis submitted for the degree of

Doctor of Philosophy

At the University of Otago, Dunedin,

New Zealand

November 2018

ABSTRACT

Existing warfarin dosing methods do not accurately predict warfarin maintenance doses for patients in the lower or upper quartile of dose requirements. It was argued that this is related to the use of the international normalised ratio (INR) as a sole marker of anticoagulation for warfarin dose individualisation. The overarching premise of this thesis was that the coagulation proteins are on the causal path from warfarin dose to INR response and that a measure of coagulation protein response in addition to the INR will be helpful in the prediction of future anticoagulant response. The aim of this thesis was to apply pharmacometric methods to understand the coagulation kinetics underpinning the warfarin dose response and to introduce a new perspective to the prediction of anticoagulant response to warfarin.

A joint model was developed to quantify the influence of warfarin on all six vitamin K-dependent coagulation proteins (factors II, VII, IX, X, and proteins C and S) simultaneously. The full correlation structures that exist between parameters at the individual level and between residual errors of different coagulation proteins were accounted for. Of all the coagulation proteins considered, factor VII was found to have the shortest degradation half-life and will therefore be the first to reach a new steady-state following a perturbation introduced by warfarin.

Subsequently, the influence of coagulation proteins and their interactions on the INR was explored based on simulations from a mechanistic coagulation network model. A sensitivity analysis revealed that INR is most sensitive to factor VII and an isobologram analysis demonstrated that the presence of more than one coagulation protein deficiencies is redundant for INR effect. It was proposed that factor VII is the most influential on the INR and that the use of factor VII as a marker of anticoagulation (in addition to the INR) may improve the prediction of the anticoagulant response.

A factor VII-based method for the prediction of anticoagulant response to warfarin was developed based on a heuristic model-order reduction of the

coagulation network model. The prediction method was shown to be associated with minimal bias and its use was illustrated using data from one typical simulated patient and two real patients supporting a proof-of-principle.

Finally, a framework for systematic evaluation of model assumptions was developed. In particular, a flowchart was proposed to evaluate assumptions based on the impact and the probability of assumption violation. The assumptions underpinning the pharmacometric analyses presented in this thesis were evaluated and used to illustrate the utility of the proposed framework.

In this thesis, both the top-down and bottom-up pharmacometric analyses were applied to explore the coagulation kinetics underpinning warfarin dose response. Standard methods such as population analysis, model simulations, isobologram analysis, and sensitivity analysis were employed. A heuristic model-order reduction method was experimented and seemed to work well although generalisation of the method to other settings requires prospective testing.

The work conducted in this thesis offered a new perspective on the prediction of anticoagulant response. The next step would be to extend the current method to the prediction of warfarin maintenance dose. This would require setting up and evaluating a dose individualisation algorithm (perhaps Bayesian) that incorporates a factor VII-INR bivariate response variable. Last but not least, a framework for systematic evaluation of assumptions was proposed. An important future step would be to apply the framework to a series of other settings to fully explore the utility and robustness of the framework to different model-building processes and model use settings.

ACKNOWLEDGMENTS

I would like to express my deepest gratitude to my primary supervisor, Professor Stephen Duffull for his constant guidance, support, and encouragement during the course of my doctoral study. I am infinitely thankful to him for introducing me to unique ways of learning and thinking about pharmacometrics – to see things (pharmacometrics) not just the way things are and how *not* to just do things but to look deeper even into everyday things to understand and see their true cause, intricacy, and significance. He is the best mentor I could ever wish for.

I am sincerely grateful to my co-supervisor, Dr Daniel Wright. He gave freely of his knowledge and encouragement. His passion and enthusiasm for clinical pharmacology are infectious and he is a source of inspiration for me to be a better science communicator.

I am also deeply grateful to my co-supervisor (clinical), Professor Geoffrey Isbister for his guidance and valuable comments.

I wish to express deep gratitude to the University of Otago for providing me with a doctoral scholarship. I am also grateful to the School of Pharmacy and the Division of Health Sciences, University of Otago for providing me with the travel grant to attend conferences and workshops.

I am grateful to the Ministry of Health Malaysia for offering a study leave for me to pursue my doctoral study. I am especially thankful to Dr Amar-Singh HSS and Dr Goh Pik Pin who had made this possible.

I would like to thank Dr Robert Tait at the Glasgow Royal Infirmary, Glasgow, Scotland who provided the clinical data for warfarin and vitamin K-dependent coagulation proteins.

I am honoured to be given the opportunity to supervise Anna Cao, a student undertaking the Bachelor of Pharmacy with Honours (BPharm(Hons)) programme in the University of Otago. The honours project allowed me to explore vitamin K as an additional aspect to the work conducted in this thesis. I would like to thank Anna for her hard work and dedication to this project.

I am particularly thankful to Dr Hesham Al-Sallami and Dr Chihiro Hasegawa from the Otago Pharmacometrics Group (OPG) who gave freely of their time for discussions and to share their experience and knowledge with us.

Special thanks go to my colleagues and friends at the OPG: Zheng Liu, Shamin, Vijay, Jaydeep, Derek, Sudeep, Yim, Isabelle, Abdallah, Salma, Jill, Shan, Vittal, Mohammed, Natalie, Dharrshinee, Mathilde, Marion, Alina, and Laura. Thank you for the good company, good food, friendly banter, and fun discussions.

I would like to thank the staff at the School of Pharmacy, University of Otago, Associate Professor Natalie Medlicott (my facilitator), Dr Dorothy Saville and Dr Allan Gamble (coordinators of the undergraduate courses that I demonstrated in), Denise (postgraduate administrator), and Tim (IT specialist) for their support during the course of my doctoral study.

A special thank you to my friends from all over the world: Anu, Jason, Pavel, Mithun, Tap, Nang, Vee-Liem, Polly, Donald, Wei Yun, Sze Hwei, Shi Chian, Chian Hui, Phiaw Chong, Wei Yang, Khai Lin, Lina, Wei Yin, Sharon, Huda, Kang Lik, Sue Lyn, Stefanie, Chee Xuan, Amy, Ryan, Bryan, Stephanie, and Jasmine. Thank you for the unfailing love and support at different stages of my life. They meant the world to me.

I am forever indebted to my mum and dad for their unconditional love and the chance at a real education that they had fought for me. Thank you for always believing in me and encouraging me to follow my dreams. A special thank you to my brothers, Alan and Andy, and my sister-in-laws, Su Wen and Kathy, for their enormous support during my PhD. Last but not least, I am grateful to my partner and best friend, Andrej, for being the pillar of strength and the voice of reason in this major undertaking.

PUBLICATIONS

THAT HAVE ARISEN FROM WORK ASSOCIATED WITH THIS THESIS

International peer-reviewed journals

Published:

- **Ooi QX**, Wright DF, Tait RC, Isbister GK, Duffull SB. *A joint model for vitamin K-dependent clotting factors and anticoagulation proteins*. Clin Pharmacokinet. 2017: 56, 1555-66.
- **Ooi QX**, Wright DF, Isbister GK, Duffull SB. *A factor VII-based method for the prediction of anticoagulant response to warfairn*. Sci Rep. 2018: 8, 12041.

In preparation:

- **Ooi QX**, Wright DF, Isbister GK, Duffull SB. *Evaluation of assumptions underpinning pharmacometric models*.

Oral Presentations

- **Ooi QX**, Wright DF, Isbister, GK, Duffull SB. *Evaluation of assumptions underpinning pharmacometric models*. Stuart Beal Methodology Session, Population Approach Group in Europe (PAGE) Meeting 2018, Montreux, Switzerland.
- **Ooi QX**, Wright DF, Isbister, GK, Duffull SB. *Evaluation of assumptions underpinning pharmacometric models*. Population Approach Group of Australia & New Zealand (PAGANZ) Meeting 2018, Melbourne, Australia. *International Society of Pharmacometrics (ISoP) Student Prize for best oral presentation (pharmacometrics)*.
- **Ooi QX**, Wright DF, Isbister, GK, Duffull SB. *A factor VII-based method for the prediction of anticoagulant response to warfarin*. Australasian Society of Clinical and Experimental Pharmacologists and Toxicologists (ASCEPT) Meeting 2017, Queentstown, New Zealand. *Evan Begg Prize for best oral presentation (clinical pharmacology)*.
- **Ooi QX**, Wright DF, Isbister, GK, Duffull SB. *Sensitivity of international normalised ratio to variations in clotting factor levels*. PAGANZ Meeting 2017, Adelaide, Australia.
- **Ooi QX**, Wright DF, Tait C, Isbister, GK, Duffull SB. *A joint model for vitamin K-dependent clotting factors and anticoagulation proteins.* World Conference on Pharmacometrics (WCoP) 2016, Brisbane, Australia.
- **Ooi QX**, Wright DF, Tait C, Isbister, GK, Duffull SB. *Quantifying the influence of vitamin K on warfarin dosing requirements*. ASCEPT Meeting 2016, Queentstown, New Zealand.

TABLE OF CONTENTS

LIST OF FIGURES

MAIN TEXT

LIST OF FIGURES

APPENDICES

LIST OF TABLES

MAIN TEXT

LIST OF TABLES

APPENDICES

LIST OF EQUATIONS

MAIN TEXT

LIST OF EQUATIONS

APPENDICES

GLOSSARY

ABBREVIATIONS

2D	Two-dimensional
3D	Three-dimensional
ADME	Absorption, distribution, metabolism, and excretion
ANOVA	Analysis of variance
AUC	Area under the curve
BSA	Body surface area
BSV	Between-subject variability
CI	Confidence interval
CV	Coefficient of variation
CWRES	Conditional weighted residuals
CYP	Cytochrome P450
dL	Decilitre
DVT	Deep vein thrombosis
EBE	Empirical Bayes estimate
EFPIA	European Federation of Pharmaceutical Industries and Associations
eGFR	Estimated glomerular filtration rate
EMA	European Medicines Agency
F1+2	Prothrombin fragment
FDA	Food and Drug Administration
FFM	Fat free mass
Fg	Fibrinogen
FO	First-order
FOCE	First-order conditional estimation
FOCE-I	First-order conditional estimation with interaction
GFR	Glomerular filtration rate
GGCX	Gamma-glutamyl carboxylase
I	Impact of assumption violation
$I_{[e]}$	Impact of assumption violation with respect to an external aim of interest
$I_{[i]}$	Impact of assumption violation with respect to an internal aim of model building
II	Factor II
II_{SS}	Steady-state factor II
iid	Independent and identically distributed
INR	International normalised ratio
INR_{SS}	Steady-state international normalised ratio
IPRED	Individual prediction
ISI	International sensitivity index for thromboplastin
IU	International unit
IX	Factor IX
L	Litre or likely

LOCF	Last observation carried forward
KPD	Kinetic-pharmacodynamic
MAP	Maximum a posteriori
mg	Milligram
mGFR	Measured glomerular filtration rate
MID3	Model-informed drug discovery and development
ML	Maximum likelihood
MPE	Mean prediction error
MTT	Mean transit time
NA	Not applicable
NCA	Non-compartmental analysis
nM	Nano-molar
NS	Non-significant
ODE	Ordinary differential equation
OFV	Objective function value
P	Probability of assumption violation
pcVPC	Prediction corrected visual predictive check
PBPK	Physiologically based pharmacokinetic modelling
PC	Protein C
PCA	Prothrombin complex activity
PD	Pharmacodynamics
$P_{[e]}$	Probability of assumption violation with respect to an external aim of interest
PE	Pulmonary embolism
$P_{[i]}$	Probability of assumption violation with respect to an internal aim of model building
PK	Pharmacokinetics
PKPD	Pharmacokinetics and pharmacodynamics
PRED	Population prediction
PS	Protein S
PT	Measured prothrombin time
$PT_{standard}$	Prothrombin time for standard normal plasma
Q-Q	Quantile-quantile
QSP	Quantitative systems pharmacology
RMSE	Root mean squared error
ROC	Receiver operating characteristic
RSE	Relative standard error
RUV	Residual unexplained variability
S	Significant
s	Seconds
SAEM	Stochastic approximation expectation maximisation
SE	Standard error
SIG	Significant digits
SI_P	Sensitivity index of the international normalised ratio to specific coagulation protein
TF	Tissue factor

TOL	Precision of integration solution
U	Unlikely
UK	Unknown
VII	Factor VII
VII_{SS}	Steady-state factor VII
VKOR	Vitamin K epoxide reductase
VPC	Visual predictive check
X	Factor X
X_{SS}	Steady-state factor X

GLOSSARY

INDICES AND SYMBOLS

a	Parameter defining the dose-dependency of the upper horizontal asymptote of the logistic function
A	Amount of an entity in a compartment
A_{50}	Amount of a drug in the body that gives half the maximum effect
$A_{t=0}$	Amount of an entity in a compartment at baseline
b	Parameter defining the dose-dependency of the magnitude of horizontal shift of the logistic function
c	Parameter defining the dose-dependency of the second-order coefficient of the quadratic function
C	Concentration of a drug
C_{50}	Concentration of a drug that gives half the maximum effect
CL	Clearance of a drug
CR	Concentration of a drug-receptor complex
D	Dose
$D_{x,drug}$	The dose of a drug that gives a predetermined x level of effect when given in combination with another drug
df	Degree of freedom
D_{ref}	Warfarin dose that is required by a typical patient to achieve a specific level of anticoagulant response
e	Exponential
E	Effect of a drug
EA_{50}	Amount of drug in the body that gives half the maximum stimulatory effect
EC_{50}	Concentration of a drug that gives half the maximum stimulatory effect
$ED_{x,drug}$	The dose of a drug that singly gives a predetermined x level of effect
EDK_{50}	Elimination rate of a drug that gives half the maximum effect
E_m	Maximum effect in a system
E_{max}	Maximum effect of a drug
ER	Elimination rate
f	Mathematical function
F	Bioavailability
$F1+2$	Concentration of prothrombin fragment
Fg	Concentration of fibrinogen
g	Magnitude of horizontal shift of the logistic function
h	Step size or upper horizontal asymptote of the logistic function
H_A	Alternative hypothesis
H_0	Null hypothesis
i	Index
I	Concentration or amount of a physiological intermediate

I_P	Inhibitory E_{max} function to describe warfarin inhibitory action on the production of a specific coagulation protein
IA_{50}	Amount of a drug in the body that gives half the maximum inhibitory effect
IC_{50}	Concentration of a drug that gives half the maximum inhibitory effect
II	Concentration of factor II
iid	Independent and identically distributed
I_{max}	Maximum inhibitory effect of a drug
INR	Value of international normalised ratio
INR_{SS}	Value of steady-state international normalised ratio
ISI	International sensitivity index for thromboplastin
IX	Concentration of factor IX
j	Index
k	First-order elimination rate constant of a drug or second-order coefficient of the quadratic function
k_{12}	First-order transfer rate constant of a drug from the central to the peripheral compartment
k_{21}	First-order transfer rate constant of a drug from the peripheral to the central compartment
k_a	First-order absorption rate constant of a drug
K_A	Equilibrium dissociation constant or reciprocal affinity parameter
K_M	Michaelis constant
k_{out}	First-order degradation rate constant
LAG	General lag parameter
M_F	Fisher information matrix
m	First-order coefficient of the quadratic function
n	Number of observations or sample size
p	Number of parameters or p value or shape parameter of the logistic function
P	Specific coagulation protein or its concentration
PC	Concentration of protein C
PS	Concentration of protein S
PT	Measured prothrombin time
$PT_{standard}$	Prothrombin time for standard normal plasma
q	Proportionality constant
$\mathbb{R}$	Real number
R_0	Concentration of available receptors in a system
r^2	Adjusted coefficient of determination
R_P	Percentage reduction in one type of coagulation protein that singly results in the predetermined level of anticoagulant effect
$R_{P,combi}$	Percentage reduction in one coagulation protein to give a predetermined level of anticoagulant effect when another coagulation protein is simultaneously reduced
R_{in}	Zero-order synthesis rate

s	Parameter defining the dose-dependency of the first-order coefficient of the quadratic function
SI_P	Sensitivity index of the international normalised ratio to changes in a specific coagulation protein
t	Time
T	Kolmogorov-Smirnov test statistic
$t_{\frac{1}{2}}$	Degradation half-life
$t_{E,max}$	Time to maximum effect of a drug
$t_{SS,INR}$	Time to steady-state international normalised ratio
V	Volume of distribution of a drug
V_1	Volume of distribution of a drug in the central compartment
V_2	Volume of distribution of a drug in the peripheral compartment
VII	Concentration of factor VII
VII_B	Concentration of factor VII in the blood compartment
VII_S	Concentration of factor VII in the storage compartment
V_{max}	Maximum rate of reaction
x	Covariate
$\bar{X}$	Sample mean
X	Concentration of factor X or input variable
y	Observations
α	Intrinsic activity or significance level
β	Fixed-effects parameter
Δ	Change or difference
ε	Residual unexplained variability or error
ε_{INR}	Tolerance in the international normalised ratio (INR) domain that defines the steady-state status of the INR
$\varepsilon_{SI_{VII}}$	Tolerance in the sensitivity index (of the international normalised ratio [INR] to changes in a specific coagulation protein) domain that defines the steady-state status of the INR
η	Between-subject variability
γ	Empirical exponent or shape parameter
λ	Parameter of the Box-Cox function
μ	Population mean
ω^2	Variance of between-subject variability
Ω	Variance-covariance matrix of between-subject variability
ρ	Pearson's linear correlation coefficient
σ^2	Variance of residual unexplained variability or error
τ	Transduction efficiency
θ	Parameter (general)
ζ	Box-Cox transformation function

STRUCTURE OF THE THESIS

Table P.1 *Overview of the thesis*

Part I	**Introduction**
	Chapter 1. Introduction
Part II	**Warfarin-coagulation proteins relationship**
	Chapter 2. A joint model for vitamin K-dependent coagulation proteins
Part III	**Warfarin-coagulation proteins-INR relationship**
	Chapter 3. Understanding the coagulation kinetics governing the international normalised ratio (INR) Chapter 4. A factor VII-based method for the prediction of anticoagulant response to warfarin
Part IV	**Evaluation of model assumptions**
	Chapter 5. Evaluation of assumptions underpinning pharmacometric models
Part V	**Discussion and future work**
	Chapter 6. Discussion and future work
Part VI	**Appendices**
	Appendix 1. Appendices to Chapter 2 Appendix 2. Appendices to Chapter 3 Appendix 3. Appendices to Chapter 4 Appendix 4. Appendices to Chapter 5 References

PART I

INTRODUCTION

Chapter 1: Introduction

1.1. Introduction to the thesis

Warfarin is the mainstay oral anticoagulant therapy that is indicated for the treatment and prevention of thomboembolic disease. The physiological response to warfarin is a reduction in the concentrations of functional vitamin K-dependent coagulation proteins (factors II, VII, IX, X, and proteins C and S) that leads to a prolonged clotting time and is usually monitored clinically using the international normalised ratio (INR). Sub-therapeutic INR is associated with increased clotting risk while supra-therapeutic INR carries a significant risk of major bleeding events [1]. The safe and effective use of warfarin is therefore dependent on maintaining the INR within a narrow therapeutic range.

The goal of warfarin dose individualisation is to predict the warfarin maintenance dose that will keep the steady-state INR (INR_{SS}) within this range. Several tools, usually with an underpinning model, have been developed to aid warfarin dose selection in the clinic. Despite a significant body of literature in this area, prediction of anticoagulant response and warfarin maintenance dose in patients remain inaccurate [2-7]. This highlights the difficulty in choosing an optimal warfarin maintenance dose for individual patient where it requires a quantitative understanding of warfarin dose response while accounting for the inherent variability between and within patients.

The work conducted in this thesis involves the application of pharmacometric methods to understand warfarin dose response. Pharmacometrics is the science of quantitative pharmacology. It involves the development and application of mathematical and statistical models to (1) describe, understand, and predict the pharmacokinetics (PK) and pharmacodynamics (PD) of a drug; (2) quantify the variability between and within patients as well as the uncertainty in predictions; (3) rationalise decision in the drug development process and optimisation of drug therapy in routine clinical setting; and (4) design studies to generate data for inferential purposes.

Pharmacometric analysis has an inherent utility in dose individualisation. It is unique in that it allows the partitioning and quantification of variability

between and within patients. Variability between patients may be predictable due to dependence of PK or PD process on individual characteristics while the remaining variability are unexplained and assumed random. Understanding the variability between patients and its effect on dose requirements is useful to rationalise dosing decisions and to tailor the dosing regimen to suit the needs of a specific patient. Indeed, this provides the basis for warfarin dose individualisations in clinical practice where patient characteristics (e.g. concomitant drugs) [8-16] and measures of anticoagulant response (e.g. INR) [12, 17, 18] are used to predict the between-patient differences in warfarin dose response. From a practical perspective, because the pharmacometric approach to analysis is based on population data (and not solely on data from any one particular patient), it has an innate ability to cope with sparse data that are typically generated during routine patient care [19-21].

The reason for the poor predictive performance of available warfarin dosing tools is not fully understood [5]. It is probable that empirical models (e.g. those using a linear function [12, 22-25]) underpinning these dosing methods are too simple to accommodate the complexity of the coagulation system. Importantly, it is believed that much of the issues with the poor predictive ability of existing tools relate to the use of INR, a blunt estimate of coagulation that is a composite of multiple coagulation proteins, as a sole marker of anticoagulant response to guide warfarin dosing [12, 17, 18, 22, 23, 25-30].

The overarching premise of this thesis is that a measure of coagulation protein in addition to the INR will better inform the prediction of anticoagulant response and warfarin dose requirement. This was argued and rationalised based on the full causal path of warfarin dose response from warfarin dose, warfarin PK, warfarin PD, coagulation proteins' response, coagulation network response to the INR response. Here, due to the its downstream location on the causal path, INR response is a conglomerate measure of the variability in all of the upstream components. Then, in theory, inclusion of the coagulation protein response will provide a signal from the system that lies causally between warfarin concentration and INR response and as such will be helpful in

delineating the different sources of variability in anticoagulant response and in elucidating the dose response relationship of warfarin. A choice of a coagulation protein that is particularly sensitive to warfarin and also influential on the INR would be appropriate.

To this end, pharmacometric models that vary in the level of mechanistic detail were developed and applied in this thesis. In the first stage, a semi-mechanistic, compartmental model was developed to quantify the time course of warfarin influence on factors II, VII, IX, and X, and proteins C and S simultaneously. Subsequently, a fully-mechanistic model of the coagulation network [31], which includes components of *in vivo* coagulation and *in vitro* blood coagulation tests (e.g. INR), was used to explore the effect of coagulation proteins and their interactions on the INR in order to identify a sensitive and influential coagulation protein for the prediction of anticoagulant response. This involves testing hypotheses and what-if scenarios via simulations from the model that are otherwise not permissible within standard experimental framework due to (1) the complex interactions between components of the coagulation network; (2) the different orders of magnitude in the rate of change and turnover rate of coagulation components; and (3) the fact that the act of drawing a blood sample can itself activate the coagulation system. In the development of a method for the prediction of warfarin anticoagulant response, a heuristic model reduction method was employed in which a statistical model was used to approximate the fully-mechanistic model such that all responses of interest were captured over an appropriate span of the input-output relationship. In doing this the statistical model is considerably simpler than the full mechanistic model and is amenable to manipulation for clinical application, particularly the potential for Bayesian forecasting. Finally, this work culminates in the development of a framework to explore and formalise model-based assumptions and limitations. This final component is critical in formally addressing the model-based components of this thesis that underpin the proposed method for the prediction of warfarin anticoagulant response.

1.1.1. Aims of the thesis

The aim of this thesis was to apply pharmacometric methods to understand the coagulation kinetics underpinning the warfarin dose response and to introduce a new perspective to the prediction of anticoagulant response to warfarin. There were four specific objectives:

1. To develop a model to quantify the relationship between warfarin and vitamin K-dependent coagulation proteins (**Chapter 2**),
2. To explore vitamin K-dependent coagulation proteins as drivers of the anticoagulant response (**Chapter 3**),
3. To develop a coagulation protein-based method for the prediction of anticoagulant response to warfarin (**Chapter 4**), and
4. To develop a framework for evaluating assumptions intrinsic to a pharmacometric model (**Chapter 5**).

1.1.2. Overview of the introduction

The introduction is divided into four sections:

1. **Section 1.2** Pharmacometrics (a brief overview of models, types of models, and model-building approaches),
2. **Section 1.3** Modelling drug concentrations and responses,
3. **Section 1.4** Modelling physiological systems, drug concentrations, effects, and responses, and
4. **Section 1.5** Warfarin and anticoagulant response.

1.2. Pharmacometrics

The term *pharmacometrics* was first coined by Benet and Rowland, the editors of the Journal of Pharmacokinetics and Biopharmaceutics in 1982 [32]. The field of pharmacometrics has enjoyed rapid advances in the past 20 years. This is attributable to successful application of pharmacometrics to various stages of the drug development process, from drug discovery (e.g. identification of drug target) through preclinical development (e.g. dose selection for first-in-human clinical trial) to clinical development (e.g. establishment of drug safety profile) to regulatory approval (e.g. labelling requirements) and post-marketing studies and optimisation (e.g. dose optimisation for special populations).

In clinical practice, pharmacometric analysis provides a useful means for *dose individualisation* by partitioning and quantification of (predictable or unpredictable) variability in dose-concentration-response relationships between and within patients. Understanding the variability between patients and its effect on dose requirements is useful to rationalise dosing decisions and to tailor the dosing regimen (dose, dosing frequency, and dosing time of a drug) to suit the needs of a specific patient. Indeed, this forms the basis of dose individualisations in clinical practice for drugs that exhibit a narrow therapeutic window and large between-subject variability in dose-concentration-response relationships. In this setting, patient covariates (e.g. renal function) and / or response measures (i.e. markers of effect of a drug) that are predictive of future responses to drug are typically used for dose individualisations. This allows the patient to derive the most benefit from medicines use while minimising the risk of adverse drug effects to the patient.

Models are an integral part of pharmacometric analysis. In the following sections, different types of pharmacometric models and model-building approaches are outlined.

1.2.1. Models

A model is a construct that represents a simplified version of the reality. For instance, a globe is a model of the earth. A globe is a miniature non-working version of the earth. Typically, it contains details such as geographic coordinate systems (longitude and latitude) and representations of land masses and water bodies, boundaries of countries, topographies, *et cetera*. An example in the context of pharmacometrics is a compartmental PK model. The compartmental structure of these models provide a framework to describe key PK processes: absorption, distribution to tissues, metabolism, and elimination of drugs. The compartments do not necessarily relate to a true physiological space but represent a simplified and abstract version of a (complex) physiological system that provides an adequate description of the observed time course of drug concentrations. A detailed description of compartmental PK model is provided in **Section 1.3.1.1**.

Pharmacometric analyses are underpinned by mathematical models to describe the relationship between input variables (e.g. drug doses) and output variables (e.g. drug concentrations and system responses). The general form of a mathematical model is given as follows:

$$\boldsymbol{y} = \boldsymbol{f}(\boldsymbol{\theta}, \boldsymbol{X}) + \boldsymbol{\varepsilon}$$

Equation 1.1 *General form of a mathematical model.*

Here, the input variables $\boldsymbol{X}(n \times p)$ are related to the output variables $\boldsymbol{y}(n \times 1)$ by a mathematical function, $\boldsymbol{f}(n \times 1)$, which contains a set of unknown constants termed *parameters*, $\boldsymbol{\theta}(p \times 1)$, and residual unexplained error that is given as $\boldsymbol{\varepsilon}(n \times 1)$. Note that in this thesis, matrices are capitalised and both matrices and vectors are written in bold font.

Besides characterising a given input-output relationship, a mathematical model can be applied to learn about the underlying system, to generate and test hypotheses, to answer what-if questions, and to make predictions about future

instances involving the system (e.g. future patients). Practical applications dictate that models must be simple enough for practical use while capturing important aspects of the relationships of interest to the level of detail that is sufficient for the intended purpose. Models are therefore not meant to reflect all of reality – a point well made by George Box, who is considered one of the great statistical minds of the 20th century, in his widely quoted remark that [33]:

"*Essentially, all models are wrong, but some are useful*".
George E. P. Box (statistician, 1918-2013)

1.2.2. Empirical versus mechanistic models

A simplistic view of pharmacometric models is that they are either developed based on data (*empirical* models) or mechanisms (*mechanistic* models). It is important to note a continuum of possibilities between fully-empirical and mechanistic models and that it is vital to consider the intended use of the model when choosing between model types during the model development process.

The development of an empirical model is driven by data and the principle of parsimony. An empirical model is (in theory) the simplest model that provides an adequate description of the data at hand. Note here that the mechanisms, be it the pharmacology or the biology, from which the data arose are not necessarily accounted for and as such empirical models typically have poor predictive performance when extrapolating to new conditions [34]. Prominent examples of empirical model are models that are based on parsimonious use of polynomials or exponentials. The E_{max} model (**Section 1.3.1.2**), which is ubiquitous in pharmacology research, is also arguably empirical if it is applied to data out of the receptor binding context. A simple clinical example of an empirical model is shown in **Equation 1.2** where INR is modelled as an empirical function of factors II, VII, X, protein C, and the prothrombin fragment (F1+2) [35]. In this example, the model provides an adequate fit to the INR data. However, the linear nature

of the model and the inclusion of protein C are unlikely to be consistent with known physiology of blood coagulation underpinning the INR test.

$$INR = \theta_1 \cdot II + \theta_2 \cdot VII + \theta_3 \cdot X + \theta_4 \cdot PC + \theta_5 \cdot (F1 + 2)$$

Equation 1.2 *An empirical model for the INR [35].*

Semi-empirical models are derived by incorporating components of essential prior information regarding the underpinning pharmacology and biology to the model [36, 37]. Typical examples of semi-empirical models are compartmental PK models (see **Section 1.3.1.1**), which are developed to characterise the time course data of drug concentrations by considering the different PK processes (absorption, distribution, metabolism and elimination of drugs) but do not necessarily delve into specifics of the physiological mechanisms involved. Semi-mechanistic models, on the other hand, contain greater level of mechanistic detail and address missing knowledge of the system by heuristic imputation of empirical functions. For the purpose of this thesis, empirical, semi-empirical, and semi-mechanistic models are collectively referred to as *top-down models*. A detailed description and examples of top-down models is provided in **Section 1.3**.

At the other end of the spectrum, mechanistic models are developed fully based on mechanisms and generally only utilise data for model calibration and validation. In contrast to top-down models, mechanistic models are not necessarily bound by the principle of parsimony and are therefore generally more complex with respect to model structure and the number of parameters. Looking beyond the model complexity, mechanistic models contain valuable systems information, allow for extrapolation and prediction of future data, and are inherently useful to improve our understanding of complex physiological systems considering that hypotheses can be generated and tested within the simulation framework to explore what-if scenarios. Prominent examples of mechanistic model are those under the banner of quantitative systems pharmacology (QSP) models (see **Section 1.4.1**). In this thesis, mechanistic

models are referred to as *bottom-up models*. Details and examples of bottom-up models are available in **Section 1.4**.

In this thesis, both top-down and bottom-up models are utilised to understand the coagulation kinetics underpinning the warfarin dose response. **Chapter 2** outlines the development of a top-down, compartmental model to quantify the observed time course of warfarin dose and effect on vitamin K-dependent coagulation proteins. **Chapter 3** describes the use of a bottom-up QSP model of the coagulation network [31, 38], which includes mechanistic components of *in vivo* coagulation and *in vitro* blood coagulation tests, to explore coagulation proteins as drivers of the INR. This is followed by **Chapter 4**, which details the development of a coagulation protein-based method for the prediction of anticoagulant response to warfarin. Here, a heuristic model-order reduction technique in which an empirical approximation to the QSP was developed. Finally, in **Chapter 5**, a framework for evaluating assumptions intrinsic to a top-down or bottom-up pharmacometric model is proposed.

1.3. Modelling drug concentrations and responses

Understanding, quantifying, and predicting drug concentrations and effects is of pivotal importance to both drug development and dose individualisation in clinical practice. Here, the expected drug concentrations and responses for a given dose, the time course of desired and adverse effects, and the associated variability between and within patients relate to the PK and PD properties of the drug [39]. In this thesis, a drug effect is distinguished from a system response. A drug effect relates to primary drug action or the influence of the drug on some components of the system, for instance, enzyme inhibition or target inactivation, whereas a response is mediated by the system and could include a measurable marker of a drug effect. Then, warfarin's inhibitory action on vitamin K epoxide reductase (VKOR) and the influence on coagulation protein concentrations are examples of drug effect. On the other hand, INR represents a response from the coagulation network where various zymogens, activating enzymes, and cofactors work in concert that culminates in a stable clot formation. In this section, basic principles of PK and PD as well as common top-down models employed to characterise drug concentrations and responses are introduced. This is followed by a description of the statistical methods used for the development of these top-down models.

1.3.1. Models for drug concentrations and responses

1.3.1.1. PK models

PK is a discipline within pharmacology that relates the given dose(s) of a drug to the time course of drug concentrations in the body. The PK properties of a drug is governed by absorption, distribution, metabolism, and excretion of the drug. These four processes are abbreviated to ADME.

The goal of a PK model is to describe and predict the time course of drug concentrations in a physiological matrix, most often, the plasma drug concentrations. The plasma drug concentrations (C) at a given time after dose (t) can be modelled as a function of the administered dose (D) and t via a vector of

parameters, $\boldsymbol{\theta_{PK}}(p_{PK} \times 1)$. The error in the prediction of C is denoted as ε_{PK}. The general mathematical form of a PK model is given in **Equation 1.3**.

$$C = f_{PK}(D, t, \boldsymbol{\theta_{PK}}) + \varepsilon_{PK}(t)$$

Equation 1.3 *General mathematical form of a PK model.*

Common PK parameters of interest include clearance (CL), volume of distribution (V), and derived parameters such as the first-order elimination rate constant ($k = \frac{CL}{V}$). CL is a proportionality constant that relates the rate of elimination to the drug concentration. It represents a measure of the functional capacity of the physiological system for drug elimination. V, on the other hand, relates to the extent of drug distribution and is influenced by body structure and composition. For drugs administered extravascularly, the bioavailability (F) and the first-order absorption rate constant (k_a), or similar rate parameter, are also of interest.

PK models are typically constructed using compartments. In compartmental modelling, the complex physiological system is reduced to a finite number of compartments to characterise drug disposition (distribution and elimination). A compartment represents a hypothetical space that consists of a group of tissues that display similar kinetic profiles. It is important to note that a compartment does not necessarily represent a true physiological space and specific tissues that make up a compartment are unknown.

The number of compartments for a PK model of a drug relates to the disposition kinetics of the drug (*not* input process) and is typically guided by the observed time course of drug concentrations. One of the simplest and most commonly applied PK models is the *one-compartment model* with first-order absorption and elimination (see *panel a*, **Figure 1.1**). Here, the drug distribution occurs so rapidly that it appears as if it is an instantaneous process. Then, when absorption and distribution are completed, the plasma drug concentrations will

exhibit a mono-exponential decline and will appear linear on the logarithmic scale (see *panel b*, **Figure 1.1**).

For this model, the rate of change of the amount of drug in the depot (A_1) and in the central compartment (A_2) after administration of a defined dose (D) can be described by the following ordinary differential equations (ODEs):

$$\frac{dA_1}{dt} = -k_a \cdot A_1; \quad A_{1_{t=0}} = F \cdot D$$

$$\frac{dA_2}{dt} = k_a \cdot A_1 - k \cdot A_2; \quad A_{2_{t=0}} = 0, k = \frac{CL}{V}, C = \frac{A_2}{V}.$$

Equation 1.4 *ODEs for a one-compartment PK model with first-order absorption and elimination. Here C represents the concentration in the central compartment.*

Solving the above-mentioned ODEs for the central compartment gives the corresponding closed-form, algebraic solution:

$$C = \frac{F \cdot D \cdot k_a}{V \cdot (k_a - \frac{CL}{V})} \cdot (e^{-\frac{CL}{V}t} - e^{-k_a t})$$

Equation 1.5 *Closed-form solution for a one-compartment PK model with first-order absorption and elimination.*

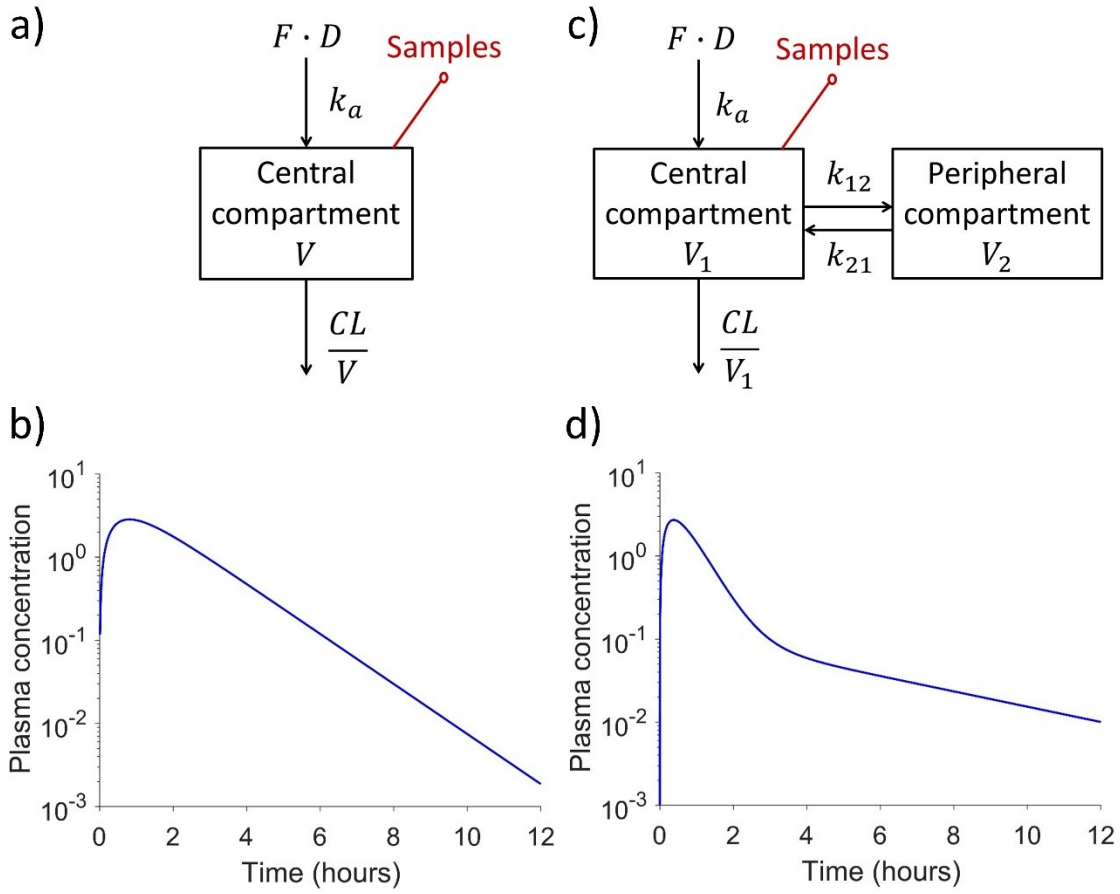

Figure 1.1 *Compartmental models. Panel a shows the schematic of a one-compartment PK model with first-order absorption and elimination. Panel b shows the corresponding time course of plasma drug concentrations (D = 10 units, F = 1, k_a = 2 h^{-1}, CL = ln 2 L/h, V = 1 L). Panel c shows the schematic of a two-compartment PK model with first-order absorption and elimination. Panel d shows the corresponding time course of plasma drug concentrations (D = 10 units, F = 1, k_a = 2 h^{-1}, CL = 3 L/h, V_1 = 1 L, k_{12} = 0.5 h^{-1}, k_{21} = 0.25 h^{-1}).*

In a *two-compartment model*, an additional compartment is included to account for the relatively slow drug distribution into some tissues which is usually termed the *peripheral compartment* (see *panel c*, **Figure 1.1**). The resulting time course of plasma drug concentrations will show a biphasic decline on the semi-logarithmic scale where a distinct phase driven predominantly by the distribution process is visually apparent (see *panel d*, **Figure 1.1**). In practice, it is rare for more than three compartments to be needed to empirically characterise the plasma PK profile for a drug.

Finally, the mathematical functions and structure of the compartmental models may be modified to account for different modes of drug administration or more complex ADME processes, for instance, absorption lag, target-mediated drug disposition, drug interactions, autoinduction and autoinhibition.

1.3.1.2. PD models

PD is a discipline within pharmacology that relates the drug concentrations to the observed pharmacological effects. The goal of a PD model is to describe and predict the drug effects (E) based on given concentrations of a drug (C) via a vector of parameters, $\boldsymbol{\theta_{PD}}$ ($p_{PD} \times 1$). The error in the prediction of E is denoted as ε_{PD}. The general mathematical form of a PD model is given in **Equation 1.6**.

$$E = f_{PD}(C, \boldsymbol{\theta_{PD}}) + \varepsilon_{PD}(C)$$

Equation 1.6 *General mathematical form of a PD model.*

Drug effects are underpinned by *classical receptor theory* [40-42]. In this thesis, receptor ligands will be discussed in the context of drugs. These terms will therefore be used interchangeably. Reversible binding of the drug to a receptor is governed by the law of mass action [41]. At equilibrium, the concentration of drug-receptor complex (CR) depends on drug concentration (C) and the equilibrium dissociation constant of the drug for the receptor (K_A), which is a reciprocal measure of affinity. Because the system has a finite number of receptors, receptor binding is limited by the total concentration (or capacity) of available receptors in a system (R_0). Receptor binding can be suitably described by using a hyperbolic function, which is typically used to characterise capacity-limited processes:

$$CR = R_0 \cdot \frac{C}{K_A + C}.$$

Equation 1.7 *Receptor binding model.*

The relationship between receptor occupancy (i.e. CR from **Equation 1.7**) and drug effect (E) can be described by using a proportionality constant known as *intrinsic activity* (α) [40]:

$$\frac{E}{E_m} = \alpha \cdot \frac{CR}{R_0}.$$

Equation 1.8 *Intrinsic activity model.*

Here, E_m represents the maximum effect in a system. Substitution of the expression for CR from **Equation 1.8** into **Equation 1.7** and upon further simplification, gives the standard hyperbolic function, the E_{max} *model*, which is one of the most frequently used PD models in pharmacology research:

$$E = E_{max} \cdot \frac{C}{C_{50} + C}.$$

Equation 1.9 *The E_{max} model.*

Here, C_{50} is the drug concentration that elicits half-maximal effect and is equal to K_A (for the case where the effect is directly linked to receptor binding). E_{max} is the maximum effect of the drug and is given by $E_{max} = \alpha \cdot E_m$. Drugs with $\alpha = 1$ and $\alpha = 0.4$ are therefore capable of eliciting 100% and 40% of system's maximum effect, respectively. In the E_{max} model, the magnitude of the drug effect depends positively on the drug concentration. However, the relationship between drug concentration and effect is nonlinear (see **Figure 1.2**) and as such doubling the concentration will not result in doubling of drug effect. The drug effects will eventually asymptote to a maximum effect (E_{max}) despite increasing concentrations.

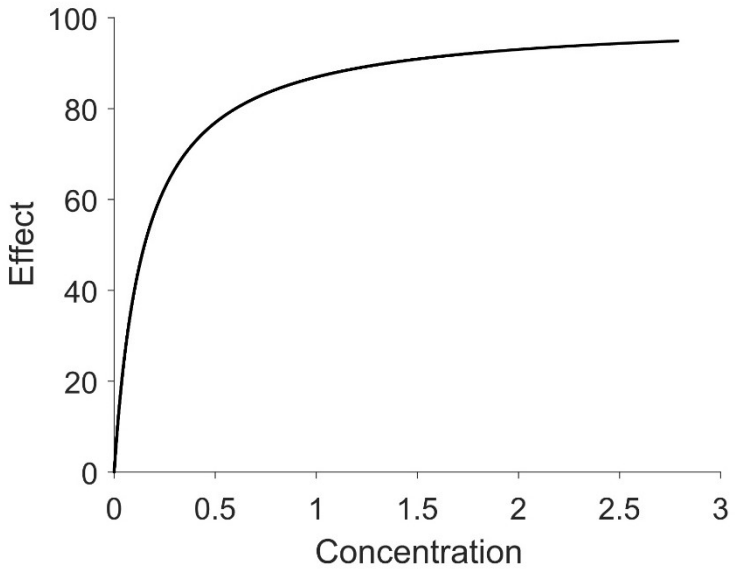

Figure 1.2 *The concentration-effect relationship for an E_{max} model. In this model, E_{max} = 100 and C_{50} = 0.15 units/L.*

One of the major drawbacks of the E_{max} model, which assumes that the drug effect is directly proportional to receptor occupancy [40], is that it does not consider the chain of events between receptor binding and emergence of drug effect (see **Figure 1.3**). Importantly, the intrinsic activity model is not generalisable to all settings, for instance, it does not explain the *receptor reserve* phenomenon where stimulation of only a fraction of the whole receptor population evokes an apparent maximal effect [43].

It was proposed that, in general, two sequential steps, receptor binding followed by signal transduction, are required for a drug to elicit an effect (see **Figure 1.3**) [42, 43]. However, the signal transduction process is typically not experimentally accessible and as such the exact functional form of the signal transduction model that relates receptor occupancy to drug effect cannot be determined based on bioassay data of the effects of the drug.

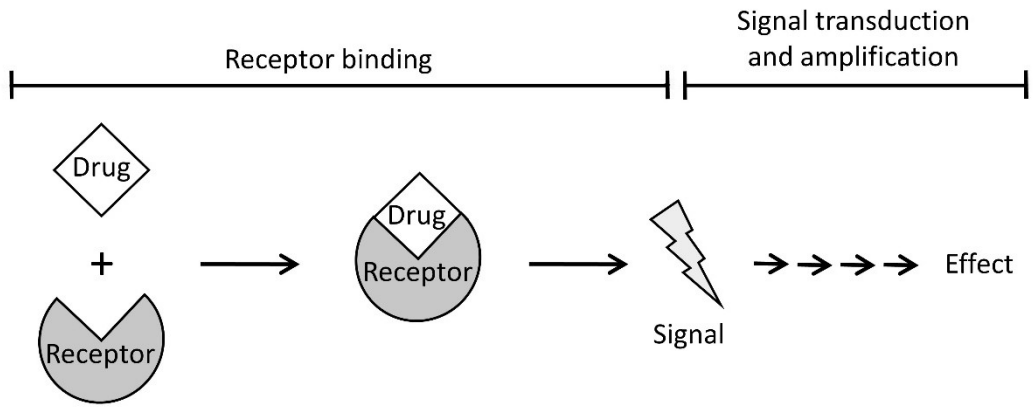

Figure 1.3 *Schematic of drug effect. The drug binds to the receptor to induce a conformational change in the receptor. A signal or stimulus is generated. The signal provokes a series of biochemical reactions that results in the observed drug effect.*

It has been shown mathematically that the function resulting from two (or more) hyperbolic functions in sequence is also a hyperbolic function [43, 44]. Then, given that the drug-receptor binding is hyperbolic (**Equation 1.7**) and that the final concentration-effect relationship observed is commonly hyperbolic, it can be deduced that the black box function for signal transduction is *necessarily* hyperbolic. For brevity, the signal transduction model and details of its derivation are not shown. A comprehensive description can be found in the landmark paper published by Black and Leff [43]. Substitution of the derived (empirical) signal transduction model in the receptor binding model (**Equation 1.7**) gives the *operational model* [43]:

$$E = \left(\frac{E_m \cdot \tau}{\tau + 1}\right) \cdot \frac{C}{\left(\frac{K_A}{\tau + 1}\right) + C}.$$

Equation 1.10 *Operational model.*

Here, τ is a measure of transduction efficiency of CR. The operational model can be simplified into an (empirical) E_{max} model (**Equation 1.9**) by assuming that $E_{max} = \frac{E_m \cdot \tau}{\tau+1}$ and $C_{50} = \frac{K_A}{\tau+1}$. It is evident that E_{max} and C_{50} are inherently correlated via parameter τ and that C_{50} is mathematically bounded to be less

than or equal to K_A assuming no change in receptor sensitivity (e.g. due to tolerance) over the course of the experiment.

An extension to the basic E_{max} model is the *sigmoidal E_{max} model* (**Equation 1.11**), which includes the estimation of an empirical exponent (γ) to modify the slope of the concentration-effect curve at half-maximal effect (see **Figure 1.4**).

$$E = E_{max} \cdot \frac{C^{\gamma}}{C_{50}^{\gamma} + C^{\gamma}}$$

Equation 1.11 *The sigmoidal E_{max} model.*

Note here that the standard E_{max} model is a special case of the sigmoidal E_{max} model when $\gamma = 1$. In theory, γ has its basis in cooperativity of ligand binding to allosteric sites of the same receptor and it itself represents the number of drug molecules binding per receptor (hence supposedly an integer) [45]. However, in modelling practice, γ is often found to achieve non-integer values and its inclusion is typically driven by data. In this case, γ is an empirical shape parameter and theoretical interpretation of γ is generally not possible.

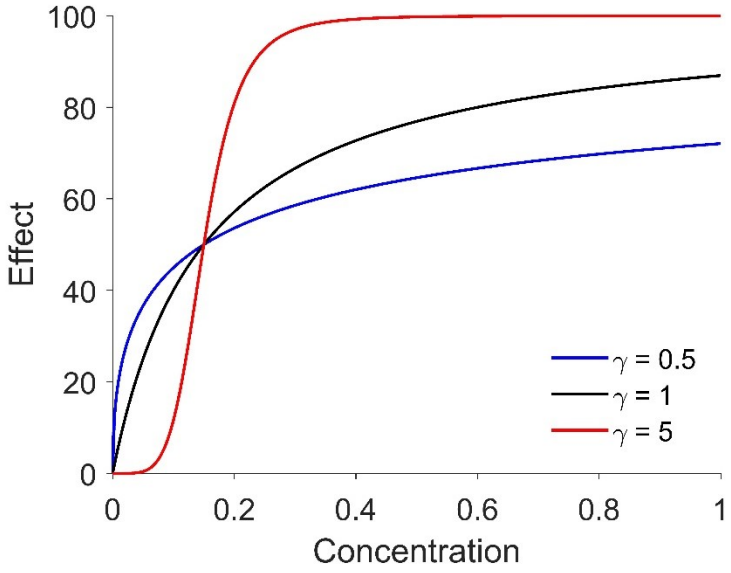

Figure 1.4 *The concentration-effect relationship for a sigmoidal E_{max} model. γ refers to the shape parameter. In this model, E_{max} = 100 and C_{50} = 0.15 units/L.*

1.3.1.3. PKPD models

The PK model that describes the time course of drug concentrations (*concentration versus time*) can be substituted into a PD model that predicts the concentration-effect relationship (*effect versus concentration*) to give the time course of drug effects (*effect versus time*). The general mathematical form of a pharmacokinetic-pharmacodynamic (PKPD) model is given in **Equation 1.12**.

$$E = f_{PD}(f_{PK}(D, t, \boldsymbol{\theta_{PK}}), \boldsymbol{\theta_{PD}}) + \varepsilon_{PKPD}(t)$$

Equation 1.12 *General mathematical form of a PKPD model.*

Here, the drug effect (E) is a function of time (t) and is dependent on the dose (D), vector of PK parameters $\boldsymbol{\theta_{PK}}(p_{PK} \times 1)$, and PD parameters $\boldsymbol{\theta_{PD}}(p_{PD} \times 1)$. The error in the prediction of $E(t)$ is denoted as ε_{PKPD}.

PKPD models can be broadly divided into two types according to the temporal differences between drug concentrations and effects: (1) *immediate effects models* and (2) *delayed effects models*.

1.3.1.3.1. Immediate effects models

When using an immediate effects PKPD model, it is assumed that the drug effect is directly linked to the drug concentration and as such there is no time lag between PK and PD. As a result, the PD profile reflects the shape of the PK profile and at each time point, the magnitude of drug effect relates positively with the drug concentration, for instance, the maximum effect is achieved at the time when the drug concentration is at its maximum (*panel a*, **Figure 1.5**). Here, since PK is linked directly to PD, drug concentration alone is sufficient to describe PD. It follows that the PD models presented in **Section 1.3.1.2** (e.g. the E_{max} model) can be used to characterise the immediate effects of a drug and that no further modification to the model structure is required. However, with few exceptions (e.g. binding of unfractionated heparins to thrombin), drug effects are delayed in relation to the plasma drug concentrations in reality.

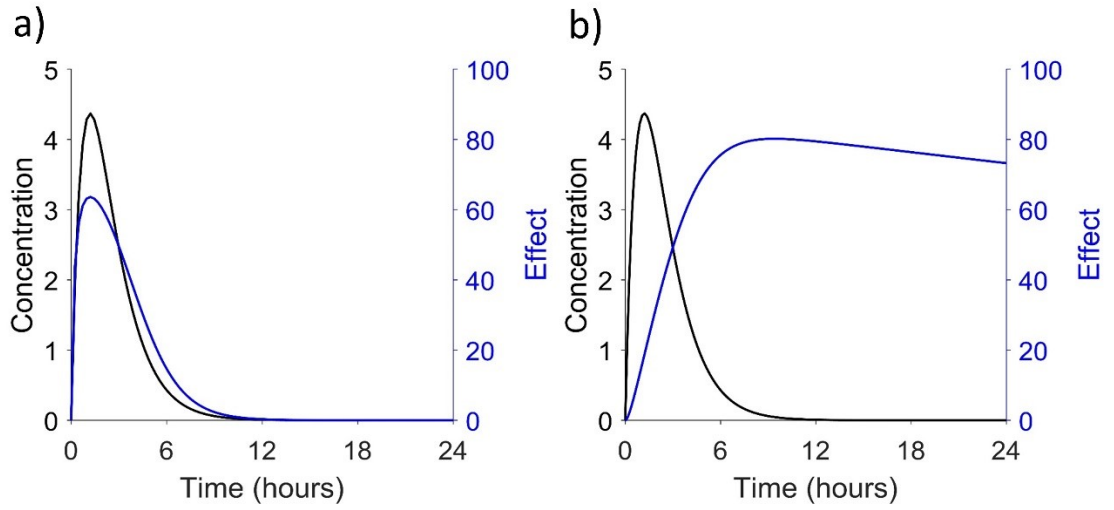

Figure 1.5 *The time course of drug concentrations and effects. Panel a shows immediate effects. Panel b displays delayed effects relative to drug concentrations (e.g. maximal drug effect occurs after the peak plasma concentration). The drug concentrations were generated using a one-compartment model with first-order input and output. The drug stimulates the production of a physiological intermediate and the delay is attributable to the turnover of the intermediates. Both models were generated using D = 10 units, F = 1,* k_a *= 1* h^{-1}*, CL = ln 2 L/h, V = 1 L,* E_{max} *= 100, and* C_{50} *= 2.5 units/L. The delayed effects model has two additional parameters:* R_{in} *= 1 unit/h and* k_{out} *= 0.003* h^{-1}*.*

1.3.1.3.2. Delayed effects models

In this setting, drug effects appear delayed in relation to the drug concentrations (*panel b*, **Figure 1.5**). There are various mechanisms for delayed effects including distributional delay to the site of drug action, slow dissociation of the drug from the receptor, and mediation of pharmacological responses by a physiological intermediate. Integration of the delay mechanism into the PKPD model is important for accurate characterisation, prediction, and extrapolation of the time course of drug effects (e.g. the onset, intensity, and duration). Distributional delay is usually accounted for using an *effect compartment model* and the delay caused by slow dissociation of the drug from the receptor is considered by the inclusion of a non-equilibrium *receptor binding model*. Neither the effect compartment model nor the non-equilibrium receptor binding model were used in the work presented in this thesis. For a description of these models refer to Gabrielsson 2012 [46], Rosenbaum 2016 [47], and Al-Sallami 2009 [39].

The mechanism of action for many drugs involves either stimulation or inhibition of the production or degradation of a physiological intermediate. Often, the turnover of these physiological intermediates is the rate-limiting step for the drug effects to be observable. For instance, warfarin inhibits the production of vitamin K-dependent coagulation proteins but its effect on the coagulation proteins is not immediately evident until existing coagulation proteins were degraded. The time course of observed response is then dependent on the degradation half-life of the coagulation protein. Delay due to the turnover of a physiological intermediate can be accommodated by the inclusion of a *turnover model* [48, 49]. There are two components to a turnover model: (1) synthesis of the physiological intermediate and (2) degradation of the intermediate. It is usually assumed in a turnover model that: (1) the precursor pool for the physiological intermediate is abundant and hence, the synthesis of the intermediate is independent of the precursor concentration i.e. a zero-order input process; and (2) the degradation of the physiological intermediate is a first-order process. Taken together, the rate of change of a physiological intermediate of interest (I) is given by the following equation:

$$\frac{dI}{dt} = R_{in} - k_{out} \cdot I; \quad I_{t=0} = \frac{R_{in}}{k_{out}}$$

Equation 1.13 *The turnover model.*

Here, R_{in} is the zero-order rate of synthesis, k_{out} is the first-order degradation rate constant, and $I_{t=0}$ is value of the physiological intermediate at equilibrium when the rate of synthesis equals to that of degradation.

A drug can either inhibit or stimulate the synthesis or the degradation of a physiological intermediate which provides the four model constructs used to describe these mechanisms (see **Table 1.1**) [48, 49]. The choice of either Model I, II, III, or IV should align with the mechanism of drug action. For instance, in **Chapter 2**, Model II (inhibition of synthesis) was deemed appropriate to describe warfarin's inhibitory action on the production of functional vitamin K-

dependent coagulation proteins. Another example is the use of Model IV (inhibition of degradation) to characterise physostigmine's inhibitory action on the degradation of acetylcholine.

At a single dose level, the time course of drug effects of Models I, II, III, and IV may be indistinguishable from that of an effect compartment model and therefore data in isolation of mechanistic insight should not be used to define the PKPD link. However, the time to maximum drug effect ($t_{E,max}$) of these models appear to increase with dose (**Figure 1.6**). On the contrary, in the effect compartment model, the $t_{E,max}$ remains constant with dose (not shown). The difference in dose-$t_{E,max}$ relationship is an important characteristic that is useful for distinguishing delayed effects that arise from distributional delay or from drug action on the turnover of a physiological intermediate.

Table 1.1 *Four basic models to represent drug action on the turnover of a physiological intermediate of interest. EC_{50} is the drug concentration that elicits half-maximal stimulatory effect. E_{max} is the maximum stimulatory effect of the drug. IC_{50} and I_{max} are the inhibitory counterparts of EC_{50} and E_{max}.*

Model ID	Mechanism	Model
I	Stimulation of synthesis	$\frac{dI}{dt} = R_{in}\left(1 + \frac{E_{max} \cdot C}{EC_{50} + C}\right) - k_{out} \cdot I; \quad I_{t=0} = \frac{R_{in}}{k_{out}}$
II	Inhibition of synthesis	$\frac{dI}{dt} = R_{in}\left(1 - \frac{I_{max} \cdot C}{IC_{50} + C}\right) - k_{out} \cdot I; \quad I_{t=0} = \frac{R_{in}}{k_{out}}$
III	Stimulation of degradation	$\frac{dI}{dt} = R_{in} - k_{out}\left(1 + \frac{E_{max} \cdot C}{EC_{50} + C}\right) \cdot I; \quad I_{t=0} = \frac{R_{in}}{k_{out}}$
IV	Inhibition of degradation	$\frac{dI}{dt} = R_{in} - k_{out}\left(1 - \frac{I_{max} \cdot C}{IC_{50} + C}\right) \cdot I; \quad I_{t=0} = \frac{R_{in}}{k_{out}}$

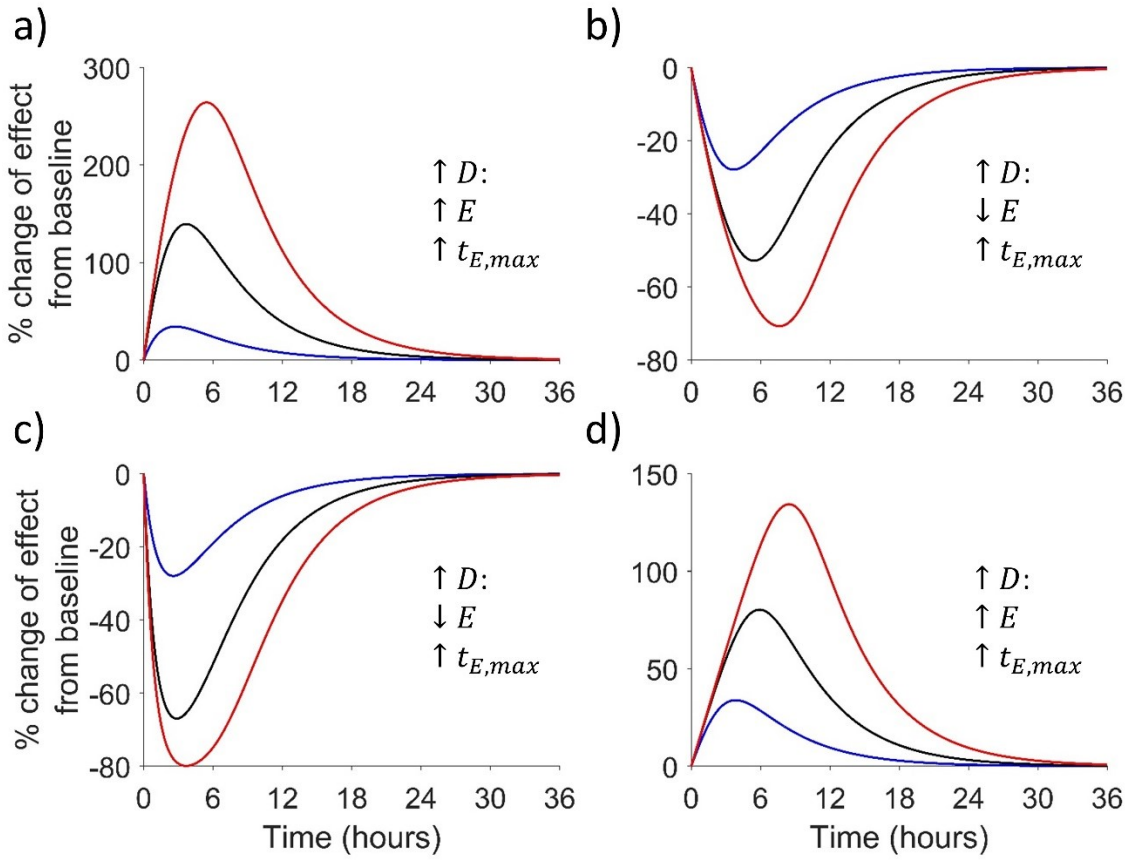

Figure 1.6 *The time course of drug effects for the four basic models used to represent drug action on the turnover of a physiological intermediate of interest. The drug effects were simulated from a one-compartment model (with first-order input and output) that is linked to a turnover model via one of the four models described in Table 1.1. Panels a, b, c, and d relate to Model I (stimulation of synthesis), II (inhibition of synthesis), III (stimulation of degradation), and IV (inhibition of degradation), respectively. Three different dose levels were simulated: D = 10 mg (blue line), D = 100 mg (black line), and D = 1000 mg (red line). In these models, F = 1, k_a = 100 h^{-1}, CL = 14 L/h, V = 20 L, R_{in} = 10 units/h, k_{out} = 0.2 h^{-1}, E_{max} = 5, EC_{50} = 1 mg/L, I_{max} = 1, and IC_{50} = 0.1 mg/L. E represents drug effect and $t_{E,max}$ is the time to maximum drug effect.*

1.3.1.4. KPD models

Both PK and PD data are required for the development of a PKPD model. For practical reasons or by means of study design, there may be few or no drug concentration data available for analysis, for instance, in phase III clinical trials and in routine clinical practice. Hence, a class of general models, the *kinetic-pharmacodynamic (KPD) model*, that is built solely on dose-effect-time data was introduced [50-53]. A schematic of a typical KPD model is shown (*panel b*, **Figure 1.7**) and is compared and contrasted to a PKPD model (*panel a*, **Figure 1.7**).

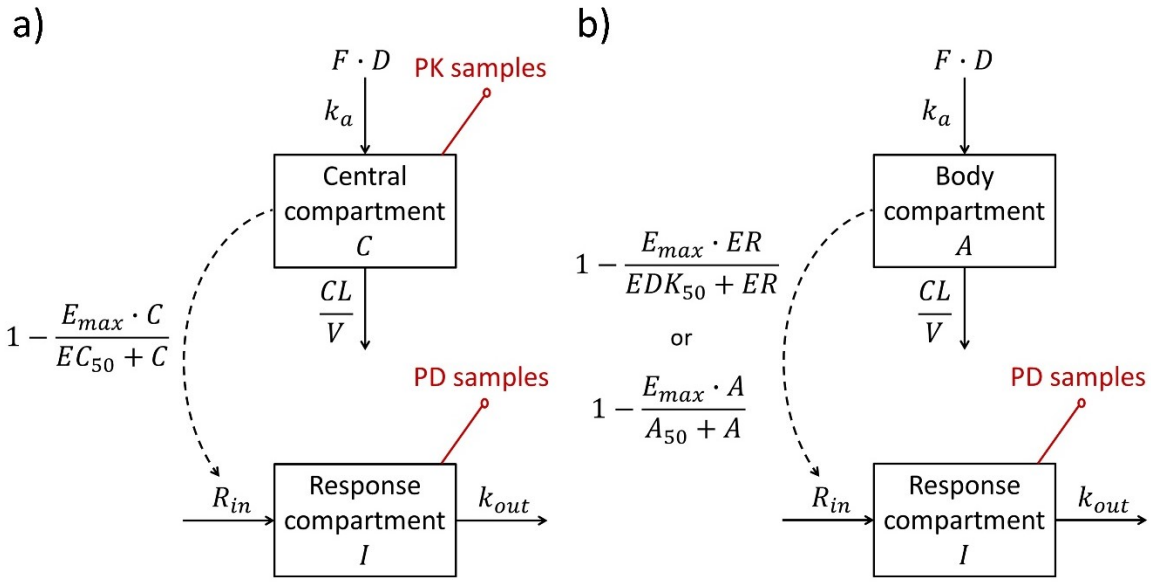

Figure 1.7 *Schematic of the structure of a PKPD model example (panel a) and a KPD model example (panel b). Note the absence of PK samples necessitates the assumption of a PK model structure for KPD modelling.*

In contrast to a PKPD model, where the drug concentrations (C) are used as driver of PD effects (**Equation 1.9**), standard KPD model uses the elimination rate of the drug (ER) to drive the PD dynamics (**Equation 1.14**) [50].

$$E = E_{max} \cdot \frac{ER}{EDK_{50} + ER}$$

Equation 1.14 *The drug effect driven by the elimination rate of the drug.*

$$EDK_{50} = CL \cdot C_{50} = \frac{CL}{V} \cdot A_{50}$$

$$A_{50} = V \cdot C_{50}$$

Equation 1.15 *Relationships between C_{50}, EDK_{50}, and A_{50}.*

Here, EDK_{50} is a conglomerate solution of C_{50} and CL (**Equation 1.15**) and it represents the drug elimination rate that gives half-maximal effect.

Alternate parameterisation of a KPD model, where the PD effect is driven by the amount of drug in the body (A), had been proposed. Essentially, this parameterisation can be thought of as a simplification of the EDK_{50} parameterisation by factoring out the influence of $\frac{CL}{V}$ (**Equation 1.15**) to give:

$$E = E_{max} \cdot \frac{A}{A_{50} + A}.$$

Equation 1.16 *The drug effect driven by the drug amount in the body.*

Here, A_{50} is a composite of C_{50} and V (**Equation 1.15**) and it represents the amount of drug in the body that gives half-maximal effect.

KPD analysis has been successfully applied to modelling a wide range of therapeutics [54-58]. In particular, the EDK_{50} parameterisation is widely applied [54, 59, 60] but from a theoretical viewpoint, how the elimination rate could drive PD is not pharmacologically intuitive and likely to be inconsistent with classical receptor theory underpinning drug effects. Furthermore, in EDK_{50} parameterisation where $ER = \frac{CL}{V} \cdot A$, a correlation between EDK_{50} and $\frac{CL}{V}$ is introduced and enforced mathematically, which means that estimation of EDK_{50} will always be dependent on $\frac{CL}{V}$ and may therefore lead to potential numerical instability during the estimation process. In this thesis, a KPD model was used to characterise the observed time course of warfarin dose and anticoagulant response. See **Chapter 2** for a detailed description.

PK and PD data provide considerable insight into both the PK and PD aspects of a drug. However, in the absence of PK data, an imputation of the PK model structure is required. In the case of a misspecification in the PK model structure, parameter estimates (e.g. A_{50}, k_{out}) may be biased and random-effects parameters (e.g. variance of between-subject variability [ω^2 in NONMEM® parlance]) may be inflated although it is possible for the goodness-of-fit of the KPD model to appear robust to the misspecification [58, 61].

Due to the absence of PK data, parameter estimation for KPD models requires special consideration. Some KPD model parameters may not be *structurally identifiable* i.e. an infinite set of parameter values results in the same output (PD predictions) even given perfect input-output conditions (dose-effect-time data) [62-65]. This was explored and reported in **Chapter 2**. In addition, in the setting of imperfect input-output data, some KPD model parameters may not be able to be estimated with reasonable precision i.e. not *deterministically identifiable* [66, 67]. Here, the use of a wider dose range, different route of administrations, and more intensive PD sampling may alleviate some of the deterministic identifiability issues.

1.3.2. Statistical methods

In pharmacometrics, top-down models are usually developed using the *nonlinear mixed-effects approach* in order to characterise the observed concentration and / or response data for a set of individuals. This approach is based on a hierarchical structure where typically, two levels of hierarchy are considered; (1) at the level of the within-subject effects (i.e. a model for the data) and (2) at the level of the between-subject effects (a model for the individuals). More levels of hierarchy may be specified as required. The nonlinear mixed-effects approach to model development will be introduced followed by a description of the estimation methods commonly used. A more detailed and technical description of nonlinear mixed-effects modelling and estimation methods is provided by Davidian and Giltinan 1995 [20], Lavielle 2014 [21], and Bonate 2011 [19].

1.3.2.1. Models for the data

The first level in the model hierarchy describes the structural model that is used for all individuals, where each individual is allowed to have different parameter values, and also includes a statistical model for residual errors i.e. the *residual unexplained variability* (RUV). Assuming additive error, observations of the ith individual, $\boldsymbol{y_i}$, can be described by the general function:

$$\boldsymbol{y_i} = \boldsymbol{f}(\boldsymbol{t_i}, \boldsymbol{\beta_i}) + \boldsymbol{\varepsilon_i}$$
$$\boldsymbol{\varepsilon} \sim iid\ N(0, \sigma^2).$$

Equation 1.17 *Model for the observations of the i[th] individual.*

Here, the model describes the systematic and random variation associated with observations of individuals. Systematic variation is characterised through the mathematical function $\boldsymbol{f}(n_i \times 1)$ that is dependent on time, $\boldsymbol{t_i}(n_i \times 1)$, and a vector of parameters, $\boldsymbol{\beta_i}$ $(p \times 1)$. Random variation, on the other hand, is represented by an assumption on the RUV, $\boldsymbol{\varepsilon}$ (i.e. $\boldsymbol{\varepsilon_i}$ for *all* individuals). It describes how observations are distributed around the values predicted by the model. RUV may arise due to various factors including process noise (e.g. error in recorded sampling time or dose), measurement noise (e.g. assay error), moment-to-moment variability, and model misspecification (e.g. "All models are wrong"). Most often, it is assumed that: (1) $\boldsymbol{\varepsilon}$ have a mean of zero, (2) $\boldsymbol{\varepsilon}$ are uncorrelated, (3) $\boldsymbol{\varepsilon}$ have common variance σ^2 and are identically distributed for all time points and covariates, and (4) $\boldsymbol{\varepsilon}$ are normally distributed. Taken together, elements of $\boldsymbol{\varepsilon}$ are independent and identically distributed (iid) from a normal distribution with a mean of zero and a variance of σ^2. If these assumptions appear to be violated (e.g. non-normality), a transformation of the $\boldsymbol{\varepsilon}$ space (via transformation of $\boldsymbol{y}$ [i.e. $\boldsymbol{y_i}$ for *all* individuals] or $\boldsymbol{\varepsilon}$ itself) can be considered to avoid assumption violation and to provide an apparent distribution that is useful for modelling the available data. An example is the Box-Cox transformation function ($\boldsymbol{\zeta}$) that transforms $\boldsymbol{y}$ via a suitably fixed or estimated parameter λ to

account for non-normality in the distribution of $\boldsymbol{\varepsilon}$ (**Equation 1.18**). Note here that logarithmic transformation is a special case of Box-Cox transformation when $\lambda = 0$.

$$\boldsymbol{\zeta}(\boldsymbol{y}) = \begin{cases} \dfrac{\boldsymbol{y}^{\lambda} - 1}{\lambda}, \lambda \neq 0 \\ ln\, \boldsymbol{y}, \lambda = 0 \end{cases}$$

Equation 1.18 *Box-Cox transformation.*

In this thesis, because all vitamin K-dependent coagulation proteins were assayed in the same blood sample, part of the assay error and all of the process error will be correlated across different coagulation proteins for the same sample. A correlation structure for $\boldsymbol{\varepsilon}$ of different coagulation proteins (termed *L2 correlation* in NONMEM® parlance) was introduced to the model (**Chapter 2**).

1.3.2.2. Models for the BSV

The second level in the model hierarchy describes the between-subject variability (BSV) in the individual parameters $\boldsymbol{\beta_i}$. Part of the BSV may be predictable. The predictability may arise from factors internal (e.g. phenotypic and genotypic characteristics) or external (e.g. extracorporeal drug removal, drug formulation, interacting drugs) to the individual. The remaining BSV are unexplained (e.g. yet to be understood influences of the genome) and assumed random. To account for these possibilities, a model for the dependence of $\boldsymbol{\beta_i}$ on systematic and random components is required:

$$\boldsymbol{\beta_i} = \boldsymbol{\psi}(\boldsymbol{\beta}, \boldsymbol{x_i}, \boldsymbol{\eta_i})$$
$$\boldsymbol{\eta} \sim N(0, \boldsymbol{\Omega})$$
$$\boldsymbol{\Omega} = \begin{bmatrix} \omega_{11}^2 & \omega_{12}^2 & \cdots & \omega_{1p}^2 \\ \omega_{21}^2 & \omega_{22}^2 & \cdots & \omega_{2p}^2 \\ \vdots & \vdots & \ddots & \vdots \\ \omega_{p1}^2 & \omega_{p2}^2 & \cdots & \omega_{pp}^2 \end{bmatrix}.$$

Equation 1.19 *Model for the parameters of the i^{th} individual.*

Here, $\boldsymbol{\beta_i}$ is modelled as a function, $\boldsymbol{\psi}(p \times 1)$, of typical value of parameters, $\boldsymbol{\beta}$ $(p \times 1)$, covariates, $\boldsymbol{x_i}(x \times 1)$, and unexplained random effects, $\boldsymbol{\eta_i}(p \times 1)$. It is usually assumed that $\boldsymbol{\eta}$ (i.e. $\boldsymbol{\eta_i}$ for *all* individuals) is normally distributed with a variance-covariance given by $\boldsymbol{\Omega}(p \times p)$. Because physiological parameters have a natural lower boundary of zero, an exponential model that constrains the parameter estimates to only positive values is usually used to describe BSV (**Equation 1.20**).

$$\beta_i = \beta \cdot e^{\eta_i}$$

Equation 1.20 *Exponential model for a parameter of the i^{th} individual that can only take on positive values.*

1.3.2.3. Software and estimation methods

Within the pharmacometric community, the most commonly used nonlinear mixed-effects modelling software program is NONMEM® (ICON Development Solutions, Ellicott City, MD, USA). In this thesis, the first-order conditional estimation (FOCE) (with interaction) method was implemented in NONMEM® for parameter estimation (see **Chapter 2**). Other parameter estimation methods, such as the first-order (FO) method, Laplacian method, expectation-maximisation (EM) method, and the stochastic approximation expectation maximisation (SAEM) method, are also available. A technical description of these estimation methods can be found elsewhere [19, 21, 68, 69].

For nonlinear mixed-effects models, the FO, FOCE, and Laplacian methods estimate the population parameters using a maximum likelihood (ML) type approach. The likelihood is defined as the probability of the data ($\boldsymbol{y}$) arising from a particular structural model, given a set of parameter values ($\boldsymbol{\beta}$, $\boldsymbol{\Omega}$, and σ^2). Unfortunately, in the nonlinear mixed-effects modelling framework it is not possible to compute the likelihood for the population model in closed form due to the nonlinear way in which the random effects enter the model. It is necessary, therefore, to linearise the model around the random effects in order to compute

the expectation and variance of the likelihood. The gradient based ML methods in NONMEM are therefore based on a linearisation process.

The FO method linearises the *nonlinear mixed-effects model* using a first-order Taylor series expansion around the expected value of zero for all elements of $\boldsymbol{\eta}$ and $\boldsymbol{\varepsilon}$ [68]. More recent estimation methods, FOCE and Laplacian methods, are developed around the *marginal likelihood* (rather than the nonlinear mixed-effects model itself) [69]. In these methods, the conditional probability distribution function of $\boldsymbol{\eta}$ (conditioned on $\boldsymbol{\Omega}$) is linearised using the Taylor series expansion to give an approximate closed form solution to the marginal likelihood function. Here, both the FOCE and Laplacian methods differ from the FO method in that the Taylor expansion uses the expectation of the empirical Bayes estimate (EBE) of $\boldsymbol{\eta}$, denoted as $\hat{\boldsymbol{\eta}}$**.** Here, the EBEs are obtained using an empirical maximum *a posteriori* (MAP) like estimation based on the present estimate of population parameters i.e. $\boldsymbol{\beta}$, $\boldsymbol{\Omega}$, and σ^2 (prior information) and individual observed data (posterior information). Note that the prior information is also based on the individual's data and hence this is not strictly a Bayesian (or MAP) technique. Whereas the FOCE method uses a first-order Taylor series expansion, the Laplacian method offers a more accurate approximation by using a second-order expansion around the EBE of $\hat{\boldsymbol{\eta}}$ [69].

Finally, population parameters, $\boldsymbol{\beta}$, $\boldsymbol{\Omega}$, and σ^2, are estimated simultaneously using the ML estimated method where value of parameters that maximise the likelihood of the data are taken as the final parameter estimates, denoted as $\widehat{\boldsymbol{\beta}}$, $\widehat{\boldsymbol{\Omega}}$, and $\hat{\sigma}^2$.

1.4. *Modelling physiological systems, drug concentrations, effects, and responses*

PK, PD, and PKPD modelling are based on a reductionist approach where a component of a system is observed and analysed in isolation of the whole system in order to provide insights into system behaviour [70, 71]. The reductionist approach to modelling, although convenient, and often works in the setting from which it was developed, it does not account for the complex interplay between the underpinning components and as such it may have poor predictive performance when used to extrapolate.

1.4.1. QSP model and its application

In the past decade, there has been a growing interest in QSP models. While PKPD models approximate the underlying physiological system using (often) simple mathematical functions (e.g. E_{max} model [**Equation 1.9**] and turnover models [**Equation 1.13**]), QSP models represent a more holistic approach to representing and understanding the system (see **Figure 1.8**). A QSP model typically includes a coherent mathematical representation of key physiological connections and system dynamics and also a quantitative characterisation of the PK and PD of a drug of interest that are consistent with the current state of knowledge [72]. With the added description of the underpinning biology, QSP model provides a rational basis to understand how a response is elicited within a system following a perturbation introduced by a drug thereby offering a complete description of the causal path of the dose and response of a drug (**Figure 1.8**). It is important to note here that **Figure 1.8** represents a generalisation of the causal path between the dose of a drug and system response. The generalisation may not be strictly accurate or hold across all instances, drugs, or models. For example, in contrast to that suggested by **Figure 1.8**, population PD models may contain a system response component.

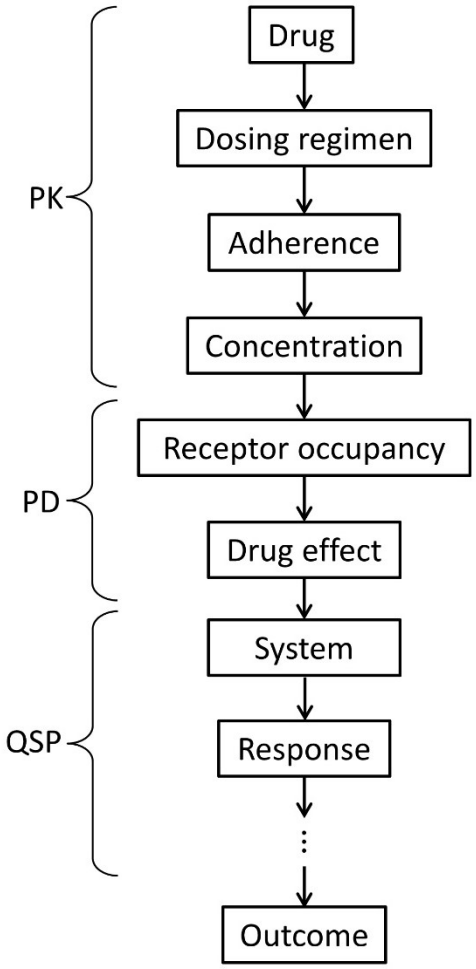

Figure 1.8 *Causal path of the dose of a drug and system response. PK relates drug dosing to concentration. PD links drug concentration to receptor occupancy and drug effect. QSP is unique in that the biological system underpinning a response is considered in addition to the PK and PD of the drug. The same figure is reproduced and explained in the context of warfarin in Figure 1.15.*

It is worth noting that QSP models are usually thought of as an extension of classical pharmacology and an area of application of systems biology. This was aptly described by Berger and colleagues that: "*systems pharmacology involves the application of systems biology approaches, combining large-scale experimental studies with model-based computational analyses, to study drug activities, targets, and effects*" [73]. A QSP model that has found a niche in relating drug pharmacology to the physiological system can thereby be distinguished from systems biology that describes a broader quantitative study of any biology.

QSP models provide a natural framework to account for both drug-specific (e.g. affinity of a drug to its target) and tissue-specific (e.g. transporter density)

properties for a comprehensive description of a drug's pharmacology. For this reason, QSP models have important potential for applications in the drug development process and clinical setting. The models can be used to test conjectures, generate hypotheses, and assess what-if scenarios regarding a drug and system of interest via simulations from the model, for instance, to identify new drug targets, biomarkers, or mechanisms that underpin drug effects and systems responses in addition to testing alternative dosing regimens. The ability of QSP models in testing hypotheses is a relatively new construct. Recent work conducted by Shivva *et al.* [74] developed a QSP model to assess mechanisms of gastrointestinal absorption of ketones. This model included knockout variants within the systems model (e.g. knockout of absorption process or site) in order to determine the most likely influence on the plasma profile. Another example is the successful application of a bone biology model [75] by the Food and Drug Administration (FDA) to identify the need for further dose optimisation of a recombinant human parathyroid hormone in the long-term treatment of hypoparathyroidism in order to address the safety concerns for hypercalciuria. Additionally, QSP models may be applied to guide future research, for example, in evaluating if the study design allows observation of important changes in safety and efficacy markers of interest. Finally, and probably most importantly, the development of the QSP model itself is helpful in both enhancing the drug development teams' level of system knowledge as well as identifying knowledge gaps particularly relating to biomarkers. This is important for a true understanding of the system and acknowledgement of the limitations attached to the model for effective model use and future refinement.

1.4.2. Model development

In general, there are six stages of QSP model development [72]:

1. identification of needs and formulation of goals,
2. determination of model scope,
3. representation of biology,
4. calibration or estimation of model parameters using data from reference subjects,
5. exploration of knowledge gap and variability, and
6. application and refinement of model.

For simplicity, the above six stages of QSP model development are presented as unidirectional, although in practice, this is rarely the case. The model development process is complex and often involves multiple learn and confirm cycles where the structural model may be tested, falsified, reduced, or expanded. Because the works reported in this thesis are based on *application* and not development of a QSP model, QSP model development is only briefly introduced here. Emphasis will be placed on representation of the biology and mathematical formalism of a QSP model, which are essential to facilitate understanding and use of a QSP model.

1.4.2.1. Representing the biology

In the QSP framework, necessary biological details are usually prioritised over the principle of parsimony. Consequently, QSP models tend to be complex with (potentially) a vast number of states and parameters. Finding an optimal granularity that is the level of detail in which the system and the drug of interest are represented in order for a QSP model to be useful, is notoriously difficult and is dependent on various factors including (1) the need for the model, (2) the amount of available information on the system and the drug of interest, as well as (3) availability of collaborators [76].

Need: The need for a QSP model typically arises from a set of high priority problems or questions that cannot be answered by using standard modelling

methodology. Here, a necessary step to QSP model development is the specification of a feasible modelling goal after considering and understanding the problem context. Subsequently, this will be used in combination with available data and knowledge to identify a suitable scope for the model.

Prior knowledge: The development of a QSP model requires integration of diverse data, existing knowledge, educated guesses, and hypotheses into a single coherent mathematical framework. To this end, a thorough review of literature is usually conducted and sometimes, expert opinions are sought regarding the drug and the target or system in which the drug acts in order to arrive at a QSP model structure (sometimes termed *model topology*) that is consistent with the current state of knowledge. Of particular interest in the search for information, are the structure (connections and interactions of components or sub-systems) of the system, mechanisms of the drug of interest, relevant parameter values as well as physiological and pathophysiological conditions for components of the system, which are of appropriate amplitude scales at, for example, molecular, cellular, tissue, organ, or sub-system level.

Most often, the information identified are heterogeneous due to variation in experimental conditions, assay methods, species (human versus animal), and the rigor in which the experiments were conducted. It is therefore necessary to carefully screen, select, and document available information for inclusion into the model. Additionally, competing hypotheses may be identified and imputation of model structure may be made based on assumptions. These uncertainties in model structure should be addressed and appropriately documented. Should the need arise, these uncertainties should be revisited and the QSP model updated according to the current state of evidence.

Collaborators: An extensive collaborative network is important for the development and application of QSP model. Long-term partnership with wet laboratories, clinics, hospitals, drug development project teams, and experts in the field of interest allow continual generation of new data and mechanistic insights that will be helpful for model refinement for effective model use.

1.4.2.2. Mathematical formalism

ODEs are the most widespread formalism of QSP models [70]. In ordinary differential equation modelling, the quantity in a state of interest is modelled as a continuous variable over time with relationships and dynamics within- and between-states defined by mathematical functions and real-valued parameters.

In the ODE setting, each state is represented by an ODE that contains two general types of rate expressions as building blocks: (1) rate of input and (2) rate of output. Different mechanisms of input (e.g. exogenous input, natural production, formation reaction) and output (e.g. natural degradation, complex formation) can be accounted for using mathematical functions. For instance, in **Equation 1.21**, output of A via diffusion, which is governed by the law of mass action and is therefore a first-order process, is characterised using a linear function whereas output of B that is transporter-dependent is described using the Michaelis-Menten equation. Finally, in the representation of the rate of change of the quantity in a state, the ODE subtracts the sum of output rate from the sum of input rate.

$$\frac{dA}{dt} = -k \cdot A; \quad A_{t=0} = A_0$$

$$\frac{dB}{dt} = k \cdot A - \frac{V_{max}}{K_M + B} \cdot B; \quad B_{t=0} = 0$$

Equation 1.21 *ODE describing conversion of A to B via a first-order process and saturable elimination of B.*

For QSP model development and application, the physical quantity in each of the states in the model over time are of primary interest. This requires solving the systems of ODEs. In some cases, the ODE systems can be expressed in exact closed forms then a solution can be obtained *algebraically*. However, QSP models usually do not have algebraic solutions due to the recursiveness (causing nonlinearity) of the system that leads to dependence of an input or output function on the state itself. For example, $k \cdot A$ of **Equation 1.21** is amenable to

algebraic representation, which allows simplification of the equation to **Equation 1.22**, whereas $\frac{V_{max}}{K_M+B} \cdot B$ part of the equation is nonlinear in response variable B and would require *time-stepping* ODE solvers to derive the solutions *numerically*.

$$\frac{dB}{dt} = k \cdot (A_0 \cdot e^{-kt}) - \frac{V_{max}}{K_M + B} \cdot B; \quad B_{t=0} = 0$$

Equation 1.22 *Simplification of Equation 1.21.*

The time-stepping procedures are numerical techniques for computing solutions to the ODE by conditioning the next step solution on the immediate previous time point. The Euler's method (**Equation 1.23**) is one of the simplest and it forms the basis to construct more complex methods for solving systems of ODEs [77]. Briefly, starting from a known initial value (y_n), the Euler's method uses the tangent line equation given by the ODE i.e. $f(t_n, y_n) = \frac{dy}{dt}$ and a small time step size (h) to approximate successive point (y_{n+1}) on the solution curve of the ODE. The solution from one time point is then advanced to the next time point and the process is continued iteratively until the desired vector of solutions $(y_0, y_1, \cdots, y_n, y_{n+1})$ is obtained.

$$y_{n+1} \approx y_n + h \cdot f(t_n, y_n)$$

Equation 1.23 *Euler's method for solving ODEs with a given initial value*

The Euler's method may require specification of a very small h to obtain reasonably accurate solutions, which typically leads to an exaggerated increase in computation time. For this reason, higher order methods such as the Runge-Kutta methods [77, 78] that adapt h according to the ODE model gradients are generally preferred for better numerical accuracy and computational efficiency. Finally, in systems where there is a large difference in the rate constants among the ODEs which may cause rapid variation in the solutions, *stiff* time-stepping

solvers may be required. In MATLAB® (The MathWorks Inc., Natick, Massachusetts, USA), ode45 and ode15s functions are commonly used for non-stiff and stiff systems, respectively. A technical explanation of these numerical methods and detailed description of the aforementioned ODE solvers can be found elsewhere [79, 80].

In contrast to PKPD models, parameters for QSP models are almost always not estimated but heuristically calibrated by modellers based on single or multiple input-output relationship(s) of interest. In QSP models, some or most parameters are not known *a priori* and due to model complexity, they are often not identifiable (definition of identifiability is provided earlier in **Section 1.3.1.4**). Then, with a flat likelihood surface with respect to the parameter(s) of interest, the driving force for the parameter search diminishes for (traditional) *derivative-based* optimisation methods (e.g. gradient method and the Newton's method). For more effective exploration of parameter space, *stochastic* optimisation methods (e.g. simulated annealing and SAEM method) can theoretically be considered [81]. However, it is important to note that QSP models are generally not amenable for estimation purposes even if all unidentifiable parameters are fixed [76, 82]. This is because fixing a parameter may bias other parameters in the system then when a large number of parameters are fixed, the bias compounded within the system may be so huge that it renders the model unusable for its intended purpose.

1.4.3. Coagulation network model

In this thesis, a QSP model of the coagulation network, which was developed by Wajima and colleagues [31] and later updated by Gulati and peers [38], was applied to explore the kinetics of coagulation proteins as driver of the INR (see **Chapter 3**) and subsequently, to derive a coagulation protein-based method for the prediction of anticoagulant response to warfarin (see **Chapter 4**). A schematic of the QSP coagulation network model is shown in **Figure 1.9**.

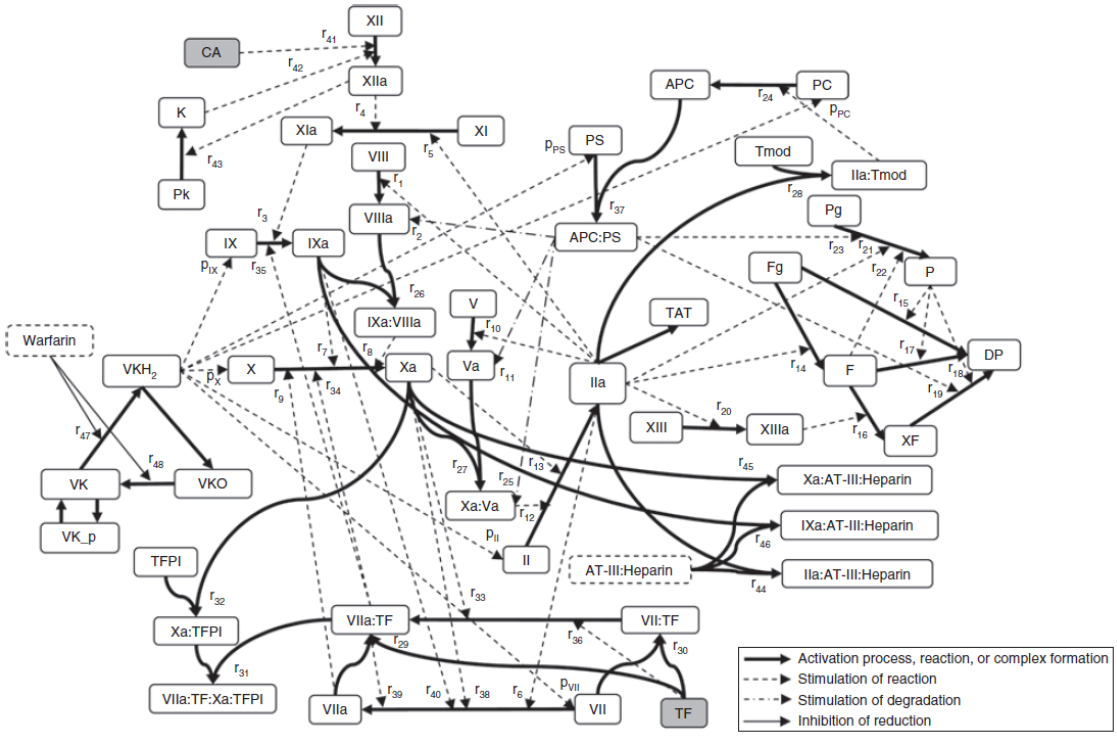

Figure 1.9 *Schematics of the coagulation network model [31]. APC represents activated protein C, AT-III antithrombin-III, CA contact activator, DP degradation product, F fibrin, Fg fibrinogen, II factor II, IIa thrombin, K kallikrein, P plasmin, PC protein C, Pg plasminogen, Pk prekallikrein, PS protein S, TAT thrombin-antithrombin complex, TF tissue factor, TFPI tissue factor pathway inhibitor, Tmod thrombomodulin, VK vitamin K, VKH_2 vitamin K hydroquinone, VKO vitamin K epoxide, XF cross-linked fibrin.*

The model accounts for various subsystems involved in *in vivo* coagulation (e.g. vitamin K cycle, intrinsic, extrinsic, and common coagulation pathways [according to classical definition], anticoagulant system, and fibrinolytic system) as well as common *in vitro* blood coagulation tests (e.g. prothrombin time (PT),

INR, and activated partial thromboplastin time tests). It also predicts the time course of drug concentrations and effects for warfarin, heparins, and vitamin K in humans. The model was previously applied to simulating PT and INR for 20 patients identified from the literature [31, 83] and was found to provide an adequate description of the observed data [31].

The model consists of 63 states, each corresponds to a specific coagulation component. The coagulation components can be broadly classified into *inactivated* components termed *zymogens* (e.g. factor II), the corresponding *activated* species, which acts as *activating enzymes* for clot formation (e.g. thrombin [factor IIa]), and *cofactors* (e.g. protein S). Briefly, *in vivo* coagulation is initiated when vascular injury exposes factor VII in the blood to tissue factor. Factor VII is activated to factor VIIa that leads to an accelerated pathway of activation of other zymogens as a result of the complex feedback and feedforward mechanisms within the coagulation network. This ultimately leads to rapid activation of factor II to thrombin, which in turn catalyses the conversion of fibrinogen to insoluble fibrin, which is cross-linked by factor XIIIa to form the stabilising component of a clot.

In the QSP coagulation network model, the zymogen, cofactor, and activated species are assumed to follow a first-order degradation process (parameterised as k_{out}) but differ in the mechanism of formation. Each zymogen or cofactor is described by a turnover model (see **Section 1.3.1.3.2**) that assumes a zero-order natural production rate (R_{in}). On the other hand, activated species is formed by activation of the zymogen and is assumed to be a time-varying reaction that depends nonlinearly on the concentration of specific activating enzyme via a Michaelis-Menten function.

By default, the coagulation system is assumed to be in equilibrium dynamics. The initial condition of the zymogens and cofactors are given by $\frac{R_{in}}{k_{out}}$ (See **Equation 1.13** in **Section 1.3.1.3.2**). On the other hand, the initial concentration of all activating enzymes (including complexes and products) are assumed to be zero so that the coagulation system is at a non-clotting condition at equilibrium.

QSP models tend to be complex. They are often difficult to work with, challenging to analyse, and generally not suitable for estimation purposes and for practical application in drug development or clinical settings [76, 82]. On the basis of parsimony and practicality, QSP models may be simplified based on a specific input-output relationship of interest. In general, model-order reduction can be achieved by either reducing the number of reactions (e.g. quasi steady-state approximation) or the number of states (e.g. proper lumping). In particular, the technique of proper lumping has been successfully applied for model-order reduction for several systems models [84-86]. However, at the time this PhD work was undertaken, no exact solutions for lumping are available for nonlinear ODEs [85]. In this work, a heuristic model-order reduction technique in which an empirical approximation to predictions from the QSP coagulation network model is used and described in **Chapter 4**.

1.5. *Warfarin and anticoagulant response*

Warfarin has been used to treat and prevent blood clots in humans for more than 60 years and despite the availability of newer oral anticoagulants, warfarin remains one of the most widely prescribed oral anticoagulants in the world. The effectiveness of warfarin is well-established for the treatment and prevention of venous thrombosis, pulmonary embolism, and systemic embolism associated with atrial fibrillation, myocardial infarction, and prosthetic heart valves [87-90].

Warfarin has a narrow therapeutic range [1, 87, 91-93] and it is a difficult drug to dose safely and accurately. It requires a working knowledge of the relationship between warfarin dose and observed anticoagulant response, a relationship that is inherently nonlinear and therefore not necessarily intuitive. The overall aim of this thesis was to understand warfarin dose response by considering the underpinning coagulation kinetics. In the next following sections, the PK and PD of warfarin underpinning this relationship will be reviewed and the current status, knowledge gap, challenge, and need for improved warfarin dosing will be summarised and discussed.

1.5.1. Physicochemical properties of warfarin

Warfarin (4-hydroxy-3-(3-oxo-1-phenylbutyl)chromen-2-one) is a synthetic derivative of dicoumarol (4-hydroxy-3-[(4-hydroxy-2-oxochromen-3-yl)methyl]chromen-2-one), which is a natural anticoagulant first discovered in spoiled sweet clover. Warfarin is a weak acid with a pKa of 5.08 and with a chemical formula of $C_{19}H_{16}O_4$, warfarin has a molecular weight of 308 g/mol [94]. Commercially available warfarin tablets is a racemic mixture of two enantiomers, *R*- and *S*-warfarin [95]. The two enantiomers do not appear to undergo stereo-conversion *in vivo* and they differ in their PK and PD properties.

1.5.2. PK of warfarin

Both *R*- and *S*-warfarin are essentially completely absorbed from the gut with an absolute bioavailability reported to be nearly 100% [96]. Warfarin is usually detectable in plasma within one hour of oral administration, and plasma concentrations peak between 0.3 to 4 hours [97, 98]. Following absorption, because warfarin is almost completely bound to plasma proteins (> 99%), principally albumin, warfarin distributes into a relatively small volume of about 10 L/70kg [99]. Here, the volume of distribution does not appear to differ significantly between *R*- and *S*-warfarin [100-103].

Warfarin is eliminated almost entirely by hepatic metabolism with only traces excreted unchanged in the urine. The metabolism of warfarin is capacity-limited, which is characterised by a low plasma clearance (0.2 L/h/70kg) relative to the hepatic blood flow [99, 104]. *S*-warfarin is metabolised principally by cytochrome P450 (CYP) 2C9 whereas *R*-warfarin is metabolised by various enzymes including CYP2C19, CYP1A2, and CYP3A4 [97, 105, 106]. The inactive metabolites are excreted in faeces (80%) and urine (20%) [107]. For a patient with CYP2C9 wild-type genotype, the oral clearance of *S*-warfarin is approximately 2 times higher (0.3 L/h/70kg) than that of *R*-warfarin (0.13 L/h/70kg) [100-103]. Since the volume of distribution of the enantiomers are largely similar, the plasma half-life of the *S*-warfarin (30 hours) is shorter than that of *R*-warfarin (45 hours). With these half-lives, warfarin requires about a week to reach its steady-state and that a relatively small fluctuation in the plasma drug concentrations is expected during each *daily* dosing interval.

Polymorphism in the CYP2C9 gene affects the metabolism of warfarin. CYP2C9*2 and CYP2C9*3 are common variant alleles with single base substitutions at residue 144 (arginine to cysteine) and residue 359 (isoleucine to leucine), respectively, encoding an enzyme with reduced activity [108]. Carriers of these variant allele(s) typically have a 30 to 85% reduction in oral clearance and therefore are expected to have greater tendency to bleed as compared to homozygotes for the wild-type allele, CYP2C9*1 [100-103, 109]. For this reason,

carriers of variant alleles usually have warfarin dose requirement that are 20 to 80% lower than those with the wild-type genotype [110].

1.5.3. PD of warfarin

Vitamin K-dependent clotting factors and anticoagulation proteins, factors II, VII, IX, X, protein C, and protein S, are biosynthesised in hepatocytes [111]. The required first step in the biosynthesis of functional clotting factors and anticoagulation proteins is the production of precursor proteins in the endoplasmic reticulum of the hepatocytes [112-114]. An important prerequisite for conversion of these precursor proteins to clotting factors and anticoagulation proteins involves oxidation of vitamin K hydroquinone to vitamin K epoxide [115, 116]. During the oxidation reaction, a short-lived oxygenated intermediate is produced to abstract the γ-proton from the glutamic acid residue on the precursor proteins [117]. This is sequentially coupled with a γ-carboxylation reaction whereby CO_2 is added to the γ-carbon of the glutamic acid residue on the precursor proteins by the gamma-glutamyl carboxylase (GGCX) [111, 116, 118]. The fully modified, mature clotting factors and anticoagulation proteins are then released from the hepatocytes for circulation as zymogens in the blood. The nomenclature regarding these factors and proteins remains somewhat confusing. Factors II, VII, IX, X and protein C are zymogens whereas protein S lacks the serine protease domain and is most likely a cofactor [119]. For simplicity, all these proteins are collectively denoted as vitamin K-dependent coagulation proteins in this thesis.

Warfarin exerts its anticoagulant effect by inhibiting the enzyme VKOR [111, 120]. VKOR reduces vitamin K epoxide to vitamin K quinone and also converts vitamin K quinone to the active vitamin K hydroquinone [121]. By inhibiting the formation of vitamin K hydroquinone, warfarin prevents the production of vitamin K-dependent coagulation proteins leading to a prolonged clotting time. Warfarin PD effect is summarised in **Figure 1.10**. It is generally believed that *S*-warfarin, which is 1.6 to 3.4 times more potent than *R*-warfarin,

is responsible for the observed anticoagulant response [95, 102, 122]. However, recent findings suggest that contribution of *R*-warfarin may be important [123].

The enzyme kinetics underpinning the interactions between warfarin and VKOR is a matter of contention. Reports from the 1980s have indicated the inhibition as irreversible [124, 125]. This was initially considered as inconsistent with the observation that warfarin effect can be rapidly reversed by using vitamin K but with emerging evidence of a salvage pathway for vitamin K reduction that is independent of VKOR, possibility of irreversible inhibition of VKOR by warfarin cannot be dismissed [126, 127]. The more prevailing belief is that the inhibition is reversible and non-competitive [128-130]. However, this was challenged by a recently published X-ray crystallography study that suggests that vitamin K epoxide, vitamin K quinone, and warfarin share the same binding site on VKOR that involves residue 55 (phenylalanine) [131].

In the literature, warfarin is often referred to as *vitamin K antagonist*. This is a misnomer as warfarin exerts its effect by the inhibition of VKOR and does not antagonise the effect of vitamin K *per se*.

Polymorphism in the gene VKORC1 has been shown to impact patient sensitivity to warfarin. Genetic variants in VKORC1 affects warfarin PD by causing a reduced expression of VKOR thereby leading to a reduction in the recycling of vitamin K [132]. Patients with the 1639A (rs992323) and 1173T (rs9934438) allele need a lower warfarin dose (24 to 26 mg/week) while patients with 9041A (rs7294) require a higher dose (40 mg/week) compared to the wild-type carriers (35 mg/week) [133-135]. Genetic differences in VKORC1 therefore represents an important source of warfarin dose variability.

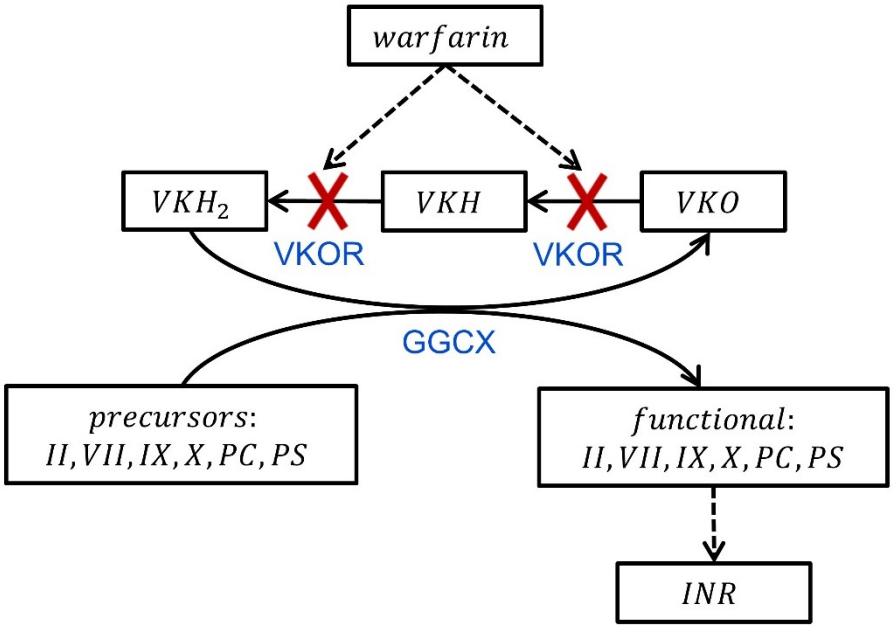

Figure 1.10 *Depletion of VKH_2 as a result of the inhibitory action of warfarin on VKOR, which leads to reduced hepatic synthesis of functional coagulation proteins and, as a result, causes prolongation of the PT and an increase in the INR. GGCX gamma-glutamyl carboxylase, II factor II, INR international normalised ratio, IX factor IX, PC protein C, PS protein S, PT prothrombin time test, VII factor VII, VK vitamin K quinone, VKH_2 vitamin K hydroquinone, VKO vitamin K epoxide, VKOR vitamin K epoxide reductase, X factor X. The rectangular box indicates a compartment. The dashed arrow indicates a functional relationship and the solid arrow indicates a mass balance relationship. A cross indicates inhibition.*

1.5.4. Monitoring anticoagulant response

Variability in the observed anticoagulant response is determined by both PK and PD factors. Warfarin drug concentrations do not reflect all of the observed variability in anticoagulant response and are therefore inadequate as a marker of anticoagulation. Since the physiological response to warfarin therapy is a prolonged clotting time, the anticoagulant response is monitored clinically using the PT test and is normally reported by the laboratory as the INR.

1.5.4.1. PT

PT is an *in vitro* test that measures the time required for a fibrin clot to form after the addition of thromboplastin (mixture of tissue factor and phospholipid) and calcium to decalcified, platelet poor plasma. Here, the tissue factor initiates

coagulation in the same way as it does in *in vivo* when vascular injury exposes factor VII in the blood to tissue factor (classically referred to as the extrinsic pathway). Hence, the PT test is sensitive to the coagulation proteins integral to the extrinsic pathway including fibrinogen, factors II, V, VII, and X [136, 137]. The PT for normal healthy individuals usually range from 12 to 14 seconds whereas for warfarin patients who have deficient level of factors II, VII, and X, the PT is usually prolonged.

1.5.4.2. INR

PT results are known to vary with the thromboplastin reagent used. For standardisation, the PT is reported as the INR:

$$INR = \left(\frac{PT}{PT_{standard}}\right)^{ISI}.$$

Equation 1.24 *INR.*

Here, PT is the measured PT of a test sample, $PT_{standard}$ is the PT for standard normal plasma, and ISI is the international sensitivity index. Inclusion of the exponent (ISI) standardises PT by correcting for the differences in sensitivity between the thromboplastin used and the international thromboplastin reference, which has a known sensitivity. Although the ISI corrects for major differences in PT results, disagreement between INR results are not uncommon, for instance, when different methods (e.g. the Quick method versus the Owren method) are used for the determination of PT [138].

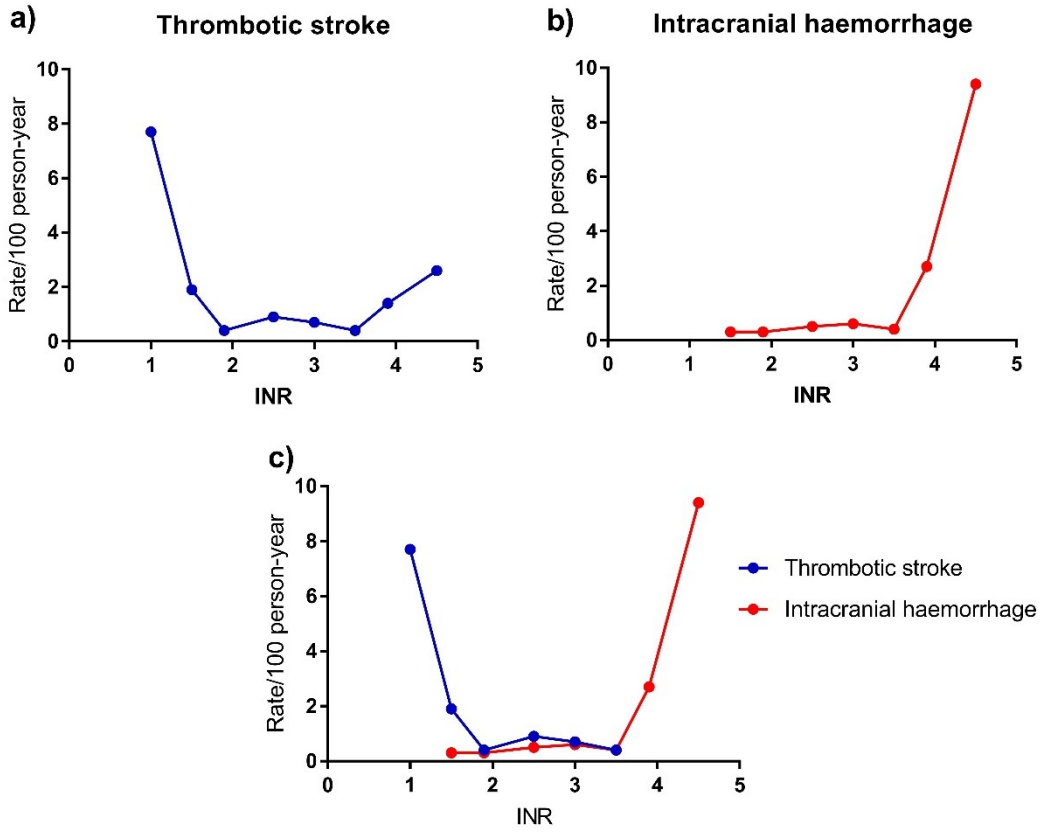

Figure 1.11 *Incidence rates of thrombotic stroke (panel a), intracranial haemorrhage (panel b), and combined data (panel c) of warfarinised patients with non-valvular atrial fibrillation versus the INR. The plots are produced based on the data from Hylek and colleagues [1].*

The INR for normal healthy individuals usually range from 1 to 1.2 whereas for warfarin patients who have deficient level of factors II, VII, and X, the INR is elevated. The work of Hylek *et al.* provided support for the functional relationships between INR and the incidence rates of thrombotic stroke and intracranial haemorrhage in patients with non-valvular atrial fibrillation (see **Figure 1.11**) [1]. *Panel c* in **Figure 1.11** identifies a safe range of INR from approximately 1.5 to 3.5 that is associated with low incidence rates of both thrombotic stroke and intracranial haemorrhage. Indeed, the INR therapeutic range for warfarin, in non-Asian patients, has been widely studied and a target INR of 2 to 3 was proposed for atrial fibrillation and for most other indications [87, 91-93]. The therapeutic range for warfarin is narrow with sub-therapeutic

INR associated with an increased risk of clotting while supra-therapeutic INR carries a significant risk of major bleeding events.

1.5.4.3. Clotting factor activity

Warfarin affects the production of vitamin K-dependent coagulation proteins. Coagulation proteins therefore provide the most direct measure of the anticoagulant response to warfarin.

Use of prothrombin complex activity (PCA) had been proposed and explored. PCA is determined based on the calibration curve constructed by plotting the measured PT against dilutions of normal plasma [98]. Then, individuals with normal clotting activity will have a PCA of 100% whereas warfarin patients with therapeutic INR usually have a PCA ranging from 20 to 40% [98, 139]. PCA is a composite measure of coagulation proteins activity and because the determination of PCA is based on PT, it is only sensitive to variation in fibrinogen, factors II, V, VII, and X [136, 137]. It is important to note that PCA is inversely proportional to INR [102, 140, 141]. Their relationship is defined by the following equation:

$$INR = \frac{a}{PCA} + b$$

Equation 1.25 *Mathematical relationship between INR and PCA.*

Here, $a = 80.65$ and $b = 0.18$ [141] although different values have been reported [102, 140].

Concentration of the vitamin K-dependent coagulation proteins provide the most direct measure of the anticoagulant response to warfarin. Factors II, VII, IX, and X are quantified in the same manner as the PCA except that specific coagulation protein-deficient-plasma is used for the construction of the calibration curve [142]. The coagulation proteins concentration for patients on stable warfarin are compared and contrasted to the reference range for normal healthy individuals in **Table 1.2**.

Table 1.2 *Vitamin K-dependent coagulation proteins concentrations for normal healthy individuals and patients on stable warfarin. Proteins C and S are not shown as their reports are sporadic. CI is the confidence interval.*

Coagulation protein	Concentration (%) $mean\ (95\%\ CI)$	
	Reference range for normal individual[a]	**Reported value for stable warfarin patient**[c]
Factor II	60 – 140[b]	24.9 (10.6 – 48.7)
Factor VII	60 – 140[b]	38.7 (19.0 – 68.4)
Factor IX	69 – 151[b]	49.7 (27.9 – 68.7)
Factor X	60 – 140[b]	16.5 (6.49 – 28.9)

[a] Sourced from Mann *et al.* 2004 ($n = 150$) [143]
[b] Mean is not reported [143]
[c] Based on data manually digitalised from Kumar *et al.* 1990 ($n = 23$), Lind *et al.* 1997 ($n = 16$), and Paul *et al.* 1987 ($n = 36$) [144-146]. Lind *et al.* 1997 did not report factor IX values. Note that the patients are on stable warfarin but their INR values are unknown.

1.5.5. Warfarin dosing methods

The goal of warfarin dose individualisation is to predict the warfarin maintenance dose that will keep the INR_{SS} within this range. There is a large body of literature exploring ways to aid warfarin dose selection in clinical practice. A brief overview of published warfarin dosing methods is provided below. However, a comprehensive review of the vast literature on this subject is beyond the scope of this thesis.

For the purposes of this thesis, warfarin dosing methods are broadly classified into two types, (1) covariate-based dosing methods and (2) response-based dosing methods, although it is acknowledged that some methods consider both covariates and anticoagulant response for warfarin dose individualisation [12, 22, 102].

1.5.5.1. Covariate-based dosing method

Body size, age, ethnicity, concomitant drugs, CYP2C9 genotype, and VKORC1 genotype have been identified to affect the PK and PD of warfarin and to explain about 50% of the between-subject variability in warfarin maintenance dose requirement [8-16]. A large number of warfarin dosing algorithms that account for individual covariates have been developed based on the multiple linear regression analysis (see **Equation 1.26** for an example) [10, 12, 22, 24, 25].

In essence, warfarin maintenance dose requirements are modelled as a linear function of one or more covariates with the inclusion of covariates guided by statistical significance.

$$D = e^{0.613+(0.425 \cdot BSA)} - (0.0075 \cdot age) + (0.156 \cdot AfricanAmerican) + \left(0.216 \cdot INR_{target}\right) - (0.257 \cdot amiodarone) + (0.108 \cdot smokes) + (0.0784 \cdot DVT/PE)$$

Equation 1.26 *Linear model underpinning the algorithm proposed by Gage et al. for the prediction of warfarin maintenance dose [10].*

Here, BSA refers to body surface area, D is the predicted warfarin daily dose, DVT is deep vein thrombosis, and PE is pulmonary embolism.

The use of patient characteristics including genotype information to predict warfarin dosing requirements *prior* to the initiation of warfarin therapy is advocated by the FDA [147]. However, the method suffers from several drawbacks. First, it relies on prior knowledge of patient's characteristics such as the CYP2C9 and VKORC1 genotypes, which may not be readily available in the clinical setting. In addition, using this approach, the intricacy and the complex interplay between warfarin, vitamin K cycle, coagulation proteins, and INR are simplified into an empirical linear regression equation. The assumption of linearity in warfarin dose-INR relationship may not necessarily hold true for the entire warfarin dose range that is clinically relevant and as a result, may have limited generalisability to other settings [5, 148]. Last but not least, while this method is useful to guide initial warfarin dosing, they provide no means of adjusting the dose of warfarin once INR responses become available.

1.5.5.2. Response-based dosing method

Measures of anticoagulant response such as the INR reflect the between-subject differences in warfarin PK and PD thereby representing a useful marker for warfarin dose individualisation.

In clinical practice, warfarin dose adjustment is a largely heuristic process with the maintenance dose for a patient determined intuitively by the prescriber, often by trial and error, based on the magnitude of observed INR values. However, accurate prediction of the warfarin maintenance dose requirement is difficult owing to the non-steady-state conditions of warfarin, coagulation proteins, and INR during warfarin initiation or after a dose change in addition to the requirement of a working knowledge of the warfarin dose-response relationship. For these reasons, various dosing tools that are based on either single or multiple observed anticoagulant responses with or without accounting for a patient's covariates simultaneously have been proposed to aid INR control in patients. Non-adaptive methods to determine dose based on measurement of a response variable fall into the general category of nomogram approaches.

Nomograms have a long history of use in clinical practice. They provide guidance for initial dose selection and recommendations for subsequent dose adjustment based on the observed INR responses. Nomograms for warfarin are most typically presented as dosing tables (see **Figure 1.12** for an example) [17, 149, 150] but may also take the form of computerised decision-support tools (see Poller *et al.* for an example [151]). Although they are easy to use, the pitfall of the nomograms lies in the often explicit assumption of a linear relationship between warfarin dose and response (though not always [**Figure 1.12**]) and the nomograms would therefore not be expected to produce credible predictions beyond the linear portion of the concentration-effect curve, i.e. at more than 20% of maximal inhibition. In addition, nomograms lack an in-built mechanism to adjust for factors such as the between-subject variability in the degradation half-life of coagulation proteins [143] that may confound the observed INR.

d5 INR	dose (for d5-7)	**d8 INR**	dose (from d8)
≤ 1.7	5mg	≤ 1.7	6mg
		1.8 - 2.4	5mg
		2.5 - 3.0	4mg
		> 3.0	3mg for 4 days
1.8 - 2.2	4mg	≤ 1.7	5mg
		1.8 - 2.4	4mg
		2.5 - 3.0	3.5mg
		3.1 - 3.5	3mg for 4 days
		> 3.5	2.5mg for 4 days
2.3 - 2.7	3mg	≤ 1.7	4mg
		1.8 - 2.4	3.5mg
		2.5 - 3.0	3mg
		3.1 - 3.5	2.5mg for 4 days
		> 3.5	2mg for 4 days
2.8 - 3.2	2mg	≤ 1.7	3mg
		1.8 - 2.4	2.5mg
		2.5 - 3.0	2mg
		3.1 - 3.5	1.5mg for 4 days
		> 3.5	1mg for 4 days
3.3 - 3.7	1mg	≤ 1.7	2mg
		1.8 - 2.4	1.5mg
		2.5 - 3.0	1mg
		3.1 - 3.5	0.5mg for 4 days
		> 3.5	omit for 4 days
> 3.7	0mg	< 2.0	1.5mg for 4 days
		2.0 - 2.9	1mg for 4 days
		3.0 - 3.5	0.5mg for 4 days

At day 15 (or day 12) check INR and make fine dose adjustment as appropriate

Figure 1.12 *Nomogram for warfarin initiation proposed by Tait et al. [17]. It relies on measuring the INR at baseline, on day 5 and day 8 to individualise warfarin dosing. The nomogram is reproduced here with permission from the British Journal of Haematology.*

Only about 50% of the between-subject variability in warfarin maintenance dose requirement are accounted for by covariates [8-16]. In a small number of recent publications, the covariate-based linear regression method described in **Section 1.5.5.1** is extended to include single INR response as a predictor for warfarin maintenance dose to account for dosing variability previously unexplained by covariates (see Lenzini *et al.* [12] for an example). These methods have been shown to have superior predictive performance compared to algorithms without anticoagulant response feedback [7].

Alternatively, warfarin dose individualisation can be achieved by the use of Bayesian forecasting methods with an underpinning PKPD or KPD model for warfarin. See Wright *et al.* [18] for an example and the underpinning warfarin KPD model [54, 152] is shown in **Figure 1.13**. Using this approach, key parameters (e.g. CL) in the warfarin model can be individualised based on the dose-INR data obtained from individual patient then as more data become available, the parameter estimates become more refined thereby allowing accurate prediction of warfarin dose that is required to achieve the therapeutic INR.

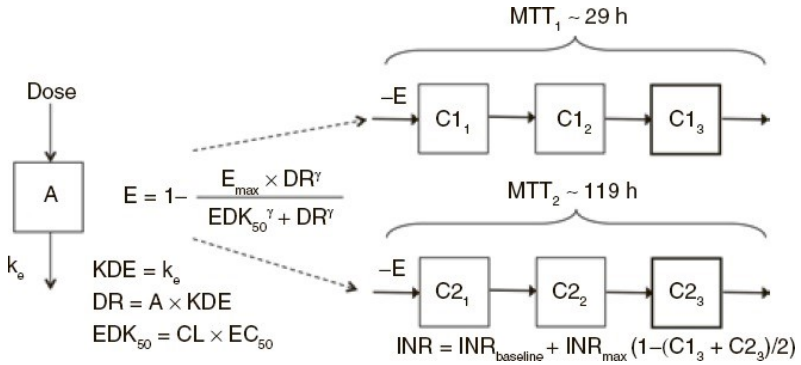

Figure 1.13 *A schematic of the warfarin KPD model developed by Hamberg et al. [54] and adopted by Wright et al. [18] for warfarin maintenance dose prediction using the Bayesian forecasting method. A is the amount of warfarin in the body, $C1_m$ and $C2_m$ are the m^{th} compartment in the two transit chains, DR dosing rate, EDK_{50} dosing rate that corresponds to 50% maximal inhibition, EFF warfarin effect, E_{max} maximum inhibition of coagulation, KDE is the first-order elimination rate constant of warfarin, MTT mean transit time, γ empirical shape parameter. The figure was published by Hamberg et al. [54] and is reproduced here with permission from the Clinical Pharmacology & Therapeutics.*

1.5.6. The need for improved warfarin dosing

1.5.6.1. Biased prediction of dose requirement

Existing warfarin dosing methods have been shown to predict warfarin dose requirements accurately on average [7, 153]. However, it was reported that current methods produce biased predictions in patients who require doses in the upper quartile (≥7 mg/day) of warfarin dose requirements [3-5, 7]. Interestingly, it was shown that even the flexibility of a Bayesian forecasting method was insufficient to accurately predict warfarin requirements in those who required higher doses [7]. In a recently published systematic review and meta-analysis that includes 47 evaluations of 22 warfarin dosing tools from 16 studies using data from 1492 patients who required warfarin doses of ≥7 mg/day, the bias in maintenance dose predictions was quantified as an average of -2.3 mg/day with a pooled estimate of under-predicted doses a staggering 92.3% (95% confidence interval 90.3% – 94.1%) [5]. The corresponding forest plot for the proportion of under-predicted doses of warfarin is reproduced here as **Figure 1.14**. In addition, warfarin dose requirements in patients who require doses in the lower quartile (≤2 mg/day) were also reported to be over-predicted [2, 6].

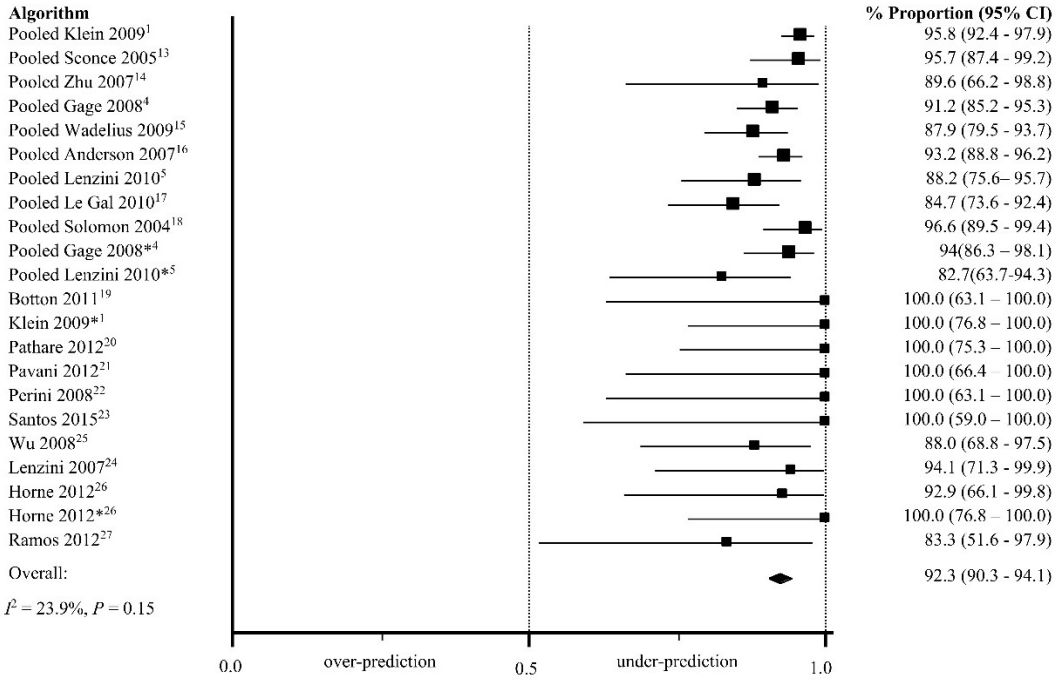

Figure 1.14 *The proportion of doses that were over- or under-predicted in patients who required ≥7 mg/day of warfarin. The line of no bias corresponds to a value of 0.5 where the proportion of over-prediction is the same as that of under-prediction. The forest plot [5] is reproduced here with permission from the Clinical Pharmacology & Therapeutics.*

It appears that current methods do not accurately predict warfarin maintenance doses for patients in the lower or upper quartile of dose requirements. These patients will be those who are at the greatest risk of over- or under-anticoagulation, and who would therefore derive the most benefit from warfarin dose individualisation.

1.5.6.2. A new perspective to warfarin dosing

The reason for the poor performance of dosing algorithms in the upper and lower quartiles of dose requirements is not understood [5]. It is probable that the empirical models underpinning these dosing methods are too simple to accommodate the complexity of the coagulation system, with many models approximating the relationship between warfarin dose and INR by linear functions [12, 22-25] or an E_{max} function [18, 54, 100, 154]. In these models, warfarin dose or concentration is linked directly and empirically to the INR. Using this approach, the vitamin K cycle and the coagulation proteins that lie

causally between warfarin dose and INR response are not considered [54, 100, 102, 139, 140, 155, 156] and the intricacy and the complex interplay between different coagulation components are simplified into an empirical equation.

In addition, to date, *all* response-based warfarin dosing methods (except Pitsiu *et al.* [157]) rely solely on the measurement of INR as feedback for warfarin dose individualisation [12, 17, 18, 22, 23, 25-30]. The INR is easily measured by commercial laboratories and has been directly linked to clinical outcomes of interest [92, 93]. This means that it is an attractive biomarker to assess the magnitude of anticoagulation and choice of warfarin dose. However, the INR is a blunt estimate of anticoagulant response that is a composite of fibrinogen, factors II, V, VII, and X [136, 137]. Its interpretation therefore relies heavily on understanding the (complex) mechanistic relationship of INR to warfarin dose. The coagulation kinetics governing the INR are poorly understood. Few studies were dedicated to improve the current state of knowledge but mostly were conducted or interpreted in cross-section, which greatly limits an in-depth understanding of the entire time course and natural variability in the coagulation proteins and INR [144-146, 158-162].

In this thesis, it is hypothesised that the issues surrounding the poor predictive power of warfarin dosing methods relate to the use of INR as a sole marker of anticoagulation in warfarin dose individualisation. A new approach to predict the INR and warfarin dosing requirement is needed. In **Figure 1.15**, INR response represents a surrogate endpoint of interest in the causal path between warfarin dose and major clotting or bleeding event. However, due to its downstream location on the causal path, INR response is a conglomerate measure of the variability in all of the upstream components: warfarin PK, PD, and the coagulation network. In theory, inclusion of warfarin concentrations (PK marker) and / or coagulation protein concentrations (PD marker) will be helpful in elucidating the relationship from warfarin dose to INR response and in delineating the different sources of variability in anticoagulant response. In this thesis, the vitamin K-dependent coagulation proteins are of primary interest. The coagulation proteins not only provide a signal from the system that lies causally

between warfarin dose and INR response but also represent a measure of the anticoagulant effect that is directly relatable to the (unobserved) warfarin-VKOR interactions (**Figure 1.15**). In addition, due to the proximity of the coagulation proteins to the INR response in the chain of causal events, the coagulation proteins are also expectedly informative and predictive of the INR response.

The overarching motivation for the work conducted in this thesis is the notion that a measure of coagulation protein response will be helpful in improving the prediction of the anticoagulant response and warfarin dose requirement. A choice of a coagulation protein that is particularly sensitive to warfarin and simultaneously, influential on the INR would be appropriate. This requires a working knowledge of the relationship between warfarin dose, warfarin concentrations, coagulation proteins, and INR response (**Figure 1.15**). In this thesis, a comprehensive description of the application of pharmacometric methods to understand the warfarin-coagulation proteins relationships (**Chapter 2**) and then to propose a coagulation protein-based method for the prediction of anticoagulant response to warfarin (**Chapters 3 & 4**) is provided. It is however important to note that the work conducted in this thesis were not set forth to propose a new framework for warfarin dosing that is instantly applicable for clinical use, but to introduce a new perspective on INR prediction.

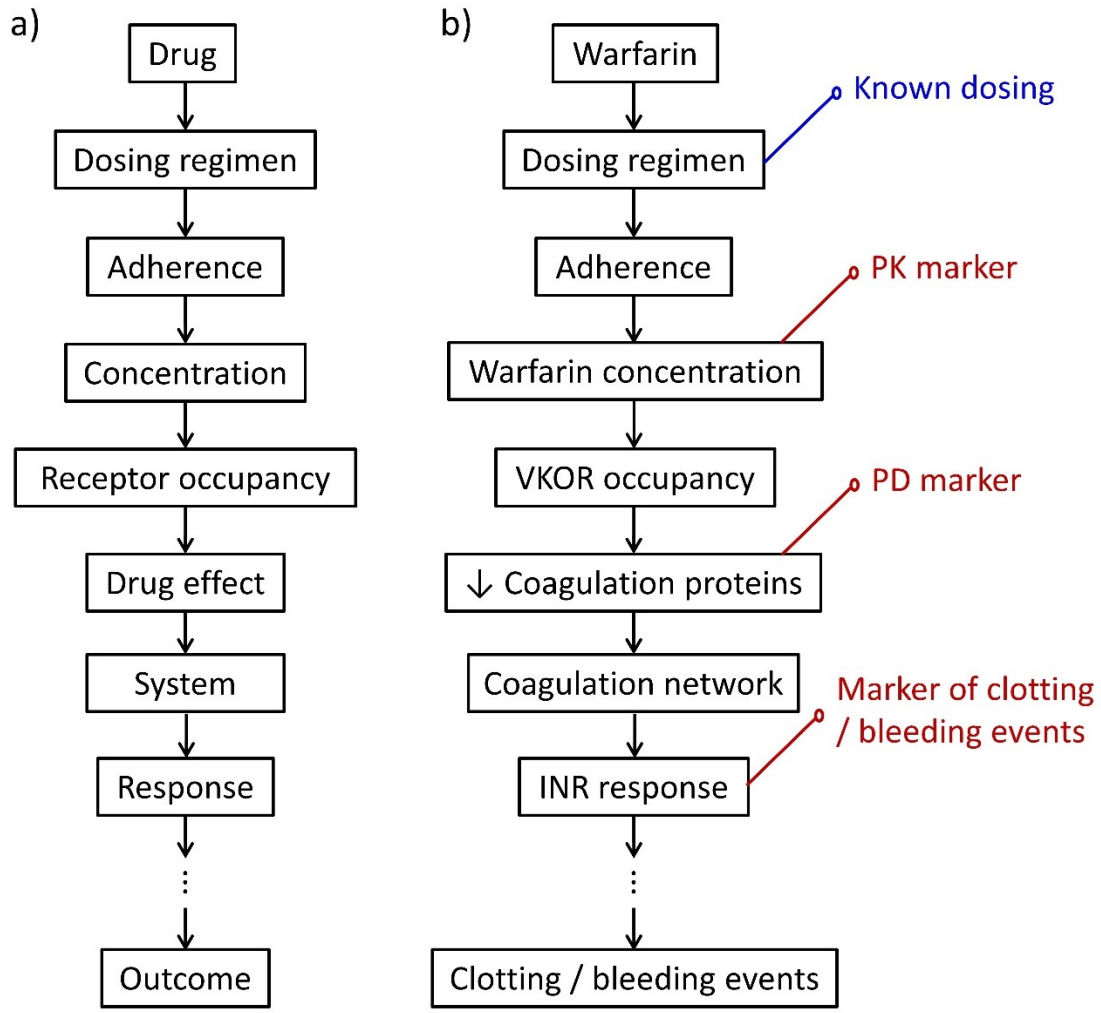

Figure 1.15 *Causal path of warfarin dose response (panel b) mapped to a general causal path framework (Figure 1.8 reproduced here as panel a). INR response is routinely measured as a surrogate marker of major clotting or bleeding events in warfarin patients. Warfarin dose is causally linked to the INR response via warfarin concentration (PK marker) and coagulation protein concentration (PD marker). INR is the international normalised ratio, PD pharmacodynamic, PK pharmacokinetic, and VKOR vitamin K epoxide reductase.*

PART II

WARFARIN-COAGULATION PROTEINS RELATIONSHIP

Chapter 2: A joint model for vitamin K-dependent coagulation proteins

This chapter is based on the following peer-reviewed publication:

Ooi QX, Wright DF, Tait RC, Isbister GK, Duffull SB. *A joint model for vitamin K-dependent clotting factors and anticoagulation proteins*. Clin Pharmacokinet. 2017: 56, 1555-66.

2.1. Introduction

Warfarin exerts its anticoagulant effect by inhibiting the enzyme vitamin K epoxide reductase (VKOR). VKOR reduces vitamin K epoxide to vitamin K quinone and also then converts vitamin K quinone to the active vitamin K hydroquinone form. By inhibiting vitamin K hydroquinone formation, warfarin prevents the production of vitamin K-dependent coagulation proteins (factors II, VII, IX, X, and proteins C and S) that leads to a prolonged clotting time. The clotting time is usually monitored clinically using the international normalised ratio (INR), which is a known marker of clinical outcomes of interest such as major clotting and bleeding events [1].

The time course of anticoagulant response to warfarin has been extensively studied [18, 54, 99, 100, 152, 154, 163, 164]. The majority of the published models link warfarin concentration directly to the INR or prothrombin complex activity, which is a composite measure of various coagulation proteins. In most cases, the published models for warfarin dose response do not account for the coagulation protein response although in theory, they provide a useful signal from the system that lies causally between warfarin concentration and INR response, thereby representing a *direct* measure of warfarin effect.

Analyses of the time course of coagulation proteins in warfarin patients are limited. Most studies employ a naïve pooled approach to analysis or examine individual coagulation protein in isolation and its time course in cross-section, thereby reducing the time courses of anticoagulant responses to snapshot(s) of single coagulation protein response to warfarin [99, 157-159, 161, 165, 166]. Such a simplistic approach to analysis, while quick and convenient, results in a loss of information and individuality of patients in addition to failing to consider the natural variability and correlation between different coagulation proteins. This may have ramifications in understanding and predicting the time course of warfarin effects, for instance, in obtaining an accurate estimate of the degradation half-life of various vitamin K-dependent coagulation proteins and in estimating the time to steady-state of anticoagulant effects.

2.2. *Aims*

The aim of this work was to develop a joint model for the vitamin K-dependent coagulation proteins, factors II, VII, IX, and X and proteins C and S, following warfarin initiation.

2.3. Methods

2.3.1. Data

Clinical data were available from a published study conducted in Glasgow, Scotland [167]. The study was approved by the North Glasgow University Hospitals Ethics Committee and written informed consent from all patients were obtained prior to enrolment.

The study included 18 adult patients (median age 70 years [range 53 - 84] and 11 were male) who were newly diagnosed with atrial fibrillation and initiated on oral daily warfarin according to the Tait and Sefcick warfarin induction regimen [17]. An initial dose of 5mg of warfarin was given for 4 days followed by adjustment of warfarin dose at days 5, 8, and 15 according to INR response [17].

A blood sample was collected at baseline, and at 1 - 5, 8, 15, and 29 days after warfarin initiation for each patient. Vitamin K-dependent coagulation proteins were measured using standard assays: (1) prothrombin time assay on ACL 3000 coagulation analyser for factors II, VII, and X; (2) activated partial thromboplastin time assay on ACL 3000 coagulation analyser for factor IX; (3) chromogenic assay on Amax 400 analyser for functional protein C; and (4) enzyme-linked immunosorbent assay for free protein S. These methods are described briefly in **Appendix A1.1** and more details can be found elsewhere [142]. The samples were not assayed for S- or R-warfarin concentrations as this was not part of the original study design.

The nominal daily dose time was 6 p.m. and the blood sampling time was 11 a.m., except for day 5 where sampling time was reported as 1.30 p.m. Missing dosing records were imputed using the last observation carried forward (LOCF) method.

2.3.2. Statistical analysis

Available data were fitted using a nonlinear mixed-effects model framework in NONMEM® Version 7.2 (ICON Development Solutions, Ellicott City, MD, United States) with the aid of a wrapper function around NONMEM®

(Wings for NONMEM® Version 720, Holford N, Auckland, New Zealand). The first-order conditional estimation method with interaction (FOCE-I) was used for model fitting. An AMD Opteron™ processor and a GNU Fortran compiler (GCC 4.6.0) were employed for the analysis. The convergence criterion was set to three to six significant digits (SIG=3 or SIG=6) and the precision of integration solution was set to nine significant digits (TOL=9).

Initially, concentration-time profiles for the vitamin K-dependent coagulation proteins were modelled independently (termed *individual model*). Then the six models were combined into a single model (termed *joint model*).

For *each* coagulation protein, the observations of the ith individual $\boldsymbol{y_i}(n_i \times 1)$ at specific observation time points $\boldsymbol{t_i}(n_i \times 1)$ was given by the following equation:

$$\boldsymbol{y_i} = \boldsymbol{f}(\boldsymbol{t_i}, \boldsymbol{\beta_i}) \cdot (1 + \boldsymbol{\varepsilon_{prop,i}}) + \boldsymbol{\varepsilon_{add,i}}.$$

Equation 2.1 *Model for the individual coagulation protein observations of the i[th] individual.*

Here, the regression function $\boldsymbol{f}(\boldsymbol{t_i}, \boldsymbol{\beta_i})(n_i \times 1)$ depends on the vector of regression parameters $\boldsymbol{\beta_i}(p \times 1)$ in a nonlinear fashion. A combined error model was used. Vector of proportional errors, $\boldsymbol{\varepsilon_{prop,i}}\ (n_i \times 1)$, corresponds to the portion of residual unexplained variability (RUV) that varies linearly with the magnitude of prediction while additive errors, $\boldsymbol{\varepsilon_{add,i}}\ (n_i \times 1)$, represent the remaining differences between observations and individual-level model predictions. Both error terms were assumed to be normally distributed with a mean of zero and variance of σ^2_{prop} and σ^2_{add}, respectively. Between-subject variability (BSV) was accounted for by a general model for regression parameters $\boldsymbol{\beta_i}$ at individual level:

$$\boldsymbol{\beta_i} = \boldsymbol{\psi}(\boldsymbol{\beta}, \boldsymbol{\eta_i}),$$

Equation 2.2 *Model for the parameters of the i[th] individual.*

where $\boldsymbol{\beta}$ is a $(p \times 1)$ vector of population parameters and $\boldsymbol{\eta_i}$ is a $(p \times 1)$ vector of corresponding between-subject random effects, which were assumed to be normally distributed with a mean of zero and variance of ω^2. $\boldsymbol{\psi}(\boldsymbol{\beta}, \boldsymbol{\eta_i})$ is a p-dimensional vector-valued function with each element linked to the corresponding element in $\boldsymbol{\beta_i}$. A log-linear model (e.g. $CL_i = CL \cdot e^{\eta_i}$) was specified for all elements of $\boldsymbol{\beta_i}$ except for baseline concentration of individual coagulation protein for which a linear model (i.e. $P_{t=0,i} = P_{t=0} + \eta_i$) was considered.

For joint modelling, all the six coagulation proteins were modelled in parallel but shared a *common* kinetic model for warfarin. **Equation 2.1** and **Equation 2.2** described earlier form the statistical basis of joint modelling. Slight modifications were made to account for multiple responses (factors II, VII, IX, X, and proteins C and S). Of primary importance is the addition of coagulation proteins (e.g. factor VII) as a higher-order level preceding individuals and observations in the hierarchical structure of the model.

In one version of the joint model, correlation between the individual parameter estimates (*L1 correlation* in NONMEM® parlance) was introduced by estimating the full covariance matrix of $\boldsymbol{\eta_i}$. The independence assumption of $\boldsymbol{\varepsilon_{prop,i}}$ and $\boldsymbol{\varepsilon_{add,i}}$ was also relaxed. Correlation in residual error space (*L2 correlation*) was allowed by introducing a general covariance structure with non-zero off-diagonal elements for $\boldsymbol{\varepsilon_{prop,i}}$ and $\boldsymbol{\varepsilon_{add,i}}$.

2.3.3. Model development

Because parameter estimations for joint model are sometimes sensitive to initial estimates, individual model for each coagulation protein was developed prior to the construction of the joint model. The final estimates from these individual models were later used as initial estimates in the joint model.

During model development, a kinetic-pharmacodynamic model was used because warfarin concentration-time data were not available. Disposition of warfarin from the body was assumed to be first-order, in accordance with previous studies [18, 31, 54, 98-100, 103, 152, 157, 164]. In our study, the amount

of warfarin in the body, A, was used to drive the inhibitory E_{max} model such that:

$$I_P = 1 - \frac{I_{max,P} \times A}{IA_{50,P} + A},$$

Equation 2.3 *Inhibitory E_{max} model to describe warfarin effect.*

where P is individual coagulation protein, $I_{max,P}$ denotes maximum inhibitory effect and $IA_{50,P}$ represents the amount of warfarin in the body that gives half the $I_{max,P}$. Concentration-time data for each coagulation protein were described with a turnover model and were assumed to have zero-order input ($R_{in,P}$) and first-order output (rate constant $k_{out,P}$). Consistent with our understanding of inhibitory action of warfarin on VKOR, the inhibitory E_{max} function was used to scale $R_{in,P}$ to give the residual synthesis rate of functional vitamin K-dependent coagulation proteins following warfarin exposure. The general system of ordinary differential equations (ODEs) is shown below:

$$\frac{dW}{dt} = -k_a \cdot W; \quad W_{t=0} = D$$

$$\frac{dA}{dt} = k_a \cdot W - \frac{CL}{V} \cdot A; \quad A_{t=0} = 0$$

$$\frac{dP}{dt} = R_{in,P} \cdot I_P - k_{out,P} \cdot P; \quad P_{t=0} = \frac{R_{in,P}}{k_{out,P}}.$$

Equation 2.4 *ODEs for warfarin and coagulation proteins.*

Here CL is the clearance of warfarin, D is the dose, t is the time after dose, V is the volume of distribution of warfarin, and W is the amount of warfarin in absorption depot.

A formal structural identifiability analysis was conducted using popt_i® Version 1.0 (Duffull SB, Dunedin, New Zealand) prior to population analysis [64, 168]. Structural identifiability relates to if a *finite* set of parameter values exist given perfect input-output conditions for the model. In popt_i®, two criteria define structural identifiability: (1) the logarithm of the determinant of the Fisher information matrix (M_F) should have a continuous relationship with the logarithm of the variance of RUV; and (2) the determinant of M_F should approach a non-infinite asymptote as the variance of RUV approaches zero [64]. In the case when the model was found structurally unidentifiable, parameters including both fixed-effects parameters (k_a, CL, V, $I_{max,P}$, $IA_{50,P}$, $P_{t=0}$, $k_{out,P}$) and the corresponding variance were fixed systematically one- or two-at-a-time until a unique solution was obtained for all remaining parameters. Note that fixing V and its variance gave a structurally identifiable model. More details of the identifiability analysis can be found in **Appendix A1.2**.

The final structural model was used for covariate analysis. Two covariates, age and sex, were available. However, age was excluded from the covariate analysis owing to the limited age range (53-84 year old) available in this dataset. Sex was tested as a covariate on liver function-related parameters (CL and $P_{t=0}$) using a forward selection process and an additive shift model.

$$CL_i = (\beta_1 + \beta_2 \cdot sex_i) \times e^{\eta_i}.$$

***Equation* 2.5** *Additive shift model for individual CL.*

2.3.4. Model evaluation

Model selection was based on a reduction in the objective function value (OFV), a reduction in variance of BSV or RUV, and precision of the parameter estimates. For nested models, the likelihood-ratio test was used whereby a reduction in OFV of ≥ 3.84 represents a statistically significant difference for one degree of freedom (df).

Precision of the final parameter estimates was also evaluated based on asymptotic estimates and either likelihood profiling (for the 95% confidence interval [CI]) or jackknife (for standard error [SE]). Likelihood profiling method is based on the likelihood ratio test where parameter estimate values associated with 3.84 units increase from the minimum OFV correspond to a (non-asymptotic) 95% CI around a particular parameter estimate of interest ($df = 1$). In delete-one jackknife analysis, new datasets, which were constructed by deleting all observations of a unique patient one-at-a-time from the original dataset, were fitted using the final model structure. The mean and standard deviation of final parameter estimates from jackknife runs were used for calculation of relative SE (RSE). Only jackknife runs that minimised successfully or ended with rounding errors were used to derive the precision measures [169].

Graphical diagnostics were based on model fits for each individual's data and prediction-corrected visual predictive checks (pcVPC) [170]. For pcVPC, a total of 1000 datasets were simulated from the model using NONMEM®. Simulation results were stratified based on dependent variables. The resulting 50th percentile (median) of the observations and the simulated data, alongside the 10th and 90th percentiles that correspond to an 80% prediction interval, were plotted against time. The corresponding 95% CI for all simulated percentiles was also constructed and graphed. A small prediction interval was chosen because of the small sample size.

2.4. Results

Eight or nine samples for each of factors II, VII, IX, and X and proteins C and S were available for 18 patients. One patient (ID 7) was administered vitamin K on day nine and was excluded from the analysis. In addition, data related to the missing dosing records of ID 6 were censored. The missing dosing records were not imputed using the LOCF method because the imputed doses (0 mg) appeared to contradict the observation that the concentration-time profile of all coagulation proteins for ID 6 were continually suppressed. Concentration-time profiles of relevant coagulation proteins for the 17 patients included in the analysis are shown in **Figure 2.1**.

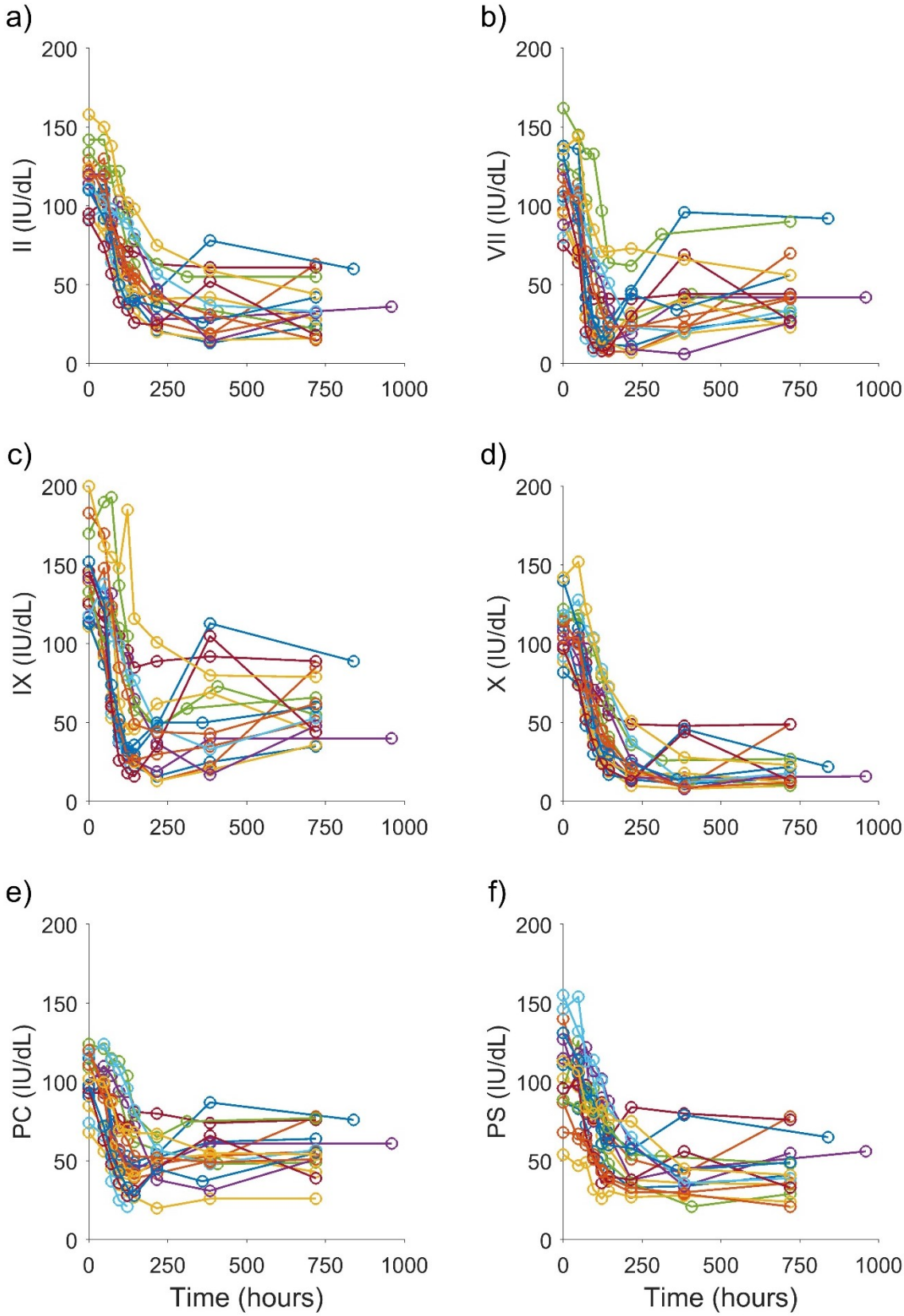

Figure 2.1 *Concentration-time profile of factors II (panel a), VII (panel b), IX (panel c), and X (panel d) and proteins C (panel e) and S (panel f) for all 17 patients after warfarin initiation at time zero. PC is protein C. PS is protein S. The marker indicates observation. The coloured solid line indicates the connector between observations by individual.*

When k_a was estimated during model development, the estimate was found to be much higher than literature values. Therefore, in the final model, k_a and its variance were fixed to values previously estimated [152]. $I_{max,P}$ was fixed to one for the inhibitory E_{max} model as $I_{max,P}$ and $IA_{50,P}$ were found to be highly correlated as shown in **Appendix A1.3**.

Two final *joint* models were developed. The models differed in accounting for natural correlation structures that exist between parameters at the individual level and between residual errors of paired samples. In this work, the joint models were heuristically named the *full joint model* and the *reduced joint model*, respectively, to signify the presence or absence of the correlation structure. It is important to note that both the full and reduced joint models were stable to different initial parameter estimates, the final parameter estimates were similar, and the empirical SE values were of the same order of magnitude. It is important to note that individual model for each coagulation protein was built for the sole purpose of providing reliable initial estimates for joint modeling. Individual models were therefore modelling aids and do not in any way represent modelling endpoints. Model-building results for the individual models are therefore *not* elaborated in this thesis. The remainder of this chapter describes the development of the joint model.

The construction of the joint models was built on several assumptions. The assumptions were evaluated in terms of the probability and impact of assumption violation. The list of assumptions and details of the evaluation are reported extensively in **Chapter 5** and **Appendix 4**.

2.4.1. Full joint model

The BSV correlation matrix has a 13 × 13 dimension corresponding to the 13 parameters (both $P_{t=0}$ and $k_{out,P}$ across all six vitamin K-dependent coagulation proteins and a lag parameter, LAG). Because all the vitamin K-dependent coagulation proteins were assayed in the same blood sample, part of the assay error and all of the process error (e.g. dosing time errors) will be correlated across different coagulation proteins for the same sample. Full L2

correlation was considered but the final model contained separate correlation matrices for proportional and additive error components. The correlation in the individual prediction error (a composite of proportional and additive errors) of the final full model for different coagulation proteins is shown in **Figure 2.2**.

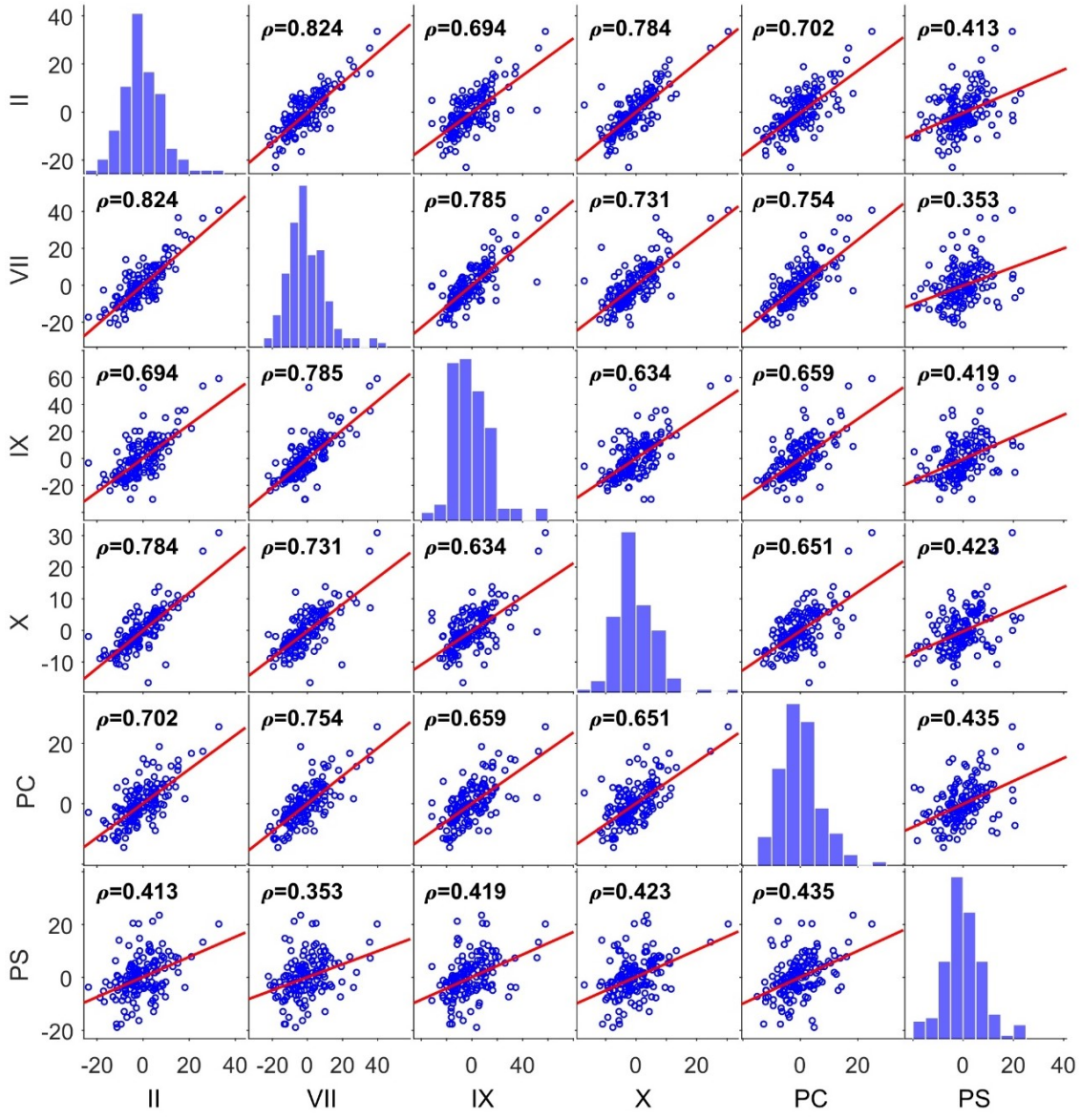

***Figure* 2.2** *Correlation between individual prediction errors of the final full model for factors II, VII, IX, X, and proteins C and S. The individual prediction error is calculated as the difference between observation and individual prediction (IPRED in NONMEM® parlance). The units are IU/dL. ρ denotes Pearson's linear correlation coefficient. PC is protein C. PS is protein S. The red line indicates the corresponding linear function.*

Since the full joint model contains 157 fixed- and random-effect parameters that were estimated from 17 patients who provided 894 data points, it was considered to be at risk of over-parameterisation. Details of the model-building process are summarised in a table in **Appendix A1.4**. The final parameter estimates and the corresponding RSEs of the full joint model are also not presented here but are given in **Appendix A1.5** should need arise to simulate from the full joint model. In view of model complexity, the NONMEM® code with the final estimates inputted for the full joint model is also provided in **Appendix A1.6**. Individual fits and pcVPC can be found in **Appendix A1.7** and **Appendix A1.8**, respectively. Precision of the parameter estimates for this model were evaluated using a jackknife procedure. The remainder of this work describes the development of the reduced joint model.

2.4.2. Reduced joint model

The reduced joint model does not include L1 (BSV) and L2 (RUV) correlation structures. It was built directly from the final joint model by the removal of the L1 and L2 correlation structures. No further model-building steps were taken because the reduced joint model performed comparably to the full model.

The reduced joint model consists of a one-compartment model with first-order absorption and elimination to describe the amount of warfarin in the body, which drives a series of six coagulation protein-specific inhibitory E_{max} functions, each linked to a turnover model. The system of ODEs for the final reduced joint model is shown in **Equation 2.6** and is accompanied by a description of the final model structure in **Figure 2.3** and presentation of the corresponding NONMEM® code with the final estimates inputted in **Appendix A1.9**.

$$\frac{dD}{dt} = -k_a \cdot D; \quad \begin{cases} t < LAG, D_{t=0} = 0 \\ t \geq LAG, D_{t=0} = Dose \end{cases}$$

$$\frac{dA}{dt} = k_a \cdot D - \frac{CL}{V} \cdot A; \quad A_{t=0} = 0$$

$$\frac{dII}{dt} = R_{in,II} \cdot I_{II} - k_{out,II} \cdot II; \quad II_{t=0} = \frac{R_{in,II}}{k_{out,II}}$$

$$\frac{dVII}{dt} = R_{in,VII} \cdot I_{VII} - k_{out,VII} \cdot VII; \quad VII_{t=0} = \frac{R_{in,VII}}{k_{out,VII}}$$

$$\frac{dIX}{dt} = R_{in,IX} \cdot I_{IX} - k_{out,IX} \cdot IX; \quad IX_{t=0} = \frac{R_{in,IX}}{k_{out,IX}}$$

$$\frac{dX}{dt} = R_{in,X} \cdot I_X - k_{out,X} \cdot X; \quad X_{t=0} = \frac{R_{in,X}}{k_{out,X}}$$

$$\frac{dPC}{dt} = R_{in,PC} \cdot I_{PC} - k_{out,PC} \cdot PC; \quad PC_{t=0} = \frac{R_{in,PC}}{k_{out,PC}}$$

$$\frac{dPS}{dt} = R_{in,PS} \cdot I_{PS} - k_{out,PS} \cdot PS; \quad PS_{t=0} = \frac{R_{in,PS}}{k_{out,PS}}$$

$$P = \{II, VII, IX, X, PC, PS\}$$

$$I_P = 1 - \frac{I_{max,P} \cdot A}{IA_{50,P} + A}$$

$$R_{in,P} = P_{t=0} \cdot k_{out,P}$$

Equation 2.6 *ODEs for the reduced joint model.*

In **Equation 2.6**, all parameters were as previously defined with the addition of LAG, which represents a delay in the dose reaching the depot compartment. The final parameter estimates of the reduced model are given in **Table 2.1**. A covariate analysis showed that sex had no significant effect on either CL or $P_{t=0}$.

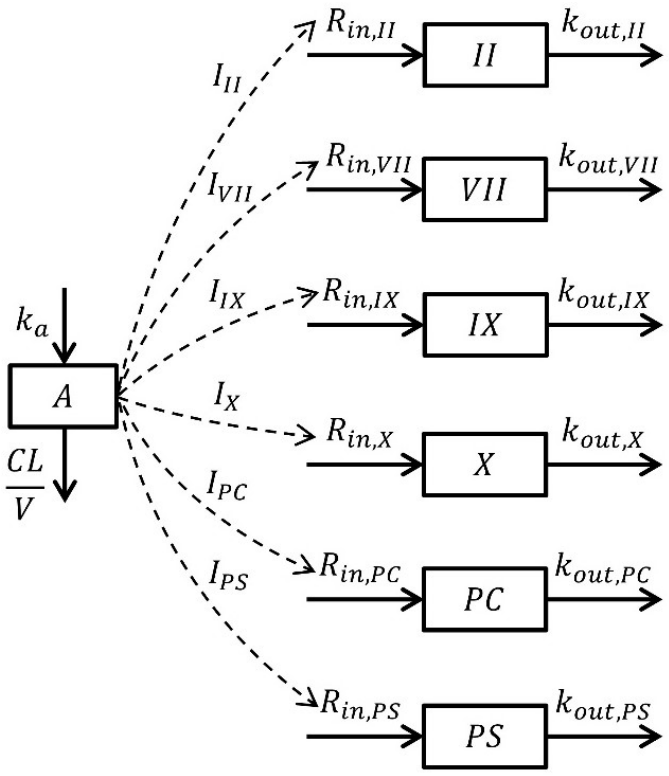

Figure 2.3 *Structure of the final joint model. CL represents the clearance of warfarin, I_P inhibitory E_{max} function, k_a first-order absorption rate constant of warfarin, $k_{out,P}$ first-order coagulation protein degradation rate constant, PC protein C, PS protein S, $P_{t=0}$ coagulation protein concentration at baseline, $R_{in,P}$ zero-order functional coagulation protein production rate (parameterised as $k_{out,P} \cdot P_{t=0}$), V volume of distribution of warfarin. The rectangular box indicates a compartment and its mass balance is represented by one of the ODEs shown in Equation 2.6. The dashed arrow indicates inhibition and the solid arrow mass balance relationship.*

Table 2.1 *Parameter estimates for the final reduced joint model. LAG represents the lag parameter. η_i between-subject variability in parameter. CI confidence interval, CV coefficient of variation, $CV_{prop}P$ coefficient of variation for the proportional error associated with model prediction, CL clearance of warfarin, F bioavailability, $IA_{50,P}$ warfarin amount in the body that gives half the maximum inhibitory effect, $I_{max,P}$ maximum inhibitory effect, k_a first-order absorption rate constant of warfarin, $k_{out,P}$ first-order coagulation protein degradation rate constant, PC protein C, PS protein S, $P_{t=0}$ coagulation protein concentration at baseline, V volume of distribution of warfarin, ω standard deviation of between-subject variability in parameter, $\sigma_{add,P}$ standard deviation for the additive error associated with model prediction. Square bracket indicates inclusive of the value stated in the bracket. Parenthesis indicates exclusive of the value stated in the parenthesis.*

Parameter	Final estimate (η_i-shrinkage)	95% CI[a]
F	1.00 fixed	–
k_a (h^{-1})	1.19 fixed[b]	–
CL (L/h)	0.211	[0.136, 0.323]
V (L)	8.06 fixed[b]	–
$I_{max,II}$	1.00 fixed	–
$I_{max,VII}$	1.00 fixed	–
$I_{max,IX}$	1.00 fixed	–
$I_{max,X}$	1.00 fixed	–
$I_{max,PC}$	1.00 fixed	–
$I_{max,PS}$	1.00 fixed	–
$IA_{50,II}$ (mg)	1.83	[1.34, 2.41]
$IA_{50,VII}$ (mg)	1.86	[1.38, 2.43]
$IA_{50,IX}$ (mg)	2.41	[1.79, 3.14]
$IA_{50,X}$ (mg)	0.875	[0.631, 1.160]
$IA_{50,PC}$ (mg)	5.21	[3.93, 6.59]
$IA_{50,PS}$ (mg)	3.35	[2.46, 4.39]
$II_{t=0}$ (IU/dL)	115	[104, 125]
$VII_{t=0}$ (IU/dL)	115	[98, 134]
$IX_{t=0}$ (IU/dL)	141	[128, 155]
$X_{t=0}$ (IU/dL)	109	[99, 118]
$PC_{t=0}$ (IU/dL)	101	[92, 111]
$PS_{t=0}$ (IU/dL)	105	[92, 118]
$k_{out,II}$ (h^{-1})	0.0135	[0.0108, 0.0171]
$k_{out,VII}$ (h^{-1})	0.0570	[0.0358, 0.0946]
$k_{out,IX}$ (h^{-1})	0.0323	[0.0208, 0.0523]
$k_{out,X}$ (h^{-1})	0.0157	[0.0129, 0.0192]
$k_{out,PC}$ (h^{-1})	0.0376	[0.0234, 0.0663]
$k_{out,PS}$ (h^{-1})	0.0122	[0.0103, 0.0146]
LAG (h)	12.5	[10.4, 14.2]
CV k_a (%)	73.0 fixed[b] (83.1%)	–

Parameter	Final estimate (η_i-shrinkage)	95% CI[a]
CV CL (%)	82.2 (0.6%)	[55.9, 145.5]
CV $IA_{50,PC}$ (%)	13.4 (45.9%)	(0, 29.2]
$\omega\ II_{t=0}$ (IU/dL)	17.8 (1.2%)	[10.6, 25.2]
$\omega\ VII_{t=0}$ (IU/dL)	26.9 (5.9%)	[17.7, 42.3]
$\omega\ IX_{t=0}$ (IU/dL)	25.0 (6.1%)	[16.2, 39.1]
$\omega\ X_{t=0}$ (IU/dL)	17.5 (1.7%)	[12.4, 26.0]
$\omega\ PC_{t=0}$ (IU/dL)	17.4 (1.7%)	[12.2, 25.8]
$\omega\ PS_{t=0}$ (IU/dL)	24.4 (-0.6%)	[17.8, 35.8]
CV $k_{out,II}$ (%)	41.4 (6.8%)	[27.3, 66.7]
CV $k_{out,VII}$ (%)	92.6 (14.7%)	[54.4, 192.1]
CV $k_{out,IX}$ (%)	89.6 (11.0 %)	[53.6, 182.0]
CV $k_{out,X}$ (%)	36.3 (4.7%)	[24.6, 56.8]
CV $k_{out,PC}$ (%)	91.2 (12.1%)	[53.9, 194.4]
CV $k_{out,PS}$ (%)	19.0 (37.5%)	(0, 38.7]
$\sigma_{add}II$ (IU/dL)	7.11	[5.62, 8.56]
CV$_{prop}II$ (%)	3.69	(0, 7.56]
$\sigma_{add}VII$ (IU/dL)	8.80	[5.34, 12.75]
CV$_{prop}VII$ (%)	15.3	(0, 24.5]
$\sigma_{add}IX$ (IU/dL)	11.0	[7.1, 14.0]
CV$_{prop}IX$ (%)	10.9	[1.5, 17.3]
$\sigma_{add}X$ (IU/dL)	5.41	[4.35, 6.64]
CV$_{prop}X$ (%)	5.96	[1.72, 8.93]
$\sigma_{add}PC$ (IU/dL)	3.89	(0, 6.69]
CV$_{prop}PC$ (%)	8.58	[2.99, 12.27]
$\sigma_{add}PS$ (IU/dL)	3.33	(0, 5.97]
CV$_{prop}PS$ (%)	10.6	[7.5, 13.5]

[a] Given by likelihood profiling. Note that the lower bound of some 95% CIs has a value of zero, which is an asymptotic value.
[b] Sourced from values estimated by Wright *et al.* [152].

A delay between warfarin exposure and coagulation protein reduction (e.g. factors VII and IX) was observed during model development. Two models for delay were proposed, a general lag model (note LAG in **Equation 2.6**) and a coagulation protein storage model.

The general lag model introduces a delay via inclusion of a parameter, LAG, that acts by delaying warfarin input into the absorption depot. In contrast, the storage model incorporates a reservoir of vitamin K-dependent coagulation proteins that needs to be depleted prior to a reduction in plasma coagulation proteins. The size of the coagulation protein storage at baseline ($P\_S_{t=0}$) therefore functions as a lag parameter. Note that once the reservoir is depleted

no further delay will be seen on subsequent warfarin doses. Using factor VII as an example, the proposed structure of the storage model is compared and contrasted with the general lag model in **Figure 2.4**.

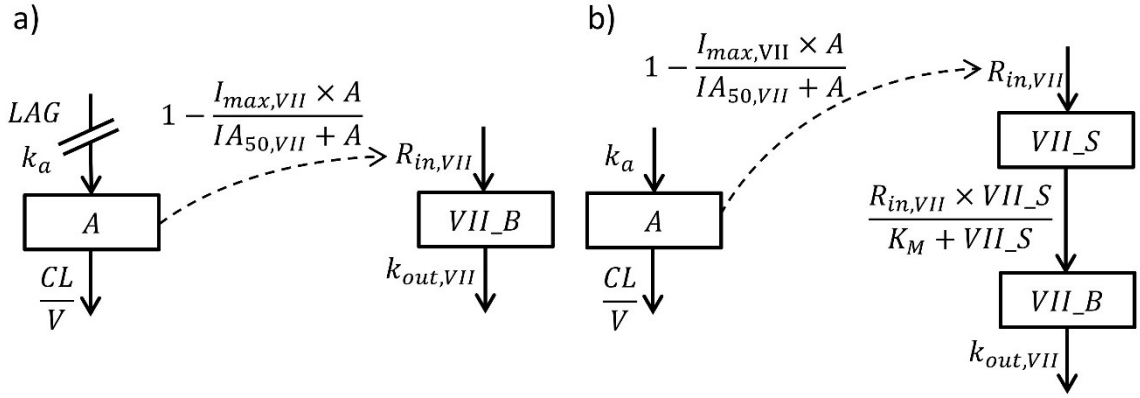

Figure 2.4 *Alternative models to account for the delay between warfarin exposure and factor VII reduction. Panel a shows the general lag model and panel b represents the storage model. A represents the warfarin in the body, CL clearance of warfarin,* $IA_{50,VII}$ *warfarin amount in the body that gives half the maximum inhibitory effect,* $I_{max,VII}$ *maximum inhibitory effect,* k_a *first-order absorption rate constant of warfarin,* K_M *Michaelis–Menten constant,* $k_{out,VII}$ *first-order degradation rate constant for factor VII, LAG general lag parameter,* $R_{in,VII}$ *zero-order production rate of functional factor VII (parameterised as* $k_{out,VII} \cdot VII\_B_{t=0}$*), V volume of distribution of warfarin, VII_B factor VII in the blood compartment,* $VII\_B_{t=0}$ *factor VII in the blood compartment at baseline, VII_S factor VII in the storage compartment. The rectangular box indicates the compartment. The dashed arrow indicates inhibition and the solid arrow indicates the mass balance relationship.*

Characteristics of the general lag model and the storage model for factor VII were explored via simulations using MATLAB® Version 2015a (The MathWorks, Inc., Natick, Massachusetts, United States). For the simulations of the general lag model, population parameter estimates from the best individual model for factor VII, which contains a LAG parameter, was used. Simulations of the storage model, on the other hand, proceeded with the removal of the LAG parameter and imputation of the factor VII storage structure (**Figure 2.4**).

For *single* warfarin dose simulation within the storage model framework, *panel a* in **Figure 2.5** shows that time to factor VII nadir appeared to be fairly insensitive to a change in K_M. *Panel b* in **Figure 2.5** reveals that time to factor VII

nadir increased with larger values of $VII\_S_{t=0}$, which confirmed the ability of $VII\_S_{t=0}$ to function as a delay parameter. Of all the storage models, storage model with $VII\_S_{t=0} = 110$ IU/dL and $K_M = 1$ IU/dL had simulated factor VII profile most similar to that of the best general lag model ($LAG = 15.9$ hours) for factor VII in terms of time to nadir.

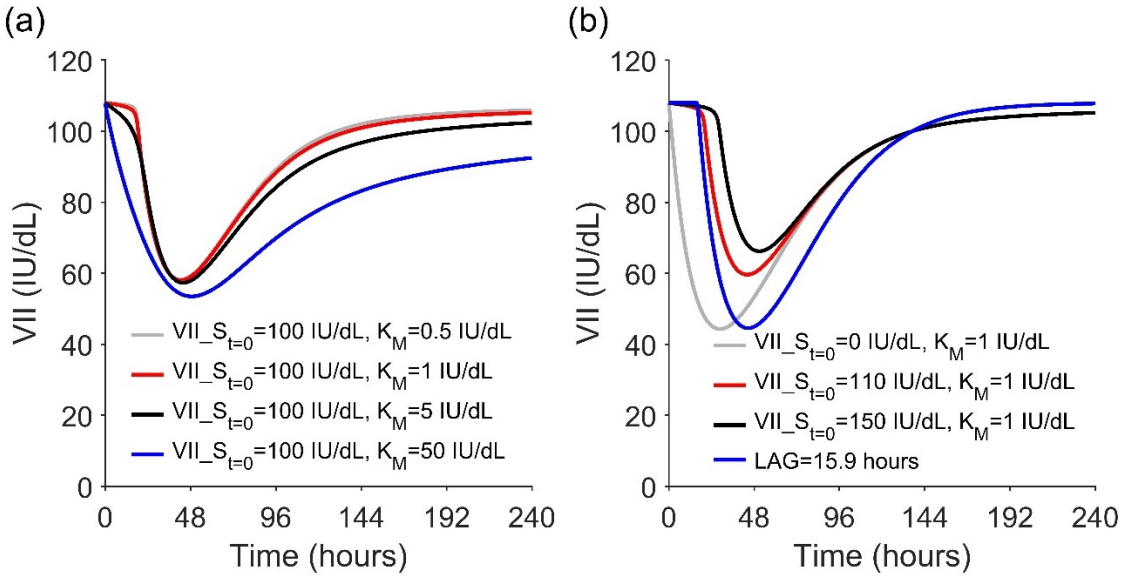

Figure 2.5 *Factor VII profiles simulated using different magnitudes of K_M (panel a) or $VII\_S_{t=0}$ (panel b) after single 5 mg warfarin dose administration. The blood compartment was observed. LAG is the general lag parameter, K_M represents the Michaelis–Menten constant and $VII\_S_{t=0}$ denotes factor VII in the storage compartment at baseline.*

Available factor VII data were fitted using the general lag model and the storage model in NONMEM®. On the basis of the likelihood-ratio test, both the general lag model ($\Delta OFV = -36.6$) and the best storage model ($\Delta OFV = -26.2$) were found to be superior to the base model for factor VII. However, the general lag model was more parsimonious and provided a better statistical representation of the data in terms of OFV. In the joint model framework, LAG was estimated as 12.5 hours and was statistically preferred to be present on each dose.

2.4.3. Model evaluation

The 95% CI of the parameter estimates was evaluated by likelihood profiling and is shown in **Table 2.1**. It is seen that all fixed- and random-effects parameters of the reduced joint model were estimated with reasonably good precision. The conditional-weighted residuals versus time plots show no discernible trend (see **Appendix A1.10**). Model misspecification was not evident.

Individual fits of the concentration–time profile of vitamin K-dependent coagulation proteins for the reduced joint model organised according to patient identifier are shown in **Appendix A1.11**. Plots of five representative individuals are shown in **Figure 2.6**. Of note, the model appeared to overpredict the nadir for factors VII and IX for ID 2, ID 4, ID 5, ID 9, ID 10, ID 11, ID 13, ID 15, ID 16 and ID 17. All data were otherwise well characterised but with a worse fit noted at later time points when sampling was sparse.

The pcVPCs of the reduced model for each vitamin K-dependent coagulation protein are depicted in **Figure 2.7**. For the reduced model, the median of the data simulated from the final model were in close agreement with that of observed data. However, as with individual fit results, overprediction of the nadir was observed whereby the median model predictions appeared to overpredict median concentrations of factors VII and IX at 41, 65 and 91.5 hours after warfarin initiation (see **Figure 2.7**).

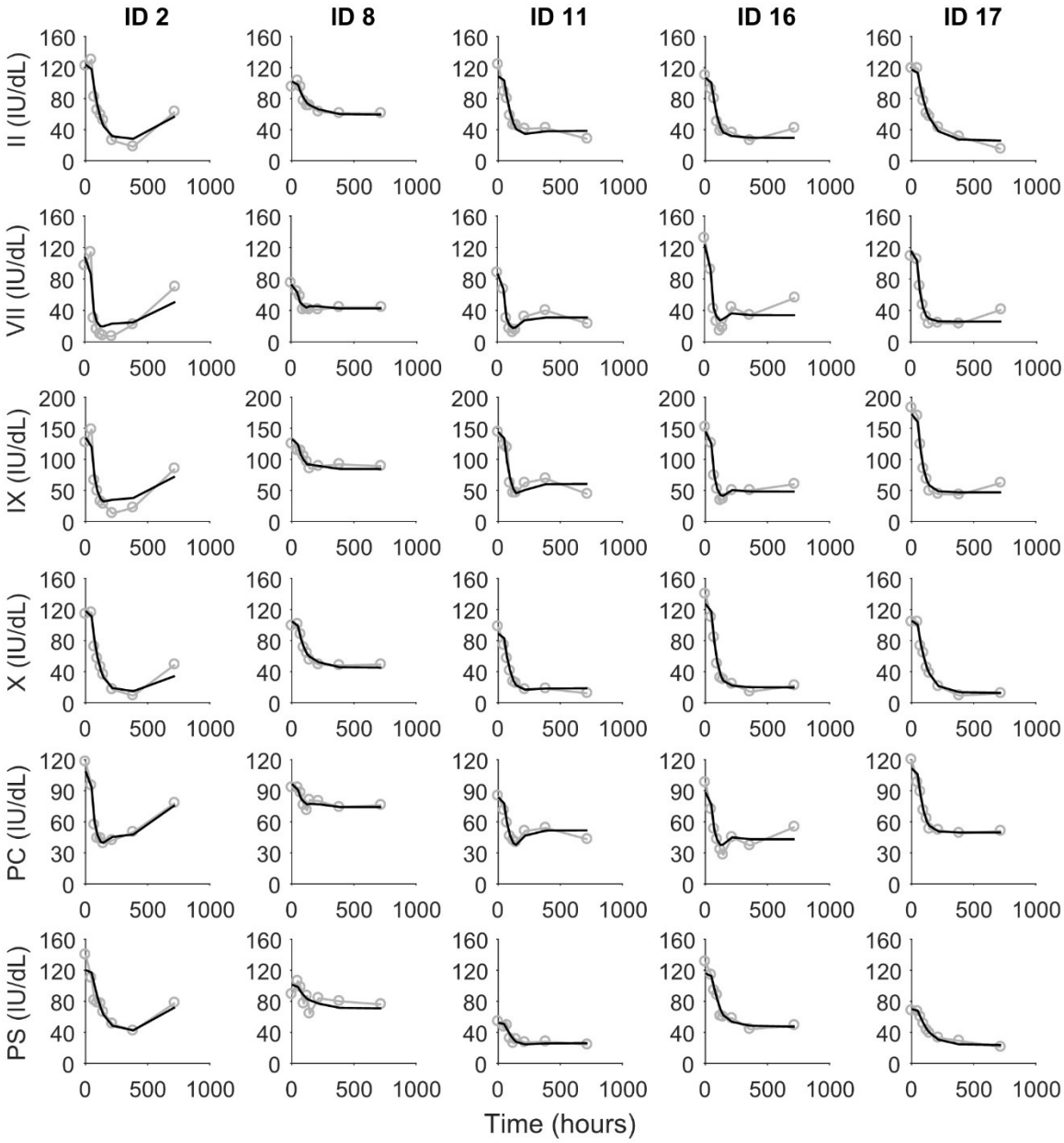

Figure 2.6 *Individual fits for the time course of factors II, VII, IX, X, and proteins C and S for five representative individuals following warfarin initiation. The black lines are predictions from the final reduced joint model. The grey markers are observations. PC denotes protein C and PS represents protein S.*

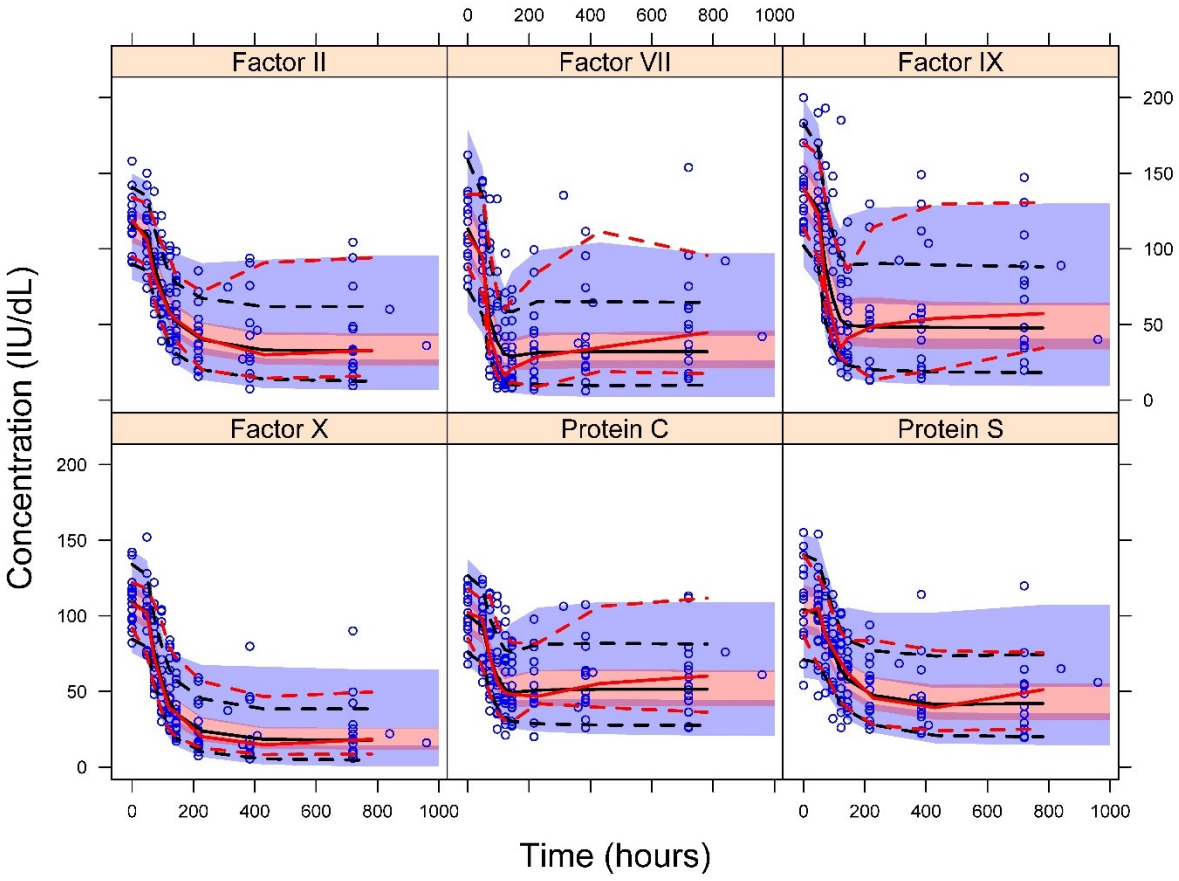

Figure 2.7 *pcVPC for factors II, VII, IX and X, and proteins C and S based on the final reduced joint model. The blue circle indicates observation. The black solid line indicates the median of simulated data. The red solid line indicates the median of observed data. The black dashed line indicates the 10th and 90th percentiles of simulated data that correspond to the 80% prediction interval. The red dashed line indicates the 10th and 90th percentiles of observed data that correspond to the 80% prediction interval. The shaded area indicates the 95% confidence interval around the simulated percentiles. pcVPC stands for prediction-corrected visual predictive checks.*

The problem of overpredicting the nadir was further investigated using the factor VII framework as an exemplar. A mixture model for $IA_{50,VII}$ as well as inclusion of a variance component for BSV of $IA_{50,VII}$ did not improve the model fit. Two causes were postulated: (1) an unaccounted for process error (e.g. unrecorded dose change) or (2) an aspect of the underlying biology was not effectively captured. Simulation of factor VII concentration–time profiles showed that accounting for possible dose adjustment or incorporating a shape parameter for the inhibitory E_{max} function, γ, provided a better prediction of

observations compared with the original model (see **Figure 2.8**). Although estimation of γ as 1.96, to some extent, alleviated the problem in some individuals, improvement in the pcVPC was not apparent (not shown). Because these two approaches were exploratory and, in this setting, model misspecification based on mechanism or on process error provided similar benefits in the model prediction, neither was taken forward into the final model.

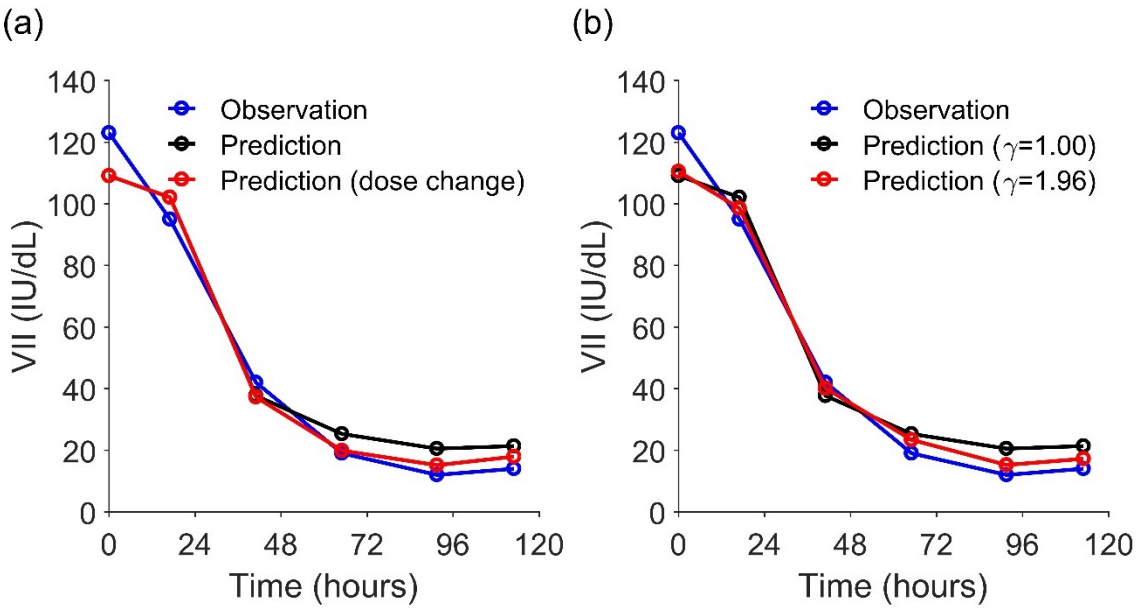

Figure 2.8 *Simulating overprediction of nadir as a result of unrecorded dose change (panel a) and biology (panel b) with duration of simulation of up to 120 hours. γ is the shape parameter for the inhibitory E_{max} function.*

2.5. Discussion

Two final joint models were developed from this work and were able to accurately describe the time course of warfarin influence on all six vitamin K-dependent coagulation proteins. In both models, the parameter values of all vitamin K-dependent coagulation proteins were estimated simultaneously but differed with respect to their correlation structures. The full joint model considered the full correlation structures that exist between parameters at the individual level and between residual errors within blood samples. However, because it is likely that the final full joint model is overparameterised owing to the sheer size of the correlation matrices that are required to be estimated, details of the full joint model are provided as additional material in the appendices and the reduced joint model is reported primarily in this chapter. The full joint model may be more useful for modellers who are interested in simulating from the model, whereas the reduced joint model is preferable for estimation purposes when computation time is a concern or when model parsimony is a priority. It is worth noting that both the full and reduced joint models are largely similar in terms of individual predictions in addition to having empirical SE values that are similar. Both models also have comparable final parameter estimates but CL estimates are somewhat different (percentage difference 49.3%). $IA_{50,P}$ estimates are also different, which most likely arise from a correlation between CL and $IA_{50,P}$.

The KPD model used differs from those reported in the published literature. In this work, the amount of warfarin in the body was used to drive the inhibitory E_{max} function (**Equation 2.3**) rather than the elimination rate [54, 59, 60]. It is thought that the use of the elimination rate as a driver of pharmacodynamic effects is not pharmacologically intuitive and likely to be inconsistent with classical receptor theory underpinning drug effects. The results of the current analysis are broadly similar to those in the published literature. The CL estimate, 0.211 (95% CI 0.136–0.323) L/h, is in close agreement with reported values that range from 0.127 to 0.333 L/h (see **Table 2.1**) [99, 104]. The degradation half-life of factors II, VII, IX and X, and proteins C and S was

estimated as 51.3, 12.2, 21.5, 44.1, 18.4, and 56.8 hours, respectively, while reported values range from 72–115, 5–35, 18–40, 35–63, 8–32, and 43 hours, respectively [99, 159, 161, 165, 171-175]. Factor VII was found to have the shortest degradation half-life compared to other coagulation proteins. Then, upon warfarin initiation, factor VII is likely the first to decline and to reach a new steady-state level. This is supported by data shown in **Figure 2.1**.

It is worth noting that the reported half-life should be interpreted with caution for coagulation proteins with a shorter plasma half-life than warfarin, i.e. when $k_{out,P} \gg k$ (e.g. factors VII, IX, and protein C), as $k_{out,P}$ was found to be less precisely estimated (see **Table 2.1**). This is not unexpected because the time course of observed coagulation protein concentrations will likely reflect the rate-limiting step in the causal path from warfarin dose to response and therefore will appear relatively uninformative of other steps. However, within the *joint* modelling framework, the same cannot be said for the estimation of k or CL when the degradation of the coagulation proteins is the rate-limiting step (i.e. $k_{out,P} \ll k$). In the joint model, even though the coagulation proteins with $k_{out,P} \ll k$ (e.g. factors II, X, and protein S) is uninformative of k, estimation of k can be informed by other coagulation proteins with $k_{out,P} \gg k$ (e.g. factors VII, IX, and protein C). This illustrate an important advantage of the joint model compared to modelling each coagulation protein individually.

There have been few published analyses examining the time course of the coagulation proteins in response to warfarin therapy. To date, only two population analyses have been performed and both modelled the warfarin-factor VII relationship [157, 165]. No models have been developed for the other coagulation proteins including factor II (prothrombin), which is an important determinant of *in vivo* prothrombin activation for clotting. In the majority of warfarin-coagulation protein studies, only the time to new steady state was quantified or, in some cases, nadir or depression of vitamin K-dependent coagulation proteins at selected time points after warfarin initiation was compared and contrasted to base concentrations [99, 157-159, 161, 165, 166]. In these studies, individual coagulation protein was studied in isolation and its

time course was typically examined in cross-section. This limits the supposed entire time course of anticoagulant responses to a snapshot of a single coagulation protein response to warfarin. In contrast, the model developed in this work, by *jointly* modelling factors II, VII, IX and X, and proteins C and S, during warfarin initiation, provides a means of quantifying the temporal influence of warfarin to all six vitamin K-dependent coagulation proteins *simultaneously*.

A delay in the onset of coagulation protein reduction was observed, which was evident for factors VII and IX. A similar delay has been reported in previous studies [140, 157, 165] but the exact mechanism for the delay is unknown. The most prevalent hypothesis to explain the delay is the presence of a storage pool of vitamin K that becomes the rate-limiting step in the inhibition of the biosynthesis of vitamin K-dependent coagulation proteins [140, 157, 176, 177]. In this study, the delay was addressed using two models: a general lag model and the storage model. In the lag model, a LAG parameter served as a heuristic solution to the observed delay and should not be interpreted as an absorption lag parameter *per se* but rather an all-purpose lag parameter that covers dose time deviation, delay in warfarin absorption, and delay in the influence of warfarin on factor production. Previously published LAG estimates for factor VII data (6.90 and 10.9 hours, respectively) and for prothrombin complex activity data (8.00 hours) are comparable to that found in this study (12.5 hours), which was consistent across all doses [140, 157, 165]. In contrast, the storage model provides a potential mechanism and accounts for a coagulation protein-specific delay. However, the storage model only accounted for a single reservoir (and hence effective for first-dose delay only) and therefore it lacks the flexibility of the general lag model in terms of modelling repeated lag. In the absence of evidence regarding the mechanism of the lag, model selection can only be guided by statistical improvements in the model. It is important to note that the mechanisms of lag presented here are by no means exhaustive. Other mechanisms of lag, for instance, process error or existence of a storage pool of vitamin K hydroquinone, could be considered and explored in future studies.

In this work, overprediction of the nadir in factors VII and IX was identified. There are many potential sources for the overprediction and these could include a process error as simple as a dose change recording error to an unexpectedly more complicated biology of warfarin activity. Both were considered in model-building and both improved the fit. In the absence of confirmatory mechanistic data, parsimony supports discounting the more complicated mechanism. It is important to note that an estimated empirical shape parameter for the sigmoid E_{max} model, γ, is not uncommon in published warfarin models to describe the time course of INR, prothrombin complex activity, or factor VII, presumably because its inclusion is associated with improved goodness-of-fit [18, 54, 100, 103, 140, 157, 165]. In this study, γ was estimated as 1.96, which is incorporated within the previous published values (range 0.424–2.83) [18, 54, 100, 103, 140, 157, 165].

Our work has several drawbacks. Because warfarin concentration–time data were not available, then V and its variance were not structurally identifiable. In addition, owing to the delayed time course of changes in coagulation proteins and sparse sampling relative to the time course of warfarin absorption, it was found that k_a of warfarin and its variance were not deterministically identifiable. A sensitivity analysis did not reveal a dependence of the final model on the choice of k_a. It is worth noting that our sample size is small ($n = 17$), thus potentially limiting generalisability of the study's results to all warfarin users. In addition, while likelihood profiling was used for precision assessment of the parameter estimates for the reduced joint model it was not used for the full joint model. Likelihood profiling requires a repeated estimation of model parameters for each instance when an individual parameter is fixed to different values. Challenges in ensuring positive definiteness in correlation matrix (over 157 correlation terms) during likelihood profiling together with significant computation time rendered likelihood profiling unsuitable for the full joint model. Instead, a delete-1 jackknife was used for the full joint model. Even though jackknife estimates of SE are asymptotically consistent and unbiased [178], it may have dubious properties for small samples [179]. Nevertheless, the

jackknife SE estimates obtained in this study appeared reliable considering their alignment with likelihood profiling for the reduced model. Furthermore, in accordance with previous studies, jackknife SE estimates even in small sample situations have been shown to be in close agreement with SE obtained by non-parametric bootstrap, which is traditionally employed to evaluate the precision of model parameters [19, 180].

The model developed provides an initial framework for mechanistic insight into warfarin exposure and response, which is traditionally studied empirically using the pharmacokinetics and INR data of warfarin. A mechanistic and comprehensive depiction of warfarin exposure and response can be obtained by the incorporation of two additional components (vitamin K cycle and INR) to the warfarin-coagulation protein model developed. Integration of the vitamin K cycle as an intermediary step between warfarin exposure and coagulation protein response would allow the complex interactions between warfarin and vitamin K to be taken into consideration. This will be useful in understanding and predicting the time course of coagulation proteins after warfarin reversal with vitamin K in warfarin toxicity or for the prevention of perioperative bleeding. A comprehensive warfarin-vitamin K-coagulation protein-INR model also represents the first step towards understanding transient warfarin resistance, a phenomenon where the use of vitamin K for warfarin reversal frequently leads to curiously prolonged resistance to warfarin (>7 days) despite warfarin reintroduction. This has important clinical utility in the determination of the appropriate vitamin K dose, time, and frequency for warfarin reversal.

2.6. Conclusions

A joint model for the vitamin K-dependent coagulation proteins following warfarin initiation is developed. The model adequately quantifies the time course of warfarin influence on factors II, VII, IX, and X, and proteins C and S simultaneously. Factor VII was found to have the shortest degradation half-life compared to other coagulation proteins thereby representing the coagulation protein that is the first to decline and to reach a new steady-state level following a perturbation introduced by warfarin. The influence of various vitamin K-dependent coagulation proteins on the INR is discussed in **Chapter 3** and **Chapter 4**.

An important future step, although beyond the scope of the thesis, would be to incorporate the vitamin K cycle as an intermediary step between warfarin exposure and response, as well as to integrate INR into the model. This provides a focused framework describing the relationships between warfarin, vitamin K cycle, vitamin K-dependent coagulation proteins, and INR that would be useful for systematic exploration of complex clinical problems (e.g. warfarin reversal with vitamin K and transient warfarin resistance) involving multiple systems and coagulation components.

PART III

WARFARIN-COAGULATION PROTEINS-INR RELATIONSHIP

Chapter 3: Understanding the coagulation kinetics governing the international normalised ratio (INR)

This chapter is based on the following peer-reviewed publication:

Ooi QX, Wright DF, Isbister GK, Duffull SB. *A factor VII-based method for the prediction of anticoagulant response to warfairn*. Sci Rep. 2018: 8, 12041.

The following two chapters outline the conception and development of a prediction method to quantify the anticoagulant response for warfarin dose individualisation. Despite a significant body of literature in this area, algorithms for predicting warfarin maintenance dose in patients remain inaccurate [2-7]. It is believed that much of these issues relate to the use of the international normalised ratio (INR) solely as a marker of coagulation. In routine clinical settings, the prediction of steady-state INR relies heavily on the interpretation of non-steady-state INR, which requires a working knowledge of the relationship between warfarin exposure, coagulation proteins and INR response, a relationship that is inherently nonlinear, and therefore, not necessarily intuitive. The motivation for this work is the overarching belief that a measure of coagulation protein response in addition to INR will better inform the steady-state INR prediction. A choice of coagulation protein that is particularly sensitive to warfarin would therefore be appropriate to aid interpretation of the observed INR value for future INR prediction.

Chapter 3 explores the coagulation kinetics underpinning the INR using a sensitivity analysis and an isobologram analysis. It seeks to identify an appropriate coagulation protein that provides a signal from the system that lies causally between warfarin exposure and INR that would be useful for INR prediction. This is followed by **Chapter 4**, which incorporates the information from the aforementioned coagulation protein of choice for the prediction of future INR in patients receiving warfarin. The methods used are based on approximations to a quantitative systems pharmacology (QSP) model and new insights are provided on the time to steady-state INR as an integral part of the process.

3.1. Introduction

The prothrombin time (PT) test, which is typically reported as the INR in routine clinical setting, is an *in vitro* blood test designed to measure the clotting time of blood as a proxy to the anticoagulant response. Both PT and INR provide a composite and blunt measure of coagulation activity related to fibrinogen, factors II, V, VII, and X but are generally unable to delineate contribution from individual coagulation proteins [136, 137].

Exploration of the coagulation kinetics using standard experimental designs is difficult [31] due to (1) the complex positive-feedback, negative-feedback, positive-feedforward, and negative-feedforward reactions that makes snapshot views of components of the coagulation network incomplete, potentially leading to descriptions that are incompatible with known mechanisms, (2) the different orders of magnitude in the rate of change of some components of the coagulation network, in addition to the diverse turnover rate of the different components ranging from seconds to days (i.e. multiscale on the time domain), and (3) the fact that the act of drawing a blood sample can itself activate the coagulation system.

Using a QSP model, experiments that would otherwise be impossible or logistically impractical to undertake can be conducted. In this work, an *in silico* approach that was based on simulations from a (mechanistic) QSP model was used for exploring the influence of coagulation proteins and their complex interactions on the INR.

3.2. *Aims and objectives*

The aim of this simulation study was to understand the coagulation kinetics underpinning the non-steady-state and steady-state INR to identify a coagulation protein of choice that is informative of the INR for future INR prediction. To this end, there were two specific objectives: (1) to evaluate the sensitivity of INR to a reduction in an individual coagulation protein in a single coagulation protein deficiency and multiple coagulation protein deficiency, and (2) to quantify the nature of interactions (sub-additivity, additivity, or supra-additivity) between coagulation proteins with respect to the INR.

3.3. Methods

The method section describes the definitions employed, model evaluation, simulation of PT and INR tests, sensitivity analysis, and isobologram analysis conducted in this work.

3.3.1. Definitions

For the purpose of this work, steady-state INR is defined as the INR that is no longer transitioning (i.e. changing over time). Mathematically, the steady-state INR is represented by $\frac{dINR}{dt} = 0$ for $t > 0$. Single coagulation protein deficiency is defined as a deficiency in a single coagulation protein whereas multiple coagulation protein deficiency refers to a deficiency in more than one coagulation protein simultaneously.

3.3.2. Model evaluation

In this work, a QSP model of the coagulation network, which was developed by Wajima and colleagues [31] and later updated by Gulati and peers [38], was used for simulation of warfarin therapy and the corresponding effect on the coagulation proteins and the INR. The model consists of 63 compartments and includes components of *in vivo* coagulation as well as *in vitro* blood coagulation tests (e.g. PT and INR tests). The model was previously applied to simulating PT and INR and was found to provide an adequate description of the data from the literature [31, 83]. See **Figure 3.1** for a schematic of the structure of the model.

An important prerequisite to the use of the model for this simulation study is that the model provides an adequate description of the relationship between warfarin, coagulation proteins, and INR. Here, the model was evaluated using an external test dataset [167, 181]. In this dataset, dosing and anticoagulant response data from 17 patients with atrial fibrillation who had warfarin therapy initiated were available for analysis. Nine blood samples were collected from each patient at baseline, and at 1-5, 8, 15 and 29 days after warfarin initiation and

assayed for factors II, VII, IX, and X, and INR. Warfarin concentration-time data were not available.

For model evaluation, missing dosing records in the external test dataset were imputed using last observation carried forward. Then, using available dosing information, factors II, VII, IX, and X, and INR response were simulated from the QSP coagulation network model in MATLAB® Version 2015a (The MathWorks Inc., Natick, Massachusetts, USA) using parameter values for a typical individual [31]. The predictive performance of the QSP coagulation network model was evaluated visually based on the level of agreement between plots of individual observed and simulated time course data.

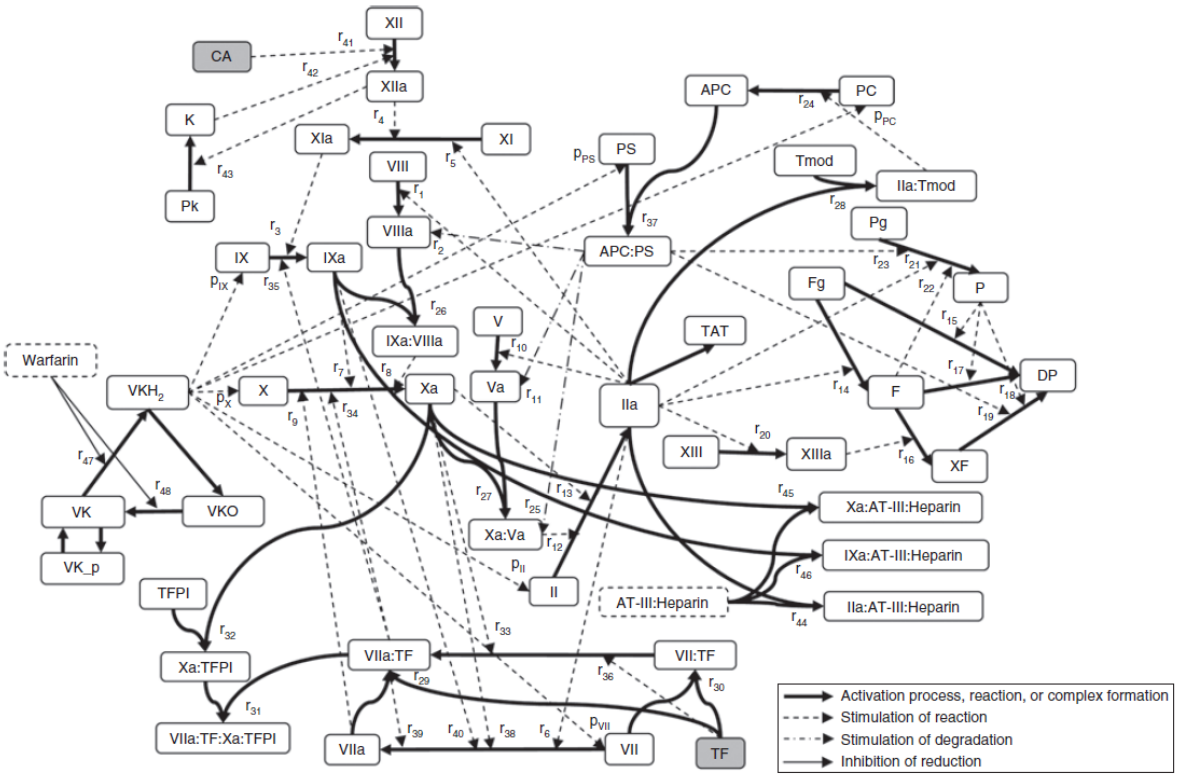

Figure 3.1 *Schematics of the coagulation network model [31]. APC represents activated protein C, AT-III antithrombin-III, CA contact activator, DP degradation product, F fibrin, Fg fibrinogen, II factor II, IIa thrombin, K kallikrein, P plasmin, PC protein C, Pg plasminogen, Pk prekallikrein, PS protein S, TAT thrombin-antithrombin complex, TF tissue factor, TFPI tissue factor pathway inhibitor, Tmod thrombomodulin, VK vitamin K, VKH_2 vitamin K hydroquinone, VKO vitamin K epoxide, XF cross-linked fibrin.*

3.3.1. Simulation of PT and INR tests

In laboratory settings, PT is quantified as the time required for a fibrin clot to form after the addition of tissue factor, phospholipid, and calcium to decalcified, platelet poor plasma.

The PT test simulation implemented using the QSP coagulation network model [31] is summarised here. For PT test simulation, the initial condition of all states was reduced to one-third of the original values to mimic the plasma dilution process as a result of the addition of tissue factor, phospholipid, and calcium to the reaction mixture. Given that the majority of the coagulation components are biosynthesised in the hepatocytes, then the endogenous production rate of these components in isolated plasma sample for *in vitro* PT test is likely to be negligible if not non-existent. Furthermore, considering the observation time window for the PT test (i.e. in seconds) is much shorter than the endogenous turnover of coagulation components (i.e. in hours or days), the endogenous production rate of these components was set to zero.

To initiate coagulation for PT test simulation, 300 nM of tissue factor (TF) was given as input into the TF compartment of the model, which subsequently was available for complex formation with factor VII. The TF:VII complex eventually led to fibrin clot formation. In this model the PT was determined as the point at which the fibrin area under the curve (AUC) reached 1500 $nM \cdot s$ (equivalent to a 30% reduction in fibrinogen from baseline) [182, 183]. Subsequently, the PT was converted to the INR according to the following equation:

$$INR = \left(\frac{PT}{PT_{standard}}\right)^{ISI}.$$

Equation 3.1 *INR.*

Here, PT is the measured (simulated) PT, $PT_{standard}$ is the PT for standard normal plasma and ISI is the international sensitivity index that quantifies the sensitivity of the PT test to the thromboplastin (mixture of tissue factor and

phospholipid). For the purpose of this work, ISI was assumed to be one and $PT_{standard}$ was taken as 12 seconds. Finally, it is important to note that the simulations were deterministic and stochastic elements were not introduced.

3.3.2. Sensitivity analysis

A simulation-based local sensitivity analysis was conducted in MATLAB® Version 2015a using the QSP coagulation network model [31] to evaluate the sensitivity of the INR to a reduction in individual coagulation protein, first in single coagulation protein deficiency, and then in multiple coagulation protein deficiency.

3.3.2.1. Single coagulation protein deficiency

Deficiency in each of fibrinogen, factors II, V, VII, IX, and X was explored one-at-a-time. The single coagulation protein deficiency was introduced by adjusting the initial condition of a coagulation protein of interest in the QSP coagulation network model to 100% to 5% of normal basal concentrations with a step size of 5% (i.e. 100%, 95%, 90%, … , 5%). At each instance, the initial values of the other coagulation components remained unchanged (i.e. were initiated at the physiological concentrations for a typical patient). Subsequently, the INR values were simulated.

In this work, sensitivity of INR to changes in coagulation protein concentration was quantified as follows:

$$SI_P = \left|\frac{\partial INR}{\partial P}\right|; \quad P \in \{Fg, II, V, VII, IX, X\}.$$

Equation 3.2 *Local sensitivity of INR to changes in coagulation protein concentration.*

Here, SI_P denotes the sensitivity index of INR to coagulation protein and P represents the concentration of a particular coagulation protein of interest. Assuming linearity in INR and coagulation protein concentration within the step size (5%), the above first partial derivative (**Equation 3.2**) was approximated by

using central differences where the difference in coagulation factor is far from the limit of zero. Values close to zero indicate that the INR is insensitive to the coagulation protein and larger values correspond to high sensitivity.

3.3.2.2. Multiple coagulation protein deficiency

Within the single coagulation protein deficiency framework, variation in multiple coagulation proteins simultaneously was not permitted. Consequently, the natural correlation that exists between coagulation proteins during warfarin therapy cannot be accounted for then it follows that the interactions between coagulation proteins with respect to the INR are unable to be characterised.

In this work, the influence of multiple coagulation protein deficiency on the INR was investigated. A hypothetical clinical scenario where a typical patient who was newly commenced on 4mg of warfarin daily was considered. In the first stage, the time course of factors II, VII, and X (vitamin K-dependent coagulation proteins identified in **Section 3.3.2.1** as influential on the INR) and INR following warfarin initiation were simulated. In the subsequent step, the local sensitivity of each of factors II (SI_{II}), VII (SI_{VII}), and X (SI_X) were quantified at each simulated time point using **Equation 3.2**. The magnitude of SI_{II}, SI_{VII}, and SI_X were compared during non-steady-state and steady-state INR. The dominating coagulation protein was identified.

3.3.3. Isobologram analysis

The isobologram analysis, which is traditionally used as an empirical way to characterise drug interactions, was used to explore the interactions between coagulation proteins with respect to the INR. In this section, components and interpretation of an isobologram are introduced from the perspective of a drug-drug interaction. This is followed by a detailed description of the isobologram analysis conducted in this work. The theory and philosophy underpinning an isobologram analysis can be found elsewhere [184-186].

3.3.3.1. Components and interpretation of an isobologram

A typical dose-normalised isobologram for two drugs is shown in **Figure 3.2**. The isobologram axes represent the dose of a drug (e.g. drug A), denoted $D_{x,A}$, that gives a predetermined level of effect (e.g. x% inhibition) when given in combination with a dose of another drug (e.g. drug B), denoted $D_{x,B}$. The axes may be normalised with the dose of the same drug that *singly* gives the predetermined level of effect i.e. the drug's potency (e.g. $ED_{x,drug}$). The normalisation process standardises the axes to range from zero to (typically) one and, importantly, yields a dimensionless dose matrix that is adjusted for the drug's potency for effective comparison across different drugs. The diagonal additivity standard on the isobologram is given by Loewe's additivity (**Equation 3.3**) [187]:

$$\frac{D_{x,A}}{ED_{x,A}} + \frac{D_{x,B}}{ED_{x,B}} = 1.$$

Equation 3.3 *Loewe's additivity.*

All the points on the isobologram that correspond to the same level of effects, when connected together, form an *isobole* (*isos* means equal and *bolus* means effect in Greek). If the isobole coincides with the line of additivity, an additive effect is indicated. Isobole located below the additivity standard represents supra-additivity whereas isobole above the standard corresponds to

sub-additivity. In the drug interaction domain, sub-additivity and supra-additivity are termed antagonism and synergism, respectively.

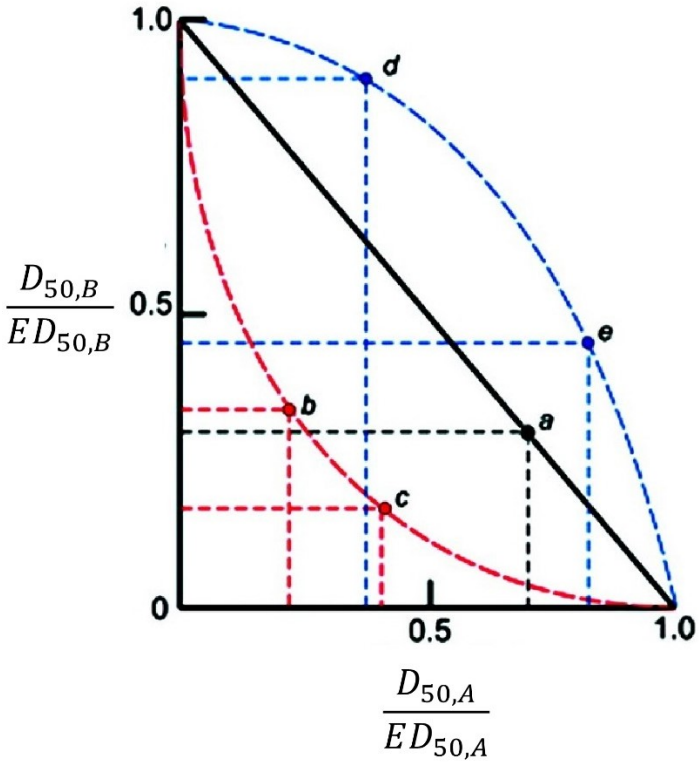

Figure 3.2 *A classic dose-normalised isobologram for two drugs, drug A and drug B. All the points on the isobologram represent combinations of drug A and drug B that give the same level of effect (e.g. 50% inhibition). When connected together, these points form an isobole. If the isobole falls on the black solid line, an additive effect is indicated. Isobole containing points b and c below the additive line is supra-additive in effect whereas the isobole containing point d and e above the additive line is sub-additive.* $D_{50,drug}$ *refers to the dose of a drug that gives half the maximal effect when given in combination with another drug.* $ED_{50,drug}$ *is the dose of a drug that singly gives half the maximal effect. The plot was adopted from a publication by Chou et al. [184].*

3.3.3.2. Constructing the isobologram

In this work, the response of interest is the INR. Three levels of INR were considered: (1) physiological INR ($INR = 1.2$ [the upper bound of normal]), (2) therapeutic INR ($INR = 2.5$), and (3) supra-therapeutic INR ($INR = 4.5$). At each level of INR considered, all pairwise combinations of factors II, VII, and X were explored: (1) factor II versus VII, (2) factor II versus X, and (3) factor VII versus

X. A total of nine normalised isobolograms were constructed. Note a full joint isobologram over the three factors was not considered (this is discussed later).

Here, the quantity that is analogous to dose is the percentage reduction in the coagulation protein of interest. $R_{P,combi}$ refers to the percentage reduction in one coagulation protein to give a predetermined level of INR when another coagulation protein is *simultaneously* reduced and is analogous to $D_{x,drug}$. On the other hand, R_P is the percentage reduction in a coagulation protein that *singly* results in the predetermined level of INR and from a drug interaction perspective, it is analogous to $ED_{x,drug}$.

The different regions on the resulting isobologram are shown in **Figure 3.3**. In this example, all the points on the isobologram correspond to the same level of effect (e.g. $INR = 2.5$) and the diagonal line represents the additivity standard. The y-axis relates to factor II and the x-axis to factor VII. At the y-intercept, since $R_{VII,combi} = 0$, then $R_{II,combi}$ is essentially the same as R_{II}. As a result, $\frac{R_{II,combi}}{R_{II}} = 1$ (i.e. y-intercept equals to one). Similarly, at the x-intercept, because $R_{II,combi} = 0$, then $R_{VII,combi} = R_{VII}$ and $\frac{R_{VII,combi}}{R_{VII}} = 1$ (i.e. x-intercept equals to one). On the other hand, the surface of the isobologram was constructed by using different combinations of factor II and factor VII (i.e. $R_{II,combi} \neq 0$ and $R_{VII,combi} \neq 0$) that give the desired level of INR. The interpretation of the isobologram is similar to that of drug interactions discussed earlier except that terminologies usually coined to describe drug interactions such as antagonism and synergism are not used.

Here, there are two prerequisite steps to constructing the isobologram: (1) to identify R_P value for the two different coagulation proteins that *singly* gives the desired level of INR (e.g. R_{II} or R_{VII} alone that gives $INR = 2.5$) and (2) to determine the $R_{P,combi}$ value for the aforementioned two coagulation proteins that *jointly* gives the predetermined level of INR (e.g. combinations of $R_{II,combi}$ and $R_{VII,combi}$ result in $INR = 2.5$). For a single level of INR, there is only one possible value of R_P for each coagulation protein whereas multiple combinations of $R_{P,combi}$ of two different coagulation proteins are permissible.

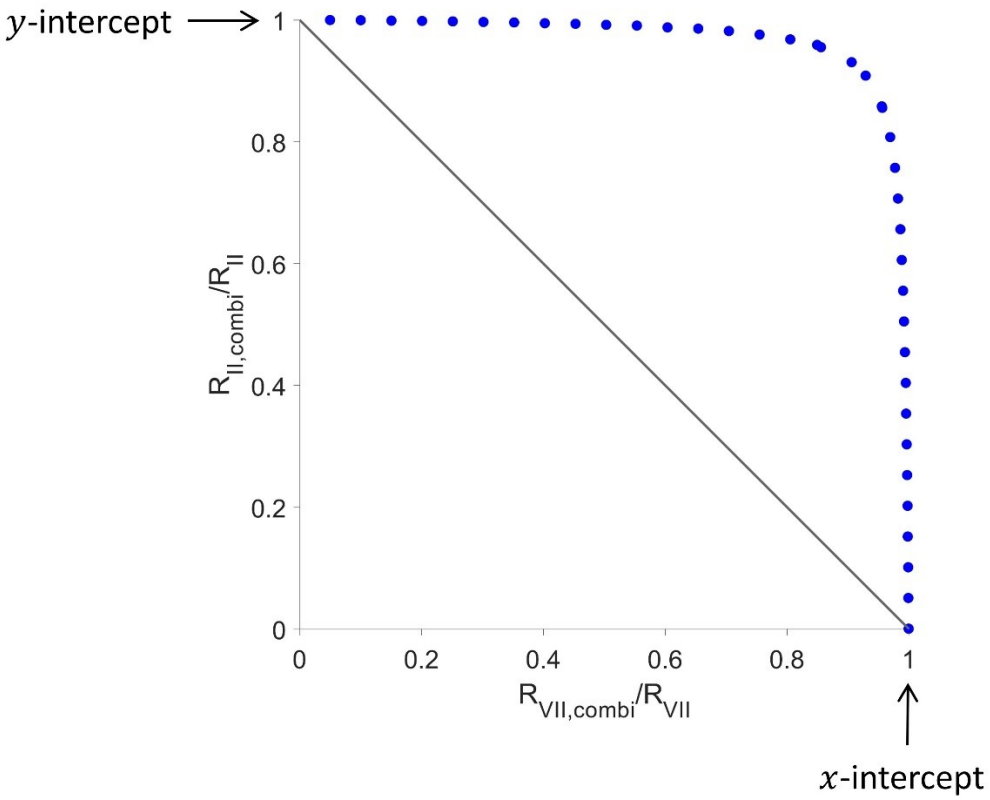

Figure 3.3 *Example of an isobologram for factors II and VII that give a predetermined level of INR (e.g. INR=2.5). The diagonal solid line is the additivity line.*

Both R_P and $R_{P,combi}$ that give a predetermined level of INR were obtained based on an adaptive grid search algorithm implemented in MATLAB® Version 2015a. R_P was searched while all other coagulation components were held at the physiological concentrations. $R_{P,combi}$ was searched in a similar manner but at fixed, reduced levels of another coagulation protein of interest.

An adaptive grid search was used for identifying isobolic combinations of the coagulation proteins. Details and the corresponding MATLAB code are included in **Appendix A2.1**. The ratio of $R_{P,combi}$ to R_P was calculated and plotted on the isobologram. Finally, the nature of interactions (sub-additivity, additivity, or supra-additivity) between coagulation proteins were qualified based on the isobologram.

3.4. Results

3.4.1. Model evaluation

The data simulated from the QSP coagulation network model (based on each patient's design [dose and timing of warfarin and blood samples]) provided a reasonable agreement, on average, to the external data for factors II, VII, IX, X, and INR at the individual level. Note that the coagulation model is built on parameters at the population level rather than individual level and hence predictions (simulations) are analogous to PRED rather than IPRED in NONMEM parlance. Discrepancies did not appear to be systematic when considered across patients suggesting that the QSP model, on the whole, provided an adequate description of the influence of warfarin on INR. Plots of five representative individuals are shown in **Figure 3.4**. Plots of all 17 patients are included in **Appendix A2.2**.

3.4.2. Sensitivity analysis

3.4.2.1. Single coagulation protein deficiency

Plots of INR and the corresponding INR sensitivity, SI_P, at different coagulation protein concentrations are shown in **Figure 3.5**. From **Figure 3.5**, INR was found to be sensitive to changes in fibrinogen, factors II, VII, and X but based on simulations from the QSP model appeared non-responsive to factors V and IX. Here, the INR sensitivity is inversely related to the concentration of influential coagulation proteins where high INR sensitivity is associated with low coagulation protein concentration and vice versa.

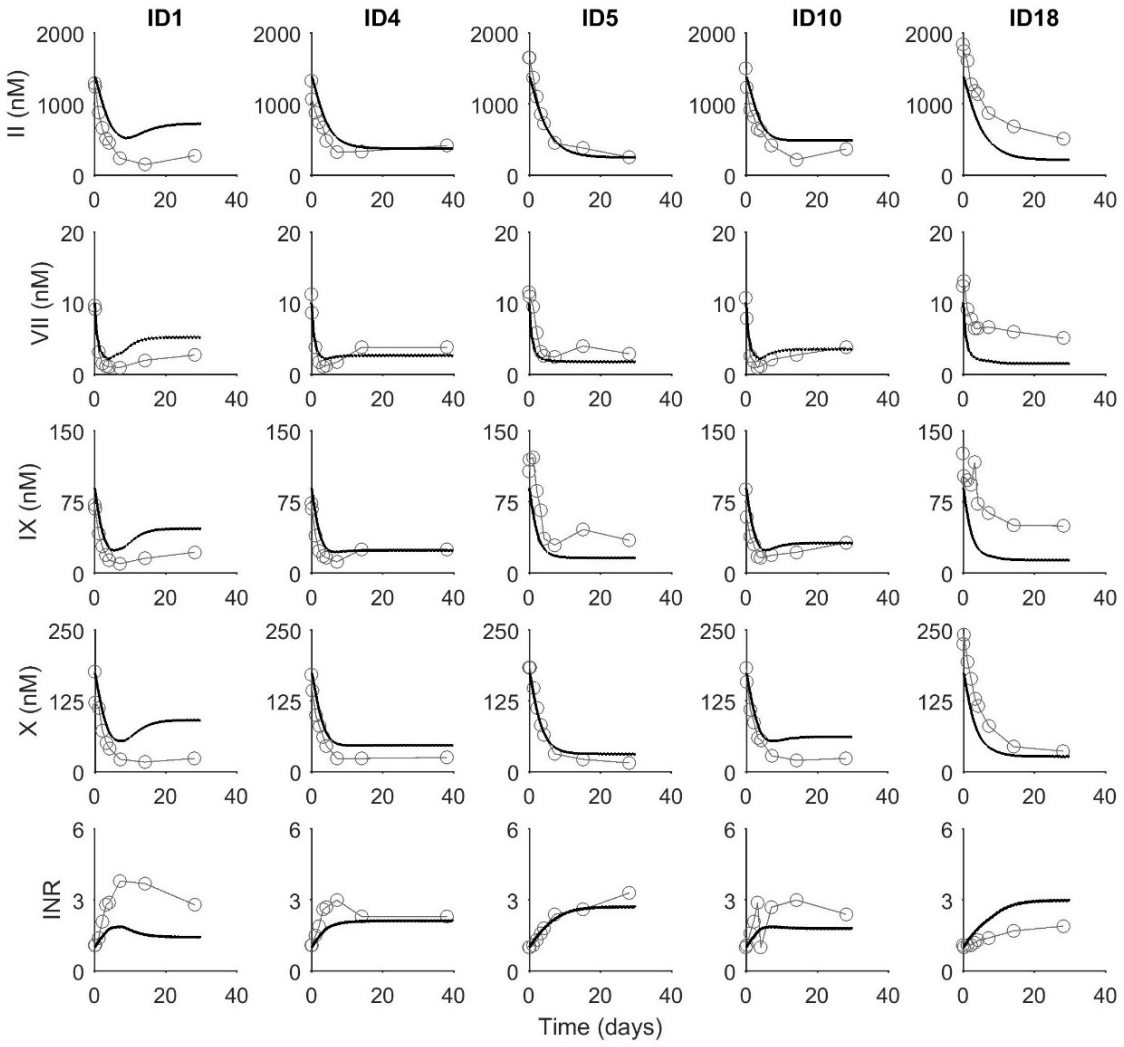

Figure 3.4 *Individual fits for the time course of factors II, VII, IX, X, and INR for five representative individuals following warfarin initiation. The black solid lines are prediction by the coagulation network model using parameters for a typical patient. The grey open circles are observations from the external dataset [167, 181]. INR refers to the international normalised ratio and nM stands for nanomolar.*

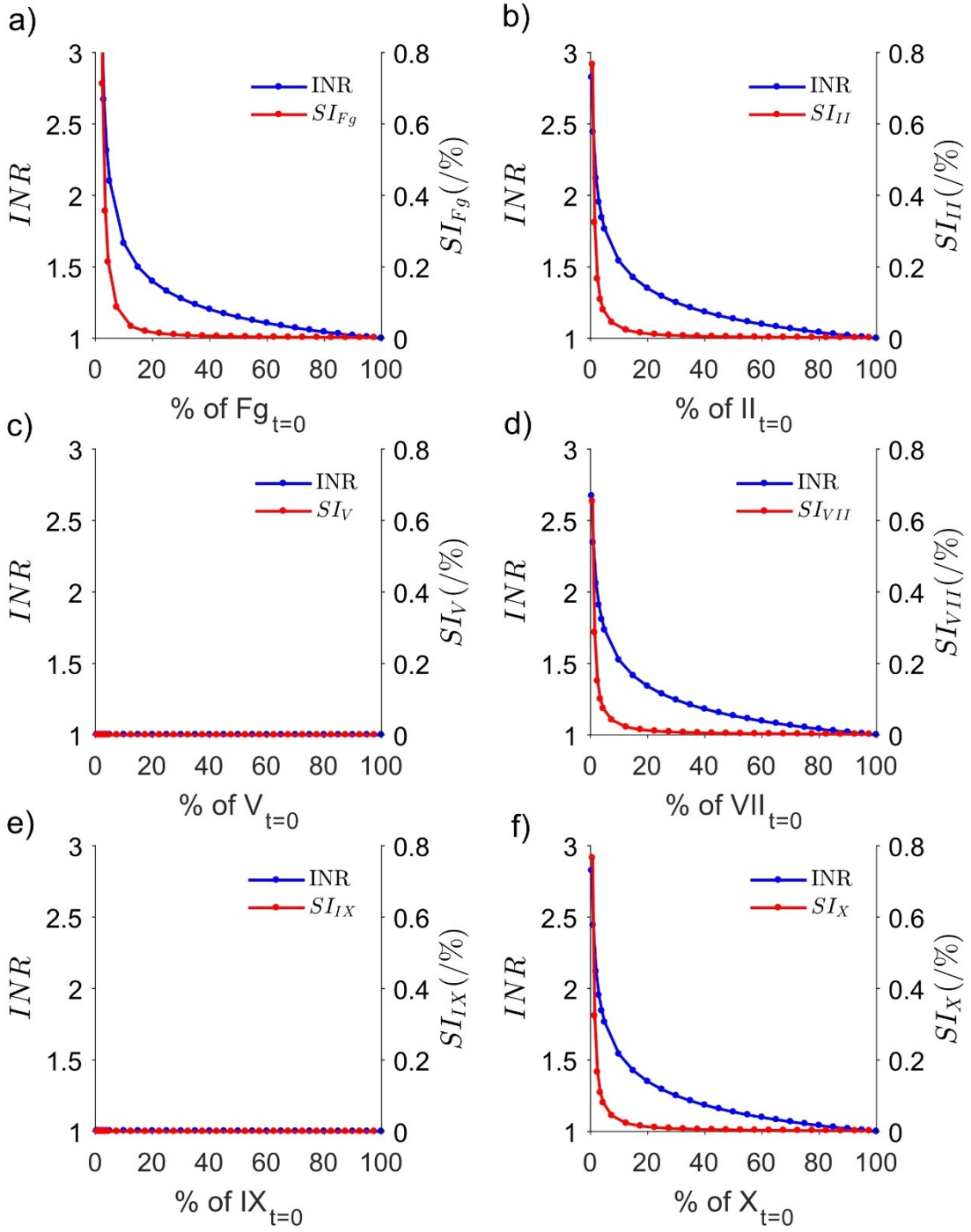

Figure 3.5 *Sensitivity of INR to changes in coagulation protein concentration in single coagulation protein deficiency: fibrinogen (panel a), factor II (panel b), factor V (panel c), factor VII (panel d), factor IX (panel e), and factor X (panel f). Fg is fibrinogen, $P_{t=0}$ is the baseline concentration of coagulation protein, INR is the international normalised ratio, SI_P is the sensitivity index of INR to coagulation protein.*

3.4.2.2. Multiple coagulation protein deficiency

The simulated time course of INR, and factors II, VII, X, and the corresponding SI_{II}, SI_{VII}, and SI_X following warfarin initiation is shown in **Figure 3.6**. After warfarin initiation, factor VII, which has a short degradation half-life ($t_{\frac{1}{2},VII} = 6\ hours$), declines rapidly and followed by factor X ($t_{\frac{1}{2},X} = 40\ hours$) and finally, factor II ($t_{\frac{1}{2},II} = 66\ hours$).

At each time point, the magnitude of SI_{II}, SI_{VII}, and SI_X were compared. It was observed that, at non-steady-state INR, SI_{VII} is persistently higher compared to SI_{II} and SI_X, whereas at steady-state INR, SI_{II}, SI_{VII}, and SI_X are similar in magnitude. These findings suggest that the INR is the most sensitive to changes in factor VII concentration at non-steady-state INR but equally sensitive to factors II, VII, and X at steady-state INR. Finally, an interesting and potentially important observation from **Figure 3.6** is that, by visual comparison, the time course of change in SI_{VII} seems similar to that of the INR. All these point to factor VII as the principal driving force for the INR.

3.4.3. Isobologram analysis

The isobologram of all pairwise combinations of factors II, VII, and X that correspond to different levels of INR are shown in **Figure 3.7**. In the isobolograms, the isoboles are located above the additivity line thereby indicating sub-additive interactions between two coagulation proteins with respect to the INR. This could be interpreted that the presence of more than one coagulation protein deficiency is redundant for INR effect. In addition, it was observed that the degree of sub-additivity increases with higher INR values. In fact, at therapeutic INR ($INR = 2.5$) and supra-therapeutic INR ($INR = 4.5$), extended horizontal and vertical segments were observed on the isobolograms. Here, INR is driven by a single coagulation protein that is the most deficient. In other words, given that a coagulation protein of interest is sufficiently deficient, then the same INR can be resulted regardless of the concentration of other coagulation proteins. This makes other coagulation protein concentrations of limited additional relevance to the changes in the INR.

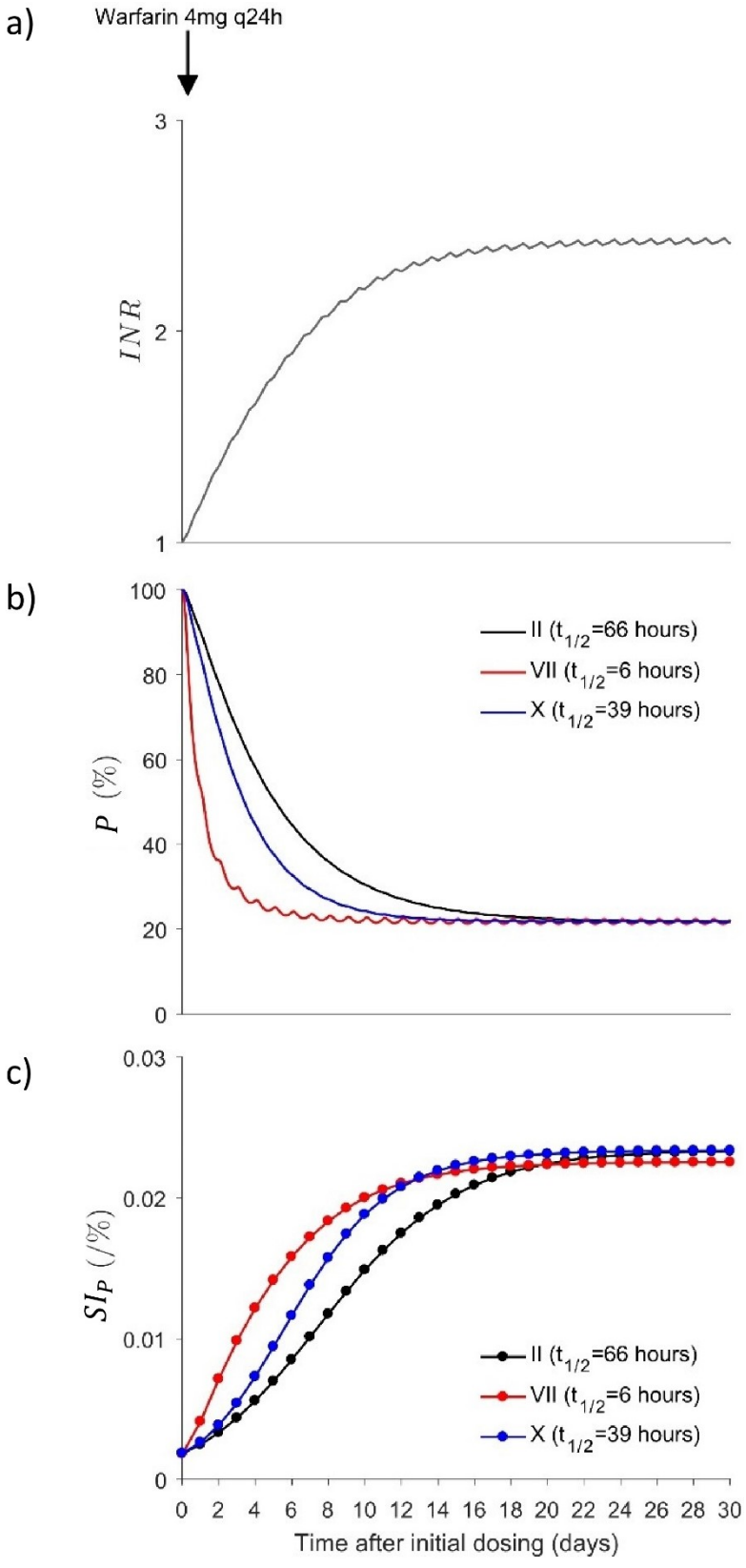

Figure 3.6 *The simulated time course of INR (panel a), and factors II, VII, and X (panel b), and SI_{II}, SI_{VII}, and SI_X (panel c) following initiation of 4mg warfarin daily. INR is the international normalised ratio, SI_P is the sensitivity index of INR to a coagulation protein and $t_{1/2,P}$ is the degradation half-life of a particular coagulation protein.*

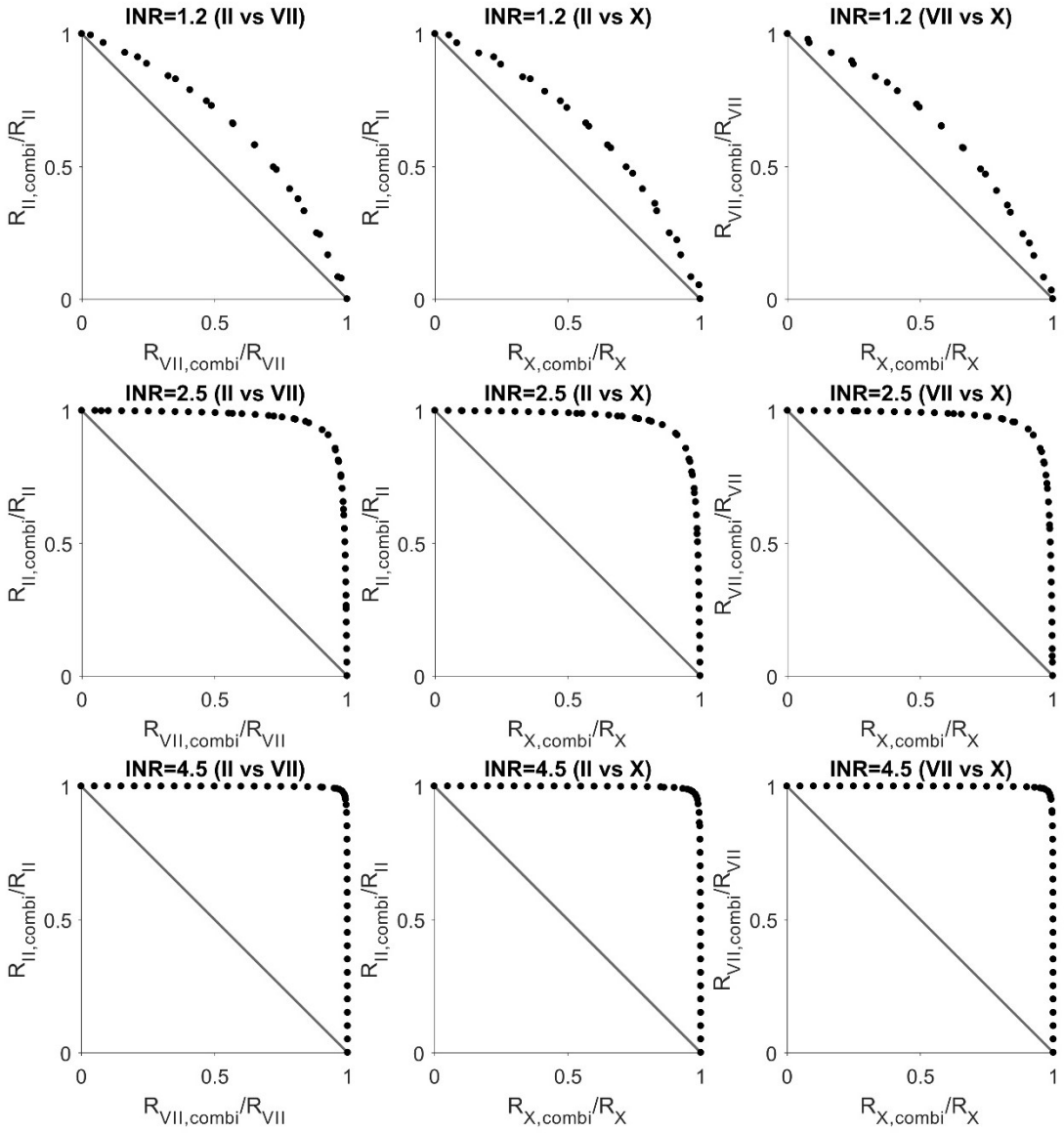

Figure 3.7 *Isobolograms of pairwise combination of factors II, VII, and X for different INRs. The top, middle and bottom rows represent physiological, therapeutic, and supra-therapeutic INR values. The columns represent different combinations of coagulation factors. The black circles correspond to pairwise combination of factors II, VII, or X that gives a predetermined INR. The diagonal solid line is the additivity line. INR is the international normalised ratio,* $R_{F,combi}$ *refers to the reduction in one coagulation protein when another coagulation protein is simultaneously reduced and* R_F *is the reduction in a single coagulation protein.*

3.4.4. Coagulation protein for INR prediction

Based on the isobologram analysis, simultaneous reduction in factors II, VII, and X leads to less than additive increases in the INR. At therapeutic and supra-therapeutic INR, the most deficient coagulation protein drives the INR whereas other coagulation proteins appear irrelevant. Given the short degradation half-life of factor VII relative to that of factors II and X, factor VII is always more deficient or of equivalent deficiency compared to the deficiency of other factors and therefore will dominate the INR. The same inference was drawn independently from the sensitivity analysis, which showed that factor VII is the principal driving force for the INR and importantly, the time course of sensitivity of the INR to factor VII was shown to provide a good approximation to the time course of INR. Here, based on this work, factor VII, a warfarin-sensitive coagulation protein appears to drive the INR, makes an attractive candidate for monitoring of anticoagulant response and future INR prediction.

3.5. Discussion

INR is sensitive to factors II, VII, and X. Of these coagulation proteins, factor VII appears to have the most dominant effect on the INR. This is attributable to the sub-additivity nature of interactions between the coagulation proteins on the INR, which implicates that INR can be driven solely by the coagulation protein that is the most deficient after warfarin initiation i.e. factor VII, which has the shortest degradation half-life amongst factors II, VII, and X. The same INR can then be resulted regardless of the concentration of other coagulation proteins. The above findings were further supported by the observation that the INR sensitivity to factor VII closely mimics the INR profile. This again highlights the potential informativeness of factor VII with respect to the INR and importantly, the ability and therefore the potential of the INR sensitivity to factor VII as an approximation to the anticoagulant response. On that basis, a measure of factor VII response accompanied by the quantification of the corresponding INR sensitivity may be useful in the prediction of future anticoagulant response for subsequent warfarin dose individualisation.

The main outcome of this work was derived from the isobologram analysis, which is traditionally used for the analysis of drug interactions [187]. It is underpinned by Loewe's additivity that implicitly assumes that dose a of drug A and dose b of drug B [termed b_a] that give the same level of effect are equivalent (*principle of dose equivalence*) and that b_a can be added to any other dose b of drug B to give the additive effect of the combination (*principle of Sham combination*) [185-187]. Here, with dose additivity for the construction of the isobologram, as long as the combination of doses give the predetermined level of effect, no particular assumption is made about the relationships between the two drugs or the doses of the two drugs, whether they are independent or correlated. The resulting isobologram is also not informative with respect to the mechanisms of drug interactions and instead serves as a black-box approach to give an empirical description of the nature of drug interactions (antagonism, additivity, or synergism) using Loewe's criterion as a reference standard for no interactions [188].

In this work, the isobologram analysis was extended beyond the usual drug interactions framework to explore interactions of *endogenous* substrates within a biological system. Here, factors II, VII, and X, which work in concert within the coagulation network for clot formation, are *inherently correlated* due to the complex series of positive-feedforward, negative-feedforward, positive-feedback, and negative-feedback reactions for maintaining haemostatic balance [31]. Based on the isobologram analysis, factors II, VII, and X were identified as sub-additive in their effects on the INR. In other words, the presence of more than one coagulation protein deficiency is *redundant* for INR effect. In this setting, terminologies usually coined to describe drug interactions are not used. For instance, *antagonism*, which relates to dampening of a biological response of interest due to receptor binding by a ligand, is underpinned by the classical receptor theory and is unsuitable to be used to describe the interactions between coagulation proteins. This is because coagulation proteins do not actually antagonise one another and in fact, they act on distinct targets. In the exploration of the effect of factors II, VII, and X on the INR, a three-dimensional (3D) isobologram can theoretically be constructed [189-192]. This is motivated by the criticism that when two-dimensional (2D) isobolograms are used to analyse three interacting coagulation proteins, one of factors II, VII, and X must be held constant, thereby rendering the analysis of interactions incomplete. However, the interpretation of a 3D isobologram is potentially difficult due to visualisation of a 3D structure on a 2D platform. For completeness, although a 3D isobologram was not constructed, the effect of varying factor X ($R_{X,combi} = 0\%, 30\%, 60\%$) on the interactions between factors II and VII with respect to the INR were briefly explored. It was observed that almost identical combinations of factors II and VII are required to give an INR of 2.5 regardless of the magnitude of reduction in factor X (see **Figure 3.8**). This lends support to our finding that if one of factors II, VII, and X is sufficiently deficient, the presence of other coagulation proteins is redundant for INR effect.

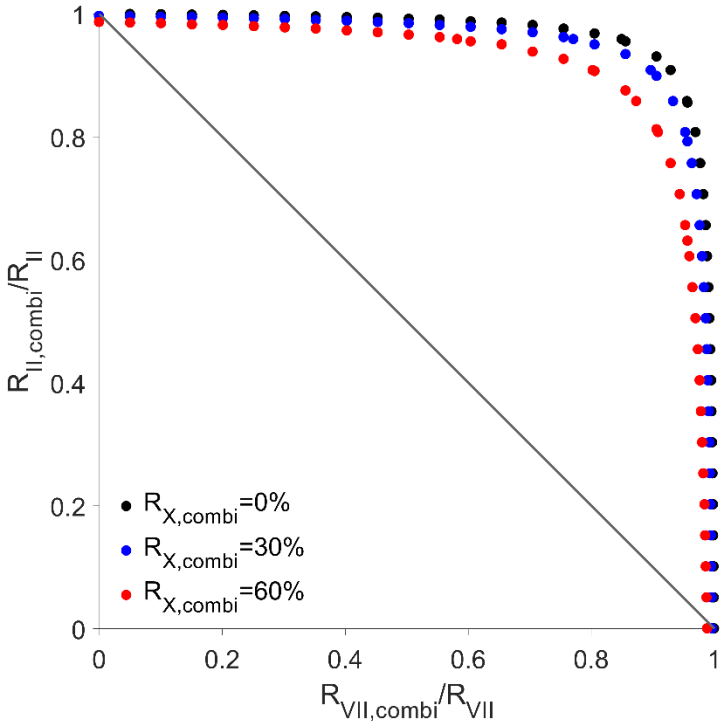

Figure 3.8 *Isobolograms of factors II and VII at different level of factor X reduction that give a predetermined level of INR (INR=2.5). The diagonal solid line is the additivity line.*

The results of our analysis are broadly similar to those reported in the published literature with respect to the sensitivity of INR to fibrinogen, factors II, VII, and X and the concentration-dependent nature of the sensitivity [136, 137]. It is well-documented in published case reports and case series that PT is prolonged (i.e. INR is elevated) in patients with isolated factor V deficiency [193-195]. However, the influence of factor V on the INR was not identified by the QSP coagulation network model, indicating that this mechanism is not correctly specified in the QSP model. Similar results were previously reported by Yoneyama and colleagues [196] who evaluated the coagulation network model. However, for the purpose of this study and subsequent works within this thesis, factor V, which is not a vitamin K-dependent coagulation protein and therefore is unaffected by warfarin, is considered peripheral to the inferences.

In this study, factor VII was identified as an important determinant of the INR. The influence of factor VII on the non-steady-state INR has been reported previously [161, 197]. In terms of steady-state INR, a conserved rank order

between steady-state factors II, VII, and X concentration was observed in warfarinised patients (see **Figure 3.9**) [144, 146, 167, 198]. Here, at steady-state INR, factor VII concentration is higher than the factor II concentration and factor II concentration is in turn is higher than the factor X concentration for all individuals (i.e. $VII_{SS} > II_{SS} > X_{SS}$). Using the same data, pairwise combinations of factors II, VII, and X were plotted (see **Figure 3.10**). A linear relationship was noted: factor II vs VII (Pearson's linear correlation coefficient, $\rho = 0.830, p < 0.05$), factor X vs VII ($\rho = 0.693, p < 0.05$), and factor II vs X ($\rho = 0.847, p < 0.05$). This consistency in trend means that given the steady-state level of one of factors II, VII, and X, steady-state level of other coagulation proteins and the resulting INR can be predicted. Of these three coagulation proteins, factor VII with a short degradation half-life achieves its steady-state rapidly following warfarin initiation and therefore provides the earliest indication of the eventual steady-state concentrations of other coagulation proteins and INR. Taken together, these findings lend support to the proposal that factor VII is potentially informative and may be useful for the prediction of steady-state INR.

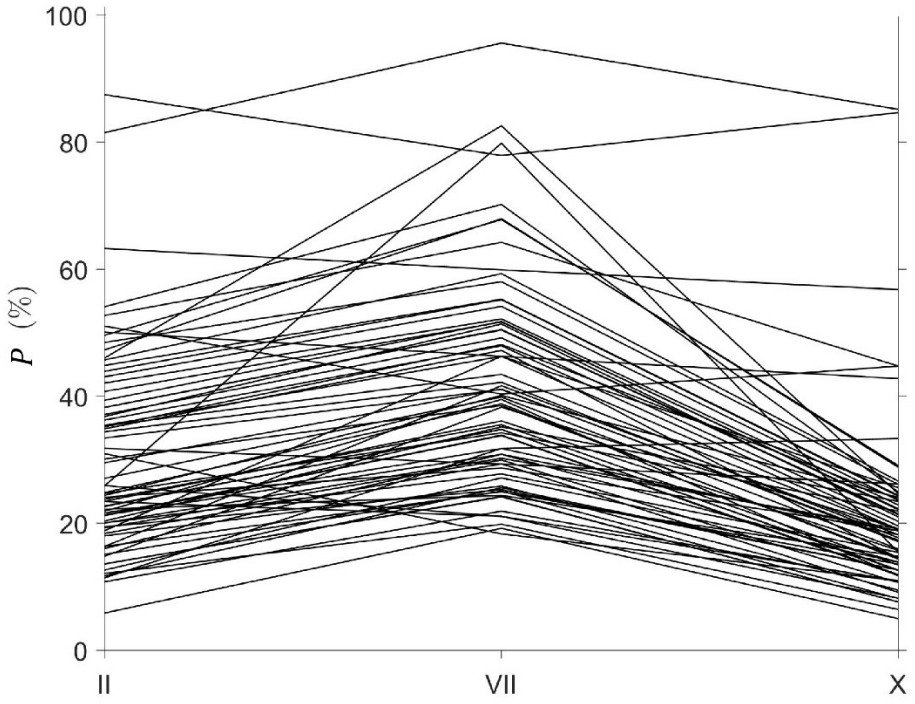

***Figure* 3.9** *Concentration of factors II, VII, and X at steady-state INR for 73 patients. The graph was reproduced based on the data from published literature: McCollum et al. 2004 [167] (n = 9), Kumar et al. 1990 [144] (n = 23), Chan et al. 1987 [198] (n = 5), and Paul et al. 1987 [146] (n = 36). Factors II, VII, and X of the same patient are connected by lines. n represents number of patients.*

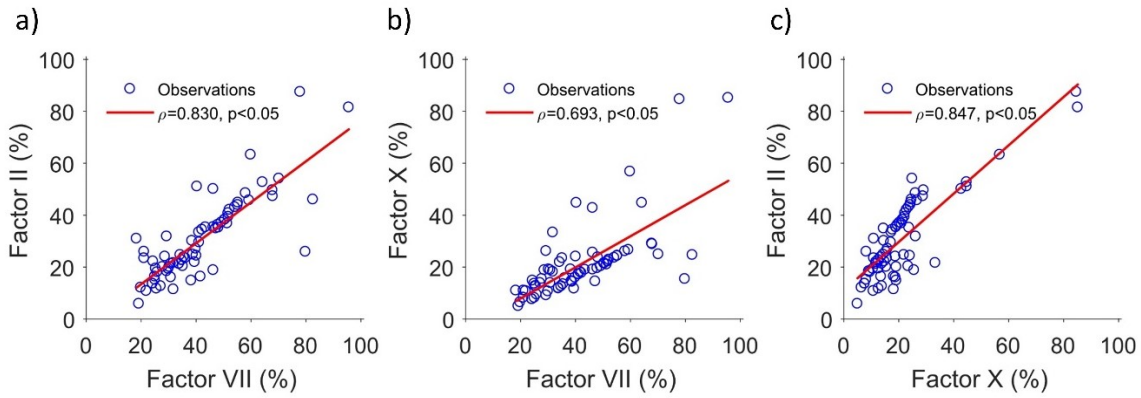

Figure 3.10 *Pairwise plots of factors II, VII, and X. Panel a shows factor II versus VII, panel b factor X versus VII, and panel c factor II versus X. Steady-state factors II, VII, and X are highly correlated. The blue circles are observations from published literature [144, 146, 167, 198] and the red lines are the linear models fitted to the observations. ρ represents the Pearson's linear correlation coefficient.*

To date, only one published study, by Pitsiu and colleagues [157], considered coagulation protein activity for the prediction of warfarin maintenance dose regimens. It was shown that factor VII response measurements alone were adequate to determine warfarin dosing requirements but the generalisability of the study results to all warfarin users is limited due to a small sample size ($n = 5$) and the use of healthy volunteers.

In this work, competing QSP coagulation models, which can mimic the PT or INR test [83, 182], were not considered and no formal evaluation was conducted to compare the predictive performance of these models to the QSP coagulation network model used. This is because these models, while able to simulate PT and INR, were not designed with the ability to simulate warfarin therapy and the corresponding coagulation protein response and therefore are not comparable and usable for this study.

A local sensitivity analysis was conducted to quantify the sensitivity of the INR to factor VII for a simulated typical patient newly commenced on warfarin. One major criticism of the local sensitivity analysis is that the sensitivity to specific input (coagulation protein of interest) variation is only valid within the immediate vicinity of a given set of input (coagulation components) values. Here, although the entire coagulation protein space was not fully explored, the space considered is immediately relevant to warfarin use since factors II, VII, and X concentrations typically observed after warfarin initiation were used for the sensitivity analysis.

In this work, factor VII was identified as sensitive to warfarin and influential to the INR thereby representing an attractive choice of anticoagulant response for future INR prediction and warfarin dose individualisation. The development and evaluation of a factor VII-based method for the prediction of anticoagulant response to warfarin is discussed in **Chapter 4**.

3.6. Conclusion

This research has identified factor VII as influential and informative of the INR following warfarin initiation. This was based on the sensitivity analysis that showed that factor VII is the principal driving force for the INR and the isobologram analysis that demonstrated that the presence of more than one coagulation protein deficiency is redundant for INR effect due to the sub-additivity nature of interactions between coagulation proteins. The use of factor VII as a marker of coagulation in addition to the INR may improve the prediction of the anticoagulant response and warfarin dosing requirements. The development and evaluation of a factor VII-based method for the prediction of anticoagulant response to warfarin is discussed in **Chapter 4**.

Chapter 4: A factor VII-based method for the prediction of anticoagulant response to warfarin

This chapter is based on the following peer-reviewed publication:

Ooi QX, Wright DF, Isbister GK, Duffull SB. *A factor VII-based method for the prediction of anticoagulant response to warfairn*. Sci Rep. 2018: 8, 12041.

4.1. Introduction

Despite a significant body of literature in this area, algorithms for predicting warfarin maintenance dose in patients remain inaccurate [2-7]. It is believed that this is related to the use of the international normalised ratio (INR) as a sole marker of anticoagulation for warfarin dose individualisation [12, 17, 18, 22, 23, 25-30].

Because the coagulation proteins are on the causal path from warfarin dose to INR response, warfarin dose response relationship can be informed by the inclusion of coagulation protein as an intermediary marker. In this setting, the coagulation proteins represent a direct measure of the anticoagulant response and because the coagulation protein response is located immediately downstream from warfarin concentration in the causal path for warfarin dose response, the response, in theory, will capture important between-subject differences in both warfarin pharmacokinetics and pharmacodynamics. Of all the vitamin K-dependent coagulation proteins, factor VII is the coagulation protein of interest due to its short degradation half-life, sensitivity to warfarin (**Chapter 2**), and profound influence on the INR (**Chapter 3**). A measure of factor VII response in addition to the INR is likely to improve the prediction of the anticoagulant response.

4.2. Aims

The aim of this work was to develop a factor VII-based method for the prediction of anticoagulant response to warfarin.

4.3. Chapter structure

The current chapter is divided into the following sections: underpinning theory; development of the prediction algorithm; application of the prediction algorithm; and finally, discussion of the proposed algorithm.

4.4. Theory

The proposed approach for the prediction of anticoagulant response to warfarin includes a 2-step process; (1) determining the time to steady-state INR ($t_{SS,INR}$) and (2) from this predicting the steady-state INR (INR_{SS}) at $t_{SS,INR}$. The predicted INR_{SS} could then provide a means of determining maintenance dose requirements.

The steady-state INR is defined as the INR that is achieved at the maximum, which is when the system is essentially at equilibrium. It follows that the steady-state INR can be defined mathematically when:

$$\frac{dINR}{dt} = 0; \quad t > 0.$$

Equation 4.1 *Definition of the steady-state INR.*

It is important to note, however, that true steady-state is an asymptotic condition and therefore the definition given in **Equation 4.1** is relaxed to a practical solution where

$$\frac{dINR}{dt} \leq \varepsilon_{INR}; \quad t > 0$$

Equation 4.2 *Relaxed definition of the steady-state INR.*

and ε_{INR} is a pre-defined level of tolerance. Here, $t_{SS,INR}$ is defined as the smallest value of t that satisfies **Equation 4.2**.

Once $t_{SS.INR}$ has been determined it is then a matter of deriving INR_{SS}. If, for simplicity, and without loss of generality, warfarin dosing is assumed to be constant over time, then the solution for INR_{SS} is a function of INR_0, the INR at baseline, and $\int_0^{t_{SS,INR}} \frac{dINR}{dt}\, dt$, the cumulative change in INR from baseline to $t_{SS,INR}$.

$$INR_{SS} \approx INR_0 + \int_0^{t_{SS,INR}} \frac{dINR}{dt}\, dt; \quad t > 0$$

Equation 4.3 *Solution for the steady-state INR.*

Generalising this to variable dosing can be solved by a series of piecewise integrals with break points at times of dose change.

Of the three coagulation proteins, factor VII has the shortest degradation half-life, of approximately 5-35 hours [159, 165, 171, 173, 181], and therefore declines at the greatest rate and is the first to attain a new steady-state concentration. Based on the assumptions that:

- **Assumption 1**: simultaneous reduction in factors II, VII, and X leads to less than additive increases in the INR,
- **Assumption 2**: the most deficient coagulation protein drives the INR,
- **Assumption 3**: under non-steady-state INR conditions, factor VII is always the most deficient, and
- **Assumption 4**: the non-steady-state INR is the most sensitive to factor VII,

then, monitoring factor VII in addition to INR will be informative for the prediction of future INR responses. These assumptions are supported by the widely-accepted notion that factor VII is the principal driving force for the non-steady-state INR [161, 197]. In addition, at steady-state INR, there exists a high correlation between the steady-state concentrations of the vitamin K-dependent factors II, VII and X and hence the steady-state concentration of factor VII would be informative of the eventual steady-state concentrations of the other factors and INR_{SS} [144, 146, 167, 198]. Assumptions 1, 2, 3, and 4 were explored in **Chapter 3** and formally evaluated in terms of the probability and impact of assumption violation in **Chapter 5**. Details of the evaluation can be found in **Appendix 4**.

If non-steady-state INR is the most sensitive to changes in factor VII, then the sensitivity of the INR to factor VII should adequately approximate the non-steady-state INR. In this study, the sensitivity of the INR to changes in the

concentration of factor VII, denoted here as SI_{VII}, is quantified as the partial derivative of the INR with respect to factor VII:

$$SI_{VII}(t) = \left|\frac{\partial INR(t)}{\partial VII(t)}\right|; \quad t > 0.$$

Equation 4.4 *Sensitivity of INR to factor VII.*

Here, INR, VII, and SI_{VII} depend on time, t, and $|\cdot|$ denotes the absolute value. SI_{VII} values close to zero indicate that INR is insensitive to factor VII whereas larger absolute values depict increased INR sensitivity to factor VII.

Subsequently, the INR, which is approximated by SI_{VII}, can be expressed as a function of SI_{VII}. Similarly, the previously defined steady-state INR status and $t_{SS,INR}$ (**Equation 4.2**) as well as INR_{SS} (**Equation 4.3**) can be expressed in terms of SI_{VII}. The steady-state INR status is considered to be achieved when SI_{VII} reaches its steady-state, accordingly:

$$\frac{dSI_{VII}}{dt} \leq \varepsilon_{SI_{VII}}; \quad t > 0$$

Equation 4.5 *Definition of the steady-state INR based on* SI_{VII}.

where $\varepsilon_{SI_{VII}}$ is analogous to ε_{INR} although scaled to SI_{VII}. The corresponding expressions for $t_{SS,INR}$ and INR_{SS} in terms of SI_{VII} are given below:

$$t_{SS,INR} \approx \min\left(t \left| \frac{dSI_{VII}}{dt} \leq \varepsilon_{SI_{VII}} \right.\right); \quad t > 0$$

Equation 4.6 *Solution for the* $t_{SS,INR}$ *based on* SI_{VII}.

$$INR_{SS} = INR_0 + \int_0^{t_{SS,INR}} l\left(\frac{dSI_{VII}}{dt}\right) dt; \quad t > 0.$$

Equation 4.7 *Solution for the* INR_{SS} *based on* SI_{VII}.

Note here that $\frac{dINR}{dt} = l\left(\frac{dSI_{VII}}{dt}\right)$. The steady-state INR, $t_{SS,INR}$, and INR_{SS}, defined from the SI_{VII} perspective, form the basis of this work.

4.5. *Development of the prediction algorithm*

In this section, the development of a four-step algorithm for the prediction of $t_{SS,INR}$ and INR_{SS} is described. A schematic of the steps is presented in **Figure 4.1**.

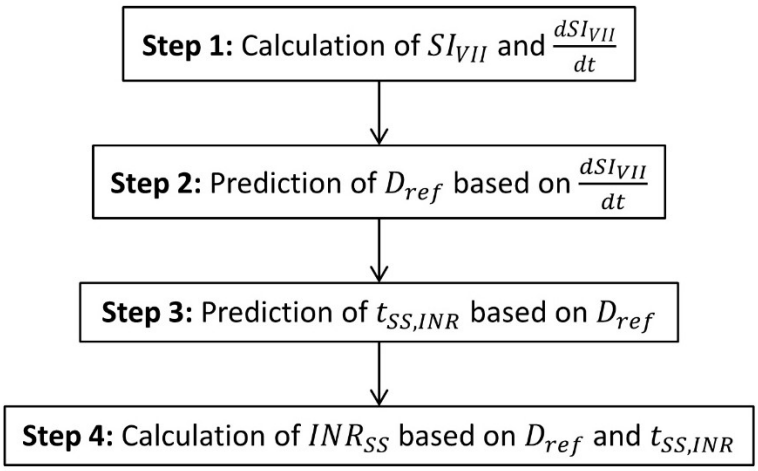

Figure 4.1 *The four-step workflow to predict $t_{SS,INR}$ and INR_{SS}. D_{ref} is the typical dose that would yield this value of INR (hence it is an indicator of the sensitivity of the patient to warfarin), INR_{SS} the steady-state INR, SI_{VII} the sensitivity index of INR to factor VII, and $t_{SS,INR}$ the time to reach steady-state INR.*

In this work, the relationships between warfarin dose, SI_{VII}, and INR, were derived empirically to match predictions from a quantitative systems pharmacology (QSP) model of the coagulation network [31]. This is a heuristic model-order reduction technique in which an empirical approximation to predictions from the QSP model was obtained. Using this approach, the mechanistic behaviour of the system over the range of simulations from the QSP were captured, albeit the mechanistic nature of the relationships was not retained. It is worth noting that, implicit to this approach, it is assumed that:

- **Assumption 5**: the QSP coagulation network model [31] is adequate in describing the warfarin-coagulation proteins-INR relationship and that
- **Assumption 6**: the simulated coagulation proteins-INR time course is representative of that of typical patients initiated with warfarin.

Of primary interest to the evaluation of these assumptions, is the predictive performance of the QSP coagulation network model. The model was previously evaluated and shown to perform well in characterising the INR based on the coagulation protein profiles of 20 patients [31, 83]. Additionally, in **Chapter 3**, predictions from the QSP coagulation network model were compared to available time course data of factors II, VII, X, and INR for 17 warfarin patients [167, 181]. The model predictions were in reasonable agreement with the observed data thereby suggesting that the QSP coagulation network model is likely to be adequate in characterising the warfarin-coagulation proteins-INR relationship. Assumptions 5 and 6 were formally evaluated in terms of the probability and impact of assumption violation in **Chapter 5**. Details of the evaluation can be found in **Appendix 4**.

4.5.1. Calculation of SI_{VII} and its derivative

The time course of factors II, VII, and X, and INR for a typical patient commenced on warfarin doses of 1 mg, 4 mg, 7 mg, 10 mg, and, 13 mg daily were simulated from the QSP coagulation network model in MATLAB® Version 2015a (The MathWorks Inc., Natick, Massachusetts, USA) [31]. SI_{VII} was quantified according to **Equation 4.4** over a vector of t_i $(n \times 1)$. A representative time course of factors II, VII, X, INR, SI_{VII} and their corresponding derivatives for a typical patient commenced on warfarin 4 mg daily is shown in **Figure 4.2**. It was observed that the time course of change in SI_{VII} (*panel f*, **Figure 4.2**) is similar to that of the INR (*panel b*, **Figure 4.2**).

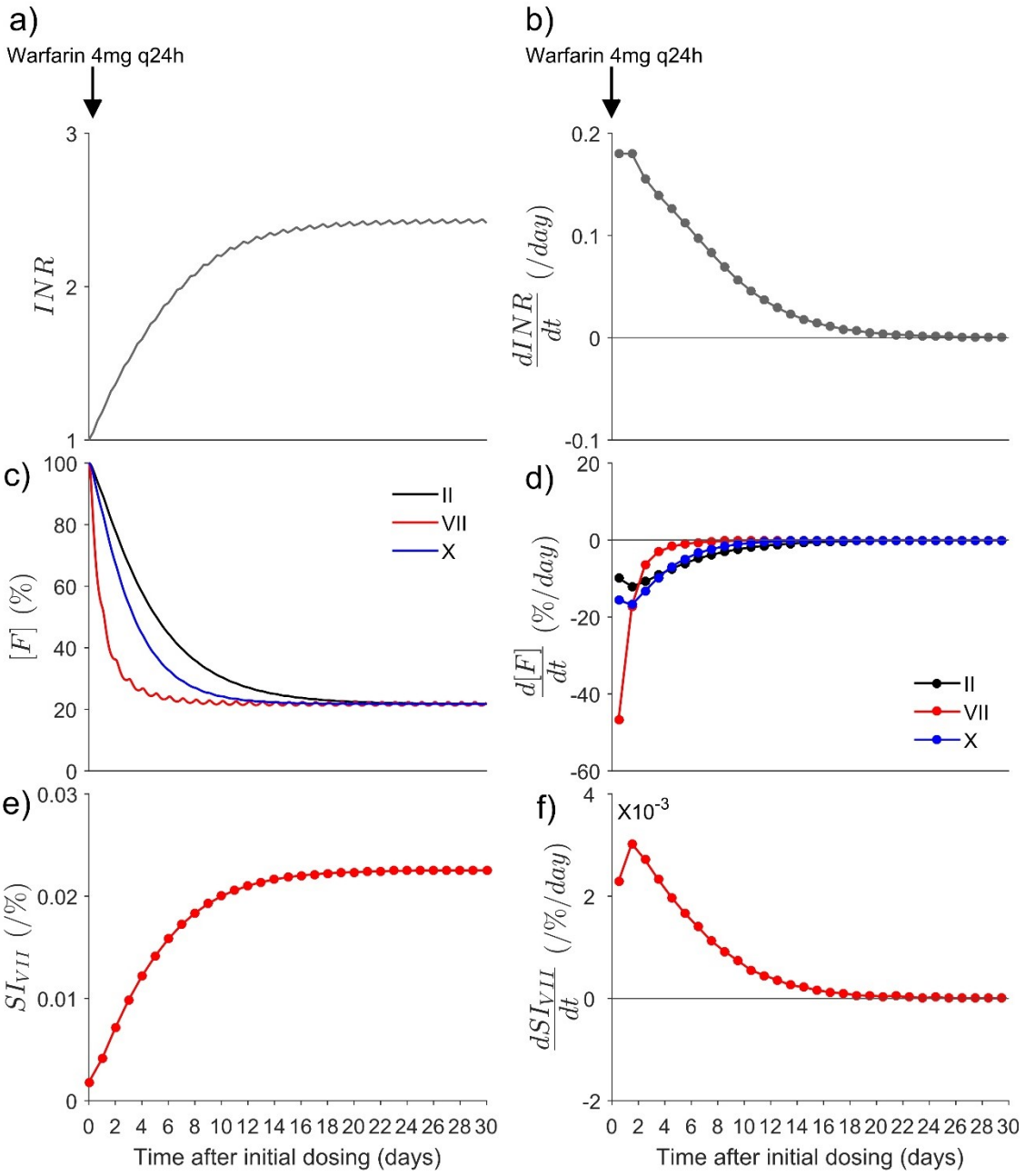

Figure 4.2 *The simulated time course of INR (panel a), factors II, VII, and X (panel c), and SI_{VII} (panel e) following initiation of 4mg warfarin daily. The corresponding derivative plots with respect to time for INR (panel b), and factors II, VII and X (panel d), and SI_{VII} (panel f) are shown in the right-hand column. SI_{VII} refers to the sensitivity index of INR to factor VII.*

For clinical application, blood samples of both factor VII and INR are needed for the calculation of SI_{VII} and $\frac{dSI_{VII}}{dt}$. To allow determination of the derivative from a single sample, a steady-state approximation was used (note that factor VII achieves steady state rapidly compared to other coagulation proteins).

$$SI_{VII_{t_i}} \approx q \times \frac{INR_{t_i}}{VII_{t_i}}; \quad t_i \geq t_{SS,VII}$$

Equation 4.8 *Approximation of SI_{VII}.*

Here, q is a proportionality constant and t_i is the time after warfarin dose change (with index i to denote a particular sampling time). A review of the relationship shown in **Equation 4.8** is shown in **Figure 4.3**. The data were fitted in MATLAB® Version 2015a using the *fitnlm* algorithm. The proportionality constant, q, was estimated to be 0.233 with a relative standard error (RSE) of 0.300%. The INR-to-factor VII ratio has intuitive appeal whereby a high INR-to-factor VII ratio indicates a high sensitivity of INR to factor VII, and vice versa, which is consistent with the original interpretation of SI_{VII}. Finally, using the INR-to-factor VII ratio as an approximation to SI_{VII}, the $\frac{dSI_{VII}}{dt}$ can now be derived from paired, timed samples of factor VII and INR (**Equation 4.9**). Higher order models were not considered given the need for more blood samples and the acceptable assumption of linearity.

$$\frac{dSI_{VII}}{dt} \approx \frac{SI_{VII_{t_2}} - SI_{VII_{t_1}}}{t_2 - t_1}; \quad t_2 > t_1 \geq t_{SS,VII}$$

Equation 4.9 *Finite difference approximation of dSI_{VII}/dt.*

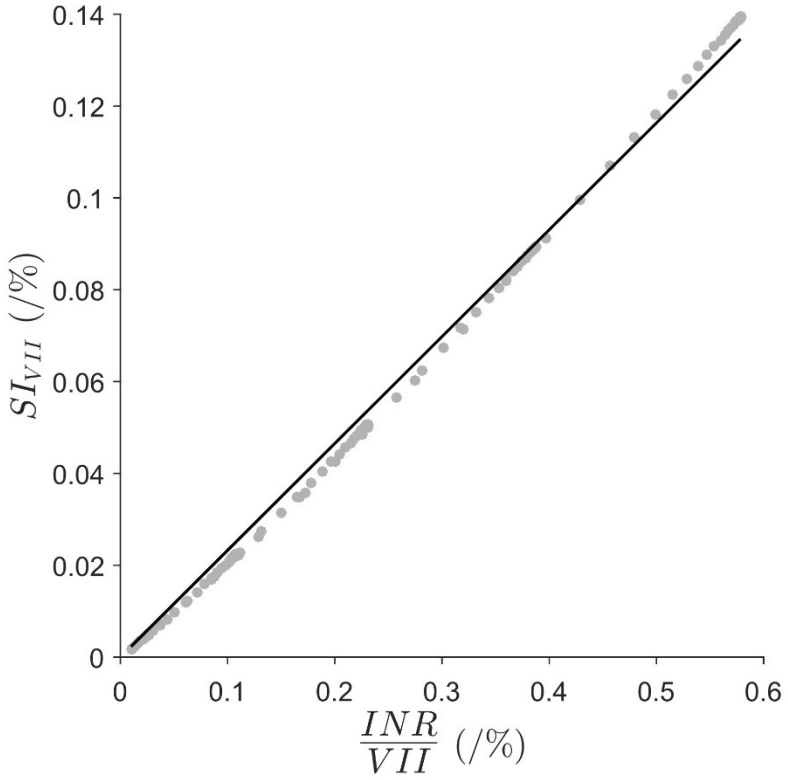

Figure 4.3 *Approximating SI_{VII} using the ratio of INR-to-factor VII. The solid line is the model prediction from a one-parameter linear model (Equation 4.8) with slope, q = 0.233 and the filled circles are the data vectors for SI_{VII} and INR-to-factor VII ratio that were simulated from the coagulation network model. SI_{VII} is the sensitivity index of INR to factor VII. The units of factor VII here are % of change from baseline and INR is dimensionless.*

4.5.2. Prediction of D_{ref}

From $\frac{dSI_{VII}}{dt}$, an individualised measure of the typical dose, D_{ref}, can be obtained. D_{ref} quantifies the sensitivity of the patient to warfarin in terms of the dose that would be taken by a typical patient to achieve the same level of anticoagulant response. For instance, if a patient is particularly sensitive to warfarin therapy then a standard warfarin dose (e.g. $D = 4\ mg/day$) will lead to an exaggerated anticoagulant response, which normally takes a much higher dose to achieve in a typical patient (e.g. $D_{ref} = 8\ mg/day$). In other words, if a patient is sensitive to warfarin then $D_{ref} > D$, if the patient displays similar sensitivity to that of a typical patient then $D_{ref} \approx D$, and if the patient is less sensitive then $D_{ref} < D$. The deviation of D_{ref} from D therefore quantifies the

difference of the patient from the typical patient. The relationships between patient's sensitivity to warfarin, D, anticoagulant responses, and D_{ref} are summarised in **Table 4.1**.

Table 4.1 *Quantification of D_{ref} based on the observed INR response and factor VII concentration for three patients who show different levels of sensitivity to warfarin. In this hypothetical example, all the patients are given the same dose of warfarin. D represents the warfarin dose administered, D_{ref} warfarin dose that would be required by a typical patient to achieve the observed anticoagulant response, INR international normalised ratio.*

Patient	D (mg/day)	INR	Factor VII concentration	D_{ref} (mg/day)
Warfarin-sensitive	4	↑	↓	8
Typical	4	↔	↔	4
Warfarin-insensitive	4	↓	↑	2

The value of D_{ref} relates to the dose-dependency of SI_{VII} and $\frac{dSI_{VII}}{dt}$ and no closed form function is available for this relationship from the QSP model. A function was, therefore, derived empirically. *Individual* model was fitted to the time course of $\frac{dSI_{VII}}{dt}$ at a specific D_{ref} (1 mg, 4 mg, 7 mg, 10 mg, and, 13 mg daily for a typical patient). A three-parameter logistic function was used such that:

$$\frac{dSI_{VII}}{dt} = \frac{h}{1 + e^{p \times (t-g)}}; \quad t > 0.$$

Equation 4.10 *Individual model for the time course of dSI_{VII}/dt at a specific D_{ref}.*

Here, h is the upper horizontal asymptote, p is the shape parameter, and g is the magnitude of horizontal shift. The individual models developed for the different levels of D_{ref} were combined into a single joint model. In the joint model, both h and g are functions of D_{ref} and p is considered independent. The full model expression is given in **Equation 4.11**.

$$\frac{dSI_{VII}}{dt} = \frac{h(D_{ref})}{1 + e^{p \times (t - g(D_{ref}))}}; \quad t > 0$$

$$h(D_{ref}) = a_0 + a_1 \times D_{ref}$$

$$g(D_{ref}) = b_0 + b_1 \times \ln D_{ref}$$

Equation 4.11 *Joint model for the time course of dSI_{VII}/dt at different D_{ref}.*

Here, a_i and b_i are parameters that define the D_{ref}-dependency of h and g, respectively. The final parameter estimates are given in **Table 4.2** and the model fits are shown in **Figure 4.4**. Details of the individual models developed for the data derived from different D_{ref} can be found in **Appendix 3.1**. Finally, given a value of $\frac{dSI_{VII}}{dt}$ (**Section 4.5.1**), D_{ref} can be quantified by solving **Equation 4.11** numerically.

Table 4.2 *Parameter estimates of the joint model for the time course of dSI_{VII}/dt at different D_{ref}. At different D_{ref}, the p estimates obtained were largely similar (range 0.260 - 0.301) and fixing of p to 0.300 resulted in an almost identical model fit. a_i defines the D_{ref}-dependency of h, b_i defines the D_{ref}-dependency of g, D_{ref} is the warfarin daily dose for a typical patient, h the upper horizontal asymptote, g the magnitude of horizontal shift, p the shape parameter, SI_{VII} the sensitivity index of INR to factor VII, r^2 the adjusted coefficient of determination, and RSE the relative standard error.*

Function	Final estimate (%RSE)		r^2
$\frac{dSI_{VII}}{dt}$	p		–
	0.300 fixed		
$h(D_{ref})$	a_0 (/%/day)	a_1 (/%/mg)	0.988
	0.000392 (123)	0.00108 (5.46)	
$g(D_{ref})$	b_0 (days)	b_1 (days)	0.995
	-1.48 (17.9)	4.13 (3.42)	

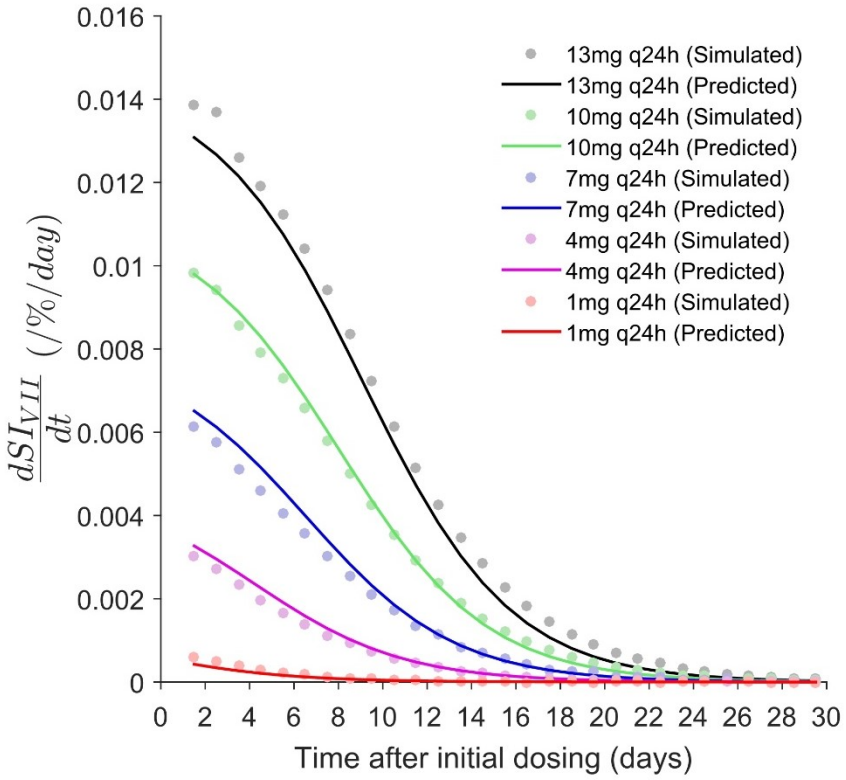

Figure 4.4 *Model fits of the joint model for the time course of dSI_{VII}/dt at different D_{ref}. The solid lines are the model predictions (Equation 4.11) and the filled circles are the data vectors for dSI_{VII}/dt that were derived based on simulations from the QSP coagulation network model. SI_{VII} is the sensitivity index of INR to factor VII.*

4.5.3. Calculation of $t_{SS,INR}$

An expression for $t_{SS,INR}$ that is now dependent on D_{ref} is obtained by combining **Equation 4.6** and **Equation 4.11**:

$$t_{SS,INR} \approx \min\left(t \left| \frac{h(D_{ref})}{1+e^{p\times(t-g(D_{ref}))}} \leq \varepsilon_{SI_{VII}} \right.\right); \quad t>0$$

$$h(D_{ref}) = a_0 + a_1 \times D_{ref}$$

$$g(D_{ref}) = b_0 + b_1 \times \ln D_{ref}.$$

Equation 4.12 *Solution for the $t_{SS,INR}$ based on D_{ref}.*

From **Equation 4.5**, a pre-requisite to the calculation of $t_{SS,INR}$ is the choice of a suitable value of $\varepsilon_{SI_{VII}}$. The choice of $\varepsilon_{SI_{VII}}$ should correctly classify a given INR as non-steady-state (or steady-state) when the INR is truly non-steady-state (or steady-state). The choice of $\varepsilon_{SI_{VII}}$ was based on optimising the receiver operating characteristic (ROC). Details of the method are provided in **Appendix 3.2**. It is seen that a choice of $\varepsilon_{SI_{VII}} = 0.000150$ provides the optimal operating characteristics of the error tolerance. Based on the D_{ref} obtained from **Section 4.5.2**, $t_{SS,INR}$ can be quantified using **Equation 4.12**.

4.5.4. Calculation of INR_{SS}

INR_{SS} can be determined based on the calculated $t_{SS,INR}$ if the function $l(\frac{dSI_{VII}}{dt})$ in **Equation 4.7** has an explicit expression. However, no mechanistic function is available and a function was derived empirically.

Factor VII and INR data were simulated from the QSP coagulation network model for different D_{ref} (1 mg, 4 mg, 7 mg, 10 mg, and, 13 mg daily). $\frac{dINR}{dt}$ and $\frac{dSI_{VII}}{dt}$ were computed. At each level of D_{ref}, individual quadratic model was fitted to the $\frac{dINR}{dt}$ versus $\frac{dSI_{VII}}{dt}$ data. Because the y-intercept was approximately zero, the following two-parameter model was used:

$$l\left(\frac{dSI_{VII}}{dt}\right) = k \times \left(\frac{dSI_{VII}}{dt}\right)^2 + m \times \frac{dSI_{VII}}{dt}; \quad t > 0.$$

Equation 4.13 *Individual model for the dINR/dt versus dSI_{VII}/dt data at a specific D_{ref}.*

Here, k is the second-order coefficient and m is the first-order coefficient of the quadratic function. Final parameter estimates and model fits for the *alternative* models considered are shown in **Appendix 3.3**. Subsequently, the five individual quadratic functions, each corresponds to a specific D_{ref}, were combined into a single joint function. In this expression, k and m were empirically expressed as a function of D_{ref},

$$l\left(\frac{dSI_{VII}}{dt}\right) = k(D_{ref}) \times \left(\frac{dSI_{VII}}{dt}\right)^2 + m(D_{ref}) \times \frac{dSI_{VII}}{dt}; \quad t > 0$$

$$k(D_{ref}) = -e^{c_0 + c_1 \times \ln D_{ref}}$$

$$m(D_{ref}) = e^{s_0 + s_1 \times \ln D_{ref}},$$

Equation 4.14 *Joint model for the dINR/dt versus dSI_{VII}/dt data at different D_{ref}.*

where, c_i and s_i are parameters defining the D_{ref}-dependency of k and m. The final parameter estimates are given in **Table 4.3**. The fit of the final model for the $\frac{dINR}{dt}$ versus $\frac{dSI_{VII}}{dt}$ data was evaluated visually by superimposing the model predictions on the simulated data (**Figure 4.5**). The quadratic model provided an adequate fit to the data.

Table 4.3 *Parameter estimates of the joint model for the dINR/dt versus dSI_{VII}/dt data at different D_{ref}. D_{ref} is the warfarin daily dose for a typical patient, k and m are coefficients of the quadratic function, c_i defines the D_{ref}-dependency of k, and s_i the D_{ref}-dependency of m, r^2 is the adjusted coefficient of determination, RSE the relative standard error, and SI_{VII} the sensitivity index of INR to factor VII.*

Function	Final estimate (%RSE)		r^2
$h(D_{ref})$	c_0	c_1	0.997
	11.9 (1.03)	-2.05 (3.18)	
$m(D_{ref})$	s_0	s_1	0.987
	5.26 (1.62)	-0.672 (6.75)	

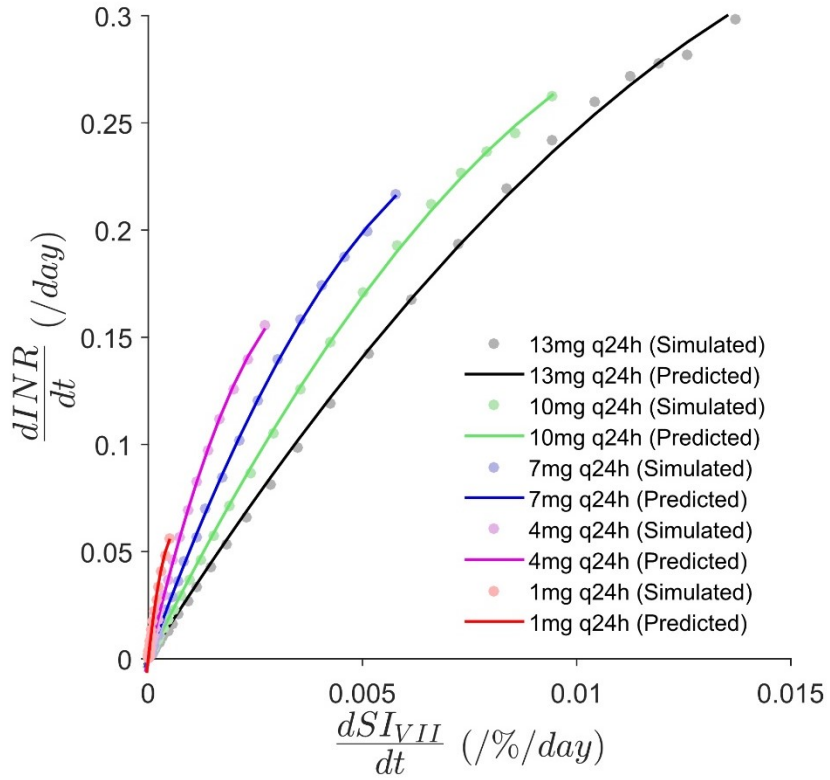

Figure 4.5 *Model fits of the joint quadratic function for the dINR/dt versus dSI_{VII}/dt data at different D_{ref}. The solid lines are the prediction from the empirical quadratic model (Equation 4.14) and the filled circles are the data that were derived based on simulations from the QSP coagulation network model. SI_{VII} is the sensitivity index of INR to factor VII.*

Equation 4.7 and **Equation 4.14** were combined to give an expression for INR_{SS}:

$$INR_{SS} \approx INR_0 + k(D_{ref}) \times \int_0^{t_{SS,INR}} \left(\frac{dSI_{VII}}{dt}\right)^2 dt + m(D_{ref}) \times \int_0^{t_{SS,INR}} \frac{dSI_{VII}}{dt} dt; \quad t > 0$$

$$k(D_{ref}) = -e^{c_0 + c_1 \times \ln D_{ref}}$$

$$m(D_{ref}) = e^{s_0 + s_1 \times \ln D_{ref}}.$$

Equation 4.15 *Solution for the INR_{SS} based on D_{ref} and $t_{SS,INR}$.*

Here, the definite integrals can be solved analytically. An algebraic solution to the definite integrals and the INR_{SS} is given in **Appendix 3.4**. This relationship

however does not hold for the first two days of warfarin initiation since factor VII level is not at equilibrium at this time.

4.5.5. Prediction algorithm

The mathematical features and parameter values of the four-step algorithm to predict $t_{SS,INR}$ and INR_{SS} are shown in **Figure 4.6**. The corresponding MATLAB® code for the implementation of the algorithm is available in **Appendix 3.5**.

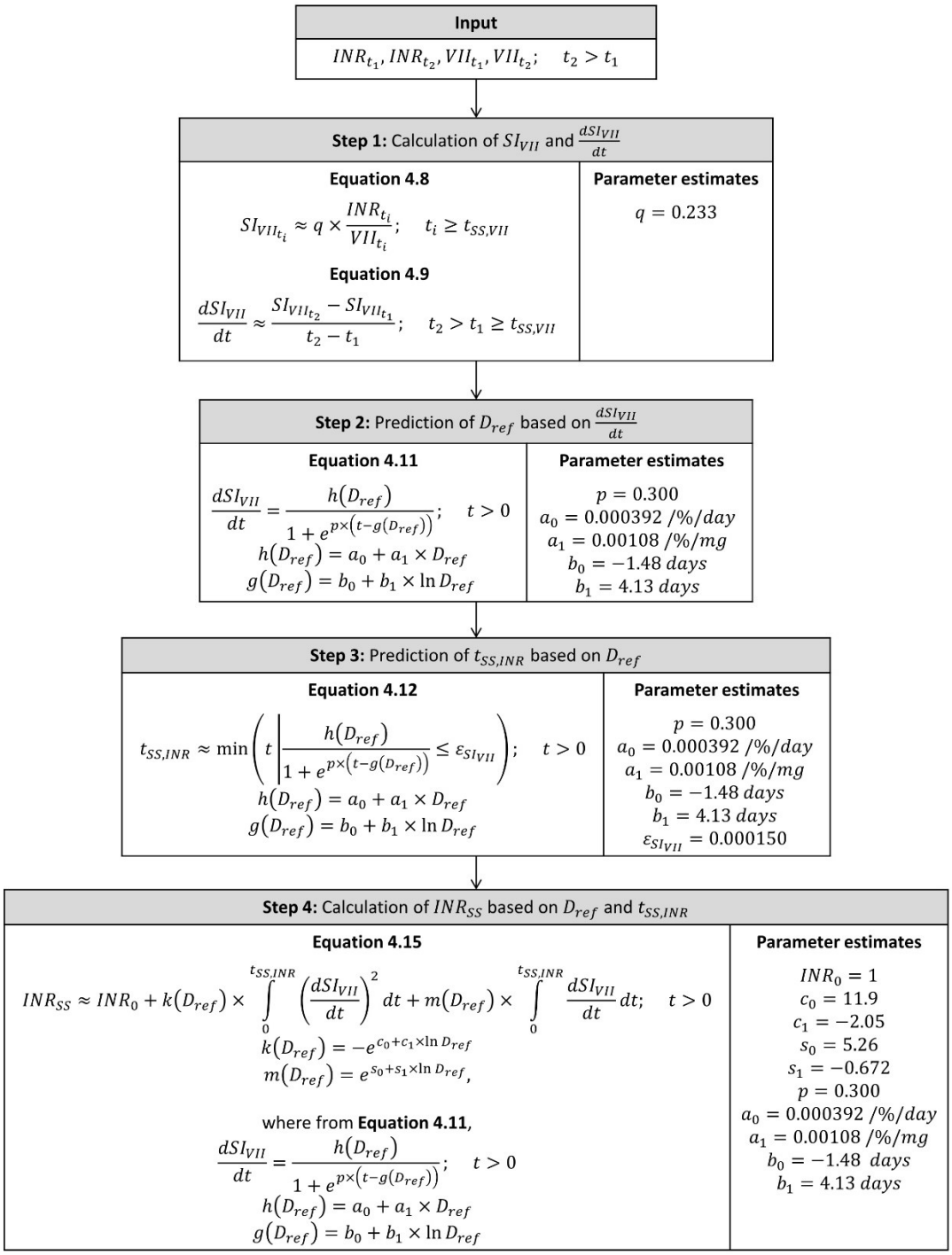

Figure 4.6 *Prediction algorithm of $t_{SS,INR}$ and INR_{SS}. a_i defines the D_{ref}-dependency of h, b_i the D_{ref}-dependency of g, c_i the D_{ref}-dependency of k, D_{ref} the typical dose that gives a specific value of INR, g the horizontal shift, h the upper horizontal asymptote, INR_{SS} the steady-state INR, INR_0 the INR at baseline, s_i defines the D_{ref}-dependency of m, k and m are the coefficients of the quadratic function, p the shape parameter, q the proportionality constant, SI_{VII} the sensitivity index of INR to factor VII, t the time after warfarin dose change (with index i to denote a particular sampling time), and ε_{SIVII} the tolerance below which the dSI_{VII}/dt corresponds to the steady-state INR.*

4.6. Application of the prediction algorithm

The proposed method was applied to a typical simulated patient and two real patients to illustrate proof-of-principle.

4.6.1. Predicting INR_{SS} for a virtual patient

Data relating to a typical patient were simulated from a QSP coagulation model [31] under different dosing scenarios. Factor VII concentrations and INR data at days 3 and 4 were simulated for typical patients who were commenced on warfarin (D =1 mg, 4 mg, 7 mg, 10 mg, or 13 mg daily). These data were analysed according to the four-step algorithm (**Figure 4.6**) and the predictions of $t_{SS,INR}$ and INR_{SS} were compared to the simulated values and reported in terms of prediction bias (predicted value minus the simulated value). The simulation and prediction results are shown in **Table 4.4**. As expected, the predicted D_{ref} is approximately equal to D since the simulated patient is a typical patient. At different simulated warfarin dosing rates, the bias was within a clinically reasonable range for both the $t_{SS,INR}$ ($\pm$2.0 days) and INR_{SS} ($\pm$0.20). One exception was that at a dose of warfarin of 1 mg/day, $t_{SS,INR}$ was under-predicted ($-$3.7 days). However, this is unlikely to be important clinically considering such a dosing rate is uncommon in clinical practice and furthermore the corresponding prediction of INR_{SS} was not evidently biased ($-$0.02).

Table 4.4 *Performance of the proposed algorithm to predict the $t_{SS,INR}$ and INR_{SS} for a simulated typical patient commenced on warfarin at different dosing rates. D denotes the warfarin daily dose given, D_{ref} the warfarin daily dose for a typical patient, INR_{SS} the steady-state INR, Obs. observed, Pred. predicted, and $t_{SS,INR}$ the time to reach steady-state INR.*

D (mg/day)	Predicted D_{ref} (mg/day)	$t_{SS,INR}$ (days)			INR_{SS}		
		Obs.	Pred.	Bias	Obs.	Pred.	Bias
1	1.35	11.5	7.8	-3.7	1.41	1.39	-0.02
4	3.97	17.5	15.6	-1.9	2.40	2.28	-0.12
7	6.78	20.5	19.5	-1.0	3.23	3.09	-0.14
10	9.90	22.5	22.3	-0.2	3.98	3.88	-0.10
13	13.3	24.5	24.5	0.0	4.70	4.66	-0.04

4.6.2. Predicting INR_{SS} for patients

The method was retrospectively assessed in two patients newly commenced on warfarin D =5 mg daily based on a previously published dataset [167, 181]. These two patients represent all of the patients who have available data that fulfil the requirements to apply the INR prediction method. $t_{SS,INR}$ and INR_{SS} were predicted using factor VII and INR available at day 3 and day 4. The factor VII and INR profiles of these two patients are shown in **Appendix 3.6**. The predicted INR_{SS} was later compared to the observed INR at day 28 for ID A and day 14 for ID B. Observed INR at later time points were not used as the observations were confounded by non-steady-state conditions introduced by warfarin dosage adjustment. Observed $t_{SS,INR}$ was also unavailable due to sparse sampling of INR. Results of the assessment using real patient data are summarised in **Table 4.5**. Both patients showed reasonable agreement in the predicted and observed INRs.

Table 4.5 *Performance of the proposed algorithm in predicting the INR_{SS} for two real patients commenced on warfarin 5 mg daily. D is the warfarin daily dose given, D_{ref} the warfarin daily dose for a typical patient, and INR_{SS} the steady-state INR.*

ID	D (mg/day)	Pred. D_{ref} (mg/day)	Pred. INR_{SS}	Obs. INR	Difference in INR
A	5	6.12	2.9	3.3 (day 28)	-0.4
B	5	7.32	3.2	3.2 (day 14)	0.0

4.7. Discussion

A factor VII-based approach to predict $t_{SS,INR}$ and INR_{SS} in patients receiving warfarin was proposed. By considering factor VII as the main driver for the INR, this allows the $t_{SS,INR}$ to be determined and from this the INR_{SS} can be calculated. The proposed method represents a unique approach to predicting the anticoagulant response to warfarin. It incorporates information from factor VII for the prediction of INR and evaluates the INR from the perspective of determining $t_{SS,INR}$. From a practical viewpoint, the proposed method requires timed, paired blood samples of INR and factor VII. The use of the method was demonstrated in a typical simulated patient and two real patients. The prediction errors were found to be within clinically acceptable limits.

The proposed method differs from those reported in the published literature. Several warfarin dosing algorithms quantify the likely anticoagulant response for warfarin maintenance dose prediction using patient characteristics known to influence warfarin dose-response such as body size, age, ethnicity, concomitant drugs, cytochrome P-450 2C9 (CYP2C9) genotype, vitamin K epoxide reductase complex subunit 1 (VKORC1) genotype (see Klein *et al.* [11] for example). These methods provide no guidance for warfarin dose adjustment once anticoagulant response data (e.g. INR) become available. Other warfarin dosing methods, including traditional initiation nomograms, rely solely on the INR, a composite and blunt measure of anticoagulant response, to guide the prediction of future INR and subsequently, warfarin dose adjustment (see Gedge *et al.* [28] for example). Bayesian forecasting methods use both prior INR and covariates for INR and warfarin dose prediction (see Wright *et al.* [18] for example). In this study, it was proposed that measuring the coagulation protein data in addition to the INR will be more informative and superior to measuring the INR alone because factors II, VII, and X bridge the gap between warfarin dose and INR response. The coagulation protein data therefore provide a *direct* measure of the anticoagulant response as well as sensitivity of the patient to warfarin therapy. Here, it is worth noting that measures of anticoagulant response, such as INR and factor VII concentration, will capture between-subject

differences in both warfarin pharmacokinetics and pharmacodynamics, including those related to CYP2C9 and VKORC1 genotypes. Therefore, in theory, once the time course of anticoagulant responses for a given warfarin dose is accounted for, it may not be necessary to consider these and other covariates separately. This would, however, require prospective evaluation. To date, only one published study (Pitsiu and colleagues [157]) considered coagulation protein activity for the prediction of warfarin maintenance dose regimens. It was shown that factor VII response measurements alone were adequate to determine dosing requirements although it is important to point out that the sample size is small ($n = 5$) and the use of healthy volunteers potentially limits generalisability of the study's results to all warfarin users.

The proposed approach also differs from those previously reported as it attempts to predict $t_{SS,INR}$ and from this, the INR_{SS} is derived. Based on simulations from the QSP coagulation network model [31], $t_{SS,INR}$ is observed to be dose-dependent (see **Figure 4.7**). It is thought that the dose-dependency of $t_{SS,INR}$ is due to the inverse relationships between INR sensitivity and coagulation protein concentrations (i.e. increasing INR sensitivity to coagulation proteins at low coagulation protein concentrations). Since greater warfarin exposure is typically associated with lower coagulation protein concentrations, then a disproportionate increase in the INR and delayed achievement of steady-state INR (i.e. longer $t_{SS,INR}$) are expected with high warfarin exposure. In this work, sensitivity of the INR to factor VII was considered and was used to provide an alternative definition for the steady-state INR, which allows the dose-dependency in $t_{SS,INR}$ to be captured and quantified. Predicting $t_{SS,INR}$ allows for a more meaningful interpretation of observed INR response data, which are frequently confounded by non-equilibrium conditions. Then, dosing decisions based on INR measured will be better informed and unnecessary dose adjustments as well as frequent INR monitoring can be avoided.

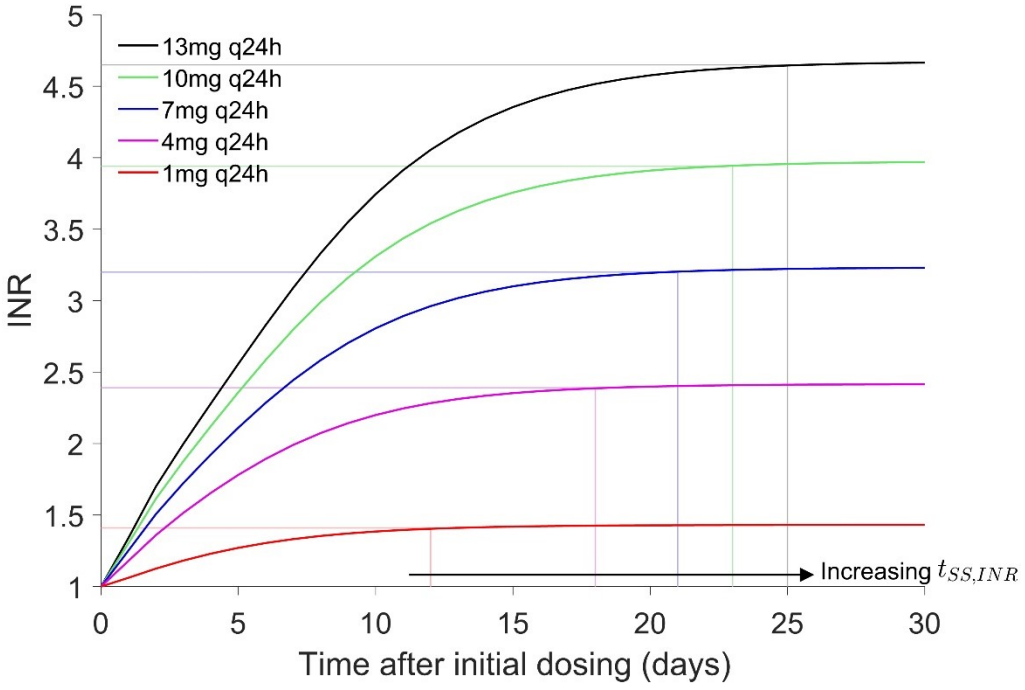

Figure 4.7 *$t_{SS,INR}$ is dose-dependent based on simulations from the QSP coagulation network model [31]. $t_{SS,INR}$ is the time to reach steady-state INR. The vertical lines represent the minimum value of time where the change in INR over time is within a predefined tolerance.*

The current work has several drawbacks. Due to the absence of explicit functions to describe the relationships between warfarin dose, SI_{VII}, and INR, the relevant functions were derived *empirically* to match predictions from a QSP coagulation network model [31]. Despite the empiricism attached to this work, the underpinning theory outlined in **Section 4.4** should remain intact and unaffected. Hence if a scale-reduced version of the QSP model is developed at a later stage then the theory could be applied to a fully mechanistic model. It is also worth noting that despite the effort to verify the QSP coagulation network model, it is acknowledged that there remain uncertainties in the applicability of the QSP coagulation network model. It is possible for a potential inconsistency in the QSP coagulation network model to propagate to the proposed INR prediction method thereby affecting the predictive performance of the method. As a result, it is essential to evaluate and if required, to recalibrate the INR prediction model using prospectively collected warfarin-factor VII-INR data in a large cohort of warfarin patients.

In this study, the observed anticoagulant response was used for individualisation of D_{ref}, which in turn was used for the prediction of $t_{SS,INR}$ and INR_{SS}. $g(D_{ref})$ is not defined when $D_{ref} \leq 0$. This defines the boundary beyond which the proposed method no longer works and thereby represents a limitation of the method. The limitation, however, is unlikely to be clinically important as the conditions where this would occur, for example if factor VII concentration increases after warfarin initiation, is unlikely in clinical practice. In addition, the individualisation of D_{ref} relies on factor VII being at steady state and therefore is confounded by factors that affect the rate of change of factor VII. For instance, an abnormally long degradation half-life of factor VII will lead to a deflated SI_{VII} estimate and a similarly depressed D_{ref} estimate, which in turn results in predicted $t_{SS,INR}$ and INR_{SS} that are biased downward. The proposed method should be adjusted to account for the between patient variability in the degradation half-life of factor VII or alternatively, to sample factor VII at later time points when its steady state has been established. It is important to recognise that the above limitations can also be circumvented by accounting for non-steady state values of factor VII – although this will require additional blood samples to enable quantification of SI_{VII}. Another limitation of the study is that the practical feasibility of the proposed method in routine clinical settings was not considered. For instance, it is assumed that an assay that is appropriately precise and accurate is available to measure blood factor VII concentrations. The proposed method was applied to a typical simulated patient and two real patients to illustrate proof-of-principle. Evaluation of the method in a larger cohort of warfarin patients is not currently possible using retrospectively available data because factor VII is not routinely measured. These results are therefore not generalisable to clinical use. Further work to evaluate the clinical utility of the method using prospectively collected warfarin, factor VII, and INR data would be required. This work would evaluate the predictive performance of the method with respect to both $t_{SS,INR}$ and INR_{SS}. Briefly, patients who will be initiated on warfarin (any indication) will be prospectively recruited. In these patients, factor VII concentrations and INRs in close temporal proximity (e.g. day

3 and day 4) will be used as input into the proposed algorithm for the prediction of $t_{SS,INR}$ and INR_{SS}. The observed and predicted $t_{SS,INR}$ and INR_{SS} will be compared using mean prediction error (MPE) and root mean square error (RMSE) to quantify the prediction bias and imprecision, respectively [199].

Finally, a note on sampling times. The sampling times after the achievement of factor VII's steady-state (e.g. $t_1 = day\,3$ and $t_2 = day\,4$) are likely to be preferable considering that steady-state factor VII is informative of INR_{SS} [144, 146, 167, 198] and that by avoiding sampling on day 1 and day 2, the lag in the onset of factor VII reduction observed in some patients can be bypassed [140, 157, 165, 181]. In addition, t_1 and t_2 should be in temporal proximity to allow accurate approximation of the derivative required for the quantification of SI_{VII}. At this stage, the sampling times are proposed based on heuristic reasons and an optimal design analysis may be able to offer better alternative sampling times – one that minimise the bias in the prediction of INR_{SS}.

It is important to note that the work conducted in this chapter was not set forth to propose a new framework that is instantly applicable for clinical use, but to introduce a new perspective on INR prediction and subsequently, for warfarin dosing. A natural succession to this work would be to extend the current method beyond the prediction of INR_{SS} to prediction of warfarin maintenance dose. This will be discussed in **Chapter 6**.

4.8. Conclusions

A conceptually different approach for the prediction of future INR has been proposed. The method was associated with minimal bias and its use was illustrated using patient data supporting a proof-of-principle. The proposed method represents a unique approach to predict the INR. It considers factor VII as the main driver for INR and furthermore, it represents the first work to evaluate the INR from the $t_{SS,INR}$ perspective. Future research to extend the method for warfarin maintenance dose prediction and to assess the predictive performance in a cohort of warfarin patients is required.

PART IV

EVALUATION OF MODEL ASSUMPTIONS

Chapter 5: Evaluation of assumptions underpinning pharmacometric models

The construction of a joint model for warfarin, vitamin K-dependent clotting factors, and anticoagulation proteins (**Chapter 2**) as well as the development of a factor VII-based method for the prediction of anticoagulant response to warfarin (**Chapter 4**) were built on several assumptions. Models or methods that are predicated on erroneous assumptions are likely to be flawed and hence evaluation of assumptions that are likely to have impact on model performance is crucial. This chapter describes the development of a framework for systematic evaluation of model assumptions. The framework was applied to the assumptions underpinning the aforementioned models. Selected assumptions from these models are shown in this chapter as examples to illustrate the utility of the framework. The current chapter is divided into the following sections: introduction, aims and objectives, workflow, definition and classification of assumptions, a flowchart for assumption evaluations, table of assumptions, application, discussion, and conclusion.

5.1. Introduction

All models are underpinned by assumptions. The validity of any inference drawn from a model depends on the appropriateness and likely impact of the underlying assumptions [34]. This makes assumption evaluation an integral part of model building and model use.

The importance of assumption evaluation is well-recognised. Current guidelines by the Food and Drug Administration (FDA) [200], the European Medicines Agency (EMA) [201, 202], and the European Federation of Pharmaceutical Industries and Associations (EFPIA) [34] stipulate that all assumptions inherent to model development and model application should be explicitly expressed in the data analysis plan and study report. A transparent description of how these assumptions were assessed and what impact they would have on model inferences should also be included. Here, the recommendations pertaining to acknowledgement, evaluation, and documentation of assumptions are applicable regardless of the type of pharmacometric analyses including: pharmacokinetic (PK) analysis [200, 201, 203-206], pharmacokinetic and pharmacodynamic (PKPD) analysis [207, 208], quantitative systems pharmacology (QSP) modelling [209], and physiologically based pharmacokinetic (PBPK) modelling [210-213].

However, assumptions inherent to model development and use are not routinely acknowledged, evaluated, or documented in journal articles reporting pharmacometric analyses. This is also apparent in the analyses submitted for regulatory review, where the EMA outlined the lack of transparent description of influential assumptions and an ineffective evaluation or reporting of the impact of assumptions on model inference to be a major limitation [214]. All these form an unequivocal barrier for effective model use and regulatory review.

Two articles were identified which provided specific frameworks for evaluating model assumptions. The first article by Karlsson and colleagues used the development of a population PK model as an exemplar to demonstrate how assumptions intrinsic to model building may be evaluated [205]. In this work, Karlsson and colleagues exhaustively stated all the assumptions associated with

the PK model, gave examples on how violations of assumptions can be detected, and introduced new models that allow some standard assumptions to be relaxed [205]. The second article was a white paper published by the EFPIA Model-Informed Drug Discovery and Development (MID3) Workgroup [34]. In this work, the importance of assumption evaluation and documentation is highlighted. Here, assumptions were broadly classified into five principal categories: (1) pharmacological assumptions, (2) physiological assumptions, (3) disease assumptions, (4) data assumptions, and (5) mathematical or statistical assumptions. Importantly, a table of assumptions was proposed for adoption by modellers to document assumptions, uncertainties, and impact of assumption violations [34].

While the importance of assumption evaluation is well-recognised, how these assumptions should be systematically approached and be effectively assessed has received limited attention. The overarching goal of this work was therefore to enrich and expand on the aforementioned frameworks for assumption evaluation in order to encourage greater transparency in the description, evaluation, and documentation of influential assumptions for model building and model use. The two common approaches to model development in pharmacometrics are: (1) top-down approach (developing model empirically i.e. based on data and usually with parsimony prioritised) and (2) bottom-up approach (building a model based on prior knowledge about a system and is not necessarily bound to the principle of parsimony). These two modelling approaches will be used to assess the assumption framework presented here.

5.2. Aims and objectives

In this work, existing frameworks [34, 205] were expanded for evaluating model assumptions systematically. The objectives of this work were: (1) to define the concept of an assumption within the context of this work, (2) to develop a flowchart for systematic evaluation of assumptions, (3) to propose a standard table for documentation of assumptions and evaluation results, and finally (4) to apply the flowchart to top-down and bottom-up modelling approaches.

5.3. *Workflow*

Existing frameworks were used as a starting point for this work. The frameworks were expanded based on an evaluation of the risk management literature, expert opinion, and logical reasoning.

A simple four-step workflow was proposed for the evaluation of model-related assumptions (**Figure 5.1**). Here, specific tools were developed to facilitate this process and will be detailed in the next following sections: (1) definition and categorisation of assumptions, (2) flowchart for systematic evaluation of assumptions, and (3) assumptions table.

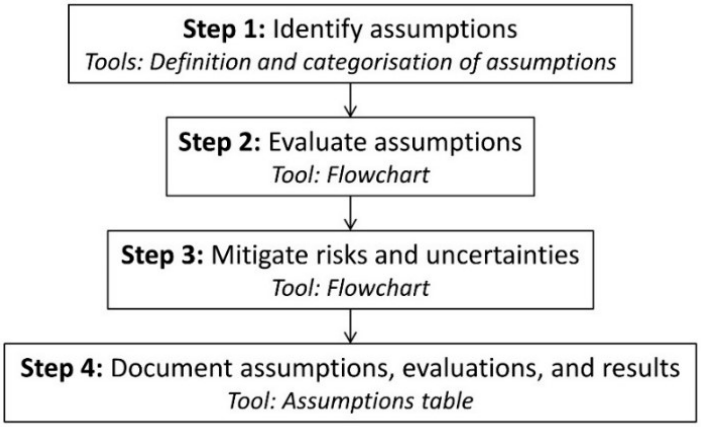

Figure 5.1 *The four-step workflow and proposed tools for assumption evaluation.*

5.4. What is an assumption?

This section is dedicated to defining assumptions. Here, the definition of an assumption and related terms are compared and contrasted. Subsequently, systems for classification of different assumptions are introduced and recommendation for systematic identification of assumptions is detailed.

5.4.1. Definition of an assumption and related terms

For the purpose of this work, an assumption is defined as an unsubstantiated claim (*belief*) about a system that is required (*need*) to be made in order for the system to be manipulated in a manner that is advantageous to the modeller (*model building or model use*). An assumption therefore is a belief that is needed to build or use a model.

A subset of these assumptions are hypotheses, which by definition, are testable. An assumption is distinguished from an axiom (a self-evident truth), a theorem (a proven belief [a truth]) and a limitation (a boundary beyond which the assumption no longer holds). The relationships between a belief, an assumption, an hypothesis, an axiom, and a theorem are summarised in **Figure 5.2**.

More elaborate definition of these terms, each accompanied by a list of examples, are provided in **Table 5.1**. Here, it is acknowledged that there may be some nuanced differences in the adopted definitions compared to that defined in other fields of study (e.g. mathematics, philosophy, psychology).

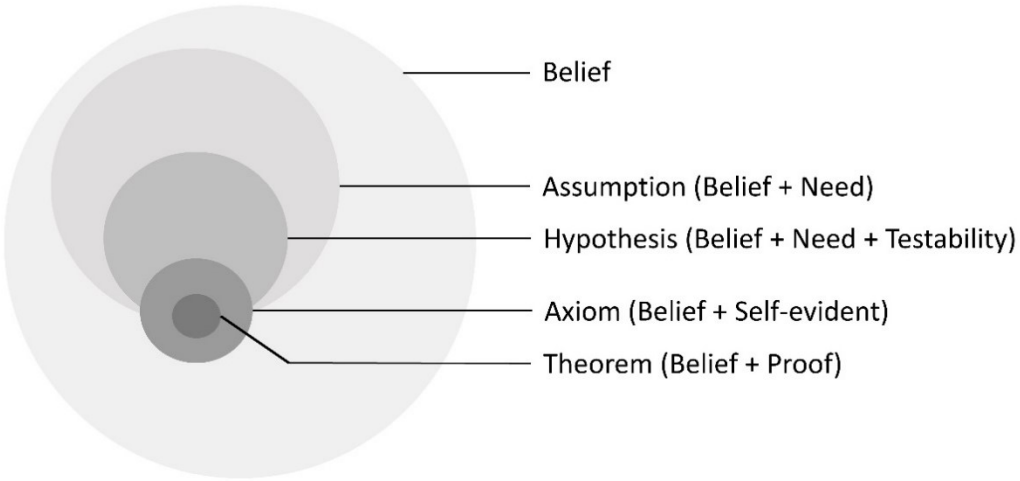

Figure 5.2 *The Venn diagram depicting the relationships between a belief, an assumption, an hypothesis, an axiom, and a theorem.*

Table 5.1 *Definition and examples of an assumption and related terms.*

Term	Definition	Examples (not exhaustive)
Belief	A belief connotes a proposition that is considered to be true but for which substantive evidence is not available.	*Example 1: Constant receptor system* The turnover of receptors are negligible if the observation time window is relatively short in *in-vitro* experiments. *Example 2: Metabolic pathways* All metabolic pathways of a drug are known. *Example 3: Paediatric versus adult population* The variability in clearance of a drug is similar between paediatric and adult patients.
Assumption	An assumption is a belief where needs define its existence and necessitate its use.	*Example 1: Accurate recorded sampling time* The recorded sampling time is free of error. *Example 2:* $\varepsilon \sim iid\ N(0, \sigma^2)$ All error terms ε are independent and identically distributed (iid) from a normal distribution with a mean of zero and a variance of σ^2. *Example 3:* $GFR \approx eGFR$ The estimated glomerular filtration rate (eGFR) obtained from the Cockcroft-Gault equation provides an unbiased measure of the actual glomerular filtration rate (GFR) of a patient.
Hypothesis	An hypothesis is a testable assumption.	*Example 1: Bioequivalence* A given generic drug is bioequivalent to the original brand-name drug. *Example 2: Hepatic clearance* The fraction of a drug administered that is metabolised is 0.4. *Example 3: Active compound* Only the parent drug is pharmacologically active.

Term	Definition	Examples (not exhaustive)
Axiom	An axiom is a belief that is regarded as self-evidently true.	*Example 1:* $CL \in \mathbb{R}^+$ Clearance of a drug (CL) is a positive quantity. *Example 2: Volume of distribution* Plasma volume represents the lower limit of the volume of distribution of any intravenously administered drugs.
Theorem	A theorem is a belief that is proven to be true based on logical or mathematical reasoning.	*Example 1: Bayes' theorem* Let X and Y be two events. Bayes' theorem states that $P(Y\|X) = \frac{P(Y)P(X\|Y)}{P(X)}$. *Example 2: Central limit theorem* Let $X_1, X_2, \cdots, X_n$ be a random sample from a distribution (any distribution) with mean μ and finite variance σ^2. If the sample size n is sufficiently large, then the sampling distribution of the sample mean ($\bar{X}$) approaches a normal distribution with a mean of μ and a variance of $\frac{\sigma^2}{n}$.
Limitation	A limitation represents the boundary beyond which the use of an assumption is unsound or invalid.	*Example 1: Linear exposure-response model* The assumed linear relationship between a drug's exposure and response may not hold beyond the dose range modelled. *Example 2: Small sample size* The sample size for the study is small thus potentially limiting generalisability of the study's results to the intended population. *Example 3: Making inferences by extrapolation* Inferences drawn from extrapolation about the clinical effects of dosing beyond the scope of the model may not be valid.

5.4.2. Classification of assumptions

Here, assumptions are classified into two groups, implicit or explicit, based on the origin of the assumptions (i.e. how does the assumption arise). Implicit and explicit assumptions are briefly introduced here. A detailed explanation and examples of implicit and explicit assumptions are provided in **Table 5.2**.

5.4.2.1. Implicit assumptions

Implicit assumptions arise from an inherent component or aspect of a method or model. They are *not* defined by the users of the method or model but based on science. For instance, the Cockcroft-Gault equation carries the implicit assumption of steady-state creatinine and the analysis of variance (ANOVA) requires the errors to be normally distributed. Here, a method or model may become invalid if the conditions required for the founding assumptions to be valid have not been met. Since the assumption attached to the method or model is not necessarily obvious, this type of assumption is termed *implicit*.

5.4.2.2. Explicit assumptions

Explicit assumptions arise from heuristic principles or the application of a method or model. Assumptions may represent a heuristic solution to a problem. They may arise due to need, lack of alternative methods or models, and parsimony. For instance, the recorded blood sampling time and dosing time are assumed to be accurate.

Explicit assumptions may also include assumptions that are originally implicit. This occurs when the knowledge of the (implicit) assumptions itself are matched to the structure of the problem to inform the choice of a method or a model. For example, since the binding equilibrium is quicker than changes in concentration, application of an E_{max} model is appropriate. Implicit and explicit assumptions are therefore not mutually exclusive.

In all cases, additional assumptions of appropriateness may be necessary. Since these assumptions are made by the user, they are termed *explicit*.

Table 5.2 *Definition and examples of implicit and explicit assumptions.*

	Implicit assumption	Explicit assumption
Origin	Arise from an inherent component or aspect of a method or model.	Arise from heuristic principles or the application of a method or model.
Definition	1. There are assumptions inherent in a method or model that underpin its derivation and use. 2. They are *not* defined by users of the method or model but derived from science.	1. Assumptions may represent a heuristic solution to a problem. They may arise due to need, lack of alternative methods or models, and parsimony. 2. Additionally, knowledge of implicit assumptions can be matched to the structure of the problem to inform decisions on the application of a method or a model. Here, assumptions that are originally implicit become explicit. 3. Additional assumptions of appropriateness are often necessary. 4. Explicit assumptions are usually user-defined.
Observations	1. Since assumptions are inherent they may not always be apparent and hence are termed *implicit*.	1. In most cases, the need for assumptions is based on a gap in knowledge, which requires an imputation. 2. In all cases, these assumptions are made by the user and hence are termed *explicit* (even if the user does not directly acknowledge the assumption).
Note	All structural models (e.g. in pharmacokinetic-pharmacodynamic (PKPD) modelling) have some implicit assumptions (see examples). These are typically related to the structure itself and also the alternative structures that are not permitted within the current framework.	Implicit and explicit assumptions are *not* mutually exclusive.

	Implicit assumption	Explicit assumption
Assumption Examples	**Assumptions related to the derivation of an equation:** 1. Cockcroft-Gault equation carries the implicit assumption of steady-state serum creatinine. 2. The E_{max} model implicitly assumes that the total ligand concentration is in excess of the concentration of the receptors. Receptor binding therefore has a negligible effect on the free ligand concentration. **Assumptions require for a method to work:** 1. The analysis of variance (ANOVA) requires the errors to be normally distributed. 2. The maximum likelihood (ML) estimation method typically requires the observations, $y_1, y_2, \cdots, y_n$, to be independent and identically distributed (iid). **Assumptions of common PKPD models:** 1. The turnover model typically assumes that the precursor pool for the physiological intermediate is abundant. 2. The relationship that specifies $CL = \frac{D \times F}{AUC}$ is predicated on elimination occurring from the central compartment (as per below). Note that AUC is the area under the concentration time curve, CL drug clearance, D dose, and F bioavailability.	**Assumptions that arise due to need, lack of alternative method or model, and parsimony:** 1. *Need / lack of alternative method or model*: The recorded blood sampling time and dosing time are accurate. 2. *Parsimony*: For a particular PKPD dataset, a linear model provides an appropriate description of the relationship between drug concentration and effect. **Explicit assumptions that are originally implicit:** 1. That binding equilibrium is quicker than changes in concentration, hence application of an E_{max} model is appropriate. 2. Since the sampling of the drug concentrations is sparse, the error terms are unlikely to be autocorrelated, hence the use of the ML estimation method is appropriate. **Assumptions of appropriateness:** 1. Cockcroft and Gault equation provides a good approximation to the measured glomerular filtration rate (mGFR) for up to 70 ml/min. 2. Application of an immediate effect model is acceptable for steady-state data even if the drug is known to have a delayed effect.

	Implicit assumption	Explicit assumption
	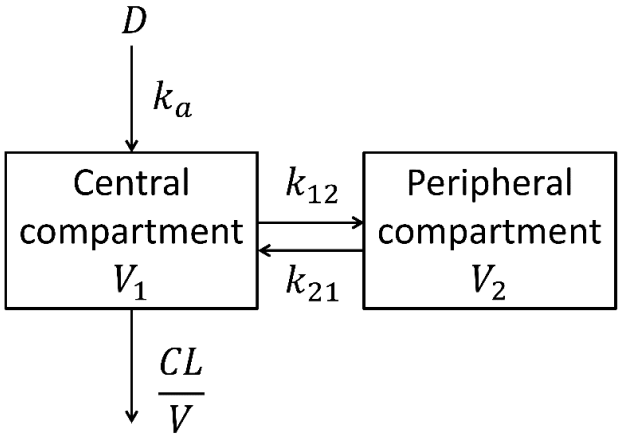	
Limitation examples	Use of Janmahasatian's equation to derive the fat free mass (FFM) for patient groups other than those of European descent.	Application of FFM equation to a patient who has recently lost weight via bariatric surgery.

5.4.3. Identification of assumptions

Identification of a potentially exhaustive list of model-related assumptions is challenging. Due to the inherent nature of some assumptions and model complexity, the very existence of some assumptions may not be immediately obvious to modellers. This represents a major barrier to assumption evaluation and subsequent mitigation of risks and uncertainties.

To spot these unknown unknowns, it is useful for modellers to adopt a systematic approach that is to list assumptions methodically according to the nature of assumptions. To this end, six categories of assumptions have previously been proposed [34]: (1) biological or physiological assumptions, (2) pathophysiological assumptions, (3) pharmacological or pharmaceutical assumptions, (4) experimental assumptions, (5) study conduct assumptions, and (6) statistical or mathematical assumptions. In this work, the definition and examples of these assumptions are provided and summarised in **Table 5.3**.

Table 5.3 *Nature of assumptions and the corresponding definition and examples.*

Nature of assumption	Definition	Examples (not exhaustive)
Biological / physiological	Relating to normal structures and functions of living organisms (including that of humans).	1. Alternative pathways for the formation of an endogenous entity X are unimportant and negligible 2. Constant receptor system 3. Bone mineral density is predictive of the risk of fractures 4. The fat free mass derived from the Janmahasatian's equation is unbiased 5. The glomerular filtration rate estimated based on the Cockcroft-Gault equation is unbiased
Pathophysiological	Relating to abnormal structures or functions of living organisms (including that of humans) associated with a disease or an injury.	1. Linear disease progression 2. A reduction in tumour size is predictive of the overall patient survival
Pharmacological / pharmaceutical	Relating to formulations, preparations, mechanisms, uses, and effects of drugs.	1. Linear pharmacokinetics 2. Constant drug's clearance (i.e. not time-varying) 3. The drug concentration obtained is at steady-state 4. The plasma drug concentration is representative of the target site concentration 5. The drug binding to the target receptor is irreversible 6. Only the parent drug is pharmacologically active 7. The effect of two drugs are non-additive
Experimental	Relating to wet lab experiments and is distinguished from *in silico* experiments or other theoretical work.	1. The drug concentration quantified based on a bioassay is accurate 2. The point of care testing device is sensitive and specific

Nature of assumption	Definition	Examples (not exhaustive)
Study conduct	Relating to the data collection process that is beyond the confines of a laboratory setting.	1. There is no study protocol violation 2. Perfect adherence 3. The recorded blood sampling time is accurate
Statistical / mathematical	Relating to statistics or mathematics.	1. The data are missing completely at random 2. The last observation carried forward method is appropriate for imputation of missing dosing history 3. Handling data that are below the limit of quantitation using the M3 method is appropriate 4. Outlying observations are not influential 5. The residual error terms are not autocorrelated

5.5. Flowchart for assumption evaluation

The typical workflow for assumption evaluation was generalised into a qualitative flowchart. A flowchart was developed in a stepwise manner. In the first step, a decision tree that mapped all possible outcomes from a sequential evaluation of the impact and the probability of assumption violation was built. In the next step, the multilevel decision tree was streamlined to a simple flowchart for systematic evaluation of assumptions. The flowchart developed is shown in **Figure 5.3**.

For each assumption, the impact, I, and the probability, P, of assumption violation are assessed. Here, both I and P were evaluated for their influence on: (1) an internal component of model building (termed *internal evaluation* and represented by subscript [i]), or (2) an external use of the model (termed *external evaluation* and represented by subscript [e]). The outcomes of the flowchart include the potential go / no-go decision for internal model-building or external use of the model, the acknolwedgement of a limitation of the model or simply the acknowledgement of the assumption and continued model use.

Evaluation of I and P as well as internal versus external evaluation are further discussed in **section 5.5.1** and **section 5.5.2**, respectively. The utility of the flowchart for decision making is illustrated in **section 5.7** for both: (1) a top-down model building process and (2) a bottom-up work based on a QSP model.

5.5.1. Evaluation of I and P

For each assumption, evaluation of the impact (I) as *significant*, *non-significant*, or *unknown* precedes the evaluation of the probability of assumption violation (P) as *likely*, *unlikely*, or *unknown*. If I is significant or unknown then P is evaluated. In this hierarchical approach, P is otherwise not tested. Here, the ratings for I and P are rated based on either prior knowledge (e.g. existing literature, logical reasoning) or, in the absence of prior information, posterior knowledge which results from a bespoke study (e.g. experimental work, simulation study, sensitivity analysis).

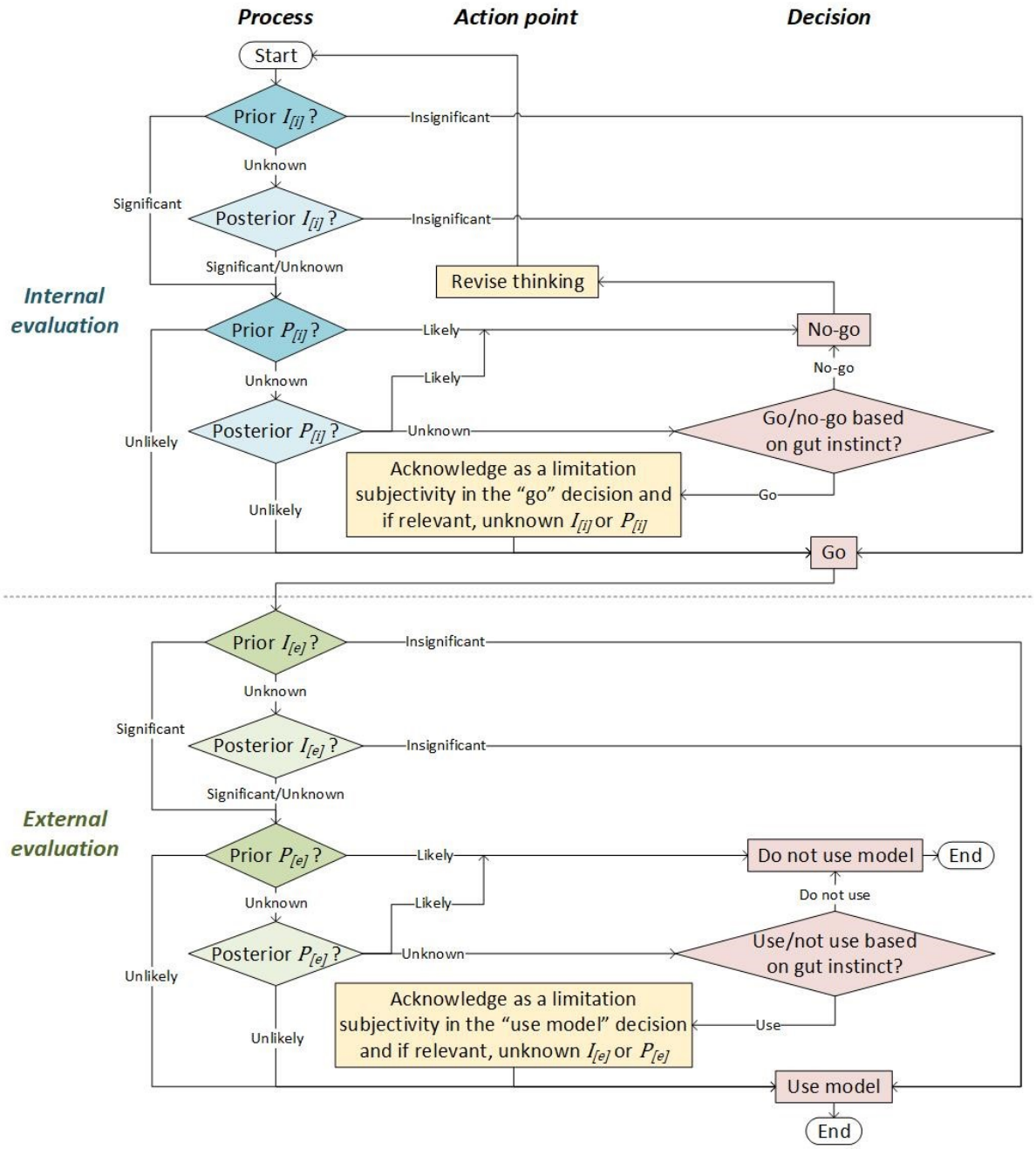

Figure 5.3 *Flowchart for systematic evaluation of model assumptions. I is the impact and P is the probability of assumption violation. The subscript [i] relates to internal evaluation (an evaluation relating to model development) and [e] external evaluation (an evaluation relating to use of the model after development).*

5.5.1. Internal versus external evaluation

For internal evaluation, both *I* and *P* are evaluated with respect to the performance of the model. Here, the goal of the assessment of *I* is to quantify the influence of a violation in the assumption on the resulting model fit and evaluation of *P* is to assess the corresponding chance of assumption violation. External evaluation is carried out in a similar manner except that it is with reference to an external aim of interest, which typically involves simulation from the final model and extrapolation beyond the original scope of the model. The evaluation of either component concludes with a go / no-go decision.

5.6. Table of assumptions

A tabular approach to documentation is proposed (with particular emphasis on recording information of interest) to enhance the effectiveness of communicating assumptions. The table is divided up into three components, *Impact*, *Probability*, and *Decision*. The impact and probability components are further divided into *Methods*, *Results*, and *Rating*. The structure of the table of assumptions, its components, and generic description of each component are shown in **Table 5.4**.

Table 5.4 *Table for documentation of assumption and their evaluation. I is the impact of assumption violation, L means likely, P is the probability of assumption violation, S means significant, NS means not significant, U means unlikely, UK means unknown, and NA not applicable.*

Assumption	**Impact (*I*)**			**Probability (*P*)**			**Decision**
	Methods	**Results**	**Rating**	**Methods**	**Results**	**Rating**	
State the assumption. Each row should contain only one assumption. Internal and external evaluations should be placed in separate rows.	State if I is not testable. If testable, state if the evaluation is based on prior knowledge or posterior test then outline the methods used briefly.	Summarise the evaluation results. Obtain supporting information for the rating assigned.	Rate I based on the evaluation results. The three possible ratings are S for significant, NS not significant, and UK unknown.	State if P is testable. If testable, state if the evaluation is based on prior knowledge or posterior test then outline the methods used briefly.	Summarise the evaluation results. Obtain supporting information for the rating assigned.	Rate P based on the evaluation results. The three possible ratings are L for likely, UL unlikely, and UK unknown.	State if it is a go or no-go decision for model building (internal evaluation) or model use (external evaluation).

5.7. Application

The utility of the flowchart and table of assumptions was illustrated for both a: (1) top-down model building process and (2) bottom-up approach based on application of a QSP model. The top-down approach was based on the joint model for warfarin and vitamin K-dependent coagulation proteins described in **Chapter 2**. For the bottom-up approach, the development of a factor VII-based method for the prediction of international normalised ratio (INR) based on simulations from a QSP coagulation network model [31] was considered (see **Chapter 4**). Selected assumptions from the top-down work are shown here as examples to illustrate the assumption evaluation process using the flowchart.

Here, four application examples are included: (1) internal evaluation of implicit assumption, (2) internal evaluation of explicit assumption, (3) external evaluation of implicit assumption, and (4) external evaluation of explicit assumption. The evaluation results of these assumptions are described in the next sections. A summary of the evaluation is also provided in **Table 5.5**.

Other assumptions underpinning the joint model (11 assumptions) and the factor VII-based method (6 assumptions) were also evaluated internally. For brevity, these are not presented here but are summarised in **Appendix A4.1** and **Appendix A4.2**, respectively.

5.7.1. Internal evaluation

5.7.1.1. Implicit assumption example

Implicit to the development of the joint model in NONMEM® Version 7.2 (ICON Development Solutions, Ellicott City, MD, USA), the residual error terms, ε, were assumed to be normally distributed with a mean of zero and have a variance of σ^2. NONMEM® is reported to be sensitive to a misspecification in the residual error model. Parameter estimates, in particular, random-effect parameters, may be biased [215]. For these reasons, *I* was conservatively rated as significant.

P was subsequently evaluated. Since no prior information were available, P was assessed by comparing the distribution of the conditional weighted residuals ($CWRES$) to a standard normal distribution using quantile-quantile (Q-Q) plots and the one-sample Kolmogorov-Smirnov goodness-of-fit tests. Here, $CWRES$ represent a composite measure of the additive and proportional error terms. In **Figure 5.4**, the majority of the $CWRES$ quantiles fall on the reference line that corresponds to a standard normal distribution. In addition, based on the Kolmogorov-Smirnov tests, $CWRES$ for factors II ($T = 0.0315, p = 0.998$), IX ($T = 0.0895, p = 0.173$), X ($T = 0.0767, p = 0.328$), proteins C ($T = 0.0588, p = 0.660$), and S ($T = 0.0432$, $p = 0.933$) do not have a distribution that is significantly different from a standard normal distribution. An exception was the $CWRES$ for factor VII ($T = 0.111, p = 0.0458$), although visually the Q-Q plot does not look significantly worse than the other plots. Taken together, these results suggest that $CWRES$ are likely to have a standard normal distribution. In other words, P was unlikely.

According to the flowchart (**Figure 5.3**), significant I and low P give a go decision for model building.

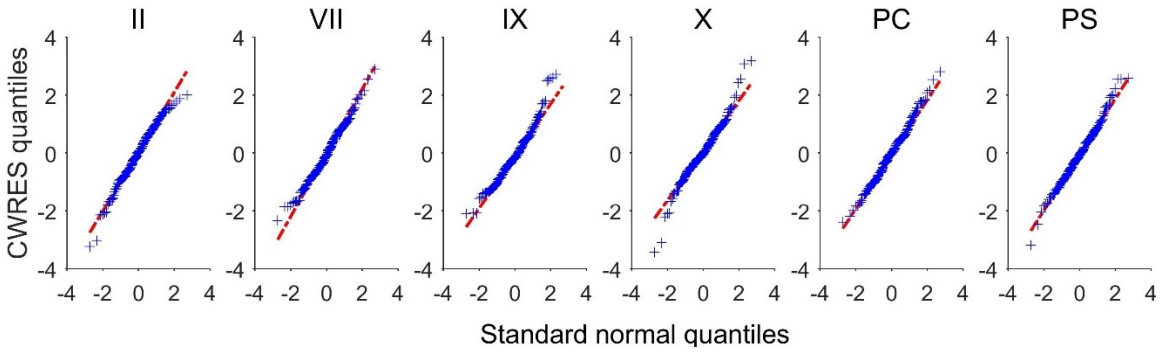

Figure 5.4 *The Q-Q plot for the CWRES of the joint model.* CWRES *is the conditional weighted residuals, PC is protein C, PS is protein S, and Q-Q plot refers to the quantile-quantile plot.*

5.7.1.2. Explicit assumption example

Actual daily dose time of warfarin were not recorded. For the joint model development, a daily dose time of 6 p.m. was assumed for all patients based on the study protocol. In the absence of prior knowledge regarding I, I was evaluated *a posteriori*. A sensitivity analysis was conducted whereby different daily dose time of 8 a.m., 10 a.m., 12 p.m., 2 p.m., 4 p.m., 8 p.m., and 10 p.m. were used as alternative imputation values for dose time. The resulting model fits and parameter estimates were compared to the original model. Identical objective function values (OFV) and final parameter estimates were obtained thereby indicating insensitivity of model fits and parameter estimations to the different imputed daily dose time. I was considered insignificant and therefore unimportant and as a result, P was not evaluated. According to the flowchart (**Figure 5.3**), this leads to an expedited go decision for model building.

5.7.2. External evaluation

For the purpose of this thesis, development of the joint model for warfarin and vitamin K-dependent coagulation proteins is of primary interest. At this stage, the model has not been used externally. However, in this section, the model was applied to explore two hypothetical external aims of interest to illustrate the external evaluation process.

5.7.2.1. Implicit assumption example

A possible external aim is to use the joint model for the prediction of the time course of coagulation protein concentrations in an external population and in this example, warfarin patients with vitamin K supplementation. Implicit to the inhibitory E_{max} model used as part of the joint model, warfarin binding to the vitamin K epoxide reductase (VKOR) enzyme is assumed to be reversible and that the binding affinity is a constant (hence time-invariant).

Based on logical reasoning, a deviation from the assumptions, for instance, if warfarin has a different binding affinity to VKOR and hence has a different

potency ($IA_{50,P}$), predictions from the model with the new $IA_{50,P}$ would be different from that produced by the original model. I was rated as significant.

Next, P was evaluated. $IA_{50,P}$ is an *apparent* potency parameter for warfarin that depends positively on the amount of vitamin K in the body. In essence, the higher the amount of vitamin K in the body, the higher is the $IA_{50,P}$ (i.e. warfarin becomes apparently less potent) and vice versa. Whereas in the model-building population where vitamin K intake is normal and rather constant, in this specific example, the new population receives vitamin K supplements. Then, $IA_{50,P}$ will vary according to the extent (e.g. upward shift of $IA_{50,P}$) and consistency (e.g. time-varying $IA_{50,P}$) in the vitamin K supplementation. Due to the discrepancy in the $IA_{50,P}$, simulations from the joint model are likely to be biased as compared to the actual time course of coagulation protein concentrations in the new population. For these reasons, P was rated as likely. According to the flowchart (**Figure 5.3**), significant I and high P result in a no-go decision for model use with respect to the external aim of interest.

5.7.2.2. Explicit assumption example

Another possible external aim of interest is to use the joint model to predict the time course of coagulation protein concentrations beyond the original dose range used for model building. In the absence of warfarin PK data, volume of distribution of warfarin (V) was found to be not structurally identifiable. V was assumed as 8 L in the joint model. In the first step of assumption evaluation, the impact of a wrongly specified V was considered with respect to the external aim of interest. Because V was structurally not identifiable given the input-output data, value of V, even if incorrectly specified, does not affect the resulting model fits (although arrives at a biased CL estimate) and as such it has no specific bearings on subsequent simulations from the model for external application (regardless of whether it is within or beyond the original dose range used for model building). I was rated as insignificant. According to the flowchart (**Figure 5.3**), evaluation of P was not required and an expedited go decision for model use was resulted.

Table 5.5 *Four assumption examples and their evaluation. I is the impact of assumption violation, L means likely, P is the probability of assumption violation, S means significant, NS means not significant, U means unlikely and NA not applicable.*

Assumption	Impact (*I*)			Probability (*P*)			Decision
	Methods	Results	Rating	Methods	Results	Rating	
Internal evaluation of implicit assumption: Example: For each coagulation protein, the errors, ε $(n \times 1)$, are assumed normally distributed with a mean of zero and a variance of σ^2	Previous evaluation of impact of non-normality available in the literature [215].	Parameter estimation for maximum likelihood estimation is sensitive to specification of the residual error. Misspecification may result in biased parameter estimates and predictions.	S	The distribution of $CWRES$ was compared to a standard normal distribution by using a Q-Q plot and a one-sample Kolmogorov-Smirnov test.	$CWRES$ of all coagulation proteins do not have a distribution that is significantly different from a standard normal distribution.	U	Go for model building.
Internal evaluation of explicit assumption: Example: The imputed daily dose time of 6 p.m. is appropriate and as a whole unbiased	A sensitivity analysis was conducted. Daily dose time of 8 a.m., 10 a.m., 12 p.m., 2 p.m., 4 p.m., 8 p.m., and 10 p.m. were considered.	The same model fits and parameter estimates were obtained regardless of the daily dose time used for imputation.	NS	NA	NA	NA	Go for model building.

Assumption	Impact (*I*)			Probability (*P*)			Decision
	Methods	Results	Rating	Methods	Results	Rating	
External evaluation of implicit assumption: Example: Reversible binding and constant binding affinity *External population with vitamin K supplementation	Thought experiment and logical reasoning.	Two models that are exactly the same but differ in the value of potency parameter ($IA_{50,P}$) will give different predictions.	S	Prior knowledge	$IA_{50,P}$ is an apparent potency parameter that depends positively on the amount of vitamin K in the body. With vitamin K supplementation, $IA_{50,P}$ is almost definitely altered.	L	No-go for model use
External evaluation of explicit assumption: Example: Volume of distribution of warfarin (V) is equal to 8 L *Extrapolation beyond the original dose range used for model building	Prior knowledge	Structural non-identifiability of V means that value of V even if incorrectly specified does not affect the model fits and subsequent simulations from the model.	NS	NA	NA	NA	Go for model use

5.8. Discussion

A framework for systematic evaluation of assumptions is proposed. The framework consists of a general workflow for assumption evaluation, definition of an assumption (and related terms), classification of assumptions, identification of assumptions, a flowchart for evaluating assumptions, and also a standardised table for documenting assumptions and evaluation results. In this work, the utility of the framework is demonstrated using both top-down and bottom-up examples. Selected assumptions are included as exemplars of implicit and explicit assumptions. Finally this work illustrates how to determine go- / no-go decisions as well as providing criteria for determining when an assumption is deemed to be a limitation of the model.

There have been few published works that address how model-related assumptions should be systematically approached and be effectively assessed. To date, only two published works are available that provide specific frameworks for evaluating model assumptions. The first work by Karlsson and colleagues used the development of a population PK model for moxonidine as an exemplar to demonstrate how assumptions intrinsic to model building may be evaluated [205]. The second article by the EFPIA MID3 Workgroup [34] provides recommendations on how assumptions may be evaluated and documented. Noteworthy, an assumptions table was proposed for modellers to document assumptions, uncertainties, and impact of assumption violations. Our work is viewed as an extension of these existing frameworks. Interested readers are referred to these works for more examples and guidance on assumption evaluation. In this work, a one-stop framework that covers the typical workflow for assumption evaluation, i.e. from identifying assumptions, evaluating assumptions, to documenting assumptions, is proposed. With this, modellers are encouraged to describe, evaluate, and document influential assumptions for effective model building and model use.

This work is not free from drawbacks. The term *assumption*, and related terms, are defined within the context of model development and use. These are rather heuristic definitions employed to empower modellers to differentiate

these closely-related but potentially confusing terms. It is acknowledged that there may be nuanced differences in the adopted definitions compared to that defined in other fields of study (e.g. mathematics, philosophy, psychology). Although this work aims to assist modellers to evaluate assumptions objectively, the use and application of the framework for assumption evaluation is somewhat subjective. For instance, the choice of evaluation methods, the rigor in which assumptions should be interrogated, and the rating assignments for *I* and *P* are all subjective and dependent on the modellers' expertise, past experience, preference, available resources, and time constraints. In addition, the required first step for assumption evaluation is successful identification of pertinent assumptions. In this work, it is suggested for the modellers to list the assumptions methodically according to the nature of assumptions. However, despite the systematic approach suggested, identification of an exhaustive list of model-related assumptions is challenging. Due to the implicit nature of some assumptions and model complexity, it is possible for some assumptions to have gone unnoticed i.e. unknown unknowns. Here, it remains unanswered as to how to mitigate the risk associated with these unknown unknowns.

This framework has been applied to both top-down and bottom-up approaches. Although these examples are sufficient to illustrate how the proposed framework may be used for assumption evaluation, it is in no way a form of validation. The robustness of the framework to the different modelling processes and model use settings as well as the utility and practicality of the framework have not been explored fully. An important next step of this work is therefore to apply the framework to other settings. Finally, in view that the bottom-up work (factor VII-based method for INR prediction) considered in this thesis is somewhat atypical to the conventional model building process for a QSP model, it is important to apply the framework to the development of a QSP model.

5.9. Conclusion

A framework for systematic evaluation of assumptions is proposed and its utility is demonstrated using both top-down and bottom-up examples. The next step of this work is to apply the framework to a series of other settings to fully assess its practicality and its value in identifying and making inference from assumptions.

PART V

DISCUSSION AND FUTURE WORK

Chapter 6: Discussion and future work

The current chapter provides a synopsis of key findings from the thesis and a discussion of these findings in the context of other work. These are followed by a summary of limitations and future work that arise from this thesis. Discussions in this chapter are targeted at the main outcome of the thesis – application of pharmacometric methods that leads to the identification of factor VII as a prominent driver of the international normalised ratio (INR) and the development of a factor VII-based method for the prediction of anticoagulant response to warfarin. Discussions specific to individual chapters of the thesis will not be reiterated here.

6.1. Synopsis and theoretical basis of the thesis

In this thesis, pharmacometric methods were applied to understand the coagulation kinetics underpinning warfarin dose response and to introduce a new perspective to the prediction of anticoagulant response to warfarin. It was argued that the issues surrounding the poor predictive performance of existing warfarin dosing methods relate to the use of the INR, a blunt measure of anticoagulant response that is a composite of the influence of several coagulation proteins, co-factors, and other causes, as a sole marker of anticoagulant response due to warfarin.

The overarching premise of this thesis was that a measure of coagulation protein response in addition to the INR response will be helpful in the prediction of the anticoagulant response and warfarin dose requirement. This was argued and rationalised based on the full causal path of warfarin dose and system response. The full causal path, which is previously presented in **Figure 1.15** in **Chapter 1**, is summarised in **Figure 6.1** in terms of the possible points of biomarker sampling to inform the prediction of anticoagulant response and warfarin dose requirement. In **Figure 6.1**, INR response represents a surrogate endpoint of interest due to its association with major clotting and bleeding events. However, due to the aforementioned conglomerate nature of INR with respect to warfarin pharmacokinetic (PK), pharmacodynamic (PD), and system variabilities, its interpretation relies heavily on understanding the mechanistic relationship between warfarin dose and INR response. To this end, the inclusion of PK marker (e.g. warfarin concentration) and / or PD marker (e.g. coagulation protein concentration) may be helpful in elucidating warfarin dose response.

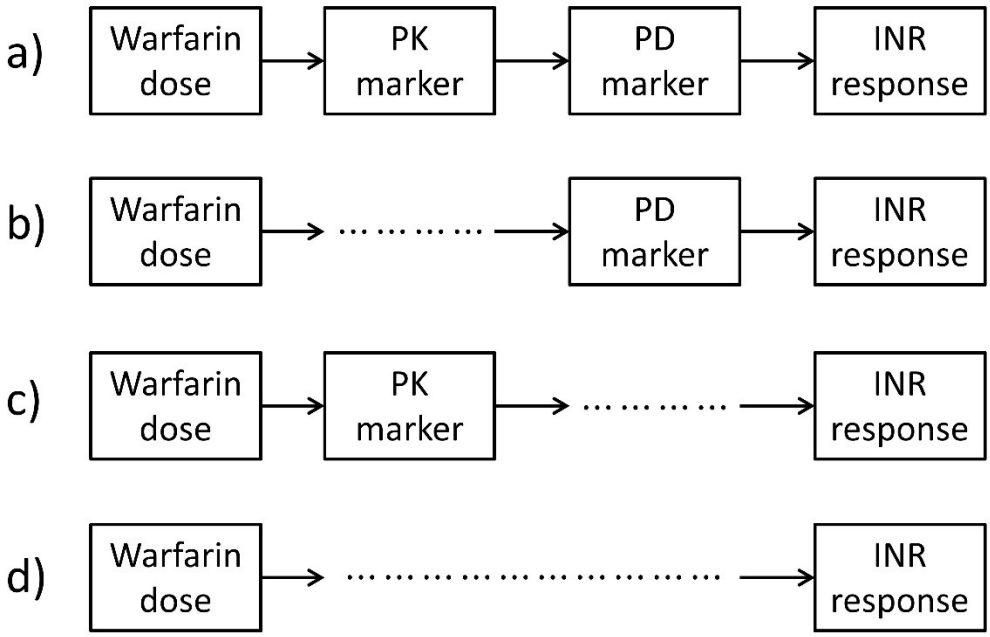

Figure 6.1 *Causal path of warfarin dose response presented in terms of the points of biomarker sampling. INR response is routinely measured as a surrogate marker of major clotting or bleeding events in warfarin patients. Warfarin dose is causally linked to the INR response via warfarin concentration (PK marker) and coagulation protein concentration (PD marker). Panel a represents an ideal case when PK, PD, and system markers are available simultaneously. Panel b (PD and system markers), panel c (PK and system markers), and panel d (system marker only) are practical approximation to Panel a. INR is the international normalised ratio, PD pharmacodynamic, and PK pharmacokinetic.*

Panel a in **Figure 6.1** represents an ideal case where PK, PD, and system markers are all observed, which can be fitted into a single coherent, multivariate prediction framework to inform the relationship from dose to response. In **Figure 6.1**, *panels b*, *c*, and *d* are practical approximations to *panel a*. Although the least informative, *panel d*, which reduces the full causal path to a simple (and often empirical) link between warfarin dose and INR response, is the most widely described method for warfarin dose individualisation literature. This includes warfarin dosing methods that adjust warfarin doses based on the observed INR responses such as the nomograms (see Tait *et al.* [17] for an example), algorithms based on the linear regression analysis (see Lenzini *et al.* [12] for an example), and prediction methods with an underpinning kinetic-pharmacodynamic (KPD) model (see Wright *et al.* [18] for an example). *Panel c*

shows the streamlined causal link between warfarin, PK marker, and INR response, which underpins the majority of warfarin pharmacokinetic-pharmacodynamic (PKPD) models (see Xue *et al.* [164] for an example).

In this thesis, the causal link of warfarin dose, PD marker, and INR response as outlined in *panel b* of **Figure 6.1** is of primary interest. This corresponds to a type of "KPD-system" framework where INR response is a system response that is downstream of the PD target effects. This approach was initially explored piecewise in **Chapter 2** of this thesis with the development of a KPD model for warfarin and coagulation proteins and in **Chapter 3** that investigated the coagulation kinetics governing the INR response based on a model of the coagulation system [31]. It was shown that, of all the vitamin K-dependent coagulation proteins, factor VII is the coagulation protein of interest due to its short degradation half-life, sensitivity to warfarin, and profound influence on the INR. On that basis, **Chapter 4** of this thesis explored the incorporation of a bivariate response variable of factor VII and INR for the prediction of future anticoagulant response to warfarin. In this setting, factor VII is a PD marker that provides a signal from the system that lies causally between warfarin dose and INR response. Here, a PD marker is arguably superior to a PK marker. This is due to its proximity to the clinical endpoints of interest in the chain of causal events (**Figure 6.1**) and its informativeness with respect to both PK and PD variabilities as compared to the PK markers, which are informative of the variability in PK only. Finally, the use of factor VII in addition to the INR response provides an opportunity to isolate the PKPD variability from system variability. This is helpful in elucidating the different sources of variability underpinning warfarin dose response.

6.2. Synopsis of individual chapters

Chapter 2 of this thesis described the development of a joint model for the vitamin K-dependent coagulation proteins (factors II, VII, IX, X, and proteins C and S) during warfarin initiation. Initially, the coagulation proteins were modelled independently, then the six models were combined into a single joint model where the full correlation structures that exist between parameters at the individual level and between residual errors of different coagulation proteins were considered. The joint model developed was able to describe accurately the time course of warfarin influence on all six coagulation proteins simultaneously. Factor VII was found to have the shortest degradation half-life compared to factors II, IX, X, and proteins C and S thereby representing the coagulation protein that is the first to decline and to reach a new steady-state level following a perturbation introduced by warfarin.

Chapter 3 of this thesis outlined the exploration of the influence of coagulation proteins and their interactions on the INR based on simulations from a previously developed quantitative systems pharmacology (QSP) coagulation network model [31]. In this chapter, of factors II, VII, and X, factor VII was found to be the most influential on the INR. This was based on the sensitivity analysis that showed that the INR is the most sensitive to factor VII and the isobologram analysis that demonstrated that the presence of more than one coagulation proteins deficiency is redundant for INR effect due to the sub-additivity nature of interactions between coagulation proteins. This led to the hypothesis that the use of factor VII as a marker of coagulation (in addition to the INR) may improve the prediction of the anticoagulant response.

Chapter 4 of this thesis builds on the findings from **Chapter 2** and **Chapter 3** to develop a factor VII-based method for the prediction of anticoagulant response to warfarin. The method was developed based on a heuristic model-order reduction technique where predictions from the QSP coagulation network [31] were empirically approximated over an appropriate span of the input-output response. The prediction method was shown to be associated with

minimal bias and its use was illustrated using data from one typical simulated patient and two real patients supporting a proof-of-principle.

The pharmacometric analyses presented in **Chapter 2** and **Chapter 4** of this thesis were founded on several assumptions. **Chapter 5** of this thesis describes the development of a framework for systematic evaluation of model assumptions. In this work, definition of an assumption and a system to classify assumptions to aid the identification of assumptions were provided. A flowchart was introduced for systematic evaluation of assumptions and a corresponding assumption table was proposed for documentation of assumptions and evaluation results. The assumptions underpinning **Chapter 2** and **Chapter 4** of this thesis were evaluated and used to illustrate the utility of the proposed framework.

6.3. The thesis findings in the context of other work

6.3.1. Application and development of pharmacometric methods

The clinical outcome of this thesis was derived from pharmacometric analyses. Pharmacometric methodologies that are unique to this work are summarised and briefly discussed in this section.

Isobologram analysis is traditionally used for the analysis of drug interactions [187]. No particular assumption is made about the relationships between the two drugs or the doses of the two drugs, whether they are independent or correlated. In **Chapter 3**, the isobologram analysis was extended beyond the usual drug interactions framework to explore interactions between factors II, VII, and X, which are known to be inherently correlated due to the complex series of interactions within the coagulation network for haemostatic control. In this setting, terminologies usually coined to describe drug interactions such as antagonism (which implies receptor binding and receptor-level interactions) were not used because coagulation proteins do not actually antagonise one another and they act on distinct targets. Here, terminologies that are neutral in the underpinning interaction mechanisms and descriptive of the observed interaction, for instance, sub-additivity in effect, were preferred. In this thesis, the isobologram analysis highlighted redundancies in the system where factors II, VII, and X were found to be sub-additive in effect. The term redundancies is used here since not all coagulation proteins are required to be depleted in order to observe a full anticoagulant effect with respect to the effect of warfarin on INR.

In the development of a method for the prediction of warfarin anticoagulant response (**Chapter 4**), a heuristic model-order reduction method was employed. In this work, a statistical model was used to approximate empirically the fully-mechanistic coagulation network model such that all anticoagulant responses of interest were captured over an appropriate span of the input-output relationships. The resulting statistical model is considerably simpler than the full mechanistic model and is amenable to manipulation for

clinical application, particularly the potential for Bayesian forecasting. A similar approach to approximate complex systems model has been described, albeit to serve a different purpose of incorporating expected variability and correlation to the output of QSP model [196, 216]. Model-order reduction can generally be achieved by either reducing the number of reactions (e.g. quasi steady-state approximation) or the number of states (e.g. proper lumping). The technique of proper lumping has been used for model-order reduction for several systems models [84-86]. In proper lumping, the original states of the model are lumped into a reduced number of pseudo-states thereby giving rise to a model of lower dimensionality but preserving similar input-output relationships of interest. However, at the time this thesis work was undertaken, no exact solutions for lumping are available for *nonlinear* ordinary differential equations (ODEs) such as that underpinning the coagulation network model. In particular, the process of proper lumping is unable to provide the parameter values for the reduced states when a system is nonlinear [85]. Recent methods suggest linearising the original nonlinear model (e.g. by inductive linearisation [217, 218]) to produce a linear system which is then ready for proper lumping. An important additional advantage of a linear system is the availability of analytical solutions (e.g. matrix exponential solutions) that are known to be accurate and associated with short solution time. Alternative methods have been described that operate within the nonlinear domain and employ lumping and empirical balanced truncation under the Petrov-Galerkin projection to achieve a reduction [219, 220].

The work conducted in this thesis is also unique in that variability in anticoagulant response between patients is accounted for and quantified within a QSP setting. **Chapter 4** describes characterisation of the sensitivity of the patient to warfarin in terms of the dose (D_{ref}) that would be taken by a typical patient to achieve the same level of observed anticoagulant response. The deviation of D_{ref} from the actual dose taken provides a quantitative assessment of the difference of the patient from a typical patient. Armed with an individualised measure of patient's sensitivity, the anticoagulant response at steady-state can be predicted. Derivation of the expected anticoagulant response

using this approach is untested but should function in theory and seems to work based on the evaluation conducted in **Chapter 4**. However, generalisation of the method to other settings requires prospective testing.

In **Chapter 5**, a framework for systematic evaluation of assumptions is proposed. The framework was developed based on expansion of existing works by Karlsson *et al.* [205], who illustrated how model-related assumptions may be evaluated using the development of a population PK model for moxonidine as an example, and the European Federation of Pharmaceutical Industries and Associations (EFPIA) Model-Informed Drug Discovery and Development (MID3) Workgroup, who provided recommendations on the evaluation and documentation of assumptions [34]. Whereas previous studies address specific aspects of assumption evaluation, the current work proposes a comprehensive, one-stop framework that encompasses the full workflow for assumption evaluation, i.e. from identifying assumptions, evaluating assumptions, to documenting assumptions and acknowledging limitations. This is critical to formally and systematically address the model-based components that form the basis of inference drawn from pharmacometric analyses such as that underpinning the proposed prediction method of warfarin anticoagulant response described in this thesis.

6.3.2. Factor VII as a driver of the INR

In this thesis, factor VII was postulated as the coagulation protein of choice for the prediction of the anticoagulant response to warfarin. Factor VII's sensitivity to warfarin and influence on the INR can be ascribed to the short degradation half-life of factor VII relative to other vitamin K-dependent coagulation proteins. Based on the joint model developed in **Chapter 2**, the degradation half-life of factors II, VII, IX, and X, and proteins C and S was 51.3, 12.2, 21.5, 44.1, 18.4, and 56.8 hours, respectively, which was in good agreement with previously reported values range from 72-115, 5-35, 18-40, 35-63, 8-32, and 43 hours, respectively [99, 159, 161, 165, 171-175]. Despite arriving at similar values, it is important to note the differences in the approaches used elsewhere

with that used here. Previous studies investigated the coagulation proteins relationship in cross-section, limiting the time course to a snapshot of the anticoagulant response to warfarin. In this work, the factors were analysed longitudinally in a joint model framework across all vitamin K-dependent coagulation proteins (factors II, VII, IX, and X, and proteins C and S) *simultaneously*. This provides a framework to account for the natural correlation that exists between parameters at the individual level and between residual errors of different coagulation proteins.

There have been few published studies examining the concentration of factors II, VII, and X at steady-state INR. At steady-state INR, factor VII concentration is consistently higher than that of factor II, which in turn is higher than the factor X concentration for patients on stable warfarin (i.e. $VII_{SS} > II_{SS} > X_{SS}$) [144, 146, 167, 198]. This consistency in trend means that given the steady-state concentration of *one* of factors II, VII, and X, the steady-state concentration of other coagulation proteins and the resulting INR can be predicted. Since factor VII has a short degradation half-life relative to that of factors II and X, it achieves the new steady-state rapidly following a perturbation in production (e.g. warfarin initiation) and thereby provides the earliest indication of the eventual steady-state concentrations of other coagulation proteins and INR.

With respect to the non-steady-state INR, the dominance of factor VII has been described previously [161, 197]. However, because the antithrombotic effect of a deficiency in factor VII was shown to be less important as compared to that of factors II and X [159, 221-225], factor VII, which governs the non-steady-state INR, is often overlooked or viewed as a nuisance factor in the monitoring of anticoagulant response using the INR. Indeed, attempts were made to factor out the influence of factor VII in the monitoring of anticoagulant response. Furie *et al.* proposed the use of factor II [221, 226] and Onundarson *et al.* designed a factor VII-insensitive prothrombin time test [224] for the monitoring of anticoagulant response to warfarin. Importantly, the goal of the work conducted as part of this thesis was not to contest the lack of antithrombotic role of a reduction in factor VII but to exploit the short degradation half-life of factor VII and its inherent

correlation with factors II and X and the INR for early and accurate prediction of anticoagulant response at steady-state.

6.3.3. Factor VII-based method to predict anticoagulant response

The proposed method differs from those reported in the published literature. A significant number of existing warfarin dosing methods quantify the likely anticoagulant response using patient covariates such as body size, age, ethnicity, concomitant drugs, cytochrome P450 2C9 (CYP2C9) genotype, and vitamin K epoxide reductase complex subunit 1 (VKORC1) genotype [8-16]. However, these methods provide no guidance for warfarin dose adjustment once measures of anticoagulant response (e.g. INR or clotting factor activity) become available. Importantly, anticoagulant response data will capture between-subject differences in warfarin dose response, including those related to patient covariates such as the CYP2C9 and VKORC1 genotypes. Therefore, in theory, once the time course of anticoagulant response for a given warfarin dose is accounted for, it may no longer be necessary to consider these covariates.

Whereas the proposed method is based on factor VII (and INR), *all* existing response-based methods rely solely on the measurement of INR for warfarin dose individualisation [12, 17, 18, 22, 23, 25-30]. This is attributable to the ease of measuring the INR and the wide availability of INR tests in the clinical setting as well as the well-established association of INR to clinical outcomes of interest (e.g. thrombotic stroke and intracranial haemorrhage) [92, 93] although INR is arguably difficult to interpret owing to its nonlinear dependence on fibrinogen, factors II, V, VII, and X [136, 137]. An exception was a published work by Pitsiu *et al.* that considered factor VII for the prediction of warfarin maintenance dose [157]. It was shown that factor VII response measurements alone were adequate to determine dosing requirements although it is important to point out that the sample size is small ($n = 5$) and the use of healthy volunteers limits generalisability of the study's results to all warfarin users.

6.4. Limitations and future work

The work conducted in this thesis was not set forth to propose a new framework for warfarin dosing that is instantly applicable for clinical use, but to introduce a new perspective on INR prediction and subsequently, for warfarin dosing. A natural succession to this work would be to extend the current method to predict warfarin maintenance dose. This would require (1) mathematical rearrangement and adaptation of the current method and (2) setting up a dose individualisation algorithm (perhaps Bayesian) as a dose prediction method that incorporates a bivariate response variable. Using a Bayesian forecasting approach, key parameters in the dose prediction algorithm can be individualised by minimising the maximum *a posteriori* (MAP) objective function based on information about the patient and the dose-factor VII-INR data obtained from individual patient. Then, as more data become available, the individual parameter estimates become more refined to allow accurate prediction of warfarin dose that is required to achieve the therapeutic INR.

In **Chapter 4**, the proposed INR prediction method was applied to a typical simulated patient and two patients. The evaluation was conducted not to illustrate clinical applicability but to show that the method may *potentially* work (i.e. akin to a proof of principle). Application of the proposed method, be it prediction of INR_{SS} or warfarin maintenance dose, relies on the availability of paired blood samples of factor VII and INR. However, factor VII is not routinely measured due to the need for factor VII-deficient plasma [142], which has not been readily available in the clinical setting and therefore it is not possible to fully evaluate the proposed method using data available retrospectively. Limited by a small sample size, the evaluation results of the proposed INR prediction method are not generalisable to clinical use.

A prospective study specially designed to systematically evaluate the method would be essential. The required first step is to prospectively assess the predictive performance of the proposed dosing algorithm by comparing the predicted INR_{SS} and / or warfarin maintenance dose to that observed in a cohort of patients initiating warfarin therapy. This allows quantification of systematic

bias in prediction and the corresponding imprecision by calculating the mean prediction error (MPE) and the root mean square error (RMSE), respectively. In addition, the time-in-therapeutic range (TTR), which is an accepted surrogate for warfarin safety and effectiveness [227], could be determined *in silico*.

Subsequently, conditioned on an acceptable predictive performance, a prospective randomised controlled trial (RCT) is needed to fully evaluate the clinical utility of the proposed warfarin dosing method. Here, patients initiating warfarin therapy would be randomised so that warfarin dosing is guided either by the proposed method or by a standard care model or an alternative dosing algorithm. The outcomes of the RCT could include incidence of major bleeding or thromboembolic events, cost effectiveness, and / or a biomarker of effect such as TTR. Importantly, because existing dosing methods produce biased predictions in patients who require doses in the upper quartile (≥7 mg/day) [3-5, 7] and lower quartile (≤2 mg/day) [2, 6] of warfarin dose requirements, these patients would be of particular interest. A stratified analysis based on dose that is sufficiently powered and with an acceptable overall type I error could be considered.

At present, the sampling times for factor VII and INR are proposed based on heuristic reasons (**Chapter 4**). An optimal design analysis may be able to offer better alternative sampling times – one that improves the precision of key parameter estimates and minimises the bias in the prediction of INR_{SS} and warfarin maintenance dose. In addition, because the proposed method was based on empirically modelling the predictions from the QSP coagulation network model [31], it is important not to extrapolate beyond the original conditions used for method development. In addition, despite the effort to verify the QSP model (**Chapter 3**), it is acknowledged that there remain uncertainties in the accuracy of the model in describing the warfarin dose-coagulation proteins-INR relationships. It is possible for a potential inconsistency in the QSP model to propagate to the proposed prediction method, which may impact the performance of the proposed method in predicting INR_{SS} and warfarin

maintenance dose requirement. Recalibration of the proposed method using prospectively collected warfarin-factor VII-INR data may be required.

In **Chapter 5**, a framework for systematic evaluation of model-related assumptions was proposed and its utility was demonstrated using both top-down and bottom-up examples. These examples are included to demonstrate how the proposed framework may be used for assumption evaluation. However, it is important to note that the framework was applied to evaluate assumptions underpinning an *application* of the bottom up model (i.e. coagulation network model), which differs from a typical model-building process for a bottom up model. The robustness of the framework to the different model-building processes and model use settings as well as the practicality of the framework have not been explored fully. The next step of this work is to apply the framework to a series of other settings, including both top-down and bottom-up works of different levels of complexity, to fully assess its practicality and its value in identifying and making inference from assumptions.

6.5. Conclusions

In this thesis, both the top-down and bottom-up approaches to pharmacometric analyses were applied to explore the coagulation kinetics underpinning the warfarin dose response and to introduce a new perspective to the prediction of anticoagulant response to warfarin.

Factor VII was identified as having a short degradation half-life and influential on the INR thereby representing an attractive marker of anticoagulant response to inform INR prediction for warfarin dose individualisation. A factor VII-based method for the prediction of anticoagulant response was developed and evaluated to illustrate proof of principle. An important next step of this work would be to extend the current method to predicting warfarin maintenance dose using the Bayesian forecasting method.

A framework for systematic evaluation of model-related assumptions was proposed and evaluated. The next step of this work is to apply the framework to a series of other settings to fully explore the utility and robustness of the framework to different model-building processes and model use settings. The framework is crucial in formally addressing and mitigating the risks attached to assumptions underpinning pharmacometric models.

The work conducted in this thesis illustrates a model-based approach to elucidate dose response of a drug. This provides a scientific basis for safe and effective use of medicines.

PART VI

APPENDICES AND REFERENCES

Appendix 1: Appendices to Chapter 2

A1.1. Assay methods

A brief description of assay methods for quantification of factors II, VII, IX, and X, and proteins C and S is provided. More details of these assays can be found elsewhere [142].

A1.1.1. Assay for factors II, VII, IX, and X

Factors II, VII, and X were quantified using an assay based on the prothrombin time on ACL 3000 coagulation analyser. Factor IX were measured in a similar manner except that an assay based on the activated partial thromboplastin time was used. The first step of coagulometric (bioactivity) assay for factors II, VII, IX, and X involved mixing the test plasma with relevant coagulation protein deficient plasma and measurement of the time required for clot formation. This was followed by comparing the clotting time obtained against a reference curve for determination of coagulation protein concentration (IU/dL).

A1.1.2. Assay for protein C

Protein C activity was measured using a chromogenic assay on Amax 400 analyser. Quantification of protein C involved the addition of an activator for activation of protein C to activated protein C, which was later measured using an amidolytic substrate.

A1.1.3. Assay for protein S

Free protein S antigen levels were quantified using an enzyme-linked immunosorbent assay. Measurement of protein S involved precipitation of C4b-bound protein S with polyethylene glycol and the free protein S was subsequently quantified using suitably labelled antibodies during the detection stage of the assay.

A1.2. Structural identifiability analysis

A1.2.1. Rationale and aim

In the absence of warfarin concentration data, some model parameters may not be structurally identifiable. The aim of this analysis was therefore to evaluate structural identifiability of the individual model to be used in population analysis.

A1.2.2. Methods

A formal structural identifiability analysis was conducted using popt_i® Version 1.0 (Duffull SB, Dunedin, New Zealand) [64, 168]. In the case when the individual model was found structurally unidentifiable, parameters including both fixed-effect parameters (k_a, CL, V, $I_{max,P}$, $IA_{50,P}$, $P_{t=0}$, $k_{out,P}$) and the corresponding between-subject variance (ω^2) were fixed systematically one- or two-at-a-time until a unique solution was obtained for all remaining parameters.

A1.2.3. Results

The model was found to be structurally not identifiable when none or just one of the parameters was fixed. Either one of the four pairwise combinations of parameters when fixed resulted in a structurally identifiable model: (1) V and $\omega^2(V)$; (2) CL and $\omega^2(CL)$; (3) V and $\omega^2(CL)$; and (4) CL and $\omega^2(V)$.

A1.2.4. Implication for population analysis

V was fixed to typical values previously estimated [152] and $\omega^2(V)$ was fixed to a value of zero to obtain a structurally identifiable model and to ensure structural identifiability during the empirical Bayesian estimation step to derive individual parameters.

A1.3. Co-dependency of $IA_{50,P}$ and $I_{max,P}$

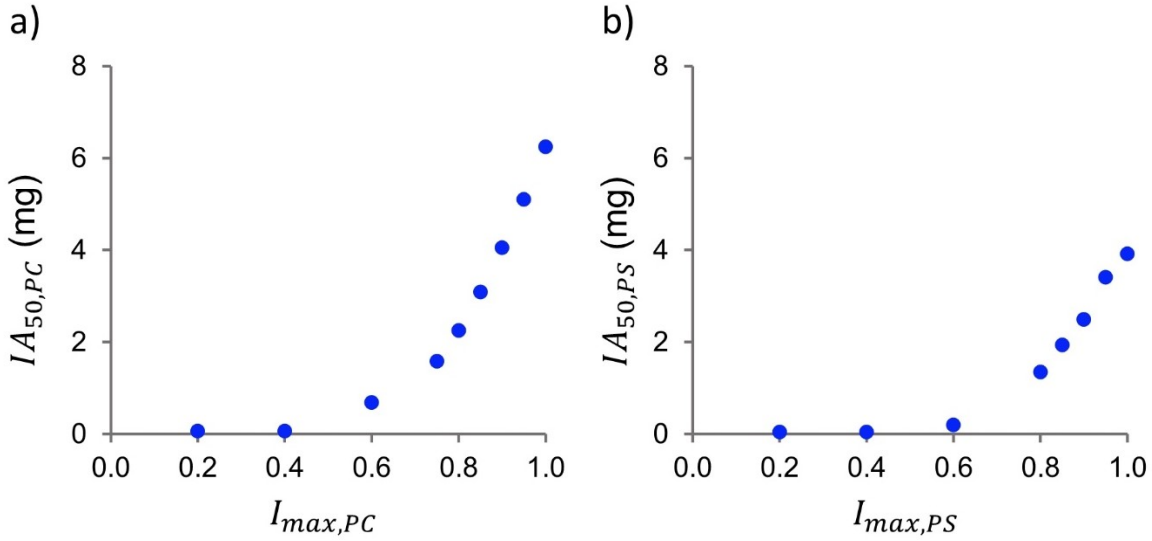

Figure A 1.1 *Co-dependency between $IA_{50,P}$ and $I_{max,P}$. This was explored by using individual model for proteins C and S. $IA_{50,P}$ was estimated at multiple instances while having $I_{max,P}$ fixed at different values. $IA_{50,P}$ was found to be highly co-dependent with $I_{max,P}$. $I_{max,P}$ for proteins C and S was fixed to one in the final models. $IA_{50,P}$ is the warfarin amount in the body that gives half the maximum inhibitory effect. $I_{max,P}$ is the maximum inhibitory effect. PC stands for protein C and PS is protein S.*

A1.4. Model-building steps for the full joint model

Due to the sheer size of the full joint model that contains 157 parameters, the parameters are separated into different tables: (1) **Table A 1.1** (fixed-effects parameters); (2) **Table A 1.2** (parameters for between-subject variability); (3) **Table A 1.3** (parameters for the residual unexplained variability); (4) **Table A 1.4** (parameters in the L1 correlation matrix), and (5) **Table A 1.5** (parameters in the L2 correlation matrices).

Table A 1.1 *Fixed-effects parameter estimates for the full joint model during important model-building steps. LAG represents the lag parameter, CL clearance of warfarin, F bioavailability of warfarin,* $IA_{50,P}$ *warfarin amount in the body that gives half the maximum inhibitory effect,* $I_{max,P}$ *maximum inhibitory effect,* k_a *first-order absorption rate constant of warfarin,* $k_{out,P}$ *first-order coagulation protein degradation rate constant, PC protein C, PS protein S,* $P_{t=0}$ *coagulation protein concentration at baseline.*

Table A 1.2 *Estimates of the BSV parameters for the full joint model during important model-building steps. BSV is the between-subject variability. CV coefficient of variation, LAG lag parameter, CL clearance of warfarin,* $k_{out,P}$ *first-order coagulation protein degradation rate constant,* ω *variance of BSV, PC protein C, PS protein S,* $P_{t=0}$ *coagulation protein concentration at baseline.*

Table A 1.3 *Estimates of the RUV parameters for the full joint model during important model-building steps. CV coefficient of variation, LAG lag parameter, CL clearance of warfarin, $k_{out,P}$ first-order coagulation protein degradation rate constant, ω variance of BSV, PC protein C, PS protein S, $P_{t=0}$ coagulation protein concentration at baseline, RUV residual unexplained variability.*

Table A 1.4 *Parameter estimates for the L1 matrix in the full joint model during important model-building steps. Note that for brevity, only selected models directly related to the inclusion of the L1 matrix are shown. η is the between-subject variability in parameter, LAG lag parameter, $k_{out,P}$ first-order coagulation protein degradation rate constant, PC protein C, PS protein S, $P_{t=0}$ coagulation protein concentration at baseline.*

Table A 1.5 *Parameter estimates for the L2 matrix in the full joint model during important model-building steps. Note that for brevity, only selected models are shown.* $\varepsilon_{prop,P}$ *is the proportional error,* $\varepsilon_{add,P}$ *additive error, PC protein C, and PS protein S.*

Model ID	Model Description	L2 correlation matrix						
M24	M20; L2 matrix (6X6) for $\varepsilon_{add,P}$.		$\varepsilon_{add,II}$	$\varepsilon_{add,VII}$	$\varepsilon_{add,IX}$	$\varepsilon_{add,X}$	$\varepsilon_{add,PC}$	$\varepsilon_{add,PS}$
		$\varepsilon_{add,II}$	1.00					
		$\varepsilon_{add,VII}$	0.882	1.00				
		$\varepsilon_{add,IX}$	0.903	1.00	1.00			
		$\varepsilon_{add,X}$	0.843	0.827	0.860	1.00		
		$\varepsilon_{add,PC}$	0.840	0.890	0.862	0.785	1.00	
		$\varepsilon_{add,PS}$	0.658	0.637	0.648	0.757	0.625	1.00
M25	M20; L2 matrix (6X6) for $\varepsilon_{prop,P}$.		$\varepsilon_{prop,II}$	$\varepsilon_{prop,VII}$	$\varepsilon_{prop,IX}$	$\varepsilon_{prop,X}$	$\varepsilon_{prop,PC}$	$\varepsilon_{prop,PS}$
		$\varepsilon_{prop,II}$	1.00					
		$\varepsilon_{prop,VII}$	0.915	1.00				
		$\varepsilon_{prop,IX}$	0.879	0.887	1.00			
		$\varepsilon_{prop,X}$	0.945	0.864	0.830	1.00		
		$\varepsilon_{prop,PC}$	0.851	0.817	0.763	0.833	1.00	
		$\varepsilon_{prop,PS}$	0.703	0.580	0.646	0.705	0.668	1.00
M26	M20; L2 matrix (6X6) $\varepsilon_{add,P}$; L2 matrix (6X6) for $\varepsilon_{prop,P}$.		$\varepsilon_{add,II}$	$\varepsilon_{add,VII}$	$\varepsilon_{add,IX}$	$\varepsilon_{add,X}$	$\varepsilon_{add,PC}$	$\varepsilon_{add,PS}$
		$\varepsilon_{add,II}$	1.00					
		$\varepsilon_{add,VII}$	0.871	1.00				
		$\varepsilon_{add,IX}$	0.894	0.989	1.00			
		$\varepsilon_{add,X}$	0.842	0.867	0.885	1.00		
		$\varepsilon_{add,PC}$	0.877	0.866	0.846	0.845	1.00	
		$\varepsilon_{add,PS}$	0.676	0.644	0.612	0.775	0.596	1.00
			$\varepsilon_{prop,II}$	$\varepsilon_{prop,VII}$	$\varepsilon_{prop,IX}$	$\varepsilon_{prop,X}$	$\varepsilon_{prop,PC}$	$\varepsilon_{prop,PS}$
		$\varepsilon_{prop,II}$	1.00					
		$\varepsilon_{prop,VII}$	0.638	1.00				
		$\varepsilon_{prop,IX}$	-0.220	0.211	1.00			
		$\varepsilon_{prop,X}$	0.00546	0.106	-0.403	1.00		
		$\varepsilon_{prop,PC}$	-0.166	0.481	0.122	-0.172	1.00	
		$\varepsilon_{prop,PS}$	-0.123	-0.0441	0.230	-0.170	0.170	1.00
M66	M65; Ensure positive definiteness of L1 and L2 matrices		$\varepsilon_{add,II}$	$\varepsilon_{add,VII}$	$\varepsilon_{add,IX}$	$\varepsilon_{add,X}$	$\varepsilon_{add,PC}$	$\varepsilon_{add,PS}$
		$\varepsilon_{add,II}$	1.00					
		$\varepsilon_{add,VII}$	0.886	1.00				
		$\varepsilon_{add,IX}$	0.896	0.983	1.00			
		$\varepsilon_{add,X}$	0.901	0.933	0.950	1.00		
		$\varepsilon_{add,PC}$	0.924	0.930	0.883	0.919	1.00	
		$\varepsilon_{add,PS}$	0.845	0.707	0.694	0.862	0.883	1.00
			$\varepsilon_{prop,II}$	$\varepsilon_{prop,VII}$	$\varepsilon_{prop,IX}$	$\varepsilon_{prop,X}$	$\varepsilon_{prop,PC}$	$\varepsilon_{prop,PS}$
		$\varepsilon_{prop,II}$	1.00					
		$\varepsilon_{prop,VII}$	0.611	1.00				
		$\varepsilon_{prop,IX}$	0.101	0.381	1.00			
		$\varepsilon_{prop,X}$	-0.571	-0.362	-0.576	1.00		
		$\varepsilon_{prop,PC}$	-0.0909	0.407	0.197	-0.414	1.00	
		$\varepsilon_{prop,PS}$	-0.103	0.131	0.319	-0.0834	0.163	1.00

A1.5. Parameter estimates for the final full joint model

Table A 1.6 *Parameter estimates for the final full joint model. LAG represents the lag parameter. η_i between-subject variability in parameter. CV coefficient of variation, $CV_{prop}P$ coefficient of variation for the proportional error associated with model prediction, CL clearance of warfarin, F bioavailability of warfarin, $IA_{50,P}$ warfarin amount in the body that gives half the maximum inhibitory effect, $I_{max,P}$ maximum inhibitory effect, k_a first-order absorption rate constant of warfarin, $k_{out,P}$ first-order coagulation protein degradation rate constant, PC protein C, PS protein S, $P_{t=0}$ coagulation protein concentration at baseline, RSE relative standard error, SE standard error, V volume of distribution of warfarin, ω standard deviation of between-subject variability in parameter, $\sigma_{add,P}$ standard deviation for the additive error associated with model prediction.*

Parameter	Final estimate (η_i-shrinkage)	Jackknife results		
		Mean[a]	SE[a]	%RSE[b]
F	1.00 fixed[c]	-	-	-
k_a (h^{-1})	1.19 fixed[c]	-	-	-
CL (L/h)	0400	0.416	0.259	62.3
V(L)	8.06 fixed[c]	–	–	–
$I_{max,II}$	1.00 fixed[c]	–	–	–
$I_{max,VII}$	1.00 fixed[c]	–	–	–
$I_{max,IX}$	1.00 fixed[c]	–	–	–
$I_{max,X}$	1.00 fixed[c]	–	–	–
$I_{max,PC}$	1.00 fixed[c]	–	–	–
$I_{max,PS}$	1.00 fixed[c]	–	–	–
$IA_{50,II}$ (mg)	0.720	0.702	0.529	75.3
$IA_{50,VII}$ (mg)	0.950	0.924	0.675	73.1
$IA_{50,IX}$ (mg)	1.15	1.12	0.823	73.3
$IA_{50,X}$ (mg)	0.324	0.316	0.258	81.5
$IA_{50,PC}$ (mg)	2.58	2.52	1.82	72.4
$IA_{50,PS}$ (mg)	1.51	1.47	1.13	76.9
$II_{t=0}$ (IU/dL)	112	112	4.71	4.2
$VII_{t=0}$ (IU/dL)	109	109	6.00	5.5
$IX_{t=0}$ (IU/dL)	136	136	6.79	5.0
$X_{t=0}$ (IU/dL)	106	107	4.13	3.9
$PC_{t=0}$ (IU/dL)	98.1	98.2	3.62	3.7
$PS_{t=0}$ (IU/dL)	104	105	6.13	5.9
$k_{out,II}$ (h^{-1})	0.00987	0.00984	0.000797	8.1
$k_{out,VII}$ (h^{-1})	0.0379	0.0377	0.00424	11.3
$k_{out,IX}$ (h^{-1})	0.0198	0.0197	0.00210	10.6
$k_{out,X}$ (h^{-1})	0.0127	0.0127	0.000794	6.3
$k_{out,PC}$ (h^{-1})	0.0204	0.0203	0.00342	16.9
$k_{out,PS}$ (h^{-1})	0.0101	0.0100	0.00131	13.0
LAG (h)	13.5	12.9	2.39	18.6

Parameter	Final estimate (η_i-shrinkage)	Jackknife results		
		Mean[a]	SE[a]	%RSE[b]
CV k_a (%)	73.0 fixed[c] (94.2%)	–	–	–
CV CL (%)	68.2 (1.6%)	67.4	23.7	35.2
CV $IA_{50,VII}$ (%)	18.0 (22.7%)	17.1	13.4	78.6
CV $IA_{50,X}$ (%)	23.1 (19.4%)	22.9	14.0	61.2
CV $IA_{50,PC}$ (%)	14.4 (27.4%)	13.8	11.5	83.0
$\omega\ II_{t=0}$ (IU/dL)	17.3 (-0.4%)	17.4	4.07	23.3
$\omega\ VII_{t=0}$ (IU/dL)	22.7 (2.7%)	23.0	3.36	14.6
$\omega\ IX_{t=0}$ (IU/dL)	28.7 (0.2%)	28.8	7.94	27.6
$\omega\ X_{t=0}$ (IU/dL)	16.9 (-0.7%)	16.9	3.49	20.6
$\omega\ PC_{t=0}$ (IU/dL)	16.9 (-0.4%)	16.9	3.65	21.6
$\omega\ PS_{t=0}$ (IU/dL)	21.9 (-1.3%)	21.8	4.68	21.5
CV $k_{out,II}$ (%)	24.3 (0.9%)	23.9	8.14	34.0
CV $k_{out,VII}$ (%)	42.6 (2.8%)	42.4	12.7	29.9
CV $k_{out,IX}$ (%)	35.5 (2.4%)	34.9	11.1	31.8
CV $k_{out,X}$ (%)	19.5 (-0.7%)	19.3	2.67	13.8
CV $k_{out,PC}$ (%)	37.4 (3.9%)	37.3	11.2	30.0
CV $k_{out,PS}$ (%)	17.4 (3.1%)	17.4	8.07	46.4
CV LAG (%)	57.9 (0.4%)	61.0	14.9	24.5
$\sigma_{add,II}$ (IU/dL)	8.75	8.64	1.48	17.1
$CV_{prop,II}$ (%)	3.21	3.62	2.62	72.2
$\sigma_{add,VII}$ (IU/dL)	10.7	10.6	1.45	13.6
$CV_{prop,VII}$ (%)	10.6	11.0	3.73	34.0
$\sigma_{add,IX}$ (IU/dL)	13.7	13.6	2.23	16.4
$CV_{prop,IX}$ (%)	10.1	10.6	2.32	22.0
$\sigma_{add,X}$ (IU/dL)	6.41	6.36	1.78	27.9
$CV_{prop,X}$ (%)	3.19	3.52	2.58	73.1
$\sigma_{add,PC}$ (IU/dL)	6.07	6.01	1.24	20.7
$CV_{prop,PC}$ (%)	5.96	5.98	1.80	30.2
$\sigma_{add,PS}$ (IU/dL)	4.79	4.82	1.21	25.0
$CV_{prop,PS}$ (%)	8.78	8.75	1.48	16.9

[a] Jackknife statistics were computed based on all 17 runs, of which 5 (29.4%) runs minimised successfully and another 12 (70.6%) runs ended with rounding errors

[b] Jackknife estimate of parameter (mean) and standard error (SE) were used for calculation of relative standard error (RSE)

[c] Sourced from estimated values by Wright et al. [152]

Table A 1.7 *Parameter estimates of the L1 correlation matrix for the final full joint model. RSE (%) is given in the bracket that follows the final estimate. LAG denotes the lag parameter. η_i between-subject variability in parameter. $P_{t=0}$ coagulation protein concentration at baseline. $k_{out,P}$ first-order coagulation protein degradation rate constant. PC protein C. PS protein S. RSE relative standard error. SE standard error.*

b_i	$II_{t=0}$	$VII_{t=0}$	$IX_{t=0}$	$X_{t=0}$	$PC_{t=0}$	$PS_{t=0}$	$k_{out,II}$	$k_{out,VII}$	$k_{out,IX}$	$k_{out,X}$	$k_{out,PC}$	$k_{out,PS}$	LAG
$II_{t=0}$	1.00												
$VII_{t=0}$	0.725 (16.1)	1.00											
$IX_{t=0}$	0.652 (35.1)	0.282 (105.7)	1.00										
$X_{t=0}$	0.609 (46.8)	0.513 (57.5)	0.506 (44.0)	1.00									
$PC_{t=0}$	0.556 (41.4)	0.495 (42.6)	0.222 (144.9)	0.473 (44.3)	1.00								
$PS_{t=0}$	-0.209 (93.3)	-0.141 (217.1)	-0.212 (101.5)	0.129 (204.5)	-0.0677 (602.7)	1.00							
$k_{out,II}$	-0.175 (132.0)	-0.0282 (1392.2)	0.028 (10755.4)	-0.438 (66.9)	-0.618 (30.4)	-0.287 (115.3)	1.00						
$k_{out,VII}$	-0.373 (78.0)	-0.194 (204.7)	-0.322 (62.5)	-0.45 (61.9)	-0.577 (53.3)	0.0881 (526.5)	0.776 (25.1)	1.00					
$k_{out,IX}$	-0.718 (34.0)	-0.491 (82.1)	-0.351 (65.6)	-0.712 (23.7)	-0.62 (41.5)	0.118 (428.2)	0.649 (27.7)	0.818 (18.5)	1.00				
$k_{out,X}$	-0.551 (43.7)	-0.294 (131.6)	-0.244 (76.6)	-0.604 (43.5)	-0.763 (16.7)	-0.117 (292.3)	0.914 (5.8)	0.788 (18.2)	0.821 (13.3)	1.00			
$k_{out,PC}$	-0.369 (77.1)	-0.242 (153.7)	-0.298 (82.2)	-0.197 (127.7)	-0.486 (74.7)	0.216 (194.3)	0.588 (36.3)	0.935 (5.6)	0.709 (29.7)	0.623 (32.4)	1.00		
$k_{out,PS}$	-0.382 (134.7)	-0.413 (175.6)	0.248 (266.0)	-0.365 (78.8)	-0.292 (124.7)	-0.218 (206.7)	0.623 (49.4)	0.464 (52.2)	0.681 (36.6)	0.652 (32.8)	0.404 (85.7)	1.00	
LAG	0.350 (78.8)	0.146 (308.2)	0.129 (718.7)	0.194 (165.1)	0.451 (71.4)	0.542 (59.0)	-0.719 (31.8)	-0.539 (70.2)	-0.446 (78.1)	-0.728 (32.9)	-0.509 (93.5)	-0.574 (44.1)	1.00

[a] Jackknife estimate of parameter (mean) and SE were used for calculation of RSE. Jackknife statistics were computed based on all 17 runs, of which 5 (29.4%) runs minimised successfully and another 12 (70.6%) runs ended with rounding errors

Table A 1.8 *Parameter estimates of the L2 correlation matrix for the final full joint model. RSE (%) is given in the bracket that follows the final estimate.* $\varepsilon_{prop,P}$ *is the proportional error.* $\varepsilon_{add,P}$ *additive error. PC protein C. PS protein S. RSE relative standard error. SE standard error.*

$\varepsilon_{prop,P}$	*II*	*VII*	*IX*	*X*	*PC*	*PS*
II	1.00					
VII	0.611 (74.0)	1.00				
IX	0.101 (251.8)	0.381 (85.5)	1.00			
X	-0.571 (398.4)	-0.362 (452.4)	-0.576 (211.7)	1.00		
PC	-0.0909 (9002.1)	0.407 (93.7)	0.197 (159.1)	-0.414 (277.7)	1.00	
PS	-0.103 (598.5)	0.131 (288.0)	0.319 (50.7)	-0.0834 (846.6)	0.163 (233.6)	1.00

$\varepsilon_{add,P}$	*II*	*VII*	*IX*	*X*	*PC*	*PS*
II	1.00					
VII	0.886 (9.7)	1.00				
IX	0.896 (7.7)	0.983 (2.5)	1.00			
X	0.901 (5.0)	0.933 (7.4)	0.950 (5.4)	1.00		
PC	0.924 (7.3)	0.930 (6.2)	0.883 (12.7)	0.919 (8.8)	1.00	
PS	0.845 (17.3)	0.707 (30.9)	0.694 (33.3)	0.862 (13.9)	0.883 (12.1)	1.00

[a] Jackknife estimate of parameter (mean) and SE were used for calculation of RSE. Jackknife statistics were computed based on all 17 runs, of which 5 (29.4%) runs minimised successfully and another 12 (70.6%) runs ended with rounding errors

A1.6. NONMEM® code for the final full joint model

```
$PROB
    FULL JOINT MODEL WARFARIN AND COAG FACTORS

$INPUT
    ID AGE SEX TIME AMT IMPUTE ADDL II VITK DV DVID MDV CMT L2 WOBS
    ; IMPUTE (indicator variable for AMT imputation by LOCF)
    ; VITK (VK dose administered for warfarin overdose)
    ; DVID (DV's identifier. Continue below)
    ; DVID (1 PT, 2 INR, 3 aPTT, 4 II, 5 VII, 6 IX, 7 X, 8 PC amido, 9 PC antigen, 10 PS total, 11 PS free)
    ; L2X (originally NONMEM data item, L2. X modifies its recognisability by NONMEM)
    ; WOBS (indicator variable for data censoring)

$DATA
    Warf_Time_Corrected_L2.csv
    IGNORE=#
    IGNORE(DVID.EQ.1) ; PT
    IGNORE(DVID.EQ.2) ; INR
    IGNORE(DVID.EQ.3) ; aPTT
    ; IGNORE(DVID.EQ.4) ; II
    ; IGNORE(DVID.EQ.5) ; VII
    ; IGNORE(DVID.EQ.6) ; IX
    ; IGNORE(DVID.EQ.7) ; X
    ; IGNORE(DVID.EQ.8) ; PC-Amido
    IGNORE(DVID.EQ.9) ; PC-Ag
    IGNORE(DVID.EQ.10) ; PS-Total Ag
    ; IGNORE(DVID.EQ.11) ; PS-Free Ag
    IGNORE(ID.EQ.7) ; ID7 VK administration
    IGNORE(WOBS.EQ.1) ; ID6 missing dosing records and LOCF inappropriate

$SUBR ADVAN6 TRANS1 TOL=9

$MODEL
    COMP=(DEPOT,DEFDOSE)
    COMP=(BODY)
    COMP=(II)
    COMP=(VII)
    COMP=(IX)
    COMP=(X)
    COMP=(C)
    COMP=(S)

$PK
    ; Warfarin kinetics model
    KA=THETA(1)*EXP(ETA(1))
    CL=THETA(2)*EXP(ETA(2))
    V2=THETA(3)
    ALAG1=THETA(28)*EXP(ETA(18))

    K=CL/V2

    ; Inhibitory Emax model
    IMAXII=THETA(4)
    IMAXVII=THETA(5)
    IMAXIX=THETA(6)
    IMAXX=THETA(7)
    IMAXC=THETA(8)
```

```
    IMAXS=THETA(9)

    ID50II=THETA(10)
    ID50VII=THETA(11)*EXP(ETA(4))
    ID50IX=THETA(12)
    ID50X=THETA(13)*EXP(ETA(5))
    ID50C=THETA(14)*EXP(ETA(3))
    ID50S=THETA(15)

    ; System response model
    II0=THETA(16)+ETA(6)
    VII0=THETA(17)+ETA(7)
    IX0=THETA(18)+ETA(8)
    X0=THETA(19)+ETA(9)
    C0=THETA(20)+ETA(10)
    S0=THETA(21)+ETA(11)

    KOUTII=THETA(22)*EXP(ETA(12))
    KOUTVII=THETA(23)*EXP(ETA(13))
    KOUTIX=THETA(24)*EXP(ETA(14))
    KOUTX=THETA(25)*EXP(ETA(15))
    KOUTC=THETA(26)*EXP(ETA(16))
    KOUTS=THETA(27)*EXP(ETA(17))

    RINII=II0*KOUTII
    RINVII=VII0*KOUTVII
    RINIX=IX0*KOUTIX
    RINX=X0*KOUTX
    RINC=C0*KOUTC
    RINS=S0*KOUTS

    A_0(3)=II0
    A_0(4)=VII0
    A_0(5)=IX0
    A_0(6)=X0
    A_0(7)=C0
    A_0(8)=S0

$DES
    EII=IMAXII*A(2)/(ID50II+A(2))
    EVII=IMAXVII*A(2)/(ID50VII+A(2))
    EIX=IMAXIX*A(2)/(ID50IX+A(2))
    EX=IMAXX*A(2)/(ID50X+A(2))
    EC=IMAXC*A(2)/(ID50C+A(2))
    ES=IMAXS*A(2)/(ID50S+A(2))

    DADT(1)=-KA*A(1) ; Warfarin
    DADT(2)=KA*A(1)-K*A(2) ; Warfarin
    DADT(3)=RINII*(1-EII)-KOUTII*A(3) ; II
    DADT(4)=RINVII*(1-EVII)-KOUTVII*A(4) ; VII
    DADT(5)=RINIX*(1-EIX)-KOUTIX*A(5) ; IX
    DADT(6)=RINX*(1-EX)-KOUTX*A(6) ; X
    DADT(7)=RINC*(1-EC)-KOUTC*A(7) ; PC-Amido
    DADT(8)=RINS*(1-ES)-KOUTS*A(8) ; PS-Free Ag
```

```
$ERROR
    IF(DVID.EQ.4) Y=F*(1+EPS(1))+EPS(7) ; II
    IF(DVID.EQ.5) Y=F*(1+EPS(2))+EPS(8) ; VII
    IF(DVID.EQ.6) Y=F*(1+EPS(3))+EPS(9) ; IX
    IF(DVID.EQ.7) Y=F*(1+EPS(4))+EPS(10) ; X
    IF(DVID.EQ.8) Y=F*(1+EPS(5))+EPS(11) ; PC-Amido
    IF(DVID.EQ.11) Y=F*(1+EPS(6))+EPS(12) ; PS-Free Ag

    IPRED=F

$THETA
    1.19 FIX ; KA
    (0,0.4) ; CL
    8.06 FIX ; V2
    1. FIX ; IMAXII
    1. FIX ; IMAXVII
    1. FIX ; IMAXIX
    1. FIX ; IMAXX
    1. FIX ; IMAXC
    1. FIX ; IMAXS
    (0,0.72) ; ID50II
    (0,0.95) ; ID50VII
    (0,1.15) ; ID50IX
    (0,0.324) ; ID50X
    (0,2.58) ; ID50C
    (0,1.51) ; ID50S
    (0,112.) ; II0
    (0,109.) ; VII0
    (0,136.) ; IX0
    (0,106.) ; X0
    (0,98.1) ; C0
    (0,104.) ; S0
    (0,0.00987) ; KOUTII
    (0,0.0379) ; KOUTVII
    (0,0.0198) ; KOUTIX
    (0,0.0127) ; KOUTX
    (0,0.0204) ; KOUTC
    (0,0.0101) ; KOUTS
    (0,13.5) ; ALAG1

$OMEGA
    0.427 FIX ; KA
    0.382 ; CL
    0.0206 ; ID50C
    0.0318 ; ID50VII
    0.0521 ; ID50X

$OMEGA BLOCK(13)
    301. ; II0
    286. 516. ; VII0
    325. 184. 824. ; IX0
    179. 197. 246. 286. ; X0
    162. 189. 108. 135. 284. ; C0
    -79.5 -70. -134. 47.9 -25. 480. ; S0
    -0.726 -0.153 0.192 -1.77 -2.49 -1.5 0.0572 ; KOUTII
    -2.65 -1.8 -3.78 -3.11 -3.98 0.789 0.0759 0.167 ; KOUTVII
```

```
    -4.29 -3.84 -3.47 -4.15 -3.6 0.895 0.0535 0.115 0.119 ; KOUTIX
    -1.85 -1.29 -1.36 -1.97 -2.49 -0.495 0.0423 0.0623 0.0547 0.0374 ; KOUTX
    -2.31 -1.99 -3.09 -1.21 -2.97 1.71 0.0509 0.138 0.0885 0.0435 0.131 ; KOUTC
    -1.15 -1.62 1.23 -1.07 -0.85 -0.827 0.0258 0.0328 0.0406 0.0218 0.0253 0.0299 ; KOUTS
    3.27 1.78 1.98 1.76 4.09 6.39 -0.0925 -0.119 -0.0826 -0.0756 -0.0991 -0.0534 0.289 ; ALAG1

$SIGMA BLOCK(6) ; Proportional component
    0.00103 ; II
    0.00207 0.0111 ; VII
    0.000329 0.00407 0.0102 ; IX
    -0.000585 -0.00122 -0.00186 0.00102 ; X
    -0.000174 0.00255 0.00119 -0.000786 0.00355 ; PC-Amido
    -0.000289 0.00121 0.00283 -0.000233 0.000849 0.00768 ; PS-Free Ag

$SIGMA BLOCK(6) ; Additive component
    76.5 ; II
    83.2 115 ; VII
    107 145 188 ; IX
    50.5 64.3 83.4 41.1 ; X
    49 60.6 73.3 35.7 36.8 ; PC-Amido
    35.4 36.4 45.5 26.4 25.6 22.9 ; PS-Free Ag

$EST MAXEVAL=99999 SIG=6 PRINT=1 METHOD=COND INTER MSFO=final_full_joint_model.msf

$TABLE
ID KA CL V2 IMAXII IMAXVII IMAXIX IMAXX IMAXC IMAXS ID50II ID50VII ID50IX ID50X ID50C
ID50S II0 VII0 IX0 X0 C0 S0 KOUTII KOUTVII KOUTIX KOUTX KOUTC KOUTS ALAG1
FIRSTONLY ONEHEADER NOAPPEND NOPRINT FILE=Full_Joint_Params.fit

$TABLE
ID TIME DVID DV PRED IPRED RES WRES CWRES
ONEHEADER NOAPPEND NOPRINT FILE=Full_Joint_GoF.fit
```

A1.7. Individual fits for the final full joint model

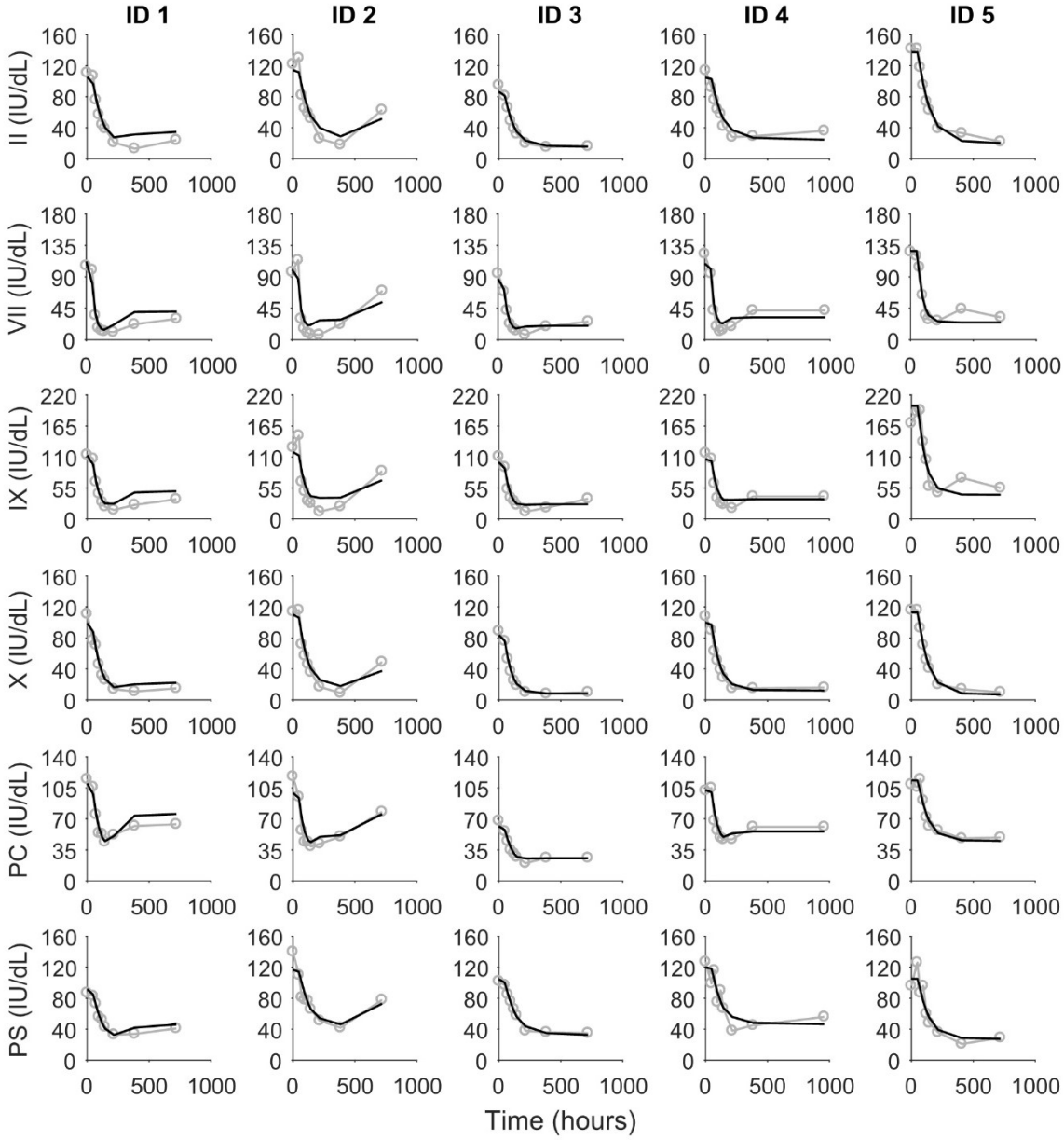

Figure A 1.2 *Individual fits for the time course of factors II, VII, IX, X, and proteins C and S following warfarin initiation. The black lines are predictions from the final full joint model. The grey markers are observations. PC denotes protein C and PS represents protein S.*

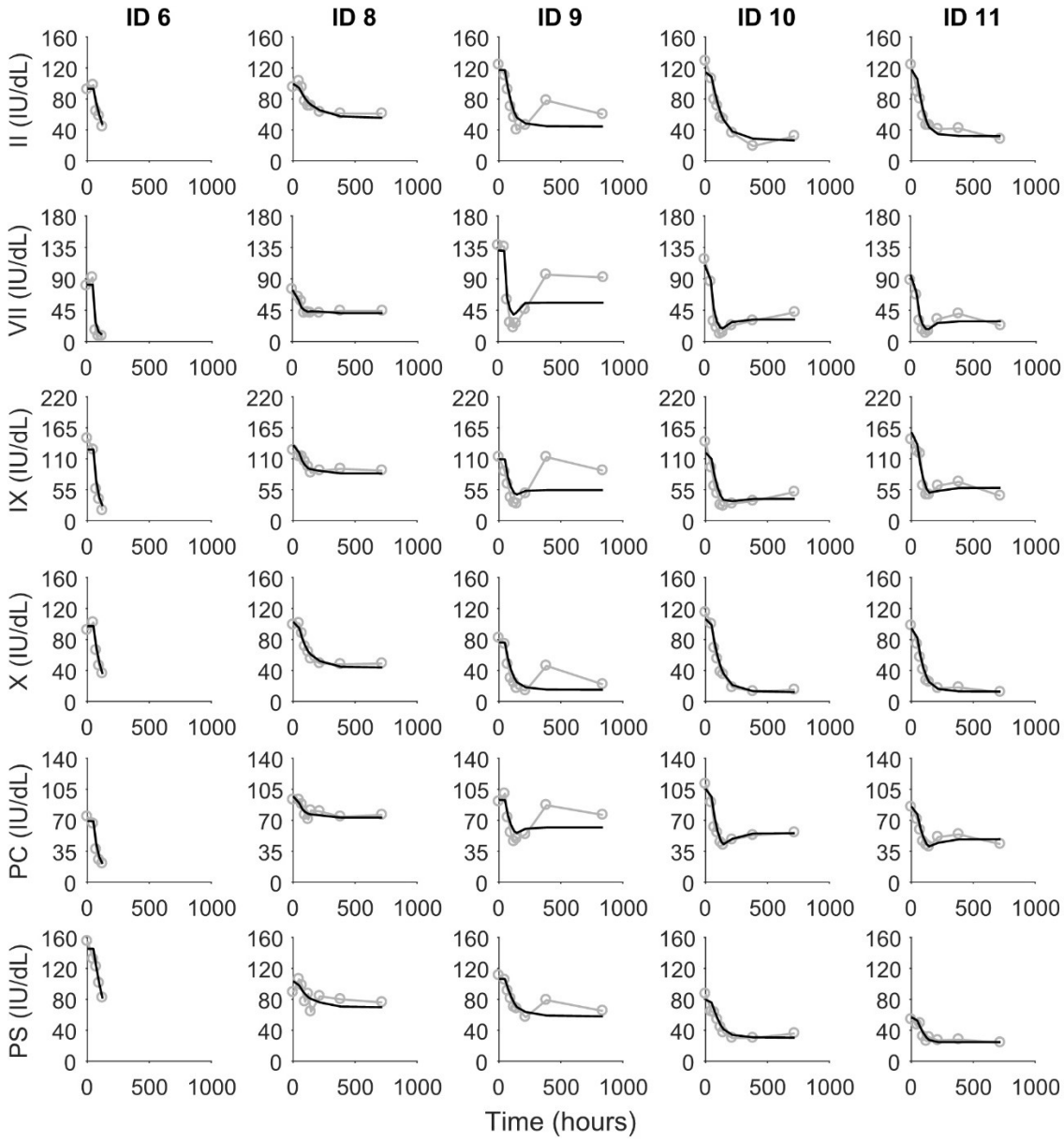

Figure A 1.2 *Continued.*

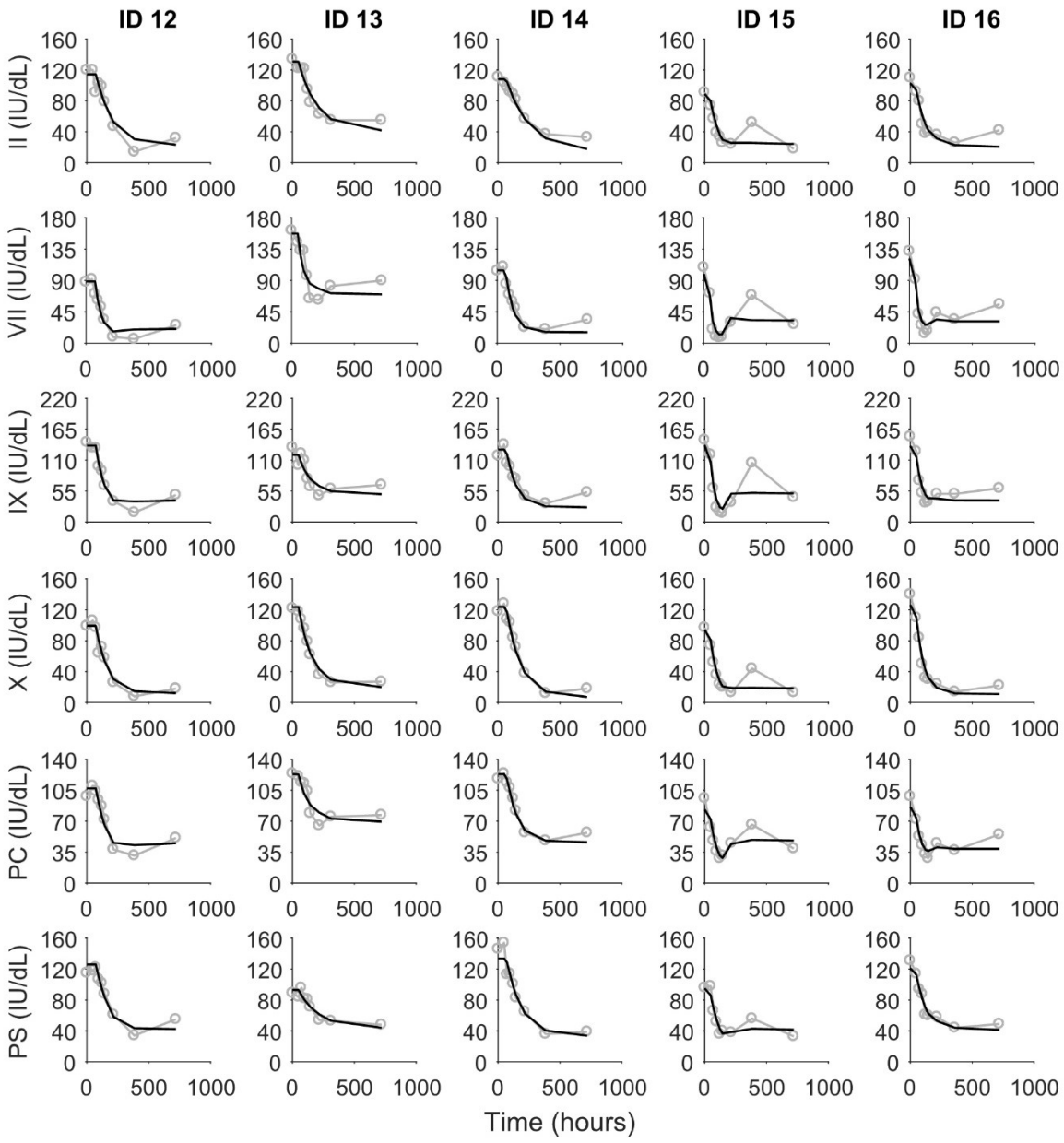

Figure A 1.2 *Continued.*

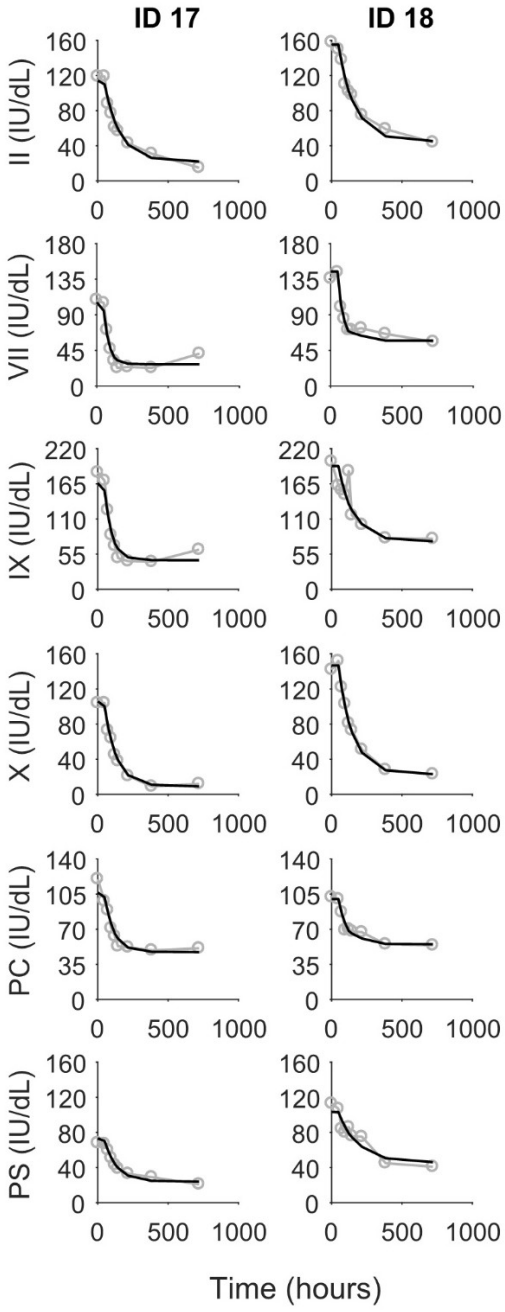

Figure A 1.2 *Continued.*

A1.8. pcVPC for the final full joint model

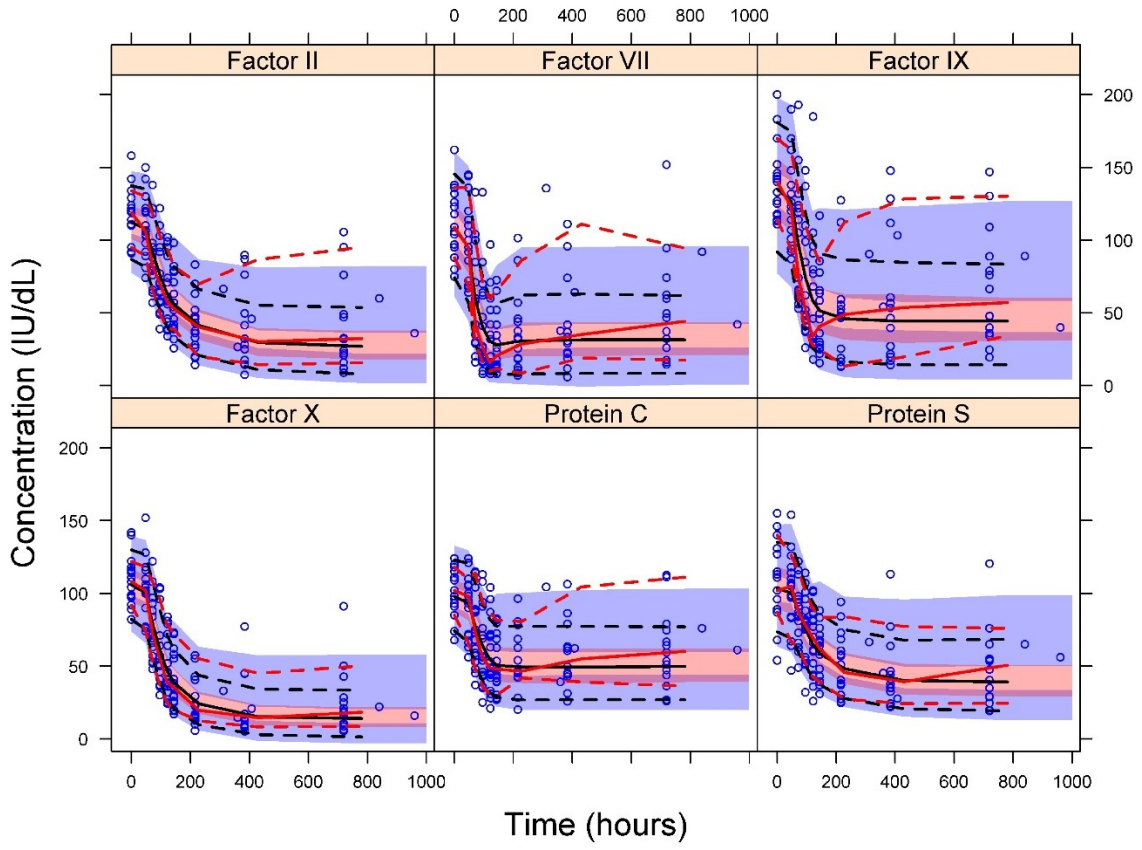

Figure A 1.3 *pcVPC for factors II, VII, IX and X, and proteins C and S based on the final full joint model. The blue circle indicates observation. The black solid line indicates the median of simulated data. The red solid line indicates the median of observed data. The black dashed line indicates the 10th and 90th percentiles of simulated data that correspond to the 80% prediction interval. The red dashed line indicates the 10th and 90th percentiles of observed data that correspond to the 80% prediction interval. The shaded area indicates the 95% confidence interval around the simulated percentiles. pcVPC stands for prediction-corrected visual predictive checks.*

A1.9. NONMEM® code for the final reduced joint model

```
$PROB
    REDUCED JOINT MODEL WARFARIN AND COAG FACTORS

$INPUT
    ID AGE SEX TIME AMT IMPUTE ADDL II VITK DV DVID MDV CMT L2X WOBS
    ; IMPUTE (indicator variable for AMT imputation by LOCF)
    ; VITK (VK dose administered for warfarin overdose)
    ; DVID (DV's identifier. Continue below)
    ; DVID (1 PT, 2 INR, 3 aPTT, 4 II, 5 VII, 6 IX, 7 X, 8 PC amido, 9 PC antigen, 10 PS total, 11 PS free)
    ; L2X (originally NONMEM data item, L2. X modifies its recognisability by NONMEM)
    ; WOBS (indicator variable for data censoring)

$DATA
    Warf_Time_Corrected_L2.csv
    IGNORE=#
    IGNORE(DVID.EQ.1) ; PT
    IGNORE(DVID.EQ.2) ; INR
    IGNORE(DVID.EQ.3) ; aPTT
    ; IGNORE(DVID.EQ.4) ; II
    ; IGNORE(DVID.EQ.5) ; VII
    ; IGNORE(DVID.EQ.6) ; IX
    ; IGNORE(DVID.EQ.7) ; X
    ; IGNORE(DVID.EQ.8) ; PC-Amido
    IGNORE(DVID.EQ.9) ; PC-Ag
    IGNORE(DVID.EQ.10) ; PS-Total Ag
    ; IGNORE(DVID.EQ.11) ; PS-Free Ag
    IGNORE(ID.EQ.7) ; ID7 VK administration
    IGNORE(WOBS.EQ.1) ; ID6 missing dosing records and LOCF inappropriate

$SUBR ADVAN6 TRANS1 TOL=9

$MODEL
    COMP=(DEPOT,DEFDOSE)
    COMP=(BODY)
    COMP=(II)
    COMP=(VII)
    COMP=(IX)
    COMP=(X)
    COMP=(C)
    COMP=(S)

$PK
    ; Warfarin kinetics model
    KA=THETA(1)*EXP(ETA(1))
    CL=THETA(2)*EXP(ETA(2))
    V2=THETA(3)
    ALAG1=THETA(28)

    K=CL/V2

    ; Inhibitory Emax model
    IMAXII=THETA(4)
    IMAXVII=THETA(5)
    IMAXIX=THETA(6)
    IMAXX=THETA(7)
    IMAXC=THETA(8)
```

```
      IMAXS=THETA(9)

      ID50II=THETA(10)
      ID50VII=THETA(11)
      ID50IX=THETA(12)
      ID50X=THETA(13)
      ID50C=THETA(14)*EXP(ETA(3))
      ID50S=THETA(15)

      ; System response model
      II0=THETA(16)+ETA(4)
      VII0=THETA(17)+ETA(5)
      IX0=THETA(18)+ETA(6)
      X0=THETA(19)+ETA(7)
      C0=THETA(20)+ETA(8)
      S0=THETA(21)+ETA(9)

      KOUTII=THETA(22)*EXP(ETA(10))
      KOUTVII=THETA(23)*EXP(ETA(11))
      KOUTIX=THETA(24)*EXP(ETA(12))
      KOUTX=THETA(25)*EXP(ETA(13))
      KOUTC=THETA(26)*EXP(ETA(14))
      KOUTS=THETA(27)*EXP(ETA(15))

      RINII=II0*KOUTII
      RINVII=VII0*KOUTVII
      RINIX=IX0*KOUTIX
      RINX=X0*KOUTX
      RINC=C0*KOUTC
      RINS=S0*KOUTS

      A_0(3)=II0
      A_0(4)=VII0
      A_0(5)=IX0
      A_0(6)=X0
      A_0(7)=C0
      A_0(8)=S0

   $DES
      EII=IMAXII*A(2)/(ID50II+A(2))
      EVII=IMAXVII*A(2)/(ID50VII+A(2))
      EIX=IMAXIX*A(2)/(ID50IX+A(2))
      EX=IMAXX*A(2)/(ID50X+A(2))
      EC=IMAXC*A(2)/(ID50C+A(2))
      ES=IMAXS*A(2)/(ID50S+A(2))

      DADT(1)=-KA*A(1) ; Warfarin
      DADT(2)=KA*A(1)-K*A(2) ; Warfarin
      DADT(3)=RINII*(1-EII)-KOUTII*A(3) ; II
      DADT(4)=RINVII*(1-EVII)-KOUTVII*A(4) ; VII
      DADT(5)=RINIX*(1-EIX)-KOUTIX*A(5) ; IX
      DADT(6)=RINX*(1-EX)-KOUTX*A(6) ; X
      DADT(7)=RINC*(1-EC)-KOUTC*A(7) ; PC-Amido
      DADT(8)=RINS*(1-ES)-KOUTS*A(8) ; PS-Free Ag
```

```
$ERROR
    IF(DVID.EQ.4) Y=F*(1+EPS(1))+EPS(7) ; II
    IF(DVID.EQ.5) Y=F*(1+EPS(2))+EPS(8) ; VII
    IF(DVID.EQ.6) Y=F*(1+EPS(3))+EPS(9) ; IX
    IF(DVID.EQ.7) Y=F*(1+EPS(4))+EPS(10) ; X
    IF(DVID.EQ.8) Y=F*(1+EPS(5))+EPS(11) ; PC-Amido
    IF(DVID.EQ.11) Y=F*(1+EPS(6))+EPS(12) ; PS-Free Ag

    IPRED=F

$THETA
    1.19 FIX ; KA
    (0,0.211) ; CL
    8.06 FIX ; V2
    1. FIX ; IMAXII
    1. FIX ; IMAXVII
    1. FIX ; IMAXIX
    1. FIX ; IMAXX
    1. FIX ; IMAXC
    1. FIX ; IMAXS
    (0,1.83) ; ID50II
    (0,1.86) ; ID50VII
    (0,2.41) ; ID50IX
    (0,0.875) ; ID50X
    (0,5.21) ; ID50C
    (0,3.35) ; ID50S
    (0,115.) ; II0
    (0,115.) ; VII0
    (0,141.) ; IX0
    (0,109.) ; X0
    (0,101.) ; C0
    (0,105.) ; S0
    (0,0.0135) ; KOUTII
    (0,0.057) ; KOUTVII
    (0,0.0323) ; KOUTIX
    (0,0.0157) ; KOUTX
    (0,0.0376) ; KOUTC
    (0,0.0122) ; KOUTS
    (0,12.5) ; ALAG1

$OMEGA
    0.427 FIX ; KA
    0.516 ; CL
    0.0177 ; ID50C
    317. ; II0
    723. ; VII0
    623. ; IX0
    306. ; X0
    302. ; C0
    596. ; S0
    0.158 ; KOUTII
    0.619 ; KOUTVII
    0.589 ; KOUTIX
    0.124 ; KOUTX
    0.605 ; KOUTC
    0.0356 ; KOUTS
```

```
$SIGMA
    ; Proportional component
    0.00136 ; II
    0.023 ; VII
    0.0119 ; IX
    0.00354 ; X
    0.00734 ; PC-Amido
    0.0112 ; PS-Free Ag

    ; Additive component
    50.6 ; II
    77.5 ; VII
    120. ; IX
    29.3 ; X
    15.1 ; PC-Amido
    11.1 ; PS-Free Ag

$EST MAXEVAL=99999 SIG=3 PRINT=1 METHOD=COND INTER MSFO=final_reduced_joint_model.msf

$TABLE
ID TIME KA CL V2 IMAXII IMAXVII IMAXIX IMAXX IMAXC IMAXS ID50II ID50VII ID50IX ID50X
ID50C ID50S II0 VII0 IX0 X0 C0 S0 KOUTII KOUTVII KOUTIX KOUTX KOUTC KOUTS ALAG1
FIRSTONLY ONEHEADER NOAPPEND NOPRINT FILE=Reduced_Joint_Params.fit

$TABLE
ID TIME DVID DV PRED IPRED RES WRES CWRES
ONEHEADER NOAPPEND NOPRINT FILE=Full_Joint_GoF.fit
```

A1.10. CWRES versus time plots for the final joint models

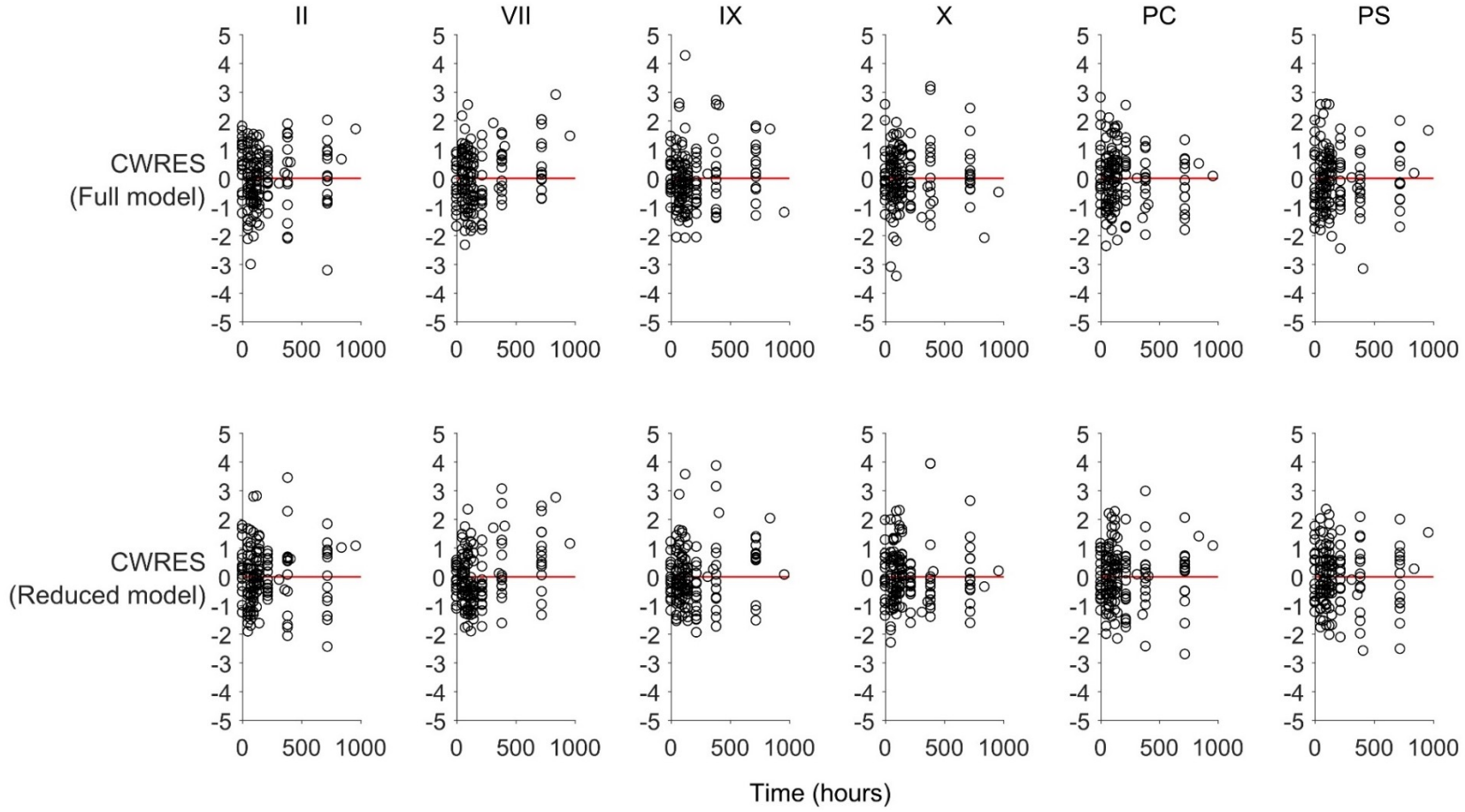

Figure A 1.4 *CWRES versus time plots for the final joint models. PC is protein C and PS is protein S.*

A1.11. Individual fits for the final reduced joint model

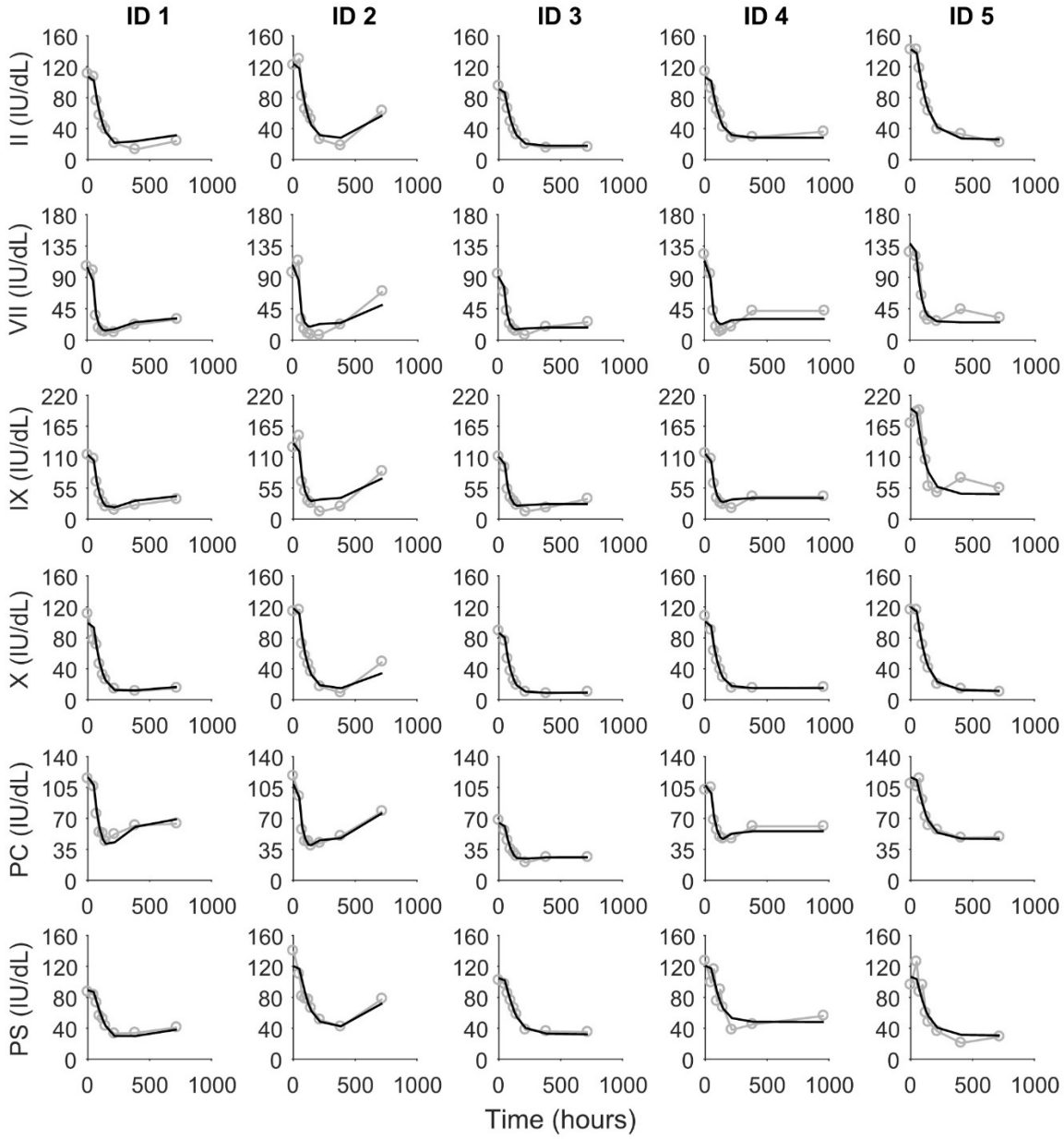

Figure A 1.5 *Individual fits for the time course of factors II, VII, IX, X, and proteins C and S following warfarin initiation. The black lines are predictions from the final reduced joint model. The grey markers are observations. PC denotes protein C and PS represents protein S.*

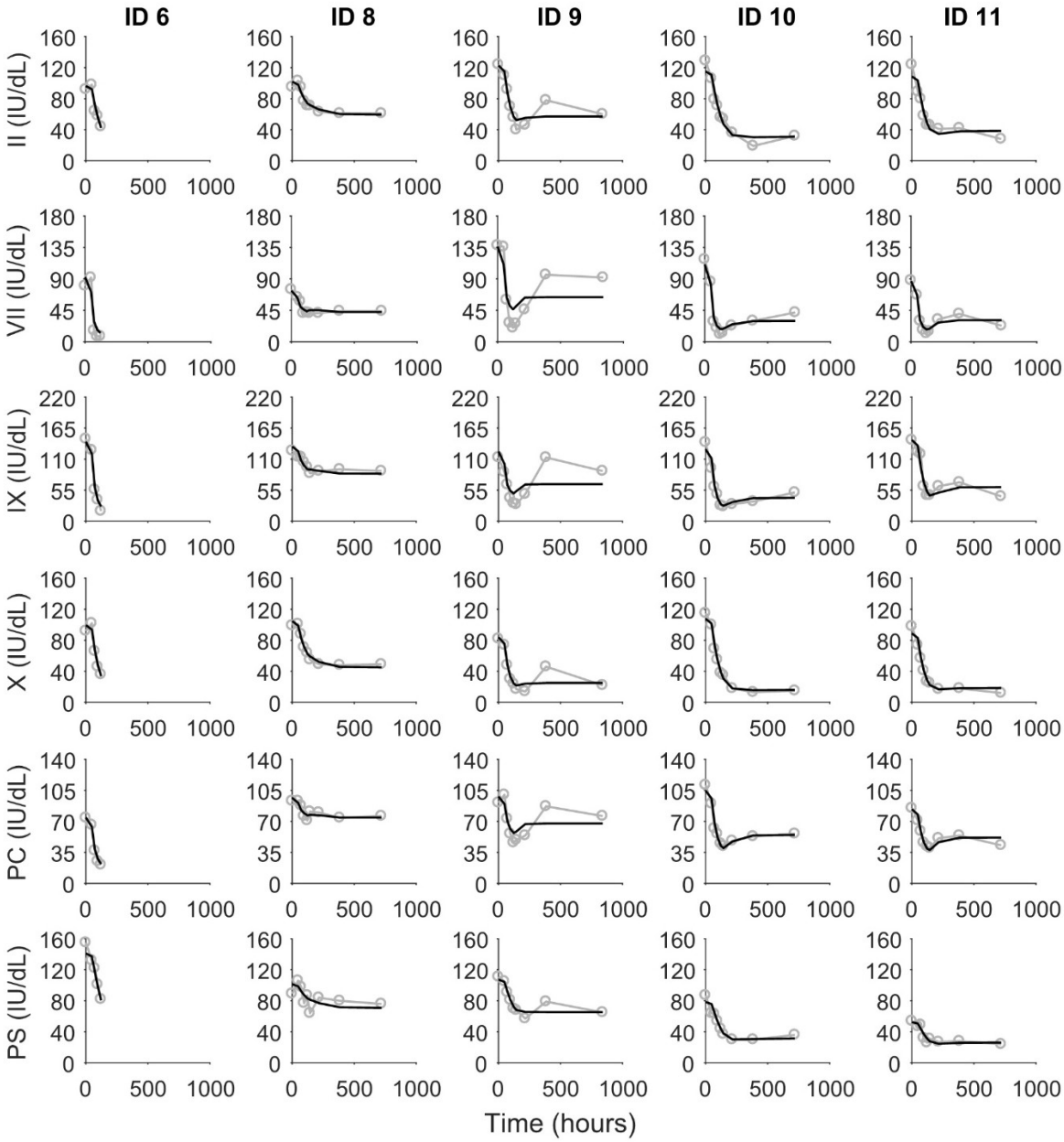

Figure A 1.5 *Continued.*

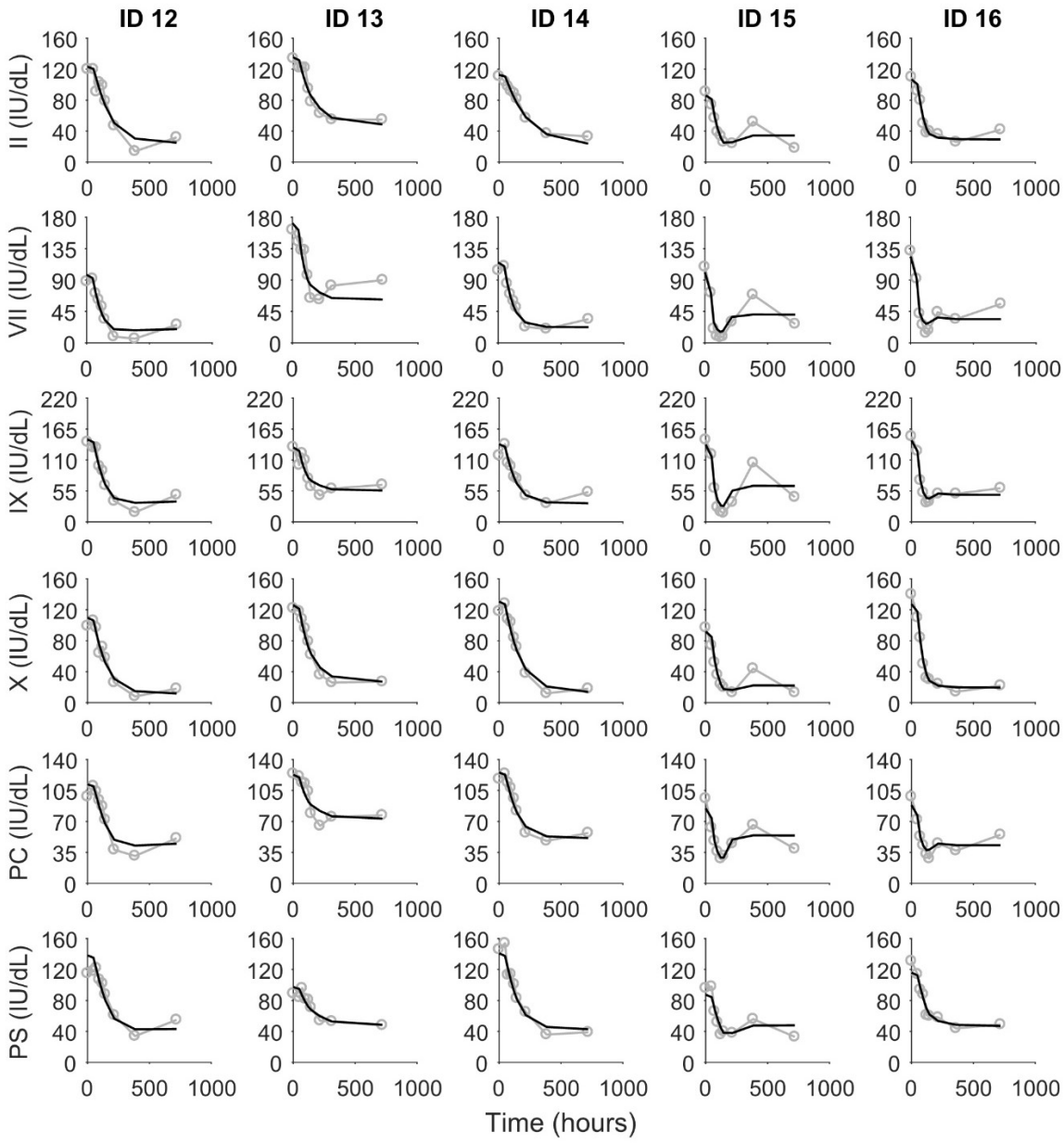

Figure A 1.5 *Continued.*

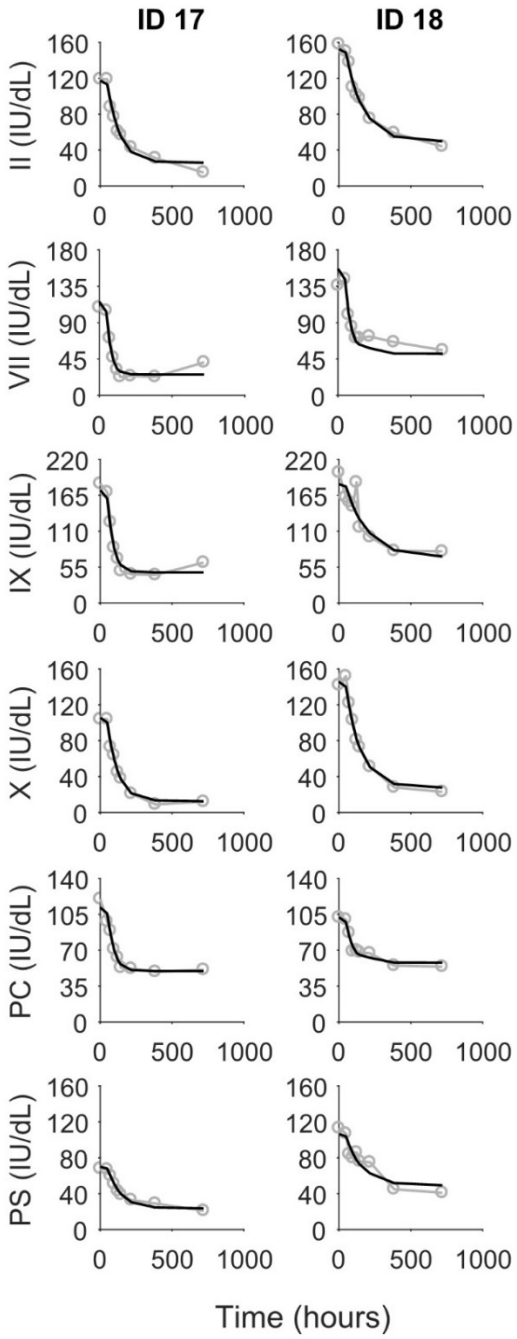

Figure A 1.5 *Continued.*

Appendix 2: Appendices to Chapter 3

A2.1. Adaptive search algorithm for R_P and $R_{P,combi}$

An adaptive grid search algorithm was implemented in MATLAB® Version 2015a (The MathWorks Inc., Natick, Massachusetts, USA) to determine the percentage reduction in a coagulation protein that singly (R_P) or jointly with reduction in another coagulation protein ($R_{P,combi}$) gives a predetermined level of INR. The simulation-based search for a reduction in factor VII, $R_{VII,combi}$, when factor II is simultaneously reduced, $R_{II,combi}$, is illustrated here as an example.

The search algorithm can be summarised in the following 7 steps. The corresponding MATLAB code is also included.

1. Fix $R_{II,combi}$ to 0%.
2. The initial search space for $R_{VII,combi}$ was set to range from 0% to 100%.
3. The 0th, 25th, 50th, 75th, and 100th percentile of the search space for $R_{VII,combi}$ were obtained.
4. The $R_{VII,combi}$ was set to each of the percentile values one-at-a-time. The corresponding INR was simulated from the QSP coagulation network model [31].
5. The two percentiles that give the INR values enveloping the INR target were used to define a more refined search space for $R_{VII,combi}$. If none of the percentile pairs contain the INR target, go to step 7.
6. Step 3 to step 5 were repeated until the smallest distance between the simulated and target INRs is less than 0.01. The corresponding percentile value was then taken as the final $R_{VII,combi}$ estimate.
7. Step 1 to step 6 were repeated for $R_{II,combi} = 5\%, \cdots, 90\%, 95\%$.

```
% Adaptive search for RVII,combi
% RVII,combi and RII,combi give a predetermined level of INR
clear all
clc

%%% User input required
INR_Target=4.5;
INR_Diff_Tol=0.01;

%%% User input not required
RF_Combi_Matrix=[];

% Step 1: Fix RII,combi to 0%, 5%, ..., 90%, 95% one-at-a-time
RII_Combi_Temp=0:0.05:0.95;
for i=1:length(RII_Combi_Temp)
    RII_Combi=RII_Combi_Temp(i);
    INR_Diff=Inf;
    Smallest_Pos_INR_Diff=Inf;
    Smallest_Neg_INR_Diff=-Inf;
    copyfile('initial_values_constants_modified_dummy.m', ...
        'initial_values_constants_modified_dummy2.m');
    find_and_replace('initial_values_constants_modified_dummy2.m', ...
        'Cue_II',num2str(RII_Combi));
    % Step 2: Define the initial search space for RVII,combi
    Lower_Bound=0;
    Upper_Bound=1;
    while abs(INR_Diff)>=INR_Diff_Tol
        % Step 3: Obtain five equally spaced percentiles from the
        % Step 3 (con'd): RVII,combi search space
        j=1;
        Search_Space=linspace(Lower_Bound,Upper_Bound,5);
        for k=1:length(Search_Space)
            % Step 4: Set RVII,combi value to percentile value
            % Step 4 (con'd): one-at-a-time and simulate INR
            copyfile('initial_values_constants_modified_dummy2.m', ...
                'initial_values_constants_modified.m');
            find_and_replace('initial_values_constants_modified.m', ...
                'Cue_VII',num2str(Search_Space(k)));
            coagInputs
            INR=results.INR;
            INR_Diff=INR-INR_Target;
```

```
            % Step 5: Define more refined search space for RVII,combi
            % Step 6: Define stop criterion as when error in INR < 0.001.
            % Step 6 (con'd): Obtain RVII,combi.
            % RVII_Combi solution
            if abs(INR_Diff)<INR_Diff_Tol
                RVII_Combi=Search_Space(k);
                RF_Combi_Matrix=[RF_Combi_Matrix;RII_Combi RVII_Combi];
                break
            % No RVII_Combi solution
            elseif j==1&&k==1&&INR_Diff>0
                RVII_Combi=NaN;
                RF_Combi_Matrix=[RF_Combi_Matrix;RII_Combi RVII_Combi];
                INR_Diff=INR_Diff_Tol/10;
                break
            % Updating upper bound
            elseif INR_Diff>0&&INR_Diff<=Smallest_Pos_INR_Diff
                Smallest_Pos_INR_Diff=INR_Diff;
                Upper_Bound=Search_Space(k);
            % Updating lower bound
            elseif INR_Diff<0&&INR_Diff>=Smallest_Neg_INR_Diff
                Smallest_Neg_INR_Diff=INR_Diff;
                Lower_Bound=Search_Space(k);
            end
        end
        j=j+1;
    end
end
```

A2.2. Model evaluation

The data simulated from the QSP coagulation network model [31] agree reasonably well with the external data for factors II, VII, IX, X, and INR at the individual level. Plots of all 17 patients are shown in **Figure A 2.1**. The model was, on the whole, considered adequate in describing the warfarin-coagulation proteins-INR relationship for subsequent use in this simulation study.

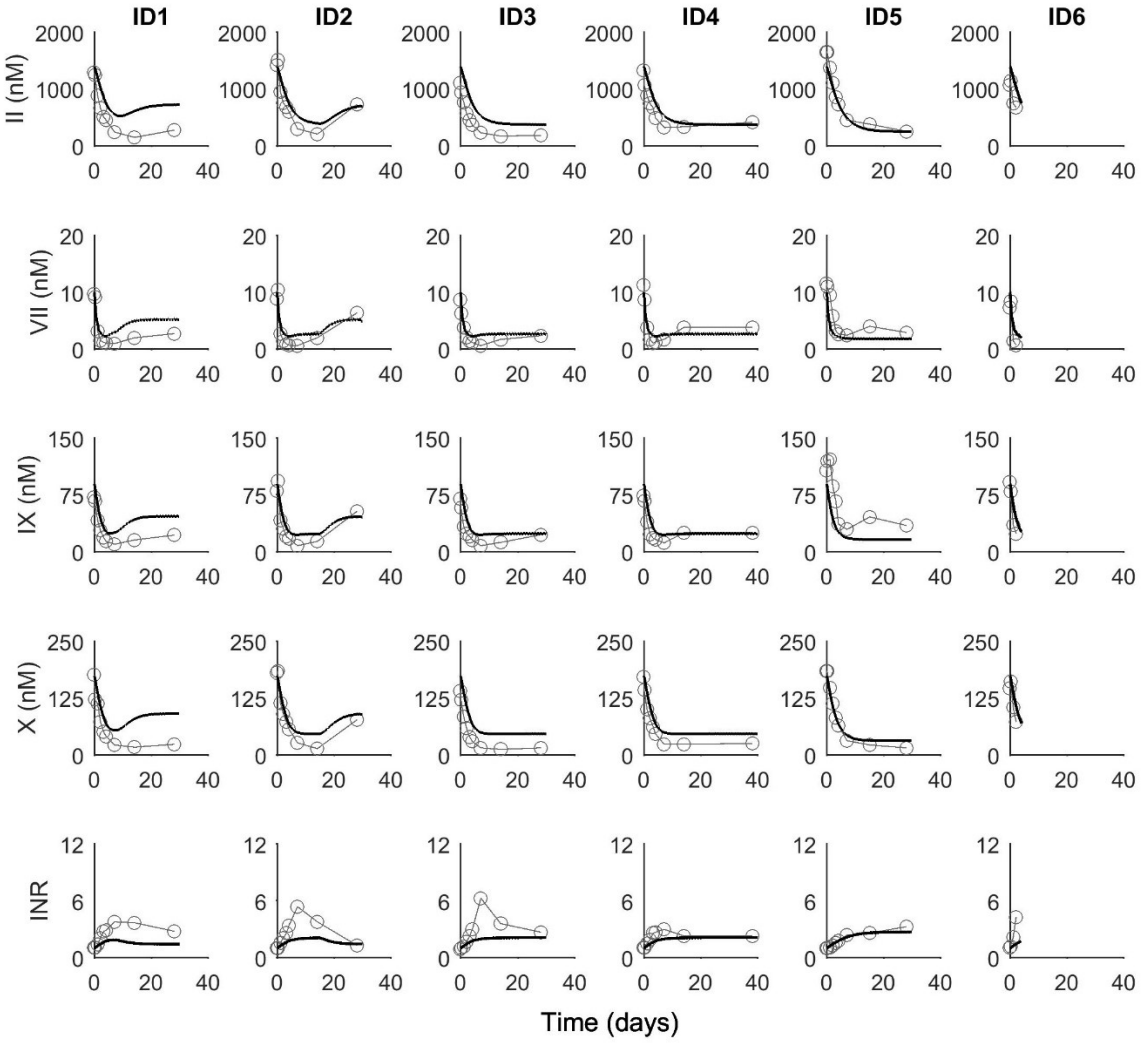

Figure A 2.1 *Individual fits for the time course of factors II, VII, IX, X, and INR for 17 patients following warfarin initiation. The black solid lines are prediction by the coagulation network model using parameters for a typical patient. The grey open circles are observations from the external test dataset [167, 181]. INR refers to the international normalised ratio and nM stands for nanomolar.*

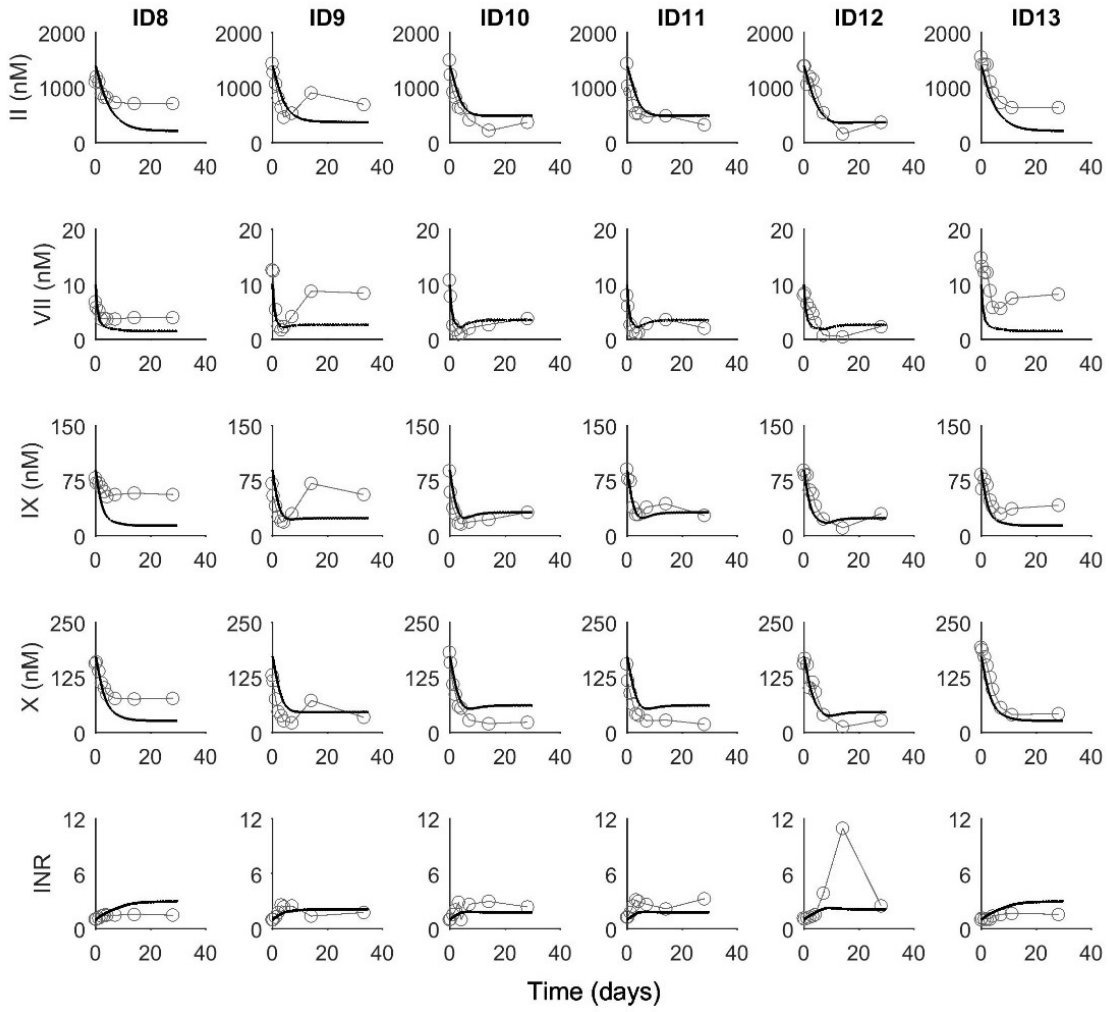

Figure A 2.1 *Continued.*

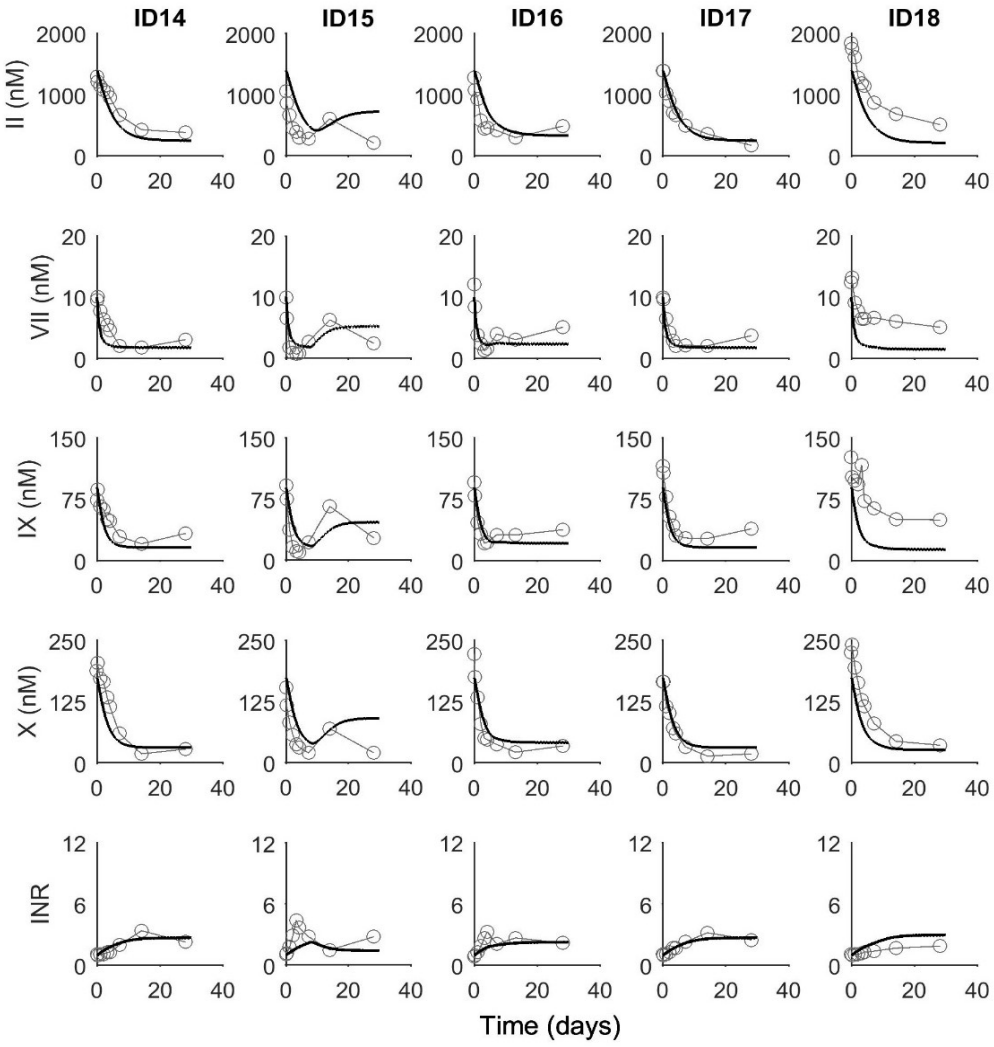

Figure A 2.1 *Continued.*

Appendix 3: Appendices to Chapter 4

A3.1. Modelling the time course of the derivative of SI_{VII}

Table A 3.1 *Parameter estimates and goodness-of-fit of the individual model for the time course of dSI_{VII}/dt at a specific D_{ref}. At different D_{ref}, the estimates for p obtained were largely similar (range 0.260 - 0.301) and fixing of p to 0.300 resulted in an almost identical model fit. D_{ref} is the warfarin daily dose for a typical patient, h the upper horizontal asymptote, g the magnitude of horizontal shift, p the shape parameter, r^2 the adjusted coefficient of determination, RSE the relative standard error, and SI_{VII} the sensitivity index of INR to factor VII.*

D_{ref}	Final estimate (%RSE)			r^2
(mg/day)	h (/%/day)	g (days)	p	
1	0.00200 (6.44)	-1.30 (21.3)	0.300 fixed	0.999
4	0.00442 (1.48)	3.96 (2.48)	0.300 fixed	0.999
7	0.00744 (1.35)	6.33 (1.76)	0.300 fixed	0.999
10	0.0109 (1.10)	8.03 (1.31)	0.300 fixed	0.998
13	0.0149 (0.883)	9.40 (1.00)	0.300 fixed	0.999

[a] Observations for $t = 0.5$ days were excluded from model-fitting.

A3.2. Determination of ε_{SIVII}

In this study, **Equation 4.12** that is based on SI_{VII} is our approximation to **Equation 4.5**, which is an approximation to the theoretical gold standard of steady-state INR given by **Equation 4.1** (via a functional relationship between $\frac{dINR}{dt}$ and $\frac{dSI_{VII}}{dt}$ described in **Section 4.5.4** in **Chapter 4**). Based on **Equation 4.12**, a pre-requisite to the prediction of $t_{SS,INR}$ is the choice of a suitable value of $\varepsilon_{SI_{VII}}$. The choice of $\varepsilon_{SI_{VII}}$ should correctly classify a given INR as non-steady-state (or steady-state) when the INR is truly non-steady-state (or steady-state). The choice of $\varepsilon_{SI_{VII}}$ was based on optimising the receiver operating characteristic (ROC). The ROC curve analysis was conducted in Stata® Version 11.2 (StataCorp LLC, College Station, Texas, USA). **Equation 4.2**, which represents a practical solution to **Equation 4.1**, was used as the gold standard to determine the achievement of steady-state INR. Here, a value of ε_{INR} was chosen to represent the target gold standard, in this case $\varepsilon_{INR} = 0.01$, for defining the steady-state INR.

The resulting ROC curve for $\frac{dSI_{VII}}{dt}$ is shown in **Figure A 3.1**. From the ROC analysis a choice of $\varepsilon_{SI_{VII}} = 0.000150$ as the tolerance for $\frac{dSI_{VII}}{dt}$ (**Equation 4.5** and **Equation 4.12**) corresponds to the steady-state INR. The associated sensitivity and specificity were 100.0% (56/56) and 93.6% (88/94), respectively.

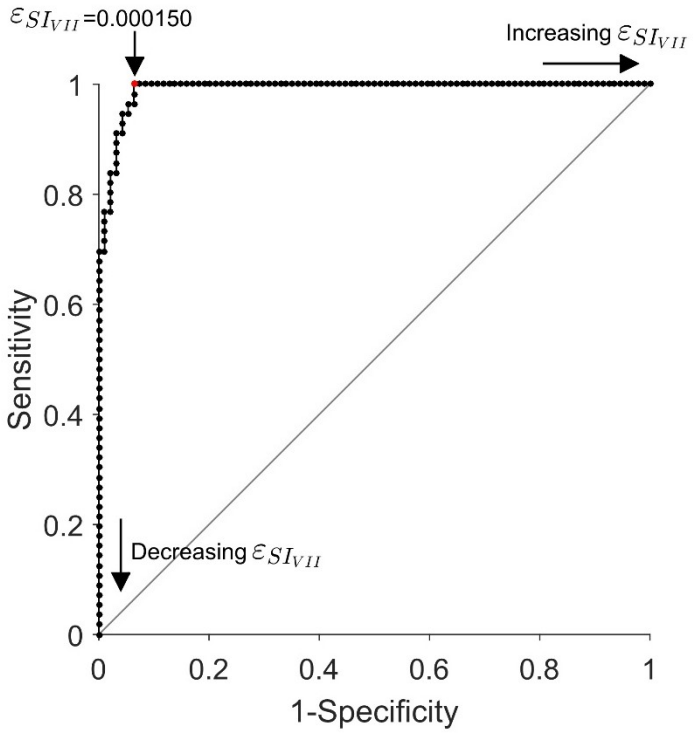

Figure A 3.1 *ROC curve for ε_{SIVII} values to define the steady-state INR status in the dSI_{VII}/dt domain compared to the presumed gold standard of $dINR/dt \leq \varepsilon_{INR}$ (where $\varepsilon_{INR} = 0.01$). The grey solid line represents the reference line for chance performance. SI_{VII} is the sensitivity index of INR to factor VII.*

A3.3. Modelling the derivative of INR as a function of the derivative of SI_{VII}

Table A 3.2 *Parameter estimates and goodness-of-fit of the 2-parameter linear model for the dINR/dt versus dSI_{VII}/dt data. D_{ref} is the warfarin daily dose for a typical patient, k the slope, m the y-intercept, r^2 the adjusted coefficient of determination, RSE the relative standard error, and SI_{VII} the sensitivity index of INR to factor VII.*

D_{ref} (mg/day)	Final estimate (%RSE)		r^2
	k (%)	m (/day)	
1	153 (2.65)	0.000770 (36.9)	0.984
4	69.8 (1.55)	0.00195 (31.9)	0.994
7	44.7 (1.45)	0.00290 (33.8)	0.995
10	32.4 (1.36)	0.00376 (34.0)	0.996
13	25.2 (1.28)	0.00446 (34.4)	0.996

[a] Observations for $t = 0.5$, $t = 1.5$, $t = 2.5$, $t = 3.5$ and $t = 4.5$ days were excluded from model-fitting.

Table A 3.3 *Parameter estimates and goodness-of-fit of the 3-parameter quadratic model for the dINR/dt versus dSI_{VII}/dt data. D_{ref} is the warfarin daily dose for a typical patient, k, m, and w are coefficients of the quadratic model, $r^2$the adjusted coefficient of determination, RSE the relative standard error, and SI_{VII} the sensitivity index of INR to factor VII.*

D_{ref} (mg/day)	Final estimate (%RSE)			r^2
	k (%²×day)	m (%)	w (/day)	
1	-131000 (0.000000464)	176 (0.856)	0.000527 (41.9)	0.996
4	-9990 (3.17)	83.6 (0.890)	0.000563 (41.7)	1.00
7	-3070 (3.20)	55.1 (0.902)	0.0000830 (435)	1.00
10	-1370 (2.88)	40.9 (0.816)	-0.000695 (60.0)	1.00
13	-735 (4.89)	32.2 (1.39)	-0.00159 (53.2)	1.00

[a] Observations for $t = 0.5$ and $t = 1.5$ days were excluded from model-fitting.

Table A 3.4 *Parameter estimates and goodness-of-fit of the 2-parameter quadratic model for the dINR/dt versus dSI_{VII}/dt data. D_{ref} is the warfarin daily dose for a typical patient, k and m are coefficients of the quadratic model, r^2 the adjusted coefficient of determination, RSE the relative standard error, and SI_{VII} the sensitivity index of INR to factor VII.*

D_{ref} (mg/day)	Final estimate (%RSE)		r^2
	k (%²×day)	m (%)	
1	-141000 (8.00)	182 (2.43)	0.996
4	-10300 (2.95)	84.7 (0.767)	1.00
7	-3080 (2.71)	55.2 (0.685)	1.00
10	-1340 (2.59)	40.5 (0.641)	1.00
13	-698 (4.50)	31.6 (1.09)	0.999

[a] Observations for $t = 0.5$ and $t = 1.5$ days were excluded from model-fitting.

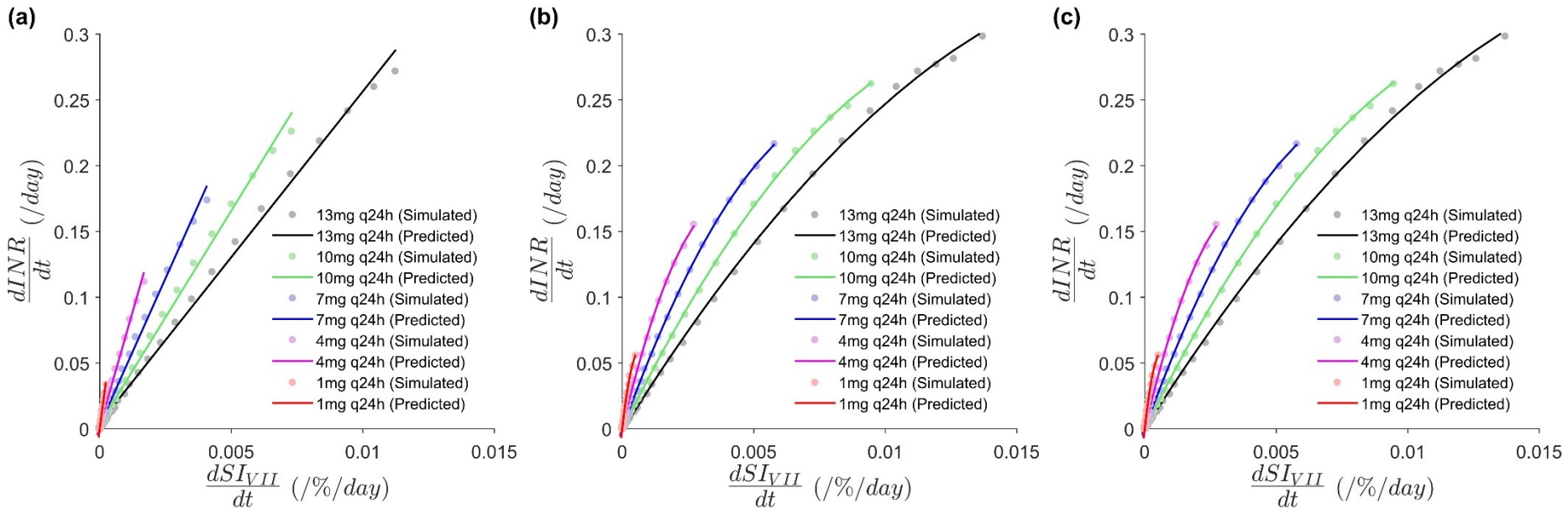

Figure A 3.2 *Model fits of (a) a 2-parameter linear model, (b) a 3-parameter quadratic model and (c) a 2-parameter quadratic model for the dINR/dt versus dSI_{VII}/dt data. The solid lines are the model predictions and the filled circles are the data that were derived based on simulations from the QSP coagulation network model [31]. SI_{VII} is the sensitivity index of INR to factor VII.*

A3.4. Symbolic solution for Equation 4.15

The symbolic solution to the definite integral, $\int_0^{t_{SS,INR}} \left(\frac{dSI_{VII}}{dt}\right)^2 dt$ in **Equation 4.15** where $\frac{dSI_{VII}}{dt} = \frac{h(D_{ref})}{1+e^{p\left(t-g\left(D_{ref}\right)\right)}}$ (**Equation 4.11**), is given below:

$$\int_0^{t_{SS,INR}} \left(\frac{dSI_{VII}}{dt}\right)^2 dt = \int_0^{t_{SS,INR}} \left(\frac{h(D_{ref})}{1+e^{p\left(t-g\left(D_{ref}\right)\right)}}\right)^2 dt$$

$$= \left[\frac{h(D_{ref})^2}{p}\left(p\left(t-g(D_{ref})\right) - \ln\left|1+e^{p\left(t-g\left(D_{ref}\right)\right)}\right| + \frac{1}{1+e^{p\left(t-g\left(D_{ref}\right)\right)}}\right)\right]_0^{t_{SS,INR}}.$$

Equation A 3.1 *Symbolic solution for the first definite integral in Equation 4.15.*

The symbolic solution to the definite integral, $\int_0^{t_{SS,INR}} \frac{dSI_{VII}}{dt} dt$ in **Equation 4.15** where $\frac{dSI_{VII}}{dt} = \frac{h(D_{ref})}{1+e^{p\left(t-g\left(D_{ref}\right)\right)}}$ (**Equation 4.11**), is given below:

$$\int_0^{t_{SS,INR}} \frac{dSI_{VII}}{dt} dt = \int_0^{t_{SS,INR}} \frac{h(D_{ref})}{1+e^{p\left(t-g\left(D_{ref}\right)\right)}} dt$$

$$= \left[\frac{h(D_{ref})}{p} \cdot \ln\left|1 - \frac{1}{1+e^{p\left(t-g\left(D_{ref}\right)\right)}}\right|\right]_0^{t_{SS,INR}}.$$

Equation A 3.2 *Symbolic solution for the second definite integral in Equation 4.15.*

Then, the full expression for INR_{SS} is given by substituting **Equation A 3.1** and **Equation A 3.2** into **Equation 4.15**:

$$INR_{SS} \approx INR_0$$
$$+k(D_{ref}) \cdot \left[\frac{h(D_{ref})^2}{p}\left(p\left(t - g(D_{ref})\right) - \ln\left|1 + e^{p\left(t-g(D_{ref})\right)}\right| + \frac{1}{1 + e^{p\left(t-g(D_{ref})\right)}}\right)\right]_0^{t_{SS,INR}}$$
$$+m(D_{ref}) \cdot \left[\frac{h(D_{ref})}{p} \cdot \ln\left|1 - \frac{1}{1 + e^{p\left(t-g(D_{ref})\right)}}\right|\right]_0^{t_{SS,INR}} \quad ; \quad t > 0$$
$$k(D_{ref}) = -e^{c_0 + c_1 \cdot \ln D_{ref}}$$
$$m(D_{ref}) = e^{s_0 + s_1 \cdot \ln D_{ref}}$$
$$h(D_{ref}) = a_0 + a_1 \cdot D_{ref}$$
$$g(D_{ref}) = b_0 + b_1 \cdot \ln D_{ref}.$$

Equation A 3.3 *Symbolic solution for Equation 4.15.*

A3.5. MATLAB® code for the implementation of the four-step algorithm for the prediction of $t_{SS,INR}$ and INR_{SS}

Main file to run (Warf_Algorithm_Main.m)

```
% Proposed algorithm for the prediction of t_SS and INR_SS

%%% No user inputs required

clear all
clc

%%% User inputs required

D=7; % Warfarin daily dose. Unit: mg/day
t1=3; % First sampling time. Unit: days
t2=4; % Second sampling time. Unit: days
INR_t1=1.72; % First INR sample. Unit: none
INR_t2=1.92; % Second INR sample. Unit: none
VII_t1=19.5; % First factor VII sample. Unit: %
VII_t2=17.2; % Second factor VII sample. Unit: %
INR_0=NaN; % Baseline INR. If not available, type 'NaN'. Unit: none.

%%% No user inputs required

Get_Parameters % Read parameter values
Calc_SI_DevSI % Step 1: Calculation of SI and DevSI
Calc_D_ref % Step 2: Prediction of D_ref based on DevSI
Calc_t_SS % Step 3: Prediction of t_SS based on D_ref
Calc_INR_SS % Step 4: Calculation of INR_SS based on D_ref and t_SS
```

Read parameter values (Get_Parameters.m)

```
% Read parameter values

q=0.23269; % Unit: none
p=0.30000; % Unit: none
a_0=0.00039173; % Unit: /%/day
a_1=0.0010791; % Unit: /%/mg
b_0=-1.4805; % Unit: days
b_1=4.1253; % Unit: days
Eps_SI=0.00015000; % Unit: none
c_0=11.942; % Unit: none
c_1=-2.0526; % Unit: none
s_0=5.2636; % Unit: none
s_1=-0.67191; % Unit: none

if isnan(INR_0)==1
INR_0=1; % Unit: none
end
```

Step 1: Calculation of SI_{VII} and $\frac{dSI_{VII}}{dt}$ (Calc_SI_DevSI.m)

```
% Step 1: Calculation of SI and DevSI

SI_t1=q*INR_t1/VII_t1; % Unit: /%
SI_t2=q*INR_t2/VII_t2; % Unit: /%

DevSI=(SI_t2-SI_t1)/(t2-t1) % Unit: /%/day
t_mid=(t1+t2)/2; % Unit: days
```

Step 2: Prediction of D_{ref} based on $\frac{dSI_{VII}}{dt}$ (Calc_D_ref.m)

```
% Step 2: Prediction of D_ref based on DevSI
% Note: An explicit, symbolic expression for D_ref cannot be obtained. D_ref is solved numerically

syms D_ref

h_syms=a_0+a_1*D_ref; % Unit: /%/day
g_syms=b_0+b_1*log(D_ref); % Unit: days

eqn=h_syms/(1+exp(p*(t_mid-g_syms)))==DevSI;
D_ref=double(solve(eqn,D_ref)) % Unit: mg/day
```

Step 3: Prediction of $t_{SS,INR}$ based on D_{ref} (Calc_t_SS.m)

```
% Step 3: Prediction of t_SS based on D_ref
% Note: Since DevSI is a continuous, monotonically declining function over t, then t_SS is the t when h/(1+exp(p*(t_SS-g)))=Eps_SI

h=a_0+a_1*D_ref; % Unit: /%/day
g=b_0+b_1*log(D_ref); % Unit: days

t_SS=1/p*log(h/Eps_SI-1)+g % Unit: days
```

Step 4: Calculation of INR_{SS} based on D_{ref} and $t_{SS,INR}$ (Calc_INR_SS.m)

```
% Step 4: Calculation of INR_SS based on D_ref and t_SS

k=-exp(c_0+c_1*log(D_ref)); % Unit: %*%*day
m=exp(s_0+s_1*log(D_ref)); % Unit: %

% Definite integral of the squared of DevSI
Integ_DevSI_SQR_2=h^2/p*(p*(t_SS-g)-log(1+exp(p*(t_SS-g)))+1/(1+exp(p*(t_SS-g)))); % Upper limit
Integ_DevSI_SQR_1=h^2/p*(p*(0-g)-log(1+exp(p*(0-g)))+1/(1+exp(p*(0-g)))); % Lower limit
Integ_DevSI_SQR=Integ_DevSI_SQR_2-Integ_DevSI_SQR_1; % Unit: /%/%/day

% Definite integral of DevSI
Integ_DevSI_2=h/p*log(1-(1/(1+exp(p*(t_SS-g))))); % Upper limit
Integ_DevSI_1=h/p*log(1-(1/(1+exp(p*(0-g))))); % Lower limit
Integ_DevSI=Integ_DevSI_2-Integ_DevSI_1; % Unit: /%

INR_SS=INR_0+k*Integ_DevSI_SQR+m*Integ_DevSI % Unit: none
```

A3.6. Patient data

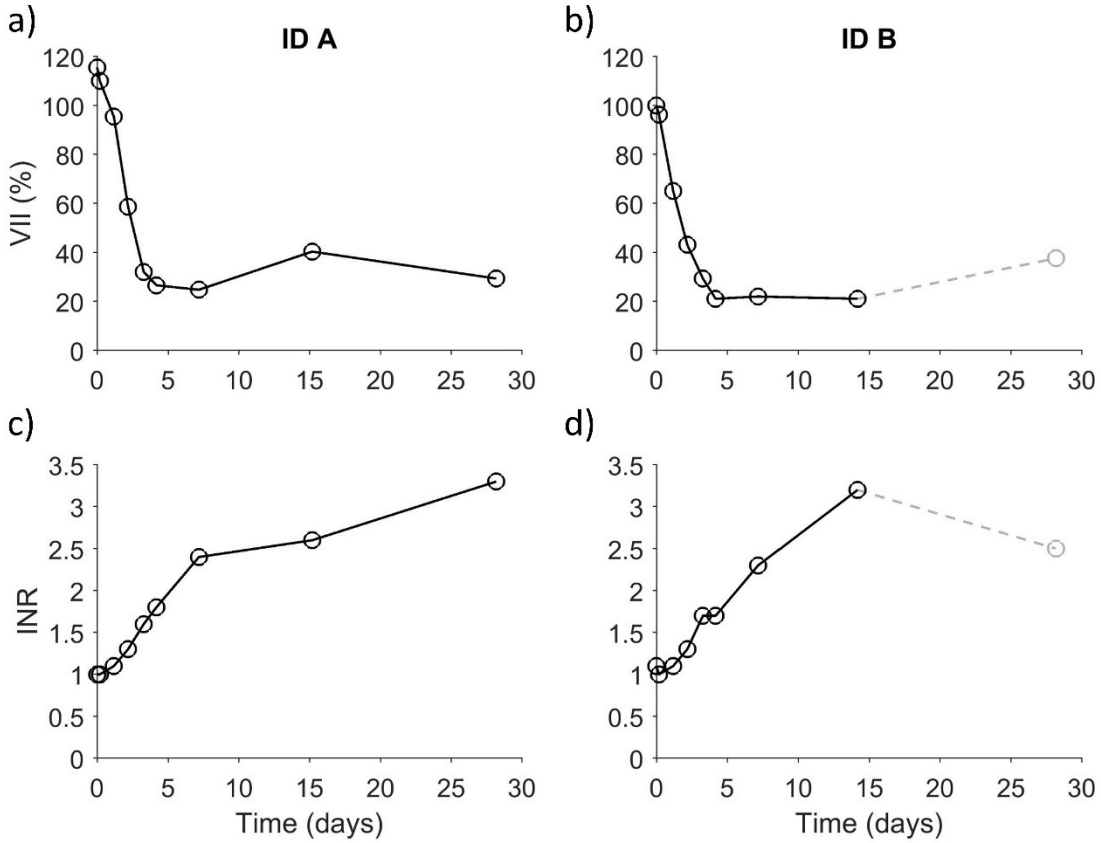

Figure A 3.3 *Factor VII and INR profiles of the two patients, ID A and ID B, used to illustrate proof-of-concept of the proposed method [167, 181]. Solid black lines indicate observations corresponding to a warfarin dosing rate of 5 mg/day. Dashed grey lines indicate observations attributable to a likely dose adjustment according to the study protocol [17] after observation of an INR of 3.2 at day 14.*

Appendix 4: Appendices to Chapter 5

A4.1. Evaluation of assumptions underpinning the joint model for warfarin and vitamin K-dependent coagulation proteins

A4.1.1. List of assumptions

Chapter 2 describes the development of a joint model to quantify the influence of warfarin on all six vitamin K-dependent coagulation proteins simultaneously. The model and its development are underpinned by the following assumptions:

- Assumption 1: A one-compartment model with first-order absorption and elimination is appropriate to describe the pharmacokinetics (PK) of warfarin,
- Assumption 2: The assumed value for the first-order absorption rate constant of warfarin, $k_a = 1.19\ h^{-1}$, is appropriate,
- Assumption 3: The assumed value for the volume of distribution of warfarin, $V = 8.06\ L$, is appropriate,
- Assumption 4: A hyperbolic model is appropriate to describe warfarin exposure and coagulation proteins response,
- Assumption 5: The assumed value for the maximum inhibitory effect of warfarin on coagulation proteins production, $I_{max,P} = 1.00$, is appropriate,
- Assumption 6: The imputed daily dose time of 6 p.m. is appropriate and as a whole unbiased,
- Assumption 7: The imputed blood sampling time of 1.30 p.m. (day 5) and 11 a.m. (all other days) are appropriate and as a whole unbiased,
- Assumption 8: All the patients enrolled were perfectly adherent,
- Assumption 9: The last observation carried forward (LOCF) method is appropriate for dose imputation,
- Assumption 10: For each coagulation protein, the errors, $\varepsilon\ (n \times 1)$, are normally distributed with a mean of zero and a variance of σ^2, and

- Assumption 11: For each coagulation protein, ε $(n \times 1)$, are independent and identically distributed (iid).

A4.1.2. Evaluation methods and results

Each of these assumptions was evaluated independently using the flowchart developed in **Chapter 5**. Here, an internal evaluation was conducted with the goal of assessing the influence of the aforementioned assumptions on the goodness-of-fit of the joint model. At this stage, where model development was of primary interest, an external evaluation was *not* carried out. It is important to note that only the reduced joint model, which is without the complex correlation structure for between-subject variability and random-unexplained variability, was evaluated.

The results of assumption evaluation are summarised in **Table A 4.1** using the assumption table structure proposed in **Chapter 5**. Evaluation methods and results for each assumption are provided in greater details in the next following subsections. Briefly, for the majority of the assumptions, the impact of violation (I) is significant but the probability of violation (P) is low. Other remaining assumptions have insignificant *I* and, as a result, the *P* was not evaluated. The risk of assumption violation was considered on the whole to be minor thereby giving a go decision for model building.

Table A 4.1 *Methods and results for internal evaluation of assumptions underpinning the warfarin-coagulation proteins model. I is the impact of assumption violation, NS means not significant, L means likely, P is the probability of assumption violation, S means significant, and U means unlikely.*

Assumption	Impact (*I*)			Probability (*P*)			Decision
	Methods	Results	Rating	Methods	Results	Rating	
1. A one-compartment model with first-order absorption and elimination is appropriate to describe the PK of warfarin	Past experience and logical reasoning.	It is possible that the joint model fit to pharmacodynamic data is robust to misspecification in the PK model but the parameter estimates may differ from its original meaning and therefore may be required to be interpreted differently.	S	Existing literature.	Available one-compartment models with first-order absorption and elimination describe warfarin PK data well [99, 103, 140, 156, 157, 165, 228-232].	U	Go for model building.
2. The assumed value for the first-order absorption rate constant of warfarin, $k_a = 1.19\ h^{-1}$, is appropriate	A sensitivity analysis was conducted. k_a fixed to 0.01, 0.1, 1, 10 and 50 h^{-1} were tried. The overall model fit (objective function value (OFV)) and the parameter estimates were compared to the original model.	The model fits appeared sensitive to the choice of k_a value. Smaller k_a value is associated with a better model fit. Lag time, t_{lag}, and first-order degradation rate constant, $k_{out,F}$, were also found sensitive to the choice of k_a value.	S	Existing literature.	The k_a value used resides well within the reported range of k_a (0.402 – 3.15 h^{-1}) [103, 140, 152, 233].		Go for model building.
3. The assumed value for the volume of distribution of warfarin, $V = 8.06\ L$, is appropriate	A structural identifiability analysis was conducted using popt_i® Version 1.0.	In the absence of PK data, V is not structurally identifiable. V is unable to influence parameter estimates and model fits.	NS	NA	NA	NA	Go for model building.

Assumption	Impact (*I*)			Probability (*P*)			Decision
	Methods	Results	Rating	Methods	Results	Rating	
4. A hyperbolic model is appropriate to describe warfarin exposure and coagulation proteins response	A sensitivity analysis was conducted. An empirical sigmoid E_{max} model was used. The overall model fit (OFV) and the parameter estimates were compared to the original model.	Based on the likelihood-ratio test, the sigmoid E_{max} model is associated with significantly better model fit compared to the original model ($\Delta OFV = -59.1$). Estimates of warfarin amount in the body that gives half the maximum effect, $IA_{50,F}$, also differ between the two models.	S	Existing literature	Warfarin inhibits vitamin K epoxide reductase (VKOR) thereby decreasing the formation of vitamin K hydroquinone, which is essential for the production of vitamin K-dependent coagulation proteins. Enzymatic binding of warfarin to VKOR can be described by a hyperbolic model [43].	U	Go for model building.
5. The assumed value for the maximum inhibitory effect of warfarin on coagulation proteins production, $I_{max,P} = 1.00$, is appropriate	A sensitivity analysis was conducted. $I_{max,P}$ fixed to 0.800, 0.850, and 0.900 was attempted. The overall model fit (OFV) and the parameter estimates were compared to the original model.	The model fits appeared sensitive to the choice of $I_{max,P}$ value, with higher $I_{max,P}$ value associated with a better model fit. Of all the parameter estimates, $IA_{50,P}$ is particularly sensitive to the $I_{max,P}$ value used.	S	Existing literature.	Almost complete inhibition of coagulation proteins synthesis by warfarin had been reported [35, 144-146, 167, 181, 234].	U	Go for model building.
6. The imputed daily dose time of 6 p.m. is appropriate and as a whole unbiased	A sensitivity analysis was conducted. Daily dose time of 8 a.m., 10 a.m., 12 p.m., 2 p.m., 4 p.m., 8 p.m., and 10 p.m. were attempted. The overall model fit (OFV) and the parameter estimates were compared to the original model.	The same model fits and parameter estimates were obtained regardless of the daily dose time used for imputation.	NS	NA	NA	NA	Go for model building.

Assumption	Impact (*I*)			Probability (*P*)			Decision
	Methods	Results	Rating	Methods	Results	Rating	
7. The imputed blood sampling time of 1.30 p.m. (day 5) and 11 a.m. (all other days) are appropriate and as a whole unbiased	A sensitivity analysis was conducted. Blood sampling time of 8 a.m., 10 a.m., 12 p.m., 2 p.m., and 4 p.m. were attempted. The overall model fit (OFV) and the parameter estimates were compared to the original model.	The same model fits and parameter estimates were obtained regardless of the blood sampling time used for imputation.	NS	NA	NA	NA	Go for model building.
8. All the patients enrolled were perfectly adherent	A published simulation study was referred. The study quantified the probability of therapeutic success 1000 patients. Imperfect adherence patterns including imperfect timing, random missed doses, and drug holiday were simulated. [235]	The probability of therapeutic success for perfect adherence was 0.58 and for imperfect adherence was 0.52. The relative forgiveness index of warfarin was 0.78, which indicates that warfarin is forgiving to imperfect adherence.	NS	NA	NA	NA	Go for model building.
9. The last observation carried forward (LOCF) method is appropriate for dose imputation	A sensitivity analysis was conducted. Observations following dose imputation were censored. The overall model fit (OFV adjusted for the number of observations) and the parameter estimates were compared to the original model.	Almost identical adjusted OFV were obtained: 5.95 (with LOCF) and 5.91 (without LOCF). Parameter estimates for the model developed without LOCF reside well within the 95% confidence interval of the final estimates of the original LOCF model.	NS	NA	NA	NA	Go for model building.

Assumption	Impact (*I*)			Probability (*P*)			Decision
	Methods	Results	Rating	Methods	Results	Rating	
10. For each coagulation protein, the errors, ε $(n \times 1)$, are normally distributed with a mean of zero and a variance of σ^2	Previous evaluation of impact of non-normality available in the literature [215].	Parameter estimation for maximum likelihood estimation is sensitive to specification of the residual error. Misspecification may result in biased parameter estimates and predictions.	S	The distribution of $CWRES$ was compared to a standard normal distribution by using a Q-Q plot and a one-sample Kolmogorov-Smirnov test.	CWRES of all coagulation proteins do not have a distribution that is significantly different from a standard normal distribution.	U	Go for model building.
11. For each coagulation protein, ε $(n \times 1)$, are independent and identically distributed (iid)	Existing literature	If autocorrelation is ignored, precision of parameter estimates [236, 237] and random-effect parameters [215] may be biased.	S	Autocorrelation was modelled using an exponential function in independent model for coagulation proteins. The resulting model fit (OFV and visual predictive checks (VPC)) were compared to the original model. Autocorrelation in the (joint) reduced model was visualised by plotting $CWRES$ time course for each patient.	For independent models, modelling autocorrelation gives significantly better model fits in terms of OFV ($\Delta OFV > 3.84, df = 1$). However, improvement in model fits is not apparent from the VPC. For the (joint) reduced model, $CWRES$ were found to be above or below zero in succession for consistent periods of time. $CWRES$ are autocorrelated.	L	No-go for model building.

A4.1.2.1. Assumption 1: A one-compartment model with first-order absorption and elimination is appropriate to describe the PK of warfarin

Interpretation

As above.

Internal evaluation of *I*

I = Significant. This was rated based on past experience and logical reasoning. There is a multitude of possibilities in the structural form that a PK model of a drug can take. However, it is difficult to judge with certainty the impact of a misspecification in the warfarin PK model on modelling the pharmacodynamic (PD) data using a kinetic-pharmacodynamic (KPD) model. From our experience, while it is possible that the KPD model fit to PD data is robust to misspecification in the PK model, parameter estimates may differ and may therefore require judicious interpretation. Here, when PK model is misspecified, PD parameter estimates may incorporate PK information that are otherwise not captured by the (misspecified) PK model. To minimise risk, *I* was conservatively rated as significant.

Internal evaluation of *P*

P = Unlikely. Based on published warfarin PK models, a one-compartment model with first-order absorption and elimination is typically adequate to describe the concentration-time data arising from clinically-relevant warfarin doses [99, 103, 140, 156, 157, 165, 228-232].

Decision

Decision = Go for model building. Even given the significant impact of violation of this assumption the probability of violation is low and hence the risk is considered to be negligible.

A4.1.2.2. Assumption 2: The assumed value $k_a = 1.19\ h^{-1}$ is appropriate

Interpretation

$k_a = 1.19\ h^{-1}$

Internal evaluation of *I*

$I =$ Significant. A sensitivity analysis was carried out to evaluate the impact of the choice of k_a value on parameter estimations and model fits. Here, k_a was fixed to arbitrarily chosen values of $0.0100\ h^{-1}$, $0.100\ h^{-1}$, $1.00\ h^{-1}$, $10.0\ h^{-1}$, and $50.0\ h^{-1}$. Estimation of k_a was also attempted. The overall model fit was assessed using the objective function value (OFV) and the parameter estimates were also compared. From **Table A 4.2**, the overall model fits appeared sensitive to the choice of k_a value, with smaller k_a value associated with a better model fit (lower OFV). Correspondingly, the final parameter estimates, particularly, the lag time, t_{lag}, and the first-order degradation rate constant of coagulation protein, $k_{out,F}$, were found sensitive to the changes in k_a value (not shown). It is worth noting that estimation of k_a, despite resulting in a good model fit, is not sensible. This is because k_a is not likely to be deterministically identifiable due to an absence of observations during the absorption phase of warfarin.

Table A 4.2 *Sensitivity of the overall model fits to the choice of k_a value. k_a is the first-order absorption rate constant of warfarin and OFV is the objective function value.*

$k_a\ (h^{-1})$	OFV
0.0100 (fixed)	5230.345
0.0385 (estimated)	5196.816
0.100 (fixed)	5213.868
0.500 (fixed)	5296.159
1.00 (fixed)	5297.467
1.19 (fixed)	5297.628
10.0 (fixed)	5298.110
50.0 (fixed)	5298.130

Internal evaluation of *P*

P = Unlikely. Previously reported values of k_a were 0.402 h^{-1} [103], 1.19 h^{-1} [152], 1.66 h^{-1} [233], and 3.15 h^{-1} [140]. The k_a = 1.19 h^{-1} value chosen resides well within the range of reported values. Also noteworthy, within the reported range of k_a, dependence of the final model fit on the choice of k_a was negligible (**Table A 4.2**).

Decision

Decision = Go for model building. Even given the significant impact of violation of this assumption the probability of violation is low and hence the risk is considered to be negligible.

A4.1.2.3. Assumption 3: The assumed value $V = 8.06\ L$ is appropriate

Interpretation

$V = 8.06\ L$

Internal evaluation of *I*

$I =$ Insignificant. A formal structural identifiability analysis was conducted using popt_i® Version 1.0 (Duffull SB, Dunedin, New Zealand). In the absence of PK data, V was found to be not structurally identifiable and therefore, by definition, is unable to influence parameter estimations and model fits.

Internal evaluation of *P*

NA.

Decision

Decision = Go for model building.

A4.1.2.4. Assumption 4: A hyperbolic model is appropriate to describe warfarin exposure and coagulation proteins response

Interpretation

As above.

Internal evaluation of *I*

I = Significant. A sensitivity analysis was conducted. An empirical sigmoid E_{max} (non-hyperbolic) model was attempted. Other commonly adopted PD models such as the linear model and the log-linear model were not tested because they are models nested within the hyperbolic model. The overall model fit was assessed using the OFV and the parameter estimates were also compared. On the basis of the likelihood-ratio test, the sigmoid E_{max} model is associated with significantly better model fit compared to the original model ($\Delta OFV = -59.1$). The final estimate for the shape parameters, γ_F, is as follows: $\gamma_{II} = 1.58$, $\gamma_{VII} = 2.20$, $\gamma_{IX} = 1.87$, $\gamma_X = 1.80$, $\gamma_{PC} = 1.02$, and $\gamma_{PS} = 1.45$. The final estimates for warfarin amount in the body that gives half the maximum inhibitory effect, $IA_{50,F}$, also differ between the sigmoid E_{max} model and the original model.

Internal evaluation of *P*

P = Unlikely. This was rated based on prior knowledge. Warfarin exerts its anticoagulant effect by inhibiting the enzyme vitamin K epoxide reductase (VKOR). VKOR is responsible to reduce vitamin K epoxide to vitamin K quinone and to reduce vitamin K quinone to its active vitamin K hydroquinone form. By inhibiting vitamin K hydroquinone formation, warfarin decreases the production of vitamin K-dependent coagulation proteins – factors II, VII, IX, X, proteins C and S. Here, the inhibitory action of warfarin is underpinned by enzymatic binding and interactions with VKOR. The use of a hyperbolic model to describe warfarin-coagulation proteins relationship is reasonable [43].

Decision

Decision = Go for model building. Even given the significant impact of violation of this assumption the probability of violation is low and hence the risk is considered to be negligible.

A4.1.2.5. Assumption 5: The assumed value $I_{max,P} = 1.00$ is appropriate

Interpretation

$I_{max,P} = 1.00$

Internal evaluation of *I*

I = Significant. A sensitivity analysis was carried out to evaluate the impact of the choice of $I_{max,P}$ value on parameter estimations and model fits. $I_{max,P}$ fixed to 0.800, 0.850, and 0.900 were attempted. Estimation of $I_{max,P}$ was also tried. The overall fit of the model was evaluated based on the OFV and the parameter estimates were compared. From **Table A 4.3**, the overall model fits appeared sensitive to the choice of $I_{max,P}$ value, with higher $I_{max,P}$ value associated with a better model fit (lower OFV). Correspondingly, the final parameter estimates particularly $IA_{50,P}$ were found sensitive to the changes in $I_{max,P}$ value (not shown).

Table A 4.3 *Sensitivity of the overall model fits to the choice of $I_{max,P}$ value. $I_{max,P}$ is the maximum inhibitory effect of warfarin and OFV is the objective function value.*

$I_{max,F}$	OFV
0.800 (fixed)	5437.406
0.850 (fixed)	5380.181
0.900 (fixed)	5340.714
1.00 (fixed)	5297.628
$I_{max,II} = 0.998$ (estimated) $I_{max,VII} = 0.998$ (estimated) $I_{max,IX} = 0.998$ (estimated) $I_{max,X} = 0.998$ (estimated) $I_{max,PC} = 0.868$ (estimated) $I_{max,PS} = 0.998$ (estimated)	5295.718

Internal evaluation of *P*

P = Unlikely. The extent of depression in the coagulation protein level is warfarin dose-dependent. Almost complete inhibition of coagulation proteins synthesis by warfarin had been observed and reported [35, 144-146, 167, 181, 234]. An $I_{max,P} = 1.00$ is probable.

Decision

Decision = Go for model building. Even given the significant impact of violation of this assumption the probability of violation is low and hence the risk is considered to be negligible.

A4.1.2.6. Assumption 6: The imputed daily dose time of 6 p.m. is appropriate and as a whole unbiased

Interpretation

As above.

Internal evaluation of *I*

I = Insignificant. A sensitivity analysis was carried out to evaluate the impact of departure from a daily dose time of 6 p.m. on parameter estimations and model fits. Daily dose time of 8 a.m., 10 a.m., 12 p.m., 2 p.m., 4 p.m., 8 p.m., and 10 p.m. were attempted. The overall fit of the model was evaluated based on the OFV and the parameter estimates were compared. Identical OFV (**Table A 4.4**) and final parameter estimates were obtained despite imputation of different daily dose times. Insensitivity of parameter estimations and model fitting process to the imputed daily dose time are attributable to the delayed time course of changes in coagulation proteins and sparse sampling (shortest sampling interval of 24 hours).

Table A 4.4 *Sensitivity of the overall model fits to the choice of daily dose time used for imputation. OFV is the objective function value.*

Daily dose time	OFV
8 a.m.	5297.628
10 a.m.	5297.628
12 p.m.	5297.628
2 p.m.	5297.628
4 p.m.	5297.628
6 p.m.	5297.628
8 p.m.	5297.628
10 p.m.	5297.628

Internal evaluation of *P*

NA.

Decision

Decision = Go for model building.

A4.1.2.7. Assumption 7: The imputed blood sampling time of 1.30 p.m. (day 5) and 11 a.m. (all other days) are appropriate and as a whole unbiased

Interpretation

As above.

Internal evaluation of *I*

I = Insignificant. A sensitivity analysis was carried out to evaluate the impact of departure from the above mentioned imputed blood sampling time on parameter estimations and model fits. Blood sampling time of 8 a.m., 10 a.m., 12 p.m., 2 p.m., and 4 p.m. were attempted. The overall fit of the model was evaluated based on the OFV and the parameter estimates were compared. Identical OFV (**Table A 4.5**) and final parameter estimates were obtained despite imputation of different blood sampling times. Insensitivity of parameter estimations and model fitting process to the imputed blood sampling time are attributable to the delayed time course of changes in coagulation proteins and sparse sampling (shortest sampling interval of 24 hours).

Table A 4.5 *Sensitivity of the overall model fits to the choice of blood sampling time used for imputation. OFV is the objective function value.*

Blood sampling time	OFV
8 a.m.	5297.628
10 a.m.	5297.628
11 a.m. (all days) 1.30 p.m. (day 5)	5297.628
12 p.m.	5297.628
2 p.m.	5297.628
4 p.m.	5297.628

Internal evaluation of *P*

NA.

Decision

Decision = Go for model building.

A4.1.2.8. Assumption 8: All the patients enrolled were perfectly adherent

Interpretation

All the patients enrolled took warfarin at the right time, had no random missed doses, and had no drug holidays.

Internal evaluation of *I*

I = Insignificant. This was rated based on the results of a published study [235]. In this work, adherence profile for 1000 patients were simulated. Imperfect adherence patterns including imperfect timing, random missed doses, and drug holiday were considered. The corresponding INR time course for these patients were simulated from a published model for warfarin and INR [54]. Here, therapeutic success was defined as where at least 55% of steady-state INR values are within the therapeutic range (INR 2 to 3.5). The simulation results showed that the probability of therapeutic success for perfect adherence was 0.58 and for imperfect adherence was 0.52. The relative forgiveness index of warfarin to imperfect adherence was 0.78. This indicates that warfarin is relatively forgiving to commonly-observed patterns of imperfect adherence. Here, the forgiving nature of warfarin suggests that imperfect adherence is likely to have minimal impact on the INR and as such it should have similarly minimal impact on parameter estimations and model fits of INR data.

Internal evaluation of *P*

NA.

Decision

Decision = Go for model building.

A4.1.2.9. Assumption 9: The LOCF method is appropriate for dose imputation

Interpretation

The dosing records for most individuals were missing after day 15. It is assumed that there is no change in warfarin dose from the last available dosing record.

Internal evaluation of *I*

I = Insignificant. A sensitivity analysis was carried out to evaluate the impact of dose imputation using LOCF method on parameter estimations and model fits. Here, observations (10.1%) following dose imputation were censored and the resulting model was compared to the original model with dose imputation using the LOCF method. The model fit was evaluated based on the OFV adjusted for the number of observations. The parameter estimates were also compared. With respect to model fit, almost identical adjusted OFV was resulted: 5.93 (with LOCF) and 5.91 (without LOCF). Differences in some final parameter estimates were observed (see **Table A 4.6**). However, this is unlikely of major importance because the final parameter estimates of the model developed without LOCF reside well within the 95% confidence interval of the final estimates of the original model (see **Table A 4.6**).

Internal evaluation of *P*

NA.

Decision

Decision = Go for model building.

Table A 4.6 *Sensitivity of the final parameter estimates to imputation using the LOCF method. LOCF refers to the last observation carried forward method.*

Parameter	With LOCF: Final estimate (95% CI)	Without LOCF: Final estimate	% Change in final estimates
CL (L/h)	0.211 [0.136, 0.323]	0.170	-19.4
$IA_{50,II}$ (mg)	1.83 [1.34, 2.41]	2.22	21.3
$IA_{50,VII}$ (mg)	1.86 [1.38, 2.43]	1.84	-1.08
$IA_{50,IX}$ (mg)	2.41 [1.79, 3.14]	2.57	6.64
$IA_{50,X}$ (mg)	0.875 [0.631, 1.160]	1.10	25.7
$IA_{50,PC}$ (mg)	5.21 [3.93, 6.59]	5.90	13.2
$IA_{50,PS}$ (mg)	3.35 [2.46, 4.39]	3.96	18.2
$II_{t=0}$ (IU/dL)	115 [104, 125]	114	-0.870
$VII_{t=0}$ (IU/dL)	115 [98, 134]	113	-1.74
$IX_{t=0}$ (IU/dL)	141 [128, 155]	141	0.000
$X_{t=0}$ (IU/dL)	109 [99, 118]	108	-0.917
$PC_{t=0}$ (IU/dL)	101 [92, 111]	102	0.990
$PS_{t=0}$ (IU/dL)	105 [92, 118]	104	-0.952
$k_{out,II}$ (h^{-1})	0.0135 [0.0108, 0.0171]	0.0141	4.44
$k_{out,VII}$ (h^{-1})	0.0570 [0.0358, 0.0946]	0.0534	-6.32
$k_{out,IX}$ (h^{-1})	0.0323 [0.0208, 0.0523]	0.0325	0.619
$k_{out,X}$ (h^{-1})	0.0157 [0.0129, 0.0192]	0.0163	3.82
$k_{out,PC}$ (h^{-1})	0.0376 [0.0234, 0.0663]	0.0425	13.0
$k_{out,PS}$ (h^{-1})	0.0122 [0.0103, 0.0146]	0.0125	2.46
LAG (h)	12.5 [10.4, 14.2]	12.7	1.60
CV CL (%)	82.2 [55.9, 145.5]	92.5	12.5
CV $IA_{50,PC}$ (%)	13.4 (0, 29.2]	18.9	41.0
ω $II_{t=0}$ (IU/dL)	17.8 [10.6, 25.2]	17.6	-1.12
ω $VII_{t=0}$ (IU/dL)	26.9 [17.7, 42.3]	22.0	-18.2
ω $IX_{t=0}$ (IU/dL)	25.0 [16.2, 39.1]	24.1	-3.60
ω $X_{t=0}$ (IU/dL)	17.5 [12.4, 26.0]	17.3	-1.14
ω $PC_{t=0}$ (IU/dL)	17.4 [12.2, 25.8]	17.3	-0.575
ω $PS_{t=0}$ (IU/dL)	24.4 [17.8, 35.8]	23.7	-2.87
CV $k_{out,II}$ (%)	41.4 [27.3, 66.7]	45.2	9.18
CV $k_{out,VII}$ (%)	92.6 [54.4, 192.1]	121	30.7
CV $k_{out,IX}$ (%)	89.6 [53.6, 182.0]	97.5	8.82
CV $k_{out,X}$ (%)	36.3 [24.6, 56.8]	38.8	6.89
CV $k_{out,PC}$ (%)	91.2 [53.9, 194.4]	110	20.6
CV $k_{out,PS}$ (%)	19.0 (0, 38.7]	31.0	63.2
$\sigma_{add}II$ (IU/dL)	7.11 [5.62, 8.56]	5.55	-21.9
$CV_{prop}II$ (%)	3.69 (0, 7.56]	5.48	48.5
$\sigma_{add}VII$ (IU/dL)	8.80 [5.34, 12.75]	8.06	-8.41
$CV_{prop}VII$ (%)	15.3 (0, 24.5]	14.6	-4.58
$\sigma_{add}IX$ (IU/dL)	11.0 [7.1, 14.0]	9.21	-16.3
$CV_{prop}IX$ (%)	10.9 [1.5, 17.3]	12.7	16.5
$\sigma_{add}X$ (IU/dL)	5.41 [4.35, 6.64]	5.23	-3.33
$CV_{prop}X$ (%)	5.96 [1.72, 8.93]	6.33	6.21
$\sigma_{add}PC$ (IU/dL)	3.89 (0, 6.69]	1.20	-69.1
$CV_{prop}PC$ (%)	8.58 [2.99, 12.27]	8.96	4.43
$\sigma_{add}PS$ (IU/dL)	3.33 (0, 5.97]	3.01	-9.61
$CV_{prop}PS$ (%)	10.6 [7.5, 13.5]	10.0	-5.66

LAG lag. CI confidence interval. CV coefficient of variation. CL clearance of warfarin. $IA_{50,F}$ warfarin amount in the body that gives half the maximum inhibitory effect. $k_{out,F}$ first-order coagulation protein degradation rate constant. ω standard deviation of between subject variability in parameter. σ_{add} standard deviation for the additive error associated with model prediction. $F_{t=0}$ coagulation protein concentration at baseline.

A4.1.2.10. Assumption 10: For each coagulation protein, ε $(n \times 1)$ are normally distributed with a mean of zero and a variance of σ^2

Interpretation

$$\varepsilon \sim N(0, \sigma^2)$$

Equation A 4.1 *Normality assumption of error terms.*

Implicit to this assumption, (1) error terms have mean zero, (2) error terms have common variance σ^2 for all individuals and covariate values; and (3) error terms are normally distributed. Note that item (2) relates to the iid assumption and therefore will be addressed in **section A4.1.2.11**.

$$CWRES \sim N(0,1)$$

Equation A 4.2 *Normality assumption of conditional weighted residuals (CWRES).*

For each coagulation protein modelled, $CWRES$ $(n \times 1)$ is the conditional weighted residuals associated with the first-order conditional estimation method implemented by NONMEM® Version 7.2 (ICON Development Solutions, Ellicott City, MD, USA). Here, note that $CWRES$ represents a composite measure of additive and proportional error terms.

Internal evaluation of *I*

$I =$ Significant. Parameter estimations in NONMEM® is reported to be sensitive to a misspecification in the residual error model. In particular, the estimation of random-effect parameters may be biased [215].

Internal evaluation of *P*

$P =$ Unlikely. The distribution of $CWRES$ was visualised by using the histogram and the quantile-quantile (Q-Q) plot. In addition, $CWRES$ was compared to a standard normal distribution by using a one-sample Kolmogorov-Smirnov goodness-of-fit test. The histogram of $CWRES$ for different coagulation proteins is approximately bell-shaped with the greatest $CWRES$ density observed at a

value of zero and all the $CWRES$ are contained within boundaries of -4 and +4. The distribution of $CWRES$ for factors VII, IX, and X is however slightly positively skewed. See **Figure A 4.1**. From the Q-Q plot, the large majority of the $CWRES$ quantiles fall on the reference line that corresponds to a standard normal distribution. Deviation of a small number of $CWRES$ quantiles from the reference line was observed at high standard normal quantiles for factor IX and X. See **Figure A 4.1**. Finally, based on the Kolmogorov-Smirnov test, $CWRES$ for factors II ($T = 0.0315, p = 0.998$), IX ($T = 0.0895, p = 0.173$), X ($T = 0.0767, p = 0.328$), proteins C ($T = 0.0588, p = 0.660$), and S ($T = 0.0432, p = 0.933$) do not have a distribution that is significantly different from a standard normal distribution. An exception was the $CWRES$ for factor VII ($T = 0.111, p = 0.0458$). Based on these results, the $CWRES$ as a whole are considered to have a standard normal distribution.

Decision

Decision = Go for model building. Even given the significant impact of violation of this assumption the probability of violation is low and hence the risk is considered to be negligible.

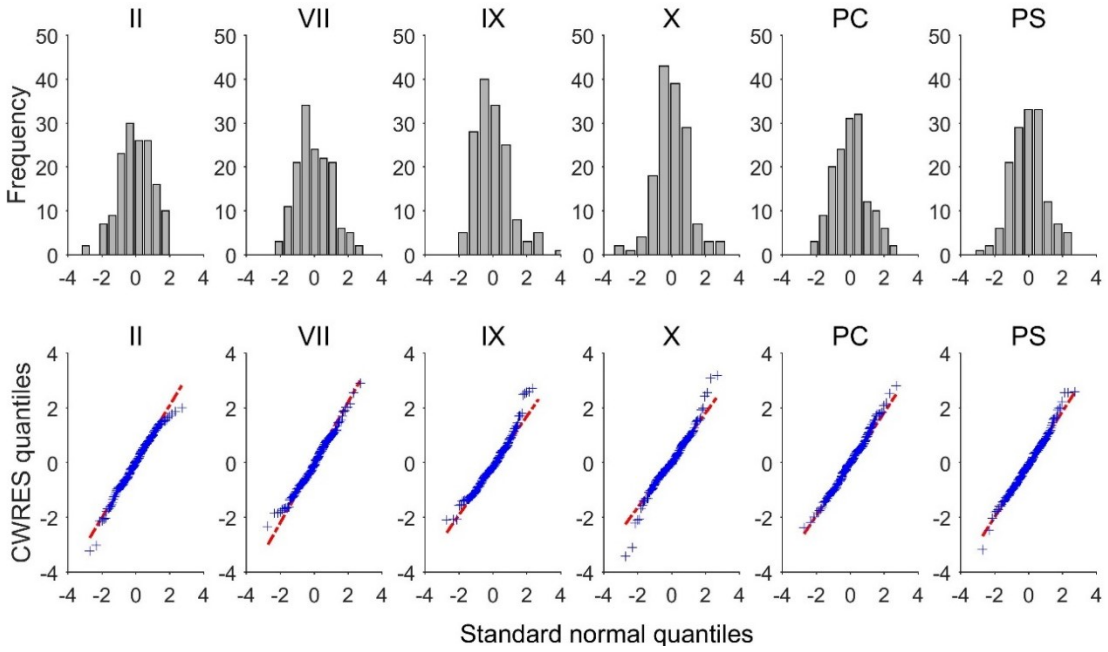

Figure A 4.1 *Histogram and Q-Q plot for the CWRES of the joint model. CWRES is the conditional weighted residuals, PC is protein C, PS is protein S, and Q-Q plot refers to quantile-quantile plot.*

A4.1.2.11. Assumption 11: For the each coagulation protein, ε $(n \times 1)$ are iid

Interpretation

In modelling repeated measure data, assumption of independence of error terms is most typically conditioned on an absence of autocorrelation (serial correlation over time) in error terms. Here, it is assumed that error terms are not correlated regardless of the temporal proximity of the observations.

Internal evaluation of *I*

I = Significant. Based on published literature, if correlation in error terms is ignored, the precision of parameter estimates can be overestimated [236, 237] and the random-effect parameter estimates (e.g. between subject variability) may be upwardly biased [215]. A violation in this assumption may potentially mislead statistical inference.

Internal evaluation of *P*

P = Likely. In the first instance, autocorrelation in error terms was considered in independent model for factors II, VII, IX, X, proteins C, and S, respectively. The autocorrelation was modelled using an exponential function:

$$\rho = e^{-k_{corr} \times \tau}.$$

Equation A 4.3 *Exponential function to describe the autocorrelation in error terms.*

ρ is the correlation between two error terms, τ is the distance between time points, and k_{corr} is the rate constant for correlation decay. It is important to note that ρ is inversely related to τ. When $\tau = 0$, $\rho = 1$ and as τ approaches infinity, asymptotically, $\rho = 0$. The resulting model fit, which was assessed based on the OFV and prediction-corrected visual predictive check (pcVPC), was compared to the original model. Modelling autocorrelation in error terms results in a better model fit ($\Delta OFV > 3.84, df = 1$) for all independent models except for protein S. ρ for the most commonly observed time distance in the dataset, $\tau = 24\ h$, was calculated based on the estimated k_{corr}. Here, the positive autocorrelation in error terms appears to be substantial in magnitude ($\rho_{\tau=24} > 0.600$) (see **Table A**

4.7). However, the pcVPC for models with autocorrelation does not seem to be superior over that of the original model without autocorrelation (see **Figure A 4.2**).

Table A 4.7 *Modelling autocorrelation in error terms in independent model of coagulation proteins. k_{corr} is the correlation decay rate constant, OFV is the objective function value, ε_{add} is additive error, ε_{prop} is proportional error, and ρ is the correlation between two error terms.*

Independent model	Autocorrelation based on	ΔOFV	k_{corr} (h^{-1})	$t_{\frac{1}{2},corr}$ (h)	$\rho_{\tau=24}$
II	ε_{add}	-12.3	0.0186	37.3	0.640
VII	ε_{prop}	-57.8	0.00670	103	0.851
	ε_{add}	-53.0	0.00287	241	0.933
IX	ε_{prop}	-33.2	0.0112	61.9	0.764
	ε_{add}	-32.1	0.00515	135	0.884
X	ε_{add}	-8.61	0.0206	33.6	0.610
PC	ε_{prop}	-34.4	0.0110	63.0	0.768
	ε_{add}	-27.1	0.00583	119	0.870
PS	ε_{prop}	-0.320	0.0754	9.19	0.164
	ε_{add}	-5.14	0.000734	944	0.983

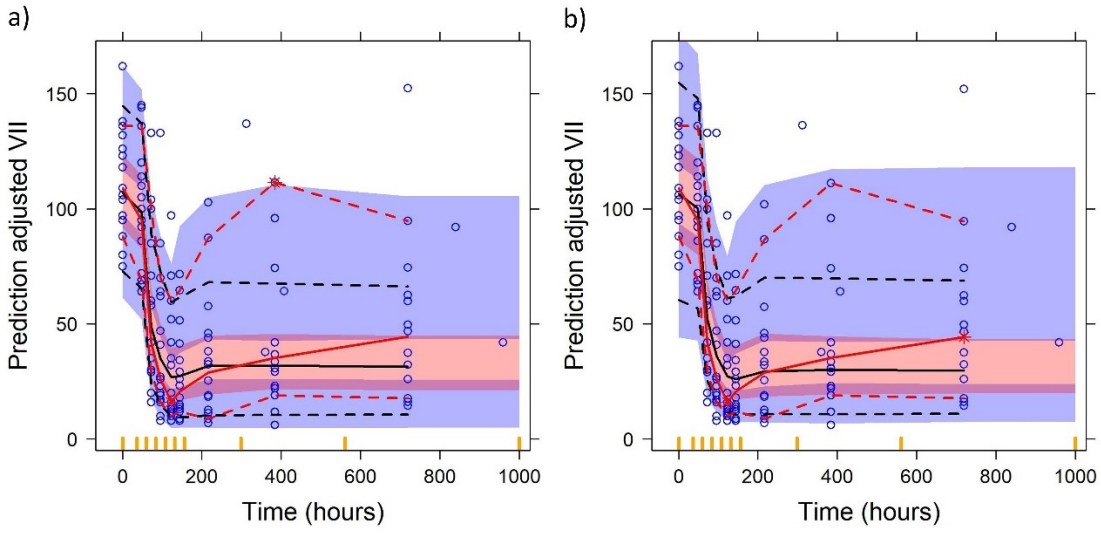

Figure A 4.2 *Prediction-corrected visual predictive check for independent model of factor VII without (a) and with (b) autocorrelation in error terms accounted for. The blue circle indicates observation. The black line indicates the 10th, 50th (median), or 90th percentile of simulated data. The red line indicates the 10th, 50th (median), or 90th percentile of observed data. The shaded area indicates the 95% confidence interval around the simulated percentiles.*

Autocorrelation in error terms was also considered in the (joint) reduced model that quantifies warfarin influence on all six coagulation proteins simultaneously. However, the estimation process was unable to be initiated successfully when autocorrelation in error terms was considered for the reduced model. It was observed earlier that the estimation run time increase drastically with inclusion of each additional coagulation protein even if the autocorrelation structure is only included for one single coagulation protein. For the purpose of evaluating this assumption, a qualitative approach was used. $CWRES$ time course for the (joint) reduced model was plotted. For the majority of patients, $CWRES$ were found to be above or below zero in succession for consistent periods of time. This is suggestive of the presence of autocorrelation in $CWRES$ (see **Figure A 4.3**). Taken together, these findings suggest that the possibility of autocorrelation in error terms cannot be excluded. Hence, P was rated as likely.

Decision

Decision = No-go for model building.

Note

Despite the no-go decision, the autocorrelation was not accounted for in the final (joint) model. Despite a reduction in OFV, improvement in model fit is not evident in graphical diagnostics. More importantly, with numerical difficulties for parameter estimations that result in unacceptably long run time, it is not practically possible at this stage to obtain a final model that accounts for autocorrelation. It is important that this limitation should be made explicit and be appropriately addressed.

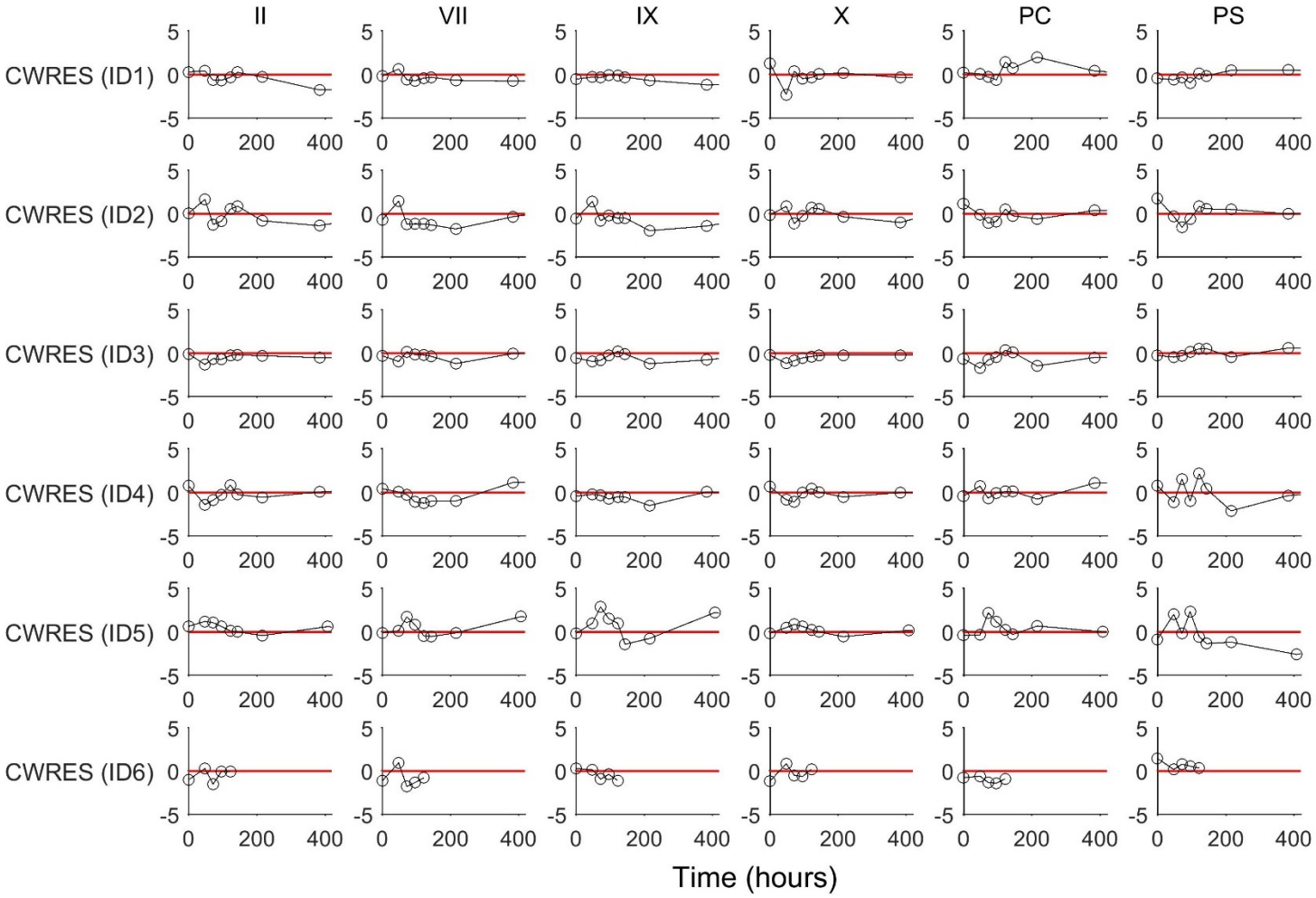

Figure A 4.3 *Conditional weighted residuals versus time plot for the (joint) reduced model. CWRES is conditional weighted residual, PC is protein C, and PS is protein S.*

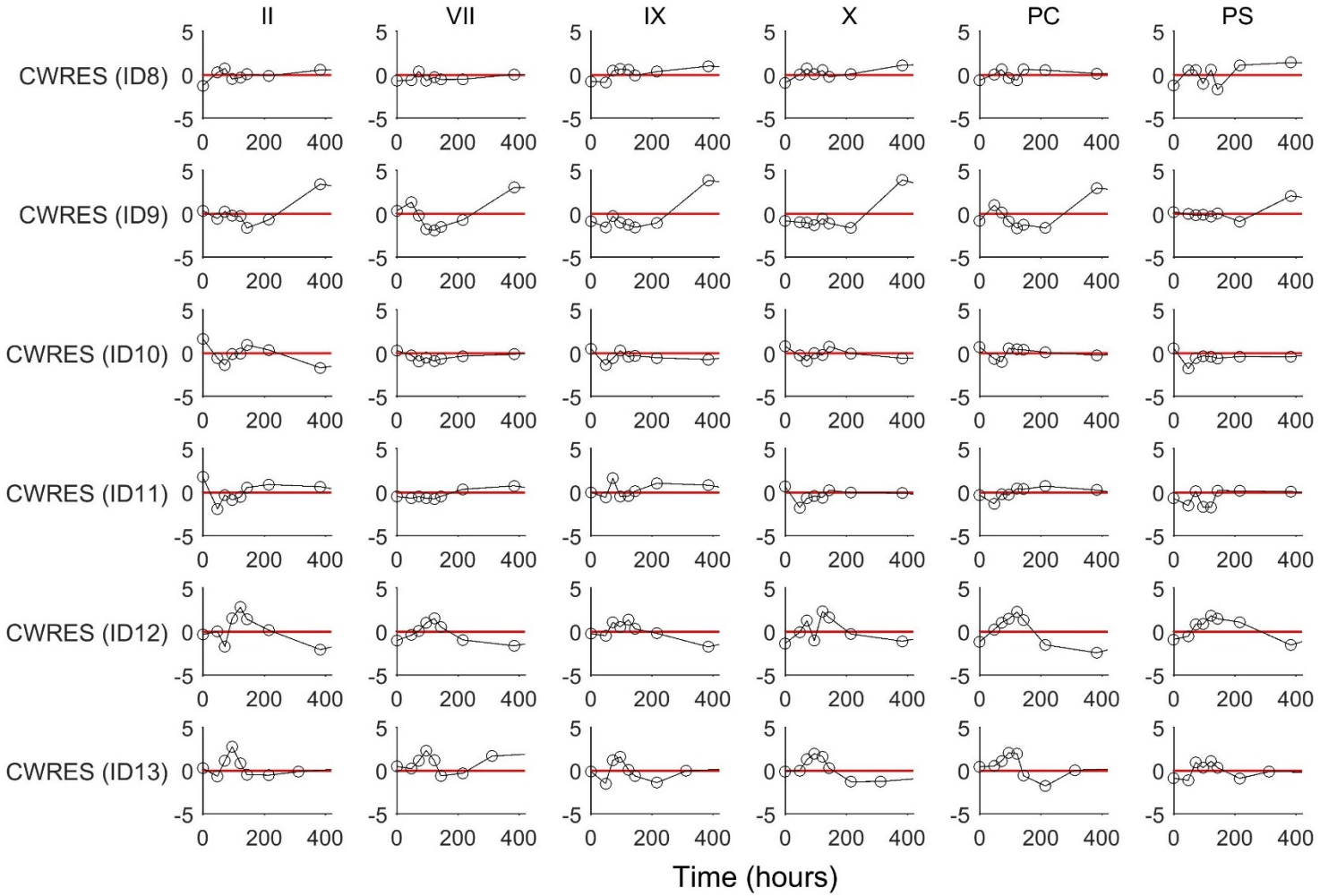

Figure A 4.3 *Continued.*

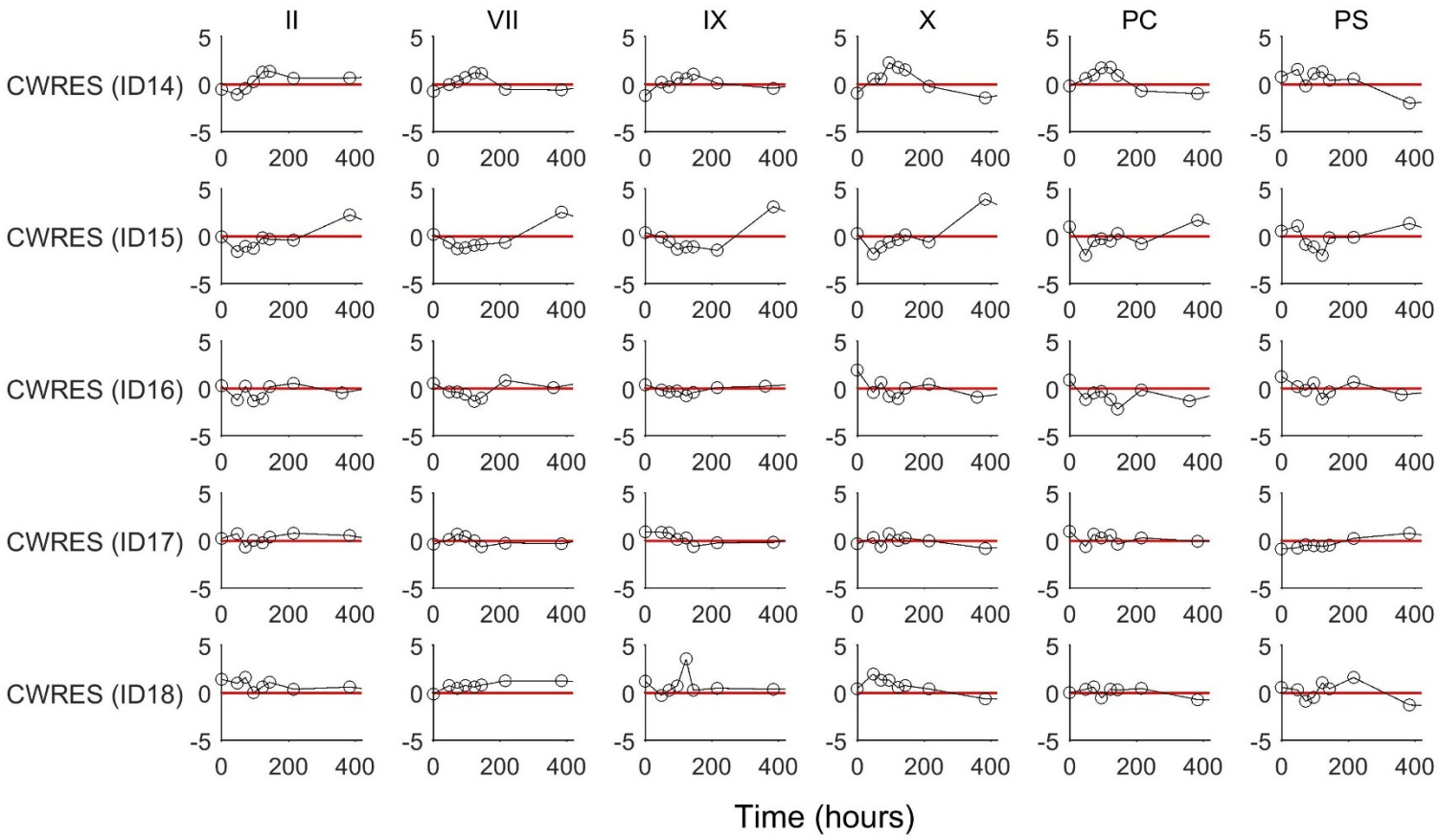

Figure A 4.3 *Continued.*

A4.2. Evaluation of assumptions underpinning the factor VII-based method for the prediction of the anticoagulant response to warfarin

A4.2.1. List of assumptions

Chapter 4 describes the development of a factor VII-based sensitivity index of the international normalised ratio (INR), SI_{VII}, to predict the anticoagulant response to warfarin. The conceptual basis of SI_{VII} to functionally approximate the INR and subsequently to provide a theoretical definition of the steady-state INR is built on the following key assumptions:

- Assumption 1: Simultaneous reduction in factors II, VII, and X leads to less than additive increases in the INR,
- Assumption 2: The most deficient coagulation protein drives the INR,
- Assumption 3: Under non-steady-state INR conditions, factor VII is always the most deficient,
- Assumption 4: Non-steady-state INR is the most sensitive to factor VII,
- Assumption 5: The quantitative systems pharmacology (QSP) coagulation network model [31] is adequate in describing the warfarin-coagulation proteins-INR relationship, and
- Assumption 6: The simulated coagulation proteins-INR time course is representative of that of typical patients initiated with warfarin.

A4.2.2. Evaluation methods and results

Each of these assumptions was evaluated independently using the flowchart developed in **Chapter 5**. Here, an internal evaluation was conducted with the goal of assessing the influence of the aforementioned assumptions on the ability of SI_{VII} to approximate the INR. At this stage where model development is of primary interest, an external evaluation was not carried out.

The results of assumption evaluation are summarised in **Table A 4.8** using the assumption table structure proposed in **Chapter 5**. Evaluation methods and results for each assumption are provided in greater details in the next following subsections. To summarise, for all the assumptions, although given the high I,

the P is low and hence the risk of assumption violation is considered on the whole to be minor. The use of these assumptions does not invalidate the use of SI_{VII} for determining steady-state INR (INR_{SS}) after warfarin dosing.

Table A 4.8 *Methods and results for internal evaluation of assumptions underpinning the factor VII-based method for INR prediction. I is the impact of assumption violation, P is the probability of assumption violation, S means significant, and U means unlikely.*

Assumption	Impact (*I*)			Probability (*P*)			Decision
	Methods	Results	Rating	Methods	Results	Rating	
1. Simultaneous reduction in factors II, VII, and X leads to less than additive increases in the international normalised ratio (INR)	Logical reasoning.	If the effects of II, VII, and X on the INR are additive or supra-additive, monitoring VII alone to inform the INR is unlikely to be adequate.	S	Isobologram analysis based on simulation of II, VII, X, and INR from the coagulation network model [31] was conducted.	All simulated points fall above the additivity line on the isobolograms thereby indicating sub-additive interactions between II, VII, and X on the INR.	U	Go for model building.
2. The most deficient coagulation protein drives the INR	Logical reasoning.	If II, VII, and X all drive the INR considerably, monitoring VII alone to inform the INR is unlikely to be adequate.	S	Isobologram analysis based on simulation of II, VII, X, and INR from the coagulation network model [31] was conducted.	At INR = 2.5 and INR = 4.5, vertical and horizontal segments were observed on the isobolograms. If either one of II, VII, and X is sufficiently deficient, the same INR will be resulted regardless of the concentration of other factors.	U	Go for model building.

Assumption	Impact (*I*)			Probability (*P*)			Decision
	Methods	Results	Rating	Methods	Results	Rating	
3. Under non-steady-state INR conditions, factor VII is always the most deficient	A sensitivity analysis was conducted. The coagulation network model [31] with a prolonged VII's degradation half-life, $t_{\frac{1}{2},VII}$ $(i.e. t_{\frac{1}{2},VII} > t_{\frac{1}{2},X})$ was used for simulation. Then, sensitivity index of INR, SI_{II}, SI_{VII}, and SI_X, were derived from the simulated data and compared to the INR.	When X replaced VII as the most deficient coagulation protein, SI_{VII} fails to approximate the INR. Instead, SI_X provides the best approximation to the INR.	S	$t_{\frac{1}{2},II}$, $t_{\frac{1}{2},VII}$, and $t_{\frac{1}{2},X}$ were simulated from the published warfarin-coagulation proteins model [181]. The rank order of $t_{\frac{1}{2},II}$, $t_{\frac{1}{2},VII}$, and $t_{\frac{1}{2},X}$ was tested using the Wilcoxon-signed rank test at an overall $\alpha = 0.05$.	$t_{\frac{1}{2},VII}$ was found to be significantly lower than both $t_{\frac{1}{2},II}$ $(Z = -27.4, p < 0.001)$ and $t_{\frac{1}{2},X}$ $(Z = -27.4, p < 0.001)$. At non-steady-state INR, VII is likely to be the most deficient.	U	Go for model building.
4. Non-steady-state INR is the most sensitive to factor VII	A sensitivity analysis was conducted. The coagulation network model [31] with a prolonged $t_{\frac{1}{2},VII}$ $(i.e. t_{\frac{1}{2},VII} > t_{\frac{1}{2},X})$ was used for simulation. Then, SI_{II}, SI_{VII}, and SI_X were derived from the simulated data and compared to the INR.	When non-steady-state INR is more sensitive to X than to VII (i.e. $SI_X > SI_{VII}$), INR is better approximated by SI_X than SI_{VII}.	S	II, VII, X, and INR were simulated from the coagulation network model [31] using typical parameters. Subsequently, SI_{II}, SI_{VII}, and SI_X were derived from the simulated data. Their magnitudes were compared.	It was observed that SI_{VII} is larger in magnitude compared to SI_{II} and SI_X at all time points during the non-steady-state INR. The non-steady-state INR is the most sensitive to VII.	U	Go for model building.
5. The coagulation network model is adequate in describing the warfarin-coagulation proteins-INR relationship	Logical reasoning.	It is self-evident that if the coagulation network model is unable to describe the warfarin-coagulation proteins-INR relationship, the SI_{VII} derived is unlikely to be fit for purpose.	S	II, VII, X, and INR were simulated from the coagulation network model [31] using typical parameters. The simulated data were compared to external data ($n = 17$) [167, 181].	The simulated data agree well with the observed data for II, VII, X, and INR at the individual level.	U	Go for model building.

Assumption	Impact (*I*)			Probability (*P*)			Decision
	Methods	Results	Rating	Methods	Results	Rating	
6. The simulated coagulation proteins-INR time course is representative of that of typical patients initiated with warfarin	Logical reasoning.	It is self-evident that generalisability will be limited if the simulation results are unrepresentative.	S	II, VII, X, and INR were simulated from the coagulation network model [31] using typical parameters. The simulated data were compared to external data ($n = 17$) [167, 181].	The simulated data agree well with the observed data for II, VII, X, and INR at the individual level.	U	Go for model building.

A4.2.2.1. Assumption 1: Simultaneous reduction in factors II, VII, and X leads to less than additive increases in the INR

Interpretation

$$\Delta INR_{\downarrow i \cap \downarrow j} < \left(\Delta INR_{\downarrow i} + \Delta INR_{\downarrow j}\right); \quad i, j \in \{II, VII, X\}, i \neq j$$

Equation A 4.4 *The mathematical representation of sub-additive interactions between coagulation proteins with respect to the INR.*

Here, $\Delta INR_{\downarrow i \cap \downarrow j}$ is the INR response to a simultaneous reduction in two different coagulation proteins. $\Delta INR_{\downarrow i}$ and $\Delta INR_{\downarrow j}$ represent the INR response to a reduction in a single coagulation protein.

Internal evaluation of *I*

I = Significant. This was rated based on logical reasoning. If the effects of factors II, VII, and X on the INR are additive or supra-additive, contribution of factors II and X to the INR will be significant then monitoring of factor VII alone to inform the INR is unlikely to be adequate.

Internal evaluation of *P*

P = Unlikely. Isobolograms of pairwise combinations of factors II, VII, and X with respect to the INR were constructed via simulation from the QSP coagulation network model [31]. All points on the same isobologram correspond to the same INR (e.g. INR=2.5). Points that fall below the additivity line indicate supra-additivity interactions whereas points that are located above the additivity line correspond to sub-additive interactions. The isobologram analysis indicates that simultaneous reduction in two coagulation proteins leads to less than additive increase in the INR (See **Figure A 4.4**).

Decision

Decision = Go for model building. Even given the significant impact of violation of this assumption the probability of violation is low and hence the risk is considered to be negligible.

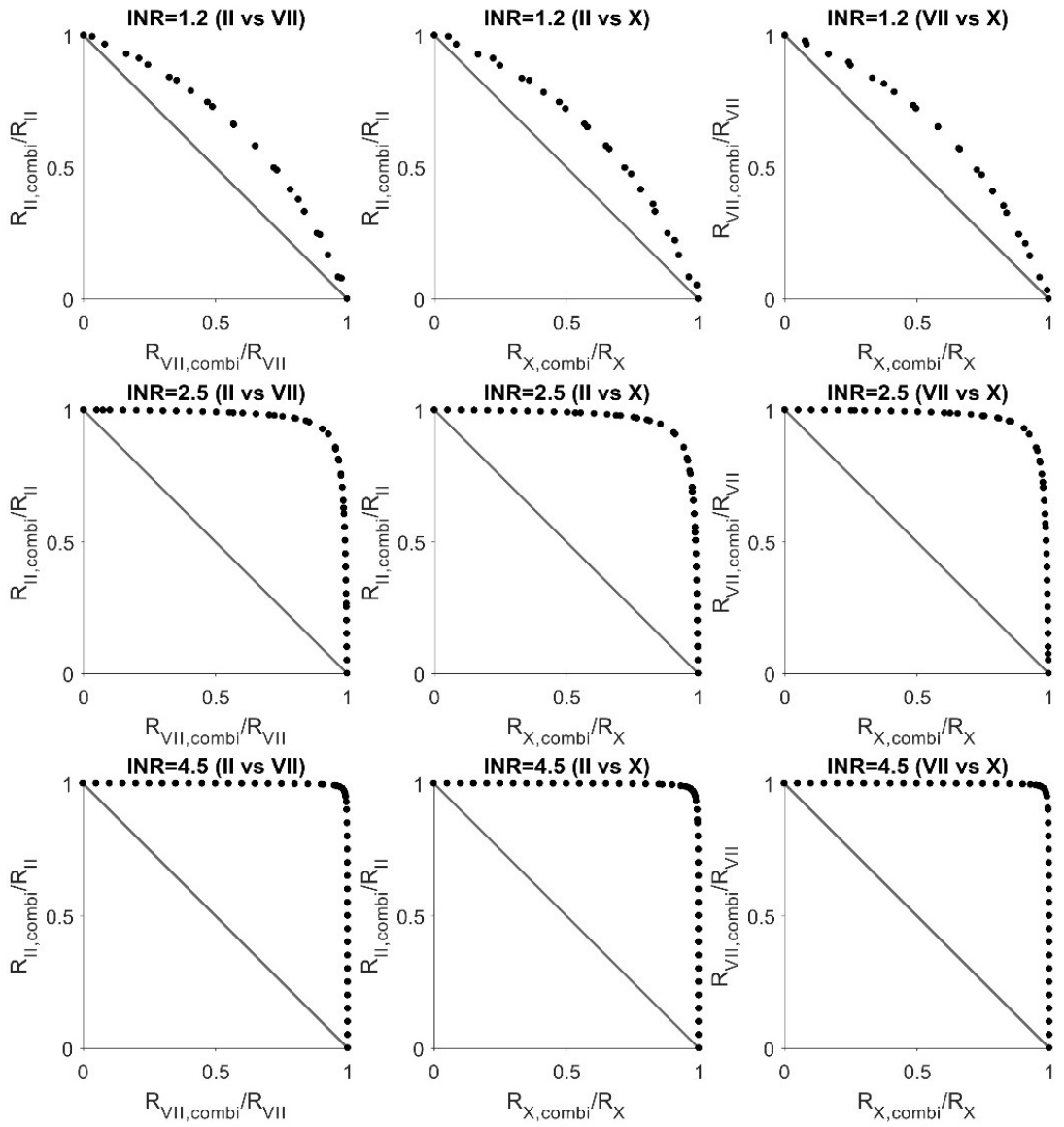

Figure A 4.4 *Isobolograms of pairwise combination of factors II, VII, and X for different INRs. The black circles correspond to pairwise combination of factors II, VII, or X that gives a predetermined INR. The diagonal solid line is the additivity line. INR is the international normalised ratio,* $R_{P,combi}$ *refers to the reduction in one coagulation protein when another coagulation protein is simultaneously reduced and* R_P *the reduction in a single coagulation protein.*

A4.2.2.2. Assumption 2: The most deficient coagulation protein drives the INR

Interpretation

Of factors II, VII, and X, the most deficient coagulation protein is the most important determinant of the INR.

Internal evaluation of *I*

I = Significant. This was rated based on logical reasoning. If factors II, VII, and X all drive the INR considerably, monitoring factor VII alone to inform the INR is unlikely to be adequate.

Internal evaluation of *P*

P = Unlikely. At high INR (e.g. INR=2.5 or INR=4.5), vertical and horizontal segments were observed on the isobolograms (see **Figure A 4.4**). This shows that if either one of the factors II, VII, and X is sufficiently deficient, then the same INR will occur regardless of the concentration of other coagulation proteins. Hence, the most deficient coagulation protein is likely the principal driving force behind the INR.

Decision

Decision = Go for model building. Even given the significant impact of violation of this assumption the probability of violation is low and hence the risk is considered to be negligible.

A4.2.2.3. Assumption 3: Under non-steady-state INR conditions, factor VII is always the most deficient

Interpretation

$$1 - P\left(\left(t_{\frac{1}{2},VII} < t_{\frac{1}{2},X}\right) \cap \left(t_{\frac{1}{2},VII} < t_{\frac{1}{2},II}\right)\right) < \alpha; \quad \alpha = 0.05$$

Equation A 4.5 *Probability of factor VII having a degradation half-life significantly longer than that of factor II or X.*

Here, $t_{\frac{1}{2},P}$ represents the degradation half-life of factors II, VII, or X and α is the overall significance level for hypothesis testing.

Internal evaluation of *I*

I = Significant. A sensitivity analysis was conducted. Here, the degradation rate constant of factor VII, $k_{out,VII}$, of the QSP coagulation network model [31] was reduced so that $t_{\frac{1}{2},VII} > t_{\frac{1}{2},X}$. Then, SI_{II}, SI_{VII}, and SI_X, respectively, were derived from INR and coagulation proteins data simulated from the QSP coagulation network model [31] using the following equation:

$$SI_P = \left|\frac{\partial INR}{\partial P}\right|; \quad P \in \{II, VII, X\}.$$

Equation A 4.6 *Local sensitivity of INR to changes in coagulation protein concentration.*

SI_{II}, SI_{VII}, and SI_X versus time were plotted and qualitatively compared to the INR versus time plot (see right-hand column of **Figure A 4.5**). When factor X replaced factor VII as the most deficient factor during the non-steady-state INR, the time course of SI_{VII} no longer bears similarity to that of the INR. Instead, the time course of SI_X appears similar to that of the INR. It appears that what matters is that the SI_P for the coagulation protein with the shortest degradation half-life is used for prediction as it provides the best approximation to the INR.

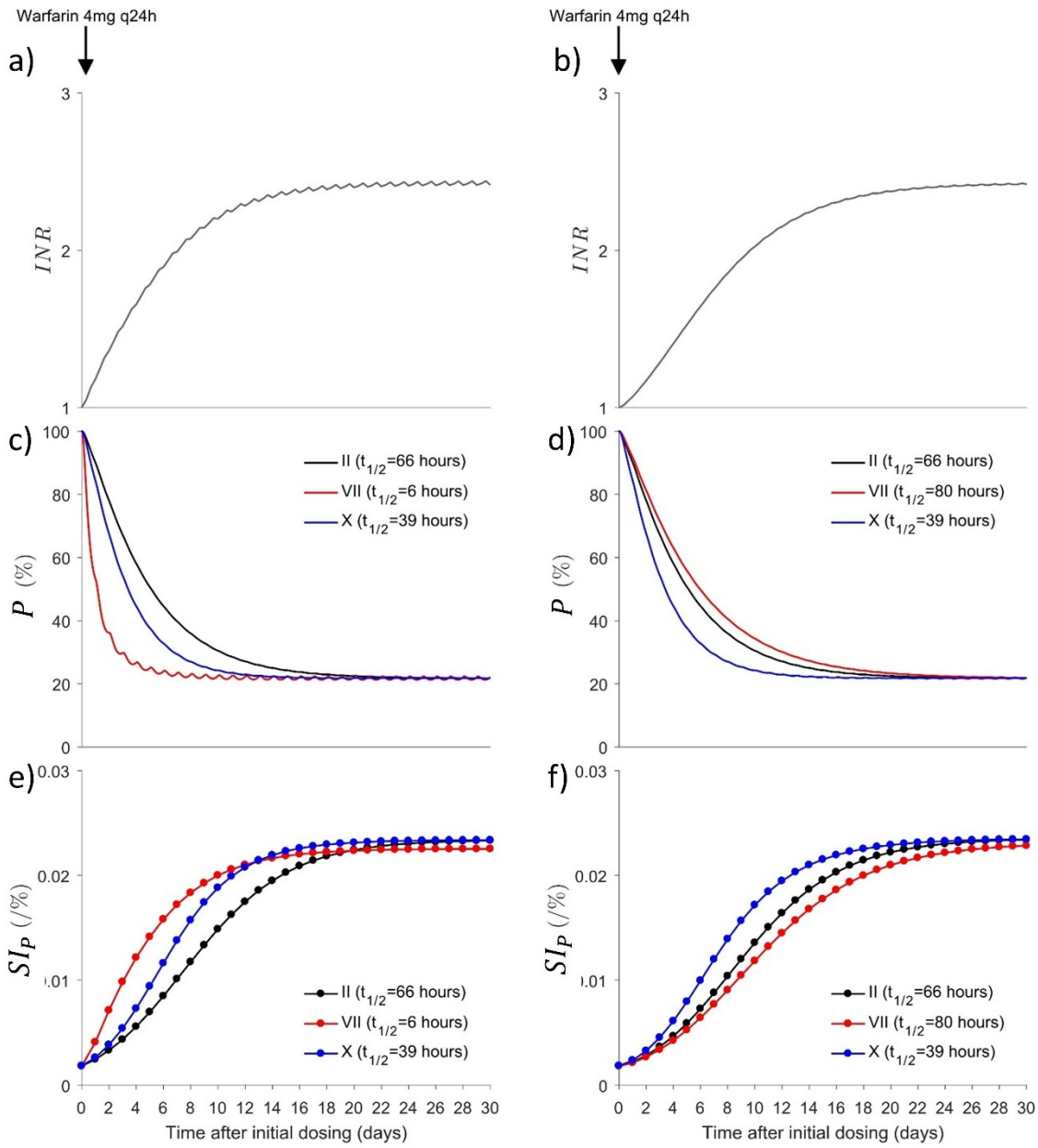

Figure A 4.5 *The simulated time course of INR (panel a and b), and factors II, VII, and X (panel c and d), and SI_{II}, SI_{VII}, and SI_X (panel e and f) following initiation of 4mg warfarin daily. The two columns of plots differ with respect to the $t_{1/2,VII}$ used for simulations. The left-hand column corresponds to $t_{1/2,VII}$ = 6 hours and the right-hand column refers to a hypothetical $t_{1/2,VII}$ = 80 hours. INR is the international normalised ratio, SI_P is the sensitivity index of INR to a specific coagulation protein and $t_{1/2,P}$ the degradation half-life of a particular coagulation protein.*

Internal evaluation of *P*

P = Unlikely. $t_{\frac{1}{2},II}$, $t_{\frac{1}{2},VII}$, and $t_{\frac{1}{2},X}$ for 1000 individuals were simulated using relevant parameters (e.g. the $k_{out,II}$, $k_{out,VII}$, $k_{out,X}$ and the corresponding variance-covariance matrix of between subject variability in parameters) from the joint model for warfarin and coagulation proteins [181]. An overarching hypothesis to test was as follows:

$$H_0: \left(t_{\frac{1}{2},VII} \geq t_{\frac{1}{2},X}\right) \cup \left(t_{\frac{1}{2},VII} \geq t_{\frac{1}{2},II}\right)$$
$$H_A: \left(t_{\frac{1}{2},VII} < t_{\frac{1}{2},X}\right) \cap \left(t_{\frac{1}{2},VII} < t_{\frac{1}{2},II}\right).$$

Equation A 4.7 *Hypotheses of the rank order of $t_{1/2,VII}$ versus $t_{1/2,II,\ and}$ $t_{1/2,X}$.*

Here, H_0 is the null hypothesis and H_A is the alternative hypothesis. Independent testing of $H_0: t_{\frac{1}{2},VII} \geq t_{\frac{1}{2},X}$ and $H_0: t_{\frac{1}{2},VII} \geq t_{\frac{1}{2},II}$ were required. Each of these hypotheses was tested using a Wilcoxon-signed rank test at $\alpha = 0.025$ (one-tailed and with Bonferroni correction). $\left(t_{\frac{1}{2},VII} - t_{\frac{1}{2},X}\right)$ was found centred at median -35.0 (IQR -39.9, -30.8) hours. $t_{\frac{1}{2},VII}$ is significantly lower than $t_{\frac{1}{2},X}$ ($Z = -27.4, p < 0.001$). In addition, $\left(t_{\frac{1}{2},VII} - t_{\frac{1}{2},II}\right)$ has a median of -50.7 (IQR -59.0, -43.4) hours. $t_{\frac{1}{2},VII}$ is significantly lower than $t_{\frac{1}{2},II}$ ($Z = -27.4, p < 0.001$). Taken together, these results provide sufficient evidence to reject the H_0.

Decision

Decision = Go for model building. Even given the significant impact of violation of this assumption the probability of violation is low and hence the risk is considered to be negligible.

A4.2.2.4. Assumption 4: Non-steady-state INR is the most sensitive to factor VII

Interpretation

SI_{VII} is greater in magnitude compared to both SI_{II} and SI_X at all time points during the non-steady-state INR.

Internal evaluation of *I*

I = Significant. A sensitivity analysis was conducted. Here, $k_{out,VII}$ of the QSP coagulation network model [31] was reduced so that $t_{\frac{1}{2},VII} > t_{\frac{1}{2},X}$. Factors II, VII, X, and INR were simulated. SI_{II}, SI_{VII}, and SI_X were derived from the simulated data. From the right column of **Figure A 4.5**, INR appears to be more sensitive to factor X than factor VII (i.e. $SI_X > SI_{VII}$) during the non-steady-state INR. Here, the time course of SI_{VII} no longer bears similarity to that of the INR. Instead, the time course of SI_X mimics that of the INR.

Internal evaluation of *P*

P = Unlikely. Factors II, VII, X, and INR were simulated from the coagulation network model [31] using parameters for a typical individuals. Subsequently, SI_{II}, SI_{VII}, and SI_X were derived from the simulated data. From the left column of **Figure A 4.5**, it was observed that SI_{VII} is larger in magnitude compared to SI_{II} and SI_X at all time points during the non-steady-state INR. It is likely that the non-steady-state INR is the most sensitive to factor VII.

Decision

Decision = Go for model building. Even given the significant impact of violation of this assumption the probability of violation is low and hence the risk is considered to be negligible.

A4.2.2.5. Assumption 5: The QSP coagulation network model is adequate in describing the warfarin-coagulation proteins-INR relationship

Interpretation

The QSP coagulation network model is able to produce physiologically-sound simulated profiles for factors II, VII, X, and INR following warfarin initiation.

Internal evaluation of *I*

I = Significant. This was rated based on logical reasoning. It is self-evident that if the QSP model is unable to accurately describe the warfarin-coagulation proteins-INR relationship, the SI_{VII} derived is unlikely to be fit for the intended purpose.

Internal evaluation of *P*

P = Unlikely. Factors II, VII, X, and INR were simulated from the QSP coagulation network model [31]. The simulated data were compared to external data (n = 17) [167, 181]. Individual observed and simulated data versus time were plotted. It is however, not possible to validate the QSP model and hence it is not possible to fully test this assumption across the whole range of INR generating pathways. The simulated data agree reasonably well with the observed data for factors II, VII, X, and INR at the individual level. See **Figure A 4.6** for plots of five representative individuals.

Decision

Decision = Go for model building. Even given the significant impact of violation of this assumption the probability of violation is low and hence the risk is considered to be negligible.

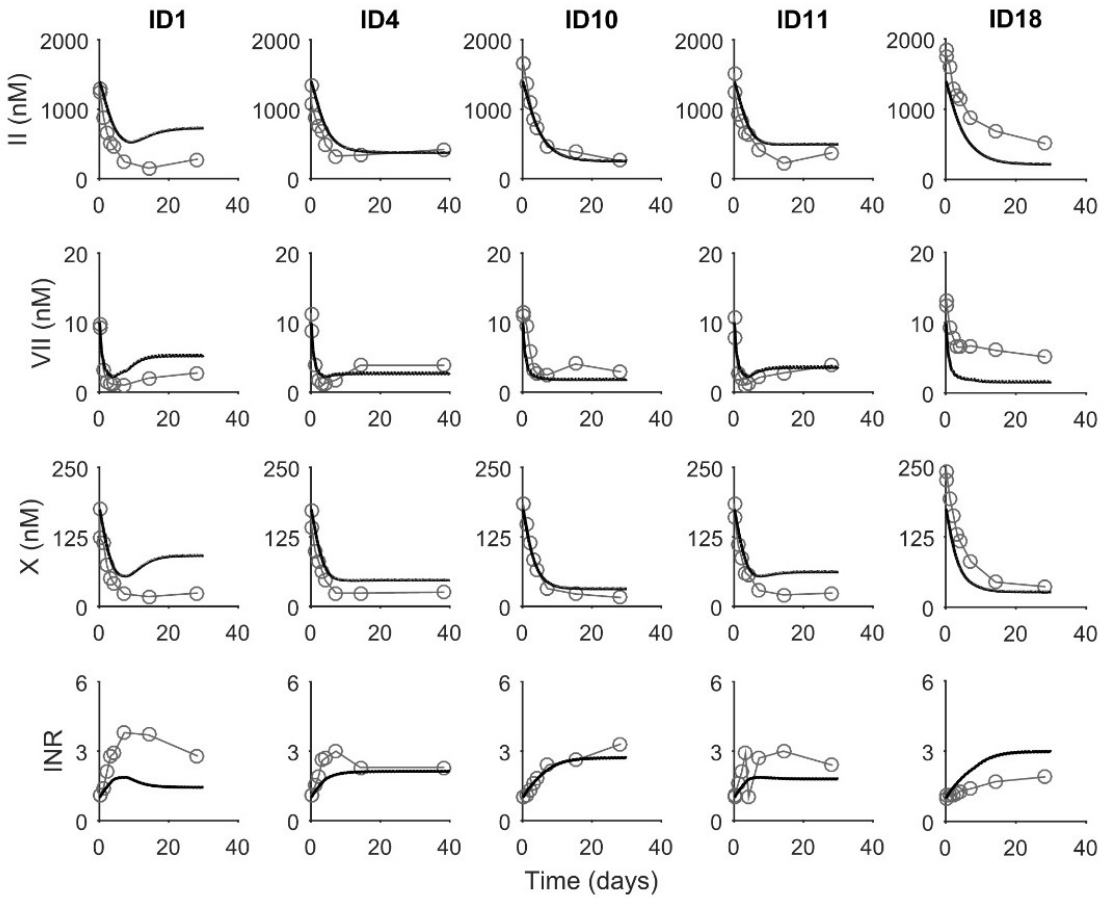

Figure A 4.6 *Individual fits for the time course of factors II, VII, X, and INR for five representative individuals following warfarin initiation. The black solid lines are prediction by the coagulation network model. The grey open circles are observations from the external test dataset [167, 181]. INR refers to the international normalised ratio and nM stands for nanomolar.*

A4.2.2.6. Assumption 6: The simulated coagulation proteins-INR time course is representative of that of typical patients initiated with warfarin

Interpretation

The simulated profiles for factors II, VII, X, and INR are representative of the majority of patients initiated with warfarin.

Internal evaluation of *I*

I = Significant. This was rated based on logical reasoning. It is self-evident that generalisability will be limited if the simulation results are unrepresentative.

Internal evaluation of *P*

P = Unlikely. Factors II, VII, X, and INR were simulated from the QSP coagulation network model [31]. The simulated data were compared to external data (n = 17) [167, 181]. Individual observed and simulated data versus time were plotted. The data simulated from the QSP coagulation network model agree reasonably well with the observed data for factors II, VII, X, and INR at the individual level. See **Figure A 4.6** above for plots of five representative individuals.

Decision

Decision = Go for model building. Even given the significant impact of violation of this assumption the probability of violation is low and hence the risk is considered to be negligible.

References

1. Hylek EM, Go AS, Chang Y, Jensvold NG, Henault LE, Selby JV, et al. Effect of intensity of oral anticoagulation on stroke severity and mortality in atrial fibrillation. N Engl J Med. 2003;349(11):1019-26.
2. Li X, Liu R, Luo ZY, Yan H, Huang WH, Yin JY, et al. Comparison of the predictive abilities of pharmacogenetics-based warfarin dosing algorithms using seven mathematical models in Chinese patients. Pharmacogenomics. 2015;16(6):583-90.
3. Marin-Leblanc M, Perreault S, Bahroun I, Lapointe M, Mongrain I, Provost S, et al. Validation of warfarin pharmacogenetic algorithms in clinical practice. Pharmacogenomics. 2012;13(1):21-9.
4. Peng Q, Huang S, Chen X, Yuan Y, Yu Y, Tao L, et al. Validation of warfarin pharmacogenetic algorithms in 586 Han Chinese patients. Pharmacogenomics. 2015;16(13):1465-74.
5. Saffian SM, Duffull SB, Wright DF. Warfarin dosing algorithms under-predict dose requirements in patients requiring >/= 7mg daily: A systematic review and meta-analysis. Clin Pharmacol Ther. 2017;102(2):297-304.
6. Yan H, Yin J, Zhang W, Li X. Possible strategies to make warfarin dosing algorithm prediction more accurately in patients with extreme dose. Clin Pharmaco Ther. 2017;103(2):184.
7. Saffian SM, Wright DF, Roberts RL, Duffull SB. Methods for predicting warfarin dose requirements. Ther Drug Monit. 2015;37(4):531-8.
8. Anderson JL, Horne BD, Stevens SM, Grove AS, Barton S, Nicholas ZP, et al. Randomized trial of genotype-guided versus standard warfarin dosing in patients initiating oral anticoagulation. Circulation. 2007;116(22):2563-70.
9. Caraco Y, Blotnick S, Muszkat M. CYP2C9 genotype-guided warfarin prescribing enhances the efficacy and safety of anticoagulation: a prospective randomized controlled study. Clin Pharmacol Ther. 2008;83(3):460-70.
10. Gage BF, Eby C, Johnson JA, Deych E, Rieder MJ, Ridker PM, et al. Use of pharmacogenetic and clinical factors to predict the therapeutic dose of warfarin. Clin Pharmacol Ther. 2008;84(3):326-31.
11. Klein TE, Altman RB, Eriksson N, Gage BF, Kimmel SE, Lee MT, et al. Estimation of the warfarin dose with clinical and pharmacogenetic data. N Engl J Med. 2009;360(8):753-64.
12. Lenzini P, Wadelius M, Kimmel S, Anderson JL, Jorgensen AL, Pirmohamed M, et al. Integration of genetic, clinical, and INR data to refine warfarin dosing. Clin Pharmacol Ther. 2010;87(5):572-8.
13. McMillin GA, Melis R, Wilson A, Strong MB, Wanner NA, Vinik RG, et al. Gene-based warfarin dosing compared with standard of care practices in an orthopedic surgery population: a prospective, parallel cohort study. Ther Drug Monit. 2010;32(3):338-45.
14. Perlstein TS, Goldhaber SZ, Nelson K, Joshi V, Morgan TV, Lesko LJ, et al. The CReating an Optimal Warfarin Nomogram (CROWN) study. Thromb Haemost. 2012;107(1):59-68.
15. Sconce EA, Khan TI, Wynne HA, Avery P, Monkhouse L, King BP, et al. The impact of CYP2C9 and VKORC1 genetic polymorphism and patient

characteristics upon warfarin dose requirements: proposal for a new dosing regimen. Blood. 2005;106(7):2329-33.
16. Wadelius M, Chen LY, Lindh JD, Eriksson N, Ghori MJ, Bumpstead S, et al. The largest prospective warfarin-treated cohort supports genetic forecasting. Blood. 2009;113(4):784-92.
17. Tait RC, Sefcick A. A warfarin induction regimen for out-patient anticoagulation in patients with atrial fibrillation. Br J Haematol. 1998;101(3):450-4.
18. Wright DF, Duffull SB. A Bayesian dose-individualization method for warfarin. Clin Pharmacokinet. 2013;52(1):59-68.
19. Bonate PL, Steimer JL. Pharmacokinetic-pharmacodynamic modeling and simulation: Springer; 2011.
20. Davidian M, Giltinan DM. Nonlinear models for repeated measurement data: Taylor & Francis; 1995.
21. Lavielle M. Mixed effects models for the population approach: models, tasks, methods and tools: Taylor & Francis; 2014.
22. Horne BD, Lenzini PA, Wadelius M, Jorgensen AL, Kimmel SE, Ridker PM, et al. Pharmacogenetic warfarin dose refinements remain significantly influenced by genetic factors after one week of therapy. Thromb Haemost. 2012;107(2):232-40.
23. Le Gal G, Carrier M, Tierney S, Majeed H, Rodger M, Wells PS. Prediction of the warfarin maintenance dose after completion of the 10 mg initiation nomogram: do we really need genotyping? J Thromb Haemost. 2010;8(1):90-4.
24. Lenzini PA, Grice GR, Milligan PE, Gatchel SK, Deych E, Eby CS, et al. Optimal initial dose adjustment of warfarin in orthopedic patients. Ann Pharmacother. 2007;41(11):1798-804.
25. Ramos AS, Seip RL, Rivera-Miranda G, Felici-Giovanini ME, Garcia-Berdecia R, Alejandro-Cowan Y, et al. Development of a pharmacogenetic-guided warfarin dosing algorithm for Puerto Rican patients. Pharmacogenomics. 2012;13(16):1937-50.
26. Choi JR, Kim JO, Kang DR, Yoon SA, Shin JY, Zhang X, et al. Proposal of pharmacogenetics-based warfarin dosing algorithm in Korean patients. J Hum Genet. 2011;56(4):290-5.
27. Fennerty A, Dolben J, Thomas P, Backhouse G, Bentley DP, Campbell IA, et al. Flexible induction dose regimen for warfarin and prediction of maintenance dose. BMJ. 1984;288(6426):1268-70.
28. Gedge J, Orme S, Hampton KK, Channer KS, Hendra TJ. A comparison of a low-dose warfarin induction regimen with the modified Fennerty regimen in elderly inpatients. Age Ageing. 2000;29(1):31-4.
29. Solomon I, Maharshak N, Chechik G, Leibovici L, Lubetsky A, Halkin H, et al. Applying an artificial neural network to warfarin maintenance dose prediction. Isr Med Assoc J. 2004;6(12):732-5.
30. Xu Q, Xu B, Zhang Y, Yang J, Gao L, Zhang Y, et al. Estimation of the warfarin dose with a pharmacogenetic refinement algorithm in Chinese patients mainly under low-intensity warfarin anticoagulation. Thromb Haemost. 2012;108(6):1132-40.

31. Wajima T, Isbister GK, Duffull SB. A comprehensive model for the humoral coagulation network in humans. Clin Pharmacol Ther. 2009;86(3):290-8.
32. Benet LZ, Rowland M. Pharmacometrics: a new journal section. J Pharmacokinet Biopharm. 1982;10(4):349-50.
33. Box GEP. Robustness in the strategy of scientific model building: Defense Technical Information Center; 1979.
34. Marshall SF, Burghaus R, Cosson V, Cheung SY, Chenel M, DellaPasqua O, et al. Good practices in model-informed drug discovery and development: practice, application, and documentation. CPT Pharmacometrics Syst Pharmacol. 2016;5(3):93-122.
35. Watala C, Golanski J, Kardas P. Multivariate relationships between international normalized ratio and vitamin K-dependent coagulation-derived parameters in normal healthy donors and oral anticoagulant therapy patients. Thromb J. 2003;1:7.
36. Upton RN, Mould DR. Basic concepts in population modeling, simulation, and model-based drug development: part 3-introduction to pharmacodynamic modeling methods. CPT Pharmacometrics Syst Pharmacol. 2014;3(1):e88.
37. Borghardt JM, Weber B, Staab A, Kloft C. Pharmacometric models for characterizing the pharmacokinetics of orally inhaled drugs. AAPS J. 2015;17(4):853-70.
38. Gulati A, Isbister GK, Duffull SB. Effect of Australian elapid venoms on blood coagulation: Australian Snakebite Project (ASP-17). Toxicon. 2013;61:94-104.
39. Al-Sallami HS, Pavan Kumar VV, Landersdorfer CB, Bulitta JB, Duffull SB. The time course of drug effects. Pharm Stat. 2009;8(3):176-85.
40. Ariens EJ. Affinity and intrinsic activity in the theory of competitive inhibition. Arch Int Pharmacodyn Ther. 1954;99(1):32-49.
41. Clark AJ. General pharmacology. Berlin: Springer; 1937.
42. Stephenson RP. A modification of receptor theory. Br J Pharmacol Chemother. 1956;11(4):379-93.
43. Black JW, Leff P. Operational models of pharmacological agonism. Proc R Soc Lond B Biol Sci. 1983;220(1219):141-62.
44. Paton WD, Rothschild AM. The changes in response and in ionic content of smooth muscle produced by acetylcholine action and by calcium deficiency. Br J Pharmacol Chemother. 1965;24:437-48.
45. Hill AV. The possible effects of the aggregation of the molecules of haemoglobin on its dissociation curves. J Physiol. 1910;40:4-7.
46. Gabrielsson J, Hjorth S. Quantitative pharmacology: an introduction to integrative pharmacokinetic-pharmacodynamic analysis: Apotekarsocieteten; 2012.
47. Rosenbaum SE. Basic pharmacokinetics and pharmacodynamics: an integrated textbook and computer simulations: Wiley; 2016.

48. Dayneka NL, Garg V, Jusko WJ. Comparison of four basic models of indirect pharmacodynamic responses. J Pharmacokinet Biopharm. 1993;21(4):457-78.
49. Sharma A, Jusko WJ. Characteristics of indirect pharmacodynamic models and applications to clinical drug responses. Br J Clin Pharmacol. 1998;45(3):229-39.
50. Jacqmin P, Snoeck E, van Schaick EA, Gieschke R, Pillai P, Steimer JL, et al. Modelling response time profiles in the absence of drug concentrations: definition and performance evaluation of the K-PD model. J Pharmacokinet Pharmacodyn. 2007;34(1):57-85.
51. Levy G. Relationship between rate of elimination of tubocurarine and rate of decline of its pharmacological activity. Br J Anaesth. 1964;36(11):694-5.
52. Levy G. Kinetic of pharmacalogic activity of succinylcholine in man. J Pharm Sci. 1967;56(12):1687-8.
53. Smolen VF. Quantitative determination of drug bioavailability and biokinetic behavior from pharmacological data for ophthalmic and oral administrations of a mydriatic drug. J Pharm Sci. 1971;60(3):354-65.
54. Hamberg AK, Wadelius M, Lindh JD, Dahl ML, Padrini R, Deloukas P, et al. A pharmacometric model describing the relationship between warfarin dose and INR response with respect to variations in CYP2C9, VKORC1, and age. Clin Pharmacol Ther. 2010;87(6):727-34.
55. Henin E, You B, VanCutsem E, Hoff PM, Cassidy J, Twelves C, et al. A dynamic model of hand-and-foot syndrome in patients receiving capecitabine. Clin Pharmacol Ther. 2009;85(4):418-25.
56. Jauslin PM, Karlsson MO, Frey N. Identification of the mechanism of action of a glucokinase activator from oral glucose tolerance test data in type 2 diabetic patients based on an integrated glucose-insulin model. J Clin Pharmacol. 2012;52(12):1861-71.
57. Gabrielsson J, Jusko WJ, Alari L. Modeling of dose-response-time data: four examples of estimating the turnover parameters and generating kinetic functions from response profiles. Biopharm Drug Dispos. 2000;21(2):41-52.
58. Gabrielsson J, Peletier LA. Dose-response-time data analysis involving nonlinear dynamics, feedback and delay. Eur J Pharm Sci. 2014;59:36-48.
59. Pillai G, Gieschke R, Goggin T, Jacqmin P, Schimmer RC, Steimer JL. A semimechanistic and mechanistic population PK-PD model for biomarker response to ibandronate, a new bisphosphonate for the treatment of osteoporosis. Br J Clin Pharmacol. 2004;58(6):618-31.
60. Tod M. Evaluation of drugs in pediatrics using K-PD models: perspectives. Fundam Clin Pharmacol. 2008;22(6):589-94.
61. Gonzalez-Sales M, Nekka F, Tanguay M, Tremblay PO, Li J. Modelling the dose-response relationship: the fair share of pharmacokinetic and pharmacodynamic information. Br J Clin Pharmacol. 2017;83(6):1240-51.
62. Raue A, Kreutz C, Maiwald T, Bachmann J, Schilling M, Klingmuller U, et al. Structural and practical identifiability analysis of partially observed dynamical models by exploiting the profile likelihood. Bioinformatics. 2009;25(15):1923-9.

63. Saccomani MP, Audoly S, Bellu G, D'Angiò L. Examples of testing global identifiability of biological and biomedical models with the DAISY software. Comput Biol Med. 2010;40(4):402-7.
64. Shivva V, Korell J, Tucker IG, Duffull SB. An approach for identifiability of population pharmacokinetic–pharmacodynamic models. CPT Pharmacometrics Syst Pharmacol. 2013;2(6):e49.
65. Bellman R, Åström KJ. On structural identifiability. Math Biosci. 1970;7(3):329-39.
66. Duffull S, Waterhouse T, Eccleston J. Some considerations on the design of population pharmacokinetic studies. J Pharmacokinet Pharmacodyn. 2005;32(3-4):441-57.
67. Mentre F, Mallet A, Baccar D. Optimal design in random-effects regression models. Biometrika. 1997;84(2):429-42.
68. Kim M, Yim D, Bae K. R-based reproduction of the estimation process hidden behind NONMEM® Part 1: first-order approximation method. TCP. 2015;23(1):1-7.
69. Wang Y. Derivation of various NONMEM estimation methods. J Pharmacokinet Pharmacodyn. 2007;34(5):575-93.
70. Gomes B. An introduction to systems biology and quantitative systems pharmacology. In: Reedijk J, editor. Reference module in chemistry, molecular sciences and chemical engineering: Elsevier; 2017. p. 488-503.
71. Duffull SB. A philosophical framework for integrating systems pharmacology models into pharmacometrics. CPT Pharmacometrics Syst Pharmacol. 2016;5(12):649-55.
72. Gadkar K, Kirouac DC, Mager DE, van der Graaf PH, Ramanujan S. A six-stage workflow for robust application of systems pharmacology. CPT Pharmacometrics Syst Pharmacol. 2016;5(5):235-49.
73. Berger SI, Ma'ayan A, Iyengar R. Systems pharmacology of arrhythmias. Sci Signal. 2010;3(118):ra30.
74. Shivva V, Tucker IG, Duffull SB. An in silico knockout model for gastrointestinal absorption using a systems pharmacology approach - development and application for ketones. PLoS One. 2016;11(9):e0163795.
75. Peterson MC, Riggs MM. A physiologically based mathematical model of integrated calcium homeostasis and bone remodeling. Bone. 2010;46(1):49-63.
76. Ribba B, Grimm HP, Agoram B, Davies MR, Gadkar K, Niederer S, et al. Methodologies for quantitative systems pharmacology (QSP) models: design and estimation. CPT Pharmacometrics Syst Pharmacol. 2017;6(8):496-8.
77. Press WH. Numerical recipes in FORTRAN: the art of scientific computing. Cambridge: Cambridge University Press; 1992.
78. Jameson A, Schmidt W, Turkel E, editors. Numerical solution of the Euler equations by finite volume methods using Runge Kutta time stepping schemes. 14th fluid and plasma dynamics conference; 1981.
79. Hamming R. Numerical methods for scientists and engineers: Dover Publications; 2012.
80. Moler CB. Numerical computing with MATLAB: Society for Industrial and Applied Mathematics; 2010.

81. Kirkpatrick S, Gelatt CD, Vecchi MP. Optimization by simulated annealing. Science. 1983;220(4598):671-80.
82. Tsamandouras N, Rostami-Hodjegan A, Aarons L. Combining the 'bottom up' and 'top down' approaches in pharmacokinetic modelling: fitting PBPK models to observed clinical data. Br J Clin Pharmacol. 2015;79(1):48-55.
83. Pohl B, Beringer C, Bomhard M, Keller F. The quick machine - a mathematical model for the extrinsic activation of coagulation. Haemostasis. 1994;24(6):325-37.
84. Dokoumetzidis A, Aarons L. Proper lumping in systems biology models. IET Syst Biol. 2009;3(1):40-51.
85. Gulati A, Isbister GK, Duffull SB. Scale reduction of a systems coagulation model with an application to modeling pharmacokinetic-pharmacodynamic data. CPT Pharmacometrics Syst Pharmacol. 2014;3:e90.
86. Pilari S, Huisinga W. Lumping of physiologically-based pharmacokinetic models and a mechanistic derivation of classical compartmental models. J Pharmacokinet Pharmacodyn. 2010;37(4):365-405.
87. Risk factors for stroke and efficacy of antithrombotic therapy in atrial fibrillation: analysis of pooled data from five randomized controlled trials. Arch Intern Med. 1994;154(13):1449-57.
88. Barritt DW, Jordan SC. Anticoagulant drugs in the treatment of pulmonary embolism. Lancet. 1960;275(7138):1309-12.
89. Hart RG, Benavente O, McBride R, Pearce LA. Antithrombotic therapy to prevent stroke in patients with atrial fibrillation: a meta-analysis. Ann Intern Med. 1999;131(7):492-501.
90. Ridker PM, Goldhaber SZ, Danielson E, Rosenberg Y, Eby CS, Deitcher SR, et al. Long-term, low-intensity warfarin therapy for the prevention of recurrent venous thromboembolism. N Engl J Med. 2003;348(15):1425-34.
91. Holbrook A, Schulman S, Witt DM, Vandvik PO, Fish J, Kovacs MJ, et al. Evidence-based management of anticoagulant therapy: antithrombotic therapy and prevention of thrombosis. Chest. 2012;141(2 Suppl):e152S-84S.
92. Hylek EM, Skates SJ, Sheehan MA, Singer DE. An analysis of the lowest effective intensity of prophylactic anticoagulation for patients with nonrheumatic atrial fibrillation. N Engl J Med. 1996;335(8):540-6.
93. Stroke Prevention in Atrial Fibrillation Investigators (SPAF III). Adjusted-dose warfarin versus low-intensity, fixed-dose warfarin plus aspirin for high-risk patients with atrial fibrillation: stroke prevention in atrial fibrillation III randomised clinical trial. Lancet. 1996;348(9028):633-8.
94. Kim SH, Thiessen PA, Bolton EE, Chen J, Fu G, Gindulyte A, et al. PubChem substance and compound databases. Nucleic Acids Res. 2016;44(Database issue):D1202-D13.
95. O'Reilly RA. Studies on the optical enantiomorphs of warfarin in man. Clin Pharmacol Ther. 1974;16(2):348-54.
96. Breckenridge A, Orme M. Kinetics of warfarin absorption in man. Clin Pharmacol Ther. 1973;14(6):955-61.
97. Kelly JG, O'Malley K. Clinical pharmacokinetics of oral anticoagulants. Clin Pharmacokinet. 1979;4(1):1-15.

98. O'Reilly RA, Aggeler PM, Leong LS. Studies on the coumarin anticoagulant drugs: the pharmacodynamics of warfarin in man. J Clin Invest. 1963;42(10):1542-51.
99. Holford NH. Clinical pharmacokinetics and pharmacodynamics of warfarin: understanding the dose-effect relationship. Clin Pharmacokinet. 1986;11(6):483-504.
100. Hamberg AK, Dahl ML, Barban M, Scordo MG, Wadelius M, Pengo V, et al. A PK-PD model for predicting the impact of age, CYP2C9, and VKORC1 genotype on individualization of warfarin therapy. Clin Pharmacol Ther. 2007;81(4):529-38.
101. Lane S, Al-Zubiedi S, Hatch E, Matthews I, Jorgensen AL, Deloukas P, et al. The population pharmacokinetics of R- and S-warfarin: effect of genetic and clinical factors. Br J Clin Pharmacol. 2012;73(1):66-76.
102. Xue L, Holford N, Ding XL, Shen ZY, Huang CR, Zhang H, et al. Theory based PKPD of S- and R-warfarin and effects on INR: influence of body size, composition and genotype in cardiac surgery patients. Br J Clin Pharmacol. 2016.
103. Yuen E, Gueorguieva I, Wise S, Soon D, Aarons L. Ethnic differences in the population pharmacokinetics and pharmacodynamics of warfarin. J Pharmacokinet Pharmacodyn. 2010;37(1):3-24.
104. Chan E, McLachlan AJ, Pegg M, MacKay AD, Cole RB, Rowland M. Disposition of warfarin enantiomers and metabolites in patients during multiple dosing with rac-warfarin. Br J Clin Pharmacol. 1994;37(6):563-9.
105. Black DJ, Kunze KL, Wienkers LC, Gidal BE, Seaton TL, McDonnell ND, et al. Warfarin-fluconazole II. A metabolically based drug interaction: in vivo studies. Drug Metab Dispos. 1996;24(4):422-8.
106. Kunze KL, Wienkers LC, Thummel KE, Trager WF. Warfarin-fluconazole I. Inhibition of the human cytochrome P450-dependent metabolism of warfarin by fluconazole: in vitro studies. Drug Metab Dispos. 1996;24(4):414-21.
107. Ufer M. Comparative pharmacokinetics of vitamin K antagonists: warfarin, phenprocoumon and acenocoumarol. Clin Pharmacokinet. 2005;44(12):1227-46.
108. Gardiner SJ, Begg EJ. Pharmacogenetics, drug-metabolizing enzymes, and clinical practice. Pharmacol Rev. 2006;58(3):521-90.
109. Kamali F, Khan TI, King BP, Frearson R, Kesteven P, Wood P, et al. Contribution of age, body size, and CYP2C9 genotype to anticoagulant response to warfarin. Clin Pharmacol Ther. 2004;75(3):204-12.
110. Lindh JD, Holm L, Andersson ML, Rane A. Influence of CYP2C9 genotype on warfarin dose requirements: a systematic review and meta-analysis. Eur J Clin Pharmacol. 2009;65(4):365-75.
111. Esmon CT, Sadowski JA, Suttie JW. A new carboxylation reaction: the vitamin K-dependent incorporation of H-14-CO3- into prothrombin. J Biol Chem. 1975;250(12):4744-8.
112. Carlisle TL, Suttie JW. Vitamin K dependent carboxylase: subcellular location of the carboxylase and enzymes involved in vitamin K metabolism in rat liver. Biochemistry. 1980;19(6):1161-7.

113. Swanson JC, Suttie JW. Prothrombin biosynthesis: characterization of processing events in rat liver microsomes. Biochemistry. 1985;24(15):3890-7.
114. McClure DB, Walls JD, Grinnell BW. Post-translational processing events in the secretion pathway of human protein C, a complex vitamin K-dependent antithrombotic factor. J Biol Chem. 1992;267(27):19710-7.
115. Dowd P, Ham SW, Hershline R. Role of oxygen in the vitamin K-dependent carboxylation reaction: incorporation of a second atom of oxygen 18 from molecular oxygen-18O2 into vitamin K oxide during carboxylase activity. J Am Chem Soc. 1992;114(20):7613-7.
116. Wood GM, Suttie JW. Vitamin K-dependent carboxylase. Stoichiometry of vitamin K epoxide formation, gamma-carboxyglutamyl formation, and gamma-glutamyl-3H cleavage. J Biol Chem. 1988;263(7):3234-9.
117. Friedman PA, Shia MA, Gallop PM, Griep AE. Vitamin K-dependent gamma-carbon-hydrogen bond cleavage and nonmandatory concurrent carboxylation of peptide-bound glutamic acid residues. Proc Natl Acad Sci U S A. 1979;76(7):3126-9.
118. Morris DP, Soute BA, Vermeer C, Stafford DW. Characterization of the purified vitamin K-dependent gamma-glutamyl carboxylase. J Biol Chem. 1993;268(12):8735-42.
119. Walker FJ. Regulation of activated protein C by a new protein: a possible function for bovine protein S. J Biol Chem. 1980;255(12):5521-4.
120. Whitlon DS, Sadowski JA, Suttie JW. Mechanism of coumarin action: significance of vitamin K epoxide reductase inhibition. Biochemistry. 1978;17(8):1371-7.
121. Suttie JW. Vitamin K-dependent carboxylase. Annu Rev Biochem. 1985;54:459-77.
122. Breckenridge A, Orme M, Wesseling H, Lewis RJ, Gibbons R. Pharmacokinetics and pharmacodynamics of the enantiomers of warfarin in man. Clin Pharmacol Ther. 1974;15(4):424-30.
123. Maddison J, Somogyi AA, Jensen BP, James HM, Gentgall M, Rolan PE. The pharmacokinetics and pharmacodynamics of single dose (R)- and (S)-warfarin administered separately and together: relationship to VKORC1 genotype. Br J Clin Pharmacol. 2013;75(1):208-16.
124. Fasco MJ, Principe LM. R- and S-Warfarin inhibition of vitamin K and vitamin K 2,3-epoxide reductase activities in the rat. J Biol Chem. 1982;257(9):4894-901.
125. Silverman RB. Model studies for a molecular mechanism of action of oral anticoagulants. J Am Chem Soc. 1981;103(13):3910-5.
126. Tie JK, Jin DY, Straight DL, Stafford DW. Functional study of the vitamin K cycle in mammalian cells. Blood. 2011;117(10):2967-74.
127. Wallin R, Gebhardt O, Prydz H. NAD(P)H dehydrogenase and its role in the vitamin K (2-methyl-3-phytyl-1,4-naphthaquinone)-dependent carboxylation reaction. Biochem J. 1978;169(1):95-101.
128. Fasco MJ, Principe LM, Walsh WA, Friedman PA. Warfarin inhibition of vitamin K 2,3-epoxide reductase in rat liver microsomes. Biochemistry. 1983;22(24):5655-60.

129. Hsia CK. Biochemical and mechanistic studies of the interactions between vitamin K antagonists and vitamin K epoxide reductase: University of Washington; 2012.
130. Thijssen HH, Baars LG, Vervoort-Peters HT. Vitamin K 2,3-epoxide reductase: the basis for stereoselectivity of 4-hydroxycoumarin anticoagulant activity. Br J Clin Pharmacol. 1988;95(3):675-82.
131. Czogalla KJ, Biswas A, Honing K, Hornung V, Liphardt K, Watzka M, et al. Warfarin and vitamin K compete for binding to Phe55 in human VKOR. Nat Struct Mol Biol. 2017;24(1):77-85.
132. Kamali F, Wynne H. Pharmacogenetics of warfarin. Annu Rev Med. 2010;61:63-75.
133. Herman D, Peternel P, Stegnar M, Breskvar K, Dolzan V. The influence of sequence variations in factor VII, gamma-glutamyl carboxylase and vitamin K epoxide reductase complex genes on warfarin dose requirement. Thromb Haemost. 2006;95(5):782-7.
134. Owen RP, Gong L, Sagreiya H, Klein TE, Altman RB. VKORC1 pharmacogenomics summary. Pharmacogenet Genomics. 2010;20(10):642-4.
135. Wadelius M, Chen LY, Downes K, Ghori J, Hunt S, Eriksson N, et al. Common VKORC1 and GGCX polymorphisms associated with warfarin dose. Pharmacogenomics J. 2005;5(4):262-70.
136. Quick AJ. The prothrombin in hemophilia and in obstructive jaundice. Am J Biol Chem. 1935;109:73.
137. Quick AJ, Hussey CV. Haemophilia-like states in girls. Lancet. 1958;271(7034):1294-8.
138. Poller L. International normalized ratios (INR): the first 20 years. J Thromb Haemost. 2004;2(6):849-60.
139. Nagashima R, O'Reilly RA, Levy G. Kinetics of pharmacologic effects in man: the anticoagulant action of warfarin. Clin Pharmacol Ther. 1969;10(1):22-35.
140. Chan E, McLachlan A, O'Reilly R, Rowland M. Stereochemical aspects of warfarin drug interactions: use of a combined pharmacokinetic-pharmacodynamic model. Clin Pharmacol Ther. 1994;56(3):286-94.
141. Jiang X, Blair EY, McLachlan AJ. Investigation of the effects of herbal medicines on warfarin response in healthy subjects: a population pharmacokinetic-pharmacodynamic modeling approach. J Clin Pharmacol. 2006;46(11):1370-8.
142. Mackie I, Cooper P, Lawrie A, Kitchen S, Gray E, Laffan M. Guidelines on the laboratory aspects of assays used in haemostasis and thrombosis. Int J Lab Hematol. 2013;35(1):1-13.
143. Mann KG, Brummel-Ziedins K, Undas A, Butenas S. Does the genotype predict the phenotype? Evaluations of the hemostatic proteome. J Thromb Haemost. 2004;2(10):1727-34.
144. Kumar S, Haigh JR, Tate G, Boothby M, Joanes DN, Davies JA, et al. Effect of warfarin on plasma concentrations of vitamin K dependent coagulation factors in patients with stable control and monitored compliance. Br J Haematol. 1990;74(1):82-5.

145. Lind SE, Callas PW, Golden EA, Joyner KA, Ortel TL. Plasma levels of factors II, VII and X and their relationship to the international normalized ratio during chronic warfarin therapy. Blood Coagul Fibrinolysis. 1997;8(1):48-53.
146. Paul B, Oxley A, Brigham K, Cox T, Hamilton PJ. Factor II, VII, IX and X concentrations in patients receiving long term warfarin. J Clin Pathol. 1987;40(1):94-8.
147. Coumadin (warfarin sodium) Prescribing Information 2015 [Available from: https://www.accessdata.fda.gov/drugsatfda_docs/label/2011/009218s107lbl.pdf.
148. Francis B, Lane S, Pirmohamed M, Jorgensen A. A review of a priori regression models for warfarin maintenance dose prediction. PLoS One. 2014;9(12):e114896.
149. Kovacs MJ, Anderson DA, Wells PS. Prospective assessment of a nomogram for the initiation of oral anticoagulation therapy for outpatient treatment of venous thromboembolism. Pathophysiol Haemost Thromb. 2002;32(3):131-3.
150. Sunderji R, Campbell L, Shalansky K, Fung A, Carter C, Gin K. Outpatient self-management of warfarin therapy: a pilot study. Pharmacotherapy. 1999;19(6):787-93.
151. Poller L, Keown M, Ibrahim S, Lowe G, Moia M, Turpie AG, et al. A multicentre randomised clinical endpoint study of PARMA 5 computer-assisted oral anticoagulant dosage. Br J Haematol. 2008;143(2):274-83.
152. Wright DF, Duffull SB. Development of a bayesian forecasting method for warfarin dose individualization. Pharm Res. 2011;28(5):1100-11.
153. Verhoef TI, Redekop WK, Daly AK, van Schie RM, de Boer A, Maitland-van der Zee AH. Pharmacogenetic-guided dosing of coumarin anticoagulants: algorithms for warfarin, acenocoumarol and phenprocoumon. Br J Clin Pharmacol. 2014;77(4):626-41.
154. Gong IY, Schwarz UI, Crown N, Dresser GK, Lazo-Langner A, Zou G, et al. Clinical and genetic determinants of warfarin pharmacokinetics and pharmacodynamics during treatment initiation. PLoS One. 2011;6(11):e27808.
155. Ferrari M, Pengo V, Barolo M, Bezzo F, Padrini R. Assessing the relative potency of (S)- and (R)-warfarin with a new PK-PD model, in relation to VKORC1 genotypes. Eur J Clin Pharmacol. 2017.
156. Sheiner LB. Computer-aided long-term anticoagulation therapy. Comput Biomed Res. 1969;2(6):507-18.
157. Pitsiu M, Parker EM, Aarons L, Rowland M. A Bayesian method based on clotting factor activity for the prediction of maintenance warfarin dosage regimens. Ther Drug Monit. 2003;25(1):36-40.
158. Bertola JP, Mazoyer E, Bergmann JF, Drouet L, Simoneau G, Mahe I. Early prediction of the sensitivity of warfarin in elderly patients by the fall in factor VIIc and protein C at the induction of treatment. Thromb Res. 2003;109(5-6):287-91.
159. D'Angelo A, Della Valle P, Crippa L, Fattorini A, Pattarini E, Vigano D'Angelo S. Relationship between international normalized ratio values, vitamin

K-dependent clotting factor levels and in vivo prothrombin activation during the early and steady phases of oral anticoagulant treatment. Haematologica. 2002;87(10):1074-80.
160. Gulati G, Hevelow M, George M, Behling E, Siegel J. International normalized ratio versus plasma levels of coagulation factors in patients on vitamin K antagonist therapy. Arch Pathol Lab Med. 2011;135(4):490-4.
161. O'Reilly RA, Aggeler PM. Studies on coumarin anticoagulant drugs. Initiation of warfarin therapy without a loading dose. Circulation. 1968;38(1):169-77.
162. Sarode R, Rawal A, Lee R, Shen YM, Frenkel EP. Poor correlation of supratherapeutic international normalised ratio and vitamin K-dependent procoagulant factor levels during warfarin therapy. Br J Haematol. 2006;132(5):604-7.
163. Sasaki T, Tabuchi H, Higuchi S, Ieiri I. Warfarin-dosing algorithm based on a population pharmacokinetic/pharmacodynamic model combined with Bayesian forecasting. Pharmacogenomics. 2009;10(8):1257-66.
164. Xue L, Holford NH, Miao L, editors. Warfarin PKPD - theory, body composition and genotype. Population Approach Group in Europe (PAGE) meeting 2016; 2016; Lisbon, Portugal.
165. Pitsiu M, Parker EM, Aarons L, Rowland M. Population pharmacokinetics and pharmacodynamics of warfarin in healthy young adults. Eur J Pharm Sci. 1993;1(3):151-7.
166. Vainieri H, Wingard LB. Effect of warfarin on the kinetics of the vitamin K-dependent clotting factors in rats. J Pharmacol Exp Ther. 1977;201(2):507-17.
167. McCollum D, Tait RC, Conkie J, Wight M, McColl MD, Walker ID. The effect of initiation of oral anticoagulation on protein Z and coagulation activation. Br J Haematol. 2004;125(Supplement s1):1.
168. Shivva V, Korell J, Tucker IG, Duffull SB. Parameterisation affects identifiability of population models. J Pharmacokinet Pharmacodyn. 2014;41(1):81-6.
169. Holford NH, Kirkpatrick C, Duffull SB, editors. NONMEM termination status is not an important indicator of the quality of bootstrap parameter estimates. Population Approach Group in Europe (PAGE) meeting 2006; 2006; Brugge, Belgium.
170. Bergstrand M, Hooker AC, Wallin JE, Karlsson MO. Prediction-corrected visual predictive checks for diagnosing nonlinear mixed-effects models. AAPS J. 2011;13(2):143-51.
171. Bowie EJ, Thompson JH, Didisheim P, Owen CA. Disappearance rates of coagulation factors: transfusion studies in factor-deficient patients. Transfusion. 1967;7(3):174-84.
172. D'Angelo A, Vigano-D'Angelo S, Esmon CT, Comp PC. Acquired deficiencies of protein S: protein S activity during oral anticoagulation, in liver disease, and in disseminated intravascular coagulation. J Clin Invest. 1988;81(5):1445-54.

173. Hjort PF, Egeberg O, Mikkelsen S. Turnover of prothrombin, factor VII and factor IX in a patient with hemophilia A. Scand J Clin Lab Invest. 1961;13(4):668-72.
174. Peyvandi F, Garagiola I, Seregni S. Future of coagulation factor replacement therapy. J Thromb Haemost. 2013;11 Suppl 1:84-98.
175. Riess H, Binsack T, Hiller E. Protein C antigen in prothrombin complex concentrates: content, recovery and half life. Blut. 1985;50(5):303-6.
176. Choonara IA, Malia RG, Haynes BP, Hay CR, Cholerton S, Breckenridge AM, et al. The relationship between inhibition of vitamin K1 2,3-epoxide reductase and reduction of clotting factor activity with warfarin. Br J Clin Pharmacol. 1988;25(1):1-7.
177. Hirsh J, Dalen J, Anderson DR, Poller L, Bussey H, Ansell J, et al. Oral anticoagulants: mechanism of action, clinical effectiveness, and optimal therapeutic range. Chest. 2001;119(1 Suppl):8S-21S.
178. Shao J, Wu CFJ. A general theory for jackknife variance estimation. Ann Stat. 1989:1176-97.
179. Bose A, Chatterjee S. Comparison of bootstrap and jackknife variance estimators in linear regression: second order results. Stat Sinica. 2002;12(2):575-98.
180. Efron B, Gong G. A leisurely look at the bootstrap, the jackknife, and cross-validation. Am Stat. 1983;37(1):36-48.
181. Ooi QX, Wright DFB, Tait RC, Isbister GK, Duffull SB. A joint model for vitamin K-dependent clotting factors and anticoagulation proteins. Clin Pharmacokinet. 2017;56(12):1555-66.
182. Khanin MA, Rakov DV, Kogan AE. Mathematical model for the blood coagulation prothrombin time test. Thromb Res. 1998;89(5):227-32.
183. Kogan AE, Kardakov DV, Khanin MA. Analysis of the activated partial thromboplastin time test using mathematical modeling. Thromb Res. 2001;101(4):299-310.
184. Chou TC. Theoretical basis, experimental design, and computerized simulation of synergism and antagonism in drug combination studies. Pharmacol Rev. 2006;58(3):621-81.
185. Tallarida RJ. An overview of drug combination analysis with isobolograms. J Pharmacol Exp Ther. 2006;319(1):1-7.
186. Geary N. Understanding synergy. Am J Physiol Endocrinol Metab. 2013;304(3):E237-53.
187. Loewe S, Käer E, Muischnek H. Über Kombinationswirkungen. Naunyn Schmiedebergs Arch Exp Pathol Pharmakol. 1927;120(1):25-40.
188. Fitzgerald JB, Schoeberl B, Nielsen UB, Sorger PK. Systems biology and combination therapy in the quest for clinical efficacy. Nat Chem Biol. 2006;2(9):458-66.
189. Martin-Betancor K, Ritz C, Fernández-Piñas F, Leganés F, Rodea-Palomares I. Defining an additivity framework for mixture research in inducible whole-cell biosensors. Sci Rep. 2015;5:17200.
190. Nishizaki M, Meyn RE, Levy LB, Atkinson EN, White RA, Roth JA, et al. Synergistic inhibition of human lung cancer cell growth by adenovirus-mediated

wild-type p53 gene transfer in combination with docetaxel and radiation therapeutics in vitro and in vivo. Clin Cancer Res. 2001;7(9):2887-97.
191. Niyazi M, Belka C. Isobologram analysis of triple therapies. Radiat Oncol. 2006;1:39-.
192. Yoon J, Urban C, Terzian C, Mariano N, Rahal JJ. In vitro double and triple synergistic activities of polymyxin B, imipenem, and rifampin against multidrug-resistant Acinetobacter baumannii. Antimicrob Agents Chemother. 2004;48(3):753-7.
193. Frotscher B, Toussaint-Hacquard M, Fouyssac F, Devignes J, Lecompte T, Briquel ME. Severe factor V deficiency in two brothers with different clinical presentations. Haemophilia. 2012;18(5):e383-5.
194. Girolami A, Scandellari R, Lombardi AM, Girolami B, Bortoletto E, Zanon E. Pregnancy and oral contraceptives in factor V deficiency: a study of 22 patients (five homozygotes and 17 heterozygotes) and review of the literature. Haemophilia. 2005;11(1):26-30.
195. Mathias M, Tunstall O, Khair K, Liesner R. Management of surgical procedures in children with severe FV deficiency: experience of 13 surgeries. Haemophilia. 2013;19(2):256-8.
196. Abstracts accepted for American Conference on Pharmacometrics 2016 (ACoP7). J Pharmacokinet Pharmacodyn. 2016;43(1):11-122.
197. Hirsh J, Poller L. The international normalized ratio: a guide to understanding and correcting its problems. Arch Intern Med. 1994;154(3):282-8.
198. Chan E, Aarons L, Serlin M, Breckenridge A, Rowland M. Inter-relationship among individual vitamin K-dependent clotting factors at different levels of anticoagulation. Br J Clin Pharmacol. 1987;24(5):621-5.
199. Sheiner LB, Beal SL. Some suggestions for measuring predictive performance. J Pharmacokinet Biopharm. 1981;9(4):503-12.
200. Food and Drug Administration (FDA). Guidance for industry: population pharmacokinetics 1999 [Available from: https://www.fda.gov/downloads/drugs/guidances/UCM072137.pdf.
201. European Medicines Agency (EMA). Guideline on reporting the results of population pharmacokinetic analyses 2007 [Available from: http://www.ema.europa.eu/docs/en_GB/document_library/Scientific_guideline/2009/09/WC500003067.pdf.
202. Manolis E, Brogren J, Cole S, Hay JL, Nordmark A, Karlsson KE, et al. Commentary on the MID3 good practices paper. CPT Pharmacometrics Syst Pharmacol. 2017;6(7):416-7.
203. Byon W, Smith MK, Chan P, Tortorici MA, Riley S, Dai H, et al. Establishing best practices and guidance in population modeling: an experience with an internal population pharmacokinetic analysis guidance. CPT Pharmacometrics Syst Pharmacol. 2013;2:e51.
204. Dykstra K, Mehrotra N, Tornøe CW, Kastrissios H, Patel B, Al-Huniti N, et al. Reporting guidelines for population pharmacokinetic analyses. J Pharmacokinet Pharmacodyn. 2015;42(3):301-14.
205. Karlsson MO, Jonsson EN, Wiltse CG, Wade JR. Assumption testing in population pharmacokinetic models: illustrated with an analysis of moxonidine

data from congestive heart failure patients. J Pharmacokinet Biopharm. 1998;26(2):207-46.
206. Wade JR, Edholm M, Salmonson T. A guide for reporting the results of population pharmacokinetic analyses: a Swedish perspective. AAPS J. 2005;7(2):45.
207. Bonate PL, Strougo A, Desai A, Roy M, Yassen A, van der Walt JS, et al. Guidelines for the quality control of population pharmacokinetic-pharmacodynamic analyses: an industry perspective. AAPS J. 2012;14(4):749-58.
208. Jamsen KM, McLeay SC, Barras MA, Green B. Reporting a population pharmacokinetic-pharmacodynamic study: a journal's perspective. Clin Pharmacokinet. 2014;53(2):111-22.
209. Timmis J, Alden K, Andrews P, Clark E, Nellis A, Naylor B, et al. Building confidence in quantitative systems pharmacology models: an engineer's guide to exploring the rationale in model design and development. CPT Pharmacometrics Syst Pharmacol. 2017;6(3):156-67.
210. Jones H, Rowland-Yeo K. Basic concepts in physiologically based pharmacokinetic modeling in drug discovery and development. CPT Pharmacometrics Syst Pharmacol. 2013;2:e63.
211. Jones HM, Chen Y, Gibson C, Heimbach T, Parrott N, Peters SA, et al. Physiologically based pharmacokinetic modeling in drug discovery and development: a pharmaceutical industry perspective. Clin Pharmaco Ther. 2015;97(3):247-62.
212. Rowland M, Peck C, Tucker G. Physiologically-based pharmacokinetics in drug development and regulatory science. Annu Rev Pharmacol Toxicol. 2011;51:45-73.
213. Zhao P, Rowland M, Huang SM. Best practice in the use of physiologically based pharmacokinetic modeling and simulation to address clinical pharmacology regulatory questions. Clin Pharmacol Ther. 2012;92(1):17-20.
214. European Medicines Agency (EMA). EFPIA-EMA modelling and simulation workshop (2011) report. . London, United Kingdom; 2012.
215. Karlsson MO, Beal SL, Sheiner LB. Three new residual error models for population PK/PD analyses. J Pharmacokinet Biopharm. 1995;23(6):651-72.
216. Gulati A, Faed JM, Isbister GK, Duffull SB. Application of adaptive DP-optimality to design a pilot study for a clotting time test for enoxaparin. Pharm Res. 2015;32(10):3391-402.
217. Duffull SB, Hegarty G. An inductive approximation to the solution of systems of nonlinear ordinary differential equations in pharmacokinetics-pharmacodynamics. J Theor Comput Sci. 2014;1(119):2.
218. Hasegawa C, Duffull SB. Exploring inductive linearization for pharmacokinetic-pharmacodynamic systems of nonlinear ordinary differential equations. J Pharmacokinet Pharmacodyn. 2017.
219. Snowden TJ, van der Graaf PH, editors. A comparison of two model reduction methodologies for a QSP bone biology system with denosumab dosing. Population Approach Group in Europe (PAGE) meeting 2018; 2018; Montreux, Switzerland.

220. Snowden TJ, van der Graaf PH, Tindall MJ. A combined model reduction algorithm for controlled biochemical systems. BMC Syst Biol. 2017;11(1):17.
221. Furie B, Diuguid CF, Jacobs M, Diuguid DL, Furie BC. Randomized prospective trial comparing the native prothrombin antigen with the prothrombin time for monitoring oral anticoagulant therapy. Blood. 1990;75(2):344-9.
222. Godal HC, Madsen K, Nissen-Meyer R. Thrombo-embolism in patients with total proconvertin (factor VII) deficiency. Acta Med Scand. 1962;171(3):325-8.
223. Gudmundsdottir BR, Francis CW, Bjornsdottir AM, Nellbring M, Onundarson PT. Critical role of factors II and X during coumarin anticoagulation and their combined measurement with a new Fiix-prothrombin time. Thromb Res. 2012;130(4):674-81.
224. Onundarson PT, Francis CW, Indridason OS, Arnar DO, Bjornsson ES, Magnusson MK, et al. Fiix-prothrombin time versus standard prothrombin time for monitoring of warfarin anticoagulation: a single centre, double-blind, randomised, non-inferiority trial. Lancet Haematol. 2015;2(6):e231-40.
225. Zivelin A, Rao LV, Rapaport SI. Mechanism of the anticoagulant effect of warfarin as evaluated in rabbits by selective depression of individual procoagulant vitamin K-dependent clotting factors. J Clin Invest. 1993;92(5):2131-40.
226. Furie B, Liebman HA, Blanchard RA, Coleman MS, Kruger SF, Furie BC. Comparison of the native prothrombin antigen and the prothrombin time for monitoring oral anticoagulant therapy. Blood. 1984;64(2):445-51.
227. Lind M, Fahlen M, Kosiborod M, Eliasson B, Oden A. Variability of INR and its relationship with mortality, stroke, bleeding and hospitalisations in patients with atrial fibrillation. Thromb Res. 2012;129(1):32-5.
228. Powers WF, Abbrecht PH, Covell DG. Systems and microcomputer approach to anticoagulant therapy. IEEE Trans Biomed Eng. 1980;27(9):520-3.
229. Svec JM, Coleman RW, Mungall DR, Ludden TM. Bayesian pharmacokinetic/pharmacodynamic forecasting of prothrombin response to warfarin therapy: preliminary evaluation. Ther Drug Monit. 1985;7(2):174-80.
230. Theofanous TG, Barile RG. Multiple-dose kinetics of oral anticoagulants: methods of analysis and optimized dosing. J Pharm Sci. 1973;62(2):261-6.
231. Vadher B, Patterson DLH, Leaning M. Prediction of the international normalized ratio and maintenance dose during the initiation of warfarin therapy. Br J Clin Pharmacol. 1999;48(1):63-70.
232. Wingard LB, O'Reilly RA, Levy G. Pharmacokinetics of warfarin enantiomers: a search for intrasubject correlations. Clin Pharmacol Ther. 1978;23(2):212-7.
233. Matthews I, Aarons L, editors. A population pharmacokinetic model for S-Warfarin application of a mixture model to determine genotype/phenotype. Population Approach Group in Europe (PAGE) meeting 2006; 2006; Bruges, Belgium.
234. Kazmier F, Spittell JA, Thompson JJ, Owen CA. Effect of oral anticoagulants on factors VII, IX, X, and II. Arch Intern Med. 1965;115:667-73.

235. Assawasuwannakit P, Braund R, Duffull SB. Quantification of the forgiveness of drugs to imperfect adherence. CPT Pharmacometrics Syst Pharmacol. 2015;4(3):e00004.
236. Beran J. Statistical methods for data with long-range dependence. Stat Sci. 1992;7(4):404-16.
237. Glasbey CA. Correlated residuals in non-linear regression applied to growth data. J Royal Stat Soc. 1979;28(3):251-9.